Novel siloxane block copolymers

by

Ingrid Staisch

Dissertation presented for the degree of

PhD (Polymer Science)

at the

University of Stellenbosch

Promoter: Prof. R.D. Sanderson

December 2008

Declaration

By submitting this dissertation electronically, I declare that the entirety of the work contained therein is my own, original work, that I am the owner of the copyright thereof (unless to the extent explicitly otherwise stated) and that I have not previously in its entirety or in part submitted it for obtaining any qualification.

Date: December 2008

Abstract

The research presented in this dissertation was concerned with the living radical polymerization (LRP) of an amphiphilic, water-soluble, bi-substituted and biologically compatible acrylamide derivative, namely *n*-acryloylmorpholine (NAM). The primary objective of this research was the synthesis of novel block copolymers containing poly(dimethylsiloxane) (PDMS) and various chain lengths of poly(acryloylmorpholine) (polyNAM) using a LRP technique, namely reversible-addition fragmentation chain transfer (RAFT) polymerization. This is the first report on the synthesis of these block copolymers using RAFT polymerization. These novel siloxane block copolymers were synthesized using a monohydroxy-terminated PDMS material which had to first be modified into a thiocarbonylthio-containing moiety in order for it to be used as macromolecular chain transfer agent (macroCTA) in the RAFT copolymerization with NAM.

Suitable reaction conditions for the synthesis of these novel block copolymers had to, firstly, be determined, and secondly, optimized. In order to determine suitable reaction conditions, a series of homopolymerizations with NAM were first performed in order to compare which chain transfer agent (CTA), solvent, temperature *etc.* could possibly be best suited for the block copolymerizations of PDMS-*b*-polyNAM. Reported in this work is the first account of the homopolymerization of NAM and 2-(dodecylsulfanyl)thiocarbonylsulfanyl-2-methyl propionic acid (DMP) as CTA using RAFT polymerization.

The resulting novel siloxane block copolymers are amphiphilic in nature and the existence of these structures was confirmed by size exclusion chromatography/multiangle light scattering (SEC/MALS), proton nuclear magnetic resonance (^{1}H-NMR) spectroscopy, gel elution chromatography (GEC) and transmission electron microscopy (TEM). Interesting phase behaviour was observed in the latter technique.

Opsomming

Die navorsing wat in hierdie proefskrif weergegee word, handel oor die lewende radikaalpolimerisasie (LRP) van 'n amfifiliese, wateroplosbare, tweevoudiggesubstitueerde en biologies versoenbare akrielamied derivaat, naamlik n-akrieloïelmorfolien (NAM). Die primêre doelwit van die navorsing is die sintese van nuwe blokkopolimere bestaande uit poli(dimetielsiloksaan) (PDMS) en verskillende kettinglengtes van poli(akrieloïelmorfolien (poliNAM), deur gebruik te maak van 'n LRP-tegniek, naamlik omkeerbare addisiefragmentasiekettingoordrag (RAFT) polimerisasie. Hierdie is die eerste bekendmaking van die sintese van hierdie blokkopolimere met behulp van RAFT-polimerisasie. Hierdie nuwe siloksaan blokkopolimere is gesintetiseer deur van 'n monohidroksiegetermineerde PDMS gebruik te maak. Die PDMS moes eers na 'n tiokarbonieltio-bevattende kern omgesit word voordat dit as makromolekulêre kettingoordragverbinding (KOV) in die RAFT-kopolimerisasie met NAM gebruik kon word.

Geskikte reaksiekondisies vir die sintese van hierdie nuwe blokkopolimere moes eers bepaal word, waarna die reaksiekondisies geoptimiseer moes word. In die proses van die bepaling van die geskikte reaksiekondisies is 'n reeks homopolimerisasies met NAM uitgevoer om sodoende te bepaal watter kettingoordragverbinding, oplosmiddel, temperatuur, ens., die beste geskik sou wees vir die blokkopolimerisasie van PDMS-*b*-poli(NAM). In hierdie proefskrif word die eerste proses van die homopolimerisasie van NAM met 2-(dodekielsulfaniel) tiokarbonielsulfaniel-2-metiel propioonsuur (DMP) as KOV deur van RAFT-polimerisasie gebruik te maak, beskryf.

Die nuutbereide siloksaan blokkopolimere is amfifilies van aard en die bestaan van hierdie strukture is deur grootte-uitsluitingschromatografie/multihoek ligverstrooiing (SEC/MALS), protonkern magnetiese resonansiespektroskopie (^{1}H-KMR), geleluering schromatografie (GEC) en transmissie elektronmikroskopie (TEM) bevestig. Met laasgenoemde tegniek is interessante fasegedrag opgemerk.

Acknowledgements

Table of Contents

Chapter 1: Introduction and objectives

Chapter 2: Historical and theoretical background: Radical polymerization

Chapter 3: PDMS macroCTA synthesis and characterization

Chapter 4: Block copolymer synthesis with poly(styrene) (PSt) using a PDMS macroCTA

Chapter 5: RAFT homopolymerizations using *n*-acryloylmorpholine (NAM)

Chapter 6: Novel siloxane block copolymers

Chapter 7: Conclusions and recommendations

List of Figures

List of Schemes

List of Tables

List of Abbreviations

AIBN	2,2'-azobis(isobutyronitrile)
[AIBN]	molar concentration of AIBN
AMPS	sodium 3-acrylamido-2-methylpropanesulfonate
ATRP	atom transfer radical polymerization
BA	butyl acrylate
BPO	benzoyl peroxide
CDB	cumyl dithiobenzoate
*t*BDB	*tertiary*-butyl dithiobenzoate
CTA	chain transfer agent
[CTA]	molar concentration of chain transfer agent
CTA (10a)	3-((benzylthio)carbonothioyl)thio)propanoic acid
CTA (10b)	2-(dodecylsulfanyl)thiocarbonylsulfanyl-2-methyl propionic acid
CTA (10c)	2-((2-phenyl-1-thioxo)thio)propanoic acid
DCC	1,3-dicyclohexylcarbodiimide
DMA	*N,N*-dimethyl acrylamide
DMAP	4-(dimethylamino)pyridine
[DMAP]	4-(dimethylamino)pyridine molar concentration
DMA-*b*-BA	poly(dimethylacrylamide)-poly(butylacrylate) block copolymer
DMP	2-(dodecylsulfanyl)thiocarbonylsulfanyl-2-methyl propionic acid
DP$_{inst}$	instantaneous degree of polymerization
DPMAm	*N*-diphenylmethylacrylamide
DSC	differential scanning calorimetry
DRI	differential refractive index
ELSD	evaporative light scattering detector
ESR	electron spin resonance
GEC	gel elution chromatography
GPC	gel permeation chromatography

HD	hexadecane
HH	head-to-head addition
HPLC	high performance liquid chromatography
HT	head-to-tail addition or 1,3-placement
H-X	hydrogen donor
$I_{scattered}$	intensity of scattered light
LRP	living radical polymerization
LS	light scattering
M:CTA	monomer to chain transfer agent ratio
[M]	molar concentration of monomer
macroCTA	macromolecular chain transfer agent
MADIX	macromolecular design by interchange of xanthate
MALDI-TOF MS	matrix-assisted laser desorption ionization time-of-flight mass spectrometry
MALS	multiangle light scattering
MMA	methyl methacrylate
NAH	*N*-acryloylazocane
NAM	*N*-acryloylmorpholine
NAP	*N*-acryloylpiperidine
NAS	*N*-acryloxysuccinimide
ODAm	*N*-octadecylacrylamide
ODN	oligonucleotide
NMP	nitroxide-mediated polymerization
PBA	poly(butylacrylate)
PDI	polydispersity index
PDMS	poly(dimethylsiloxane)
PDMS-OH	monohydroxy-terminated poly(dimethylsiloxane)
PDMS-*b*-PSt	poly(dimethylsiloxane)-poly(styrene) block copolymer
PDMS-*b*-polyNAM	poly(dimethylsiloxane)-poly(acryloylmorpholine) block copolymer
PEG	poly(ethyleneglycol)
polyNAM	homopolymer *n*-acryloylmorpholine

PMA-*b*-P(NAS-co-NAM)	poly(methylacrylate)-poly(*N*-(acryloyloxy)succinimide-*co*-(*N*-acryloylmorpholine)) block copolymer
PMMA	poly(methyl methacrylate)
PNIPAM-*b*-NAM	poly(isopropylacrylamide)-poly(acryloylmorpholine) block copolymer
PRE	persistent radical effect
PSt	poly(styrene)
R	leaving group
RAFT	reversible addition-fragmentation chain transfer
RGD	Rayleigh-Gans-Debye
RX	transfer agent
ROMP	ring-opening metathesis polymerizations
SDS	sodium dodecyl sulphate
SEC	size exclusion chromatography
SFRP	stable free radical polymerization
SG1	*N-tert*-butyl-*N*-(1-diethylphosphonate-2,2-dimethylpropyl)nitroxide
TBAm	*N-tert*-butylacrylamide
TEM	transmission electron microscopy
TEMPO	2,2,6,6-tetramethylpiperidin-1-oxy
THF	tetrahydrofuran
TIPNO	*N-tert*-butyl-2-methyl-1-phenylpropyl nitroxide
TIPNO-styryl	2,2,5-trimethyl-3-(phenylethoxy)-4-phenyl-3-azahexane
TLC	thin-layer chromatography
TM	transition metal
TT	tail-to-tail addition
UV	ultraviolet

List of Symbols

Chapter 2

A•	active radical
B•	stable radical
$\overline{}$, M_n	number-average molecular weight
$\overline{}$, M_w	weight-average molecular weight
C_{tr}	chain transfer constant
$[CTA]_0$	molar concentration of chain transfer agent at time zero
$-d[I]/dt$	rate of initiator loss
$-d[M]/dt$	rate of monomer loss
f	initiator efficiency
$[I]_0$	molar concentration of initiator at time zero
$[I]_t$	molar concentration of initiator at time t
k_{add}	rate coefficient of addition of polymeric radicals
k_{-add}	rate coefficient of fragmentation of polymeric radicals
k_d	rate coefficient for initiator decomposition
k_β	rate coefficient for the addition reaction of the R group to a polymeric RAFT species
$k_{-\beta}$	fragmentation rate coefficient of the R group
K_{eq}	equilibrium constant
k_{ex}	rate of exchange
k_i	rate coefficient for initiation
k_p	rate coefficient for propagation
k_{ri}	rate coefficient for re-initiation of R• and monomer
k_t	rate coefficient of termination
$\langle k_t \rangle$	average rate coefficient of termination
M	molar concentration in mol/dm^3
M_1•	first monomer adduct
$[M]_0$	molar concentration of monomer at time zero

[M]	molar concentration of monomer
[M•]	the total molar concentration of all chain-radicals of size M_1• or larger
[M]$_t$	molar concentration of monomer at time t
M_1•	first monomer adduct
TM(I)/L	transition metal complex
M$_{CTA}$	molecular weight of chain transfer agent
M$_I$	molecular weight of initiator
M$_M$	molecular weight of monomer
P$_n$•	polymeric chain radical with n number of monomer units
P$_m$•	polymeric chain radical with m number of monomer units
R•	primary radical species
R-X	alkylhalide initiator species used in ATRP
R$_i$–X	dormant species
R_d	rate of producing primary radicals by thermal homolysis
R_i	rate of initiation
R_p	rate of propagation
R_{tr}	rate of chain transfer
X•	persistent radical

Chapter 3

T$_g$	glass transition temperature
C$_6$D$_6$	deuterated chloroform

Chapter 4

$\overline{n}_{RAFT^{-1}}$	average number of propagating radicals per particle in a RAFT polymerization miniemulsion system
$\overline{n}_{blank^{-1}}$	average number of radicals per particle in a RAFT-free miniemulsion polymerization system

Chapter 5

$\Delta\eta$	difference in refractive index (or refractive index change)
η_s	refractive index of the sample
η_r	refractive index of the reference solvent
φ	phase shift difference
l	length of cell used in the interferometric refractometer
λ_0	vacuum wavelength of the incident light
λ	wavelength of incident light
(dn/dc)	specific refractive index increment
Δc	change in concentration increment relative to the pure solvent
ΔV	change in voltage output
d	displacement distance of the split beams
β	constant relating displacement to voltage change
T	temperature
t_0	time at beginning of reaction
N_A	Avogadro's constant
R_Θ	excess Rayleigh ratio
$P(\Theta)$	scattering function
A_2	second virial coefficient
$d\tau$	volume element
τ	distance
N	molecular concentration
η	number of segments of each molecule
$\rho(r)$	radial distribution function of the segments in the molecule
V	total volume of the scattering molecules
r	distance between two segments
s	vector difference between unit vectors in the directions of the incident and scattered light rays

i	incident light
j	scattered light
ρ_1	internal probability
ρ_2	external probability
Θ	theta angle
X	an integral representing the short range interaction between pairs of segments

Chapter I

Introduction and objectives

Abstract

A brief introduction to the dissertation follows in order to briefly summarize the main objectives of the work and to allow the reader to gain an understanding as to the basis of each chapter.

1.1   Introduction

The work that follows was conducted as part of a doctoral thesis undertaken at The University of Stellenbosch, South Africa. The field of chemistry that it was involved in is polymer chemistry. A specific area of polymer chemistry was employed in the laboratory synthesis of a range of polymeric materials, namely, living radical polymerization (LRP). One of the LRP techniques, namely, reversible-addition fragmentation chain transfer (RAFT) polymerization was the method of choice for the polymerizations performed in this research.

This work is the first report on the synthesis of a block copolymer consisting of poly(dimethylsiloxane) (PDMS) and various chain lengths of poly(acryloylmorpholine) (polyNAM) using RAFT polymerization. It was opted to use RAFT polymerization in the synthesis of these novel siloxane block copolymers as this technique is suitable for use in industrial syntheses and applications. RAFT polymerization also allows the synthesis of homo- and copolymers with well-defined macromolecular architectures and molecular weights. Another advantage of using RAFT polymerization compared to atom transfer radical polymerization (ATRP) is that the final polymeric product contains a thiocarbonylthio moiety instead of a metal compound which can be strategically placed to provide easy removal hereof, which may be a stringent requirement in certain applications. In terms of this dissertation, RAFT polymerization was considered the most suitable LRP technique to employ as it appears to be the most versatile of the LRP approaches for controlling the homo- and copolymerization of a wide range of (meth)acrylamide derivatives (refer to Chapter 5 for references).

This thesis should be considered a development thesis as the author, in arriving successfully at the final aim, has presented to the reader in detail the weaknesses that were identified in the literature and experienced upon entering the research. Some of the work learned in the literature, which was to be used as crucial initial steps in the synthesis of the novel block copolymers, needed further investigation. In addition to this, availability and access to certain equipment in-house during the earlier stages of the research, namely SEC-MALS, had presented the author with numerous difficulties, although these were overcome towards the final stages of the research project. The scientific methodology of optimizing these weaknesses are shown in a step by step process to highlight to the reader the need to fully understand the science behind these very important reaction variables which were to be used in efficiently and effectively synthesizing the novel siloxane block copolymers.

1.2   Contents of thesis

The contents of the following seven chapters are summarized as follows:

□   <u>Chapter 1: Introduction and objectives</u>

This chapter consists of a brief introduction to the dissertation identifying the primary and secondary objective(s) of this work.

□   <u>Chapter 2: Historical and theoretical background: Radical polymerizations</u>

This chapter is a literature review of conventional radical chain polymerizations and LRP systems whilst focusing on the mechanism used for the synthesis of the homo- and block copolymers described in further chapters, namely RAFT polymerization. Important variables to consider in RAFT polymerizations are described in further detail.

□   <u>Chapter 3: PDMS macroCTA synthesis and characterization</u>

Chapter 3 describes the synthesis of the PDMS macromolecular chain transfer agent (PDMS macroCTA) that was used for further syntheses with monomers to form block copolymers. This PDMS macroCTA was used for the synthesis of the novel siloxane block copolymers referred to in the primary and secondary objective(s) of this dissertation. Various investigations were performed in order to optimize the degree of conversion and obtain high purity.

□ Chapter 4: Block copolymer synthesis with poly(styrene) (PSt) using a PDMS macroCTA

This chapter was used to explain model polymerization reactions performed with the PDMS macroCTA synthesized in Chapter 3 and styrene, in order to determine whether this technique of using these PDMS macroCTAs as starting blocks would lead to the successful copolymerization of poly(dimethylsiloxane)-*b*-poly(styrene) block copolymers (PDMS-*b*-PSt). Size exclusion chromatography (SEC) and nuclear magnetic resonance (NMR) were the main analytical techniques used to characterize the materials.

□ Chapter 5: RAFT homopolymerizations with *n*-acryloylmorpholine (NAM)

Chapter 5 presents various RAFT homopolymerization reactions performed with NAM, the monomer of choice for the synthesis of the novel siloxane block copolymers described in Chapter 6. It was considered an important first step to establish optimized reaction conditions for the homopolymerization reactions before proceeding to synthesize the block copolymers.

□ Chapter 6: Novel siloxane block copolymers

After establishing optimal conditions for the homopolymerization of NAM in dioxane at various temperatures, appropriate conditions for the synthesis of the novel siloxane block copolymer were obtained. The diblock copolymers were prepared by RAFT polymerization using the PDMS macroCTA described in Chapter 3. Various chain lengths were synthesized in order to compare the effects that individual block lengths may have on the chemical properties. The rest of the chapter presents the various characterization results of the block copolymers.

□ Chapter 7: Conclusions and recommendations

This final chapter summarizes the conclusions to the experimental work as well as scientific findings developed by the author. To end off the dissertation, included are some recommendations for future applications as proposed by the author.

1.3   Objectives

1.3.1   Primary objective

The primary objective of this dissertation is to synthesize novel siloxane block copolymers that could find application in the personal care and cosmetics industry. At the onset, it was

not clear what properties the new silicone-containing polymer would bring, although it was anticipated that such a material would bring about the numerous beneficial skin feel and conditioning properties to potential formulations that silicone materials alone already possess. Silicone materials are widely used in personal care and cosmetic formulations and are non-toxic and biocompatible to the human body.[1-5] As this novel material is a block copolymer, it consists of two different types of polymer, and if it were to be used for the desired application it would imply that both parts should be biocompatible and non-toxic as well.

The second material that was used as part of the synthesized block copolymer is NAM, which is an amphiphilic, water-soluble and organic-soluble bi-substituted acrylamide derivative which has been used extensively in molecular biology and applications intended for use in the body (particularly effective as drug carriers).[6-11] This polymer can be synthesized to high molecular weights with a virtual lack of toxicity.

Block copolymers are highly useful macromolecules which show interesting phase behavior and are useful in many applications. The question now arises, "Why the need to synthesize a block copolymer for such an application?". The simple answer is that by synthesizing a new material consisting of two different segments, the new properties or, properties possessed by each part may be transferred to the block copolymer. Superior and improved chemical and physical properties could be achieved compared to the individual polymers. Also, the ability to tailor the length of block copolymers for certain applications is a useful property (*e.g.* use large size block copolymers in applications where transportation through the skin is not desirable).

Amphiphilic block copolymers consist of hydrophilic and hydrophobic segments and are self-assembling materials, which are capable of forming polymeric associates in aqueous solutions. These novel siloxane block copolymers are amphiphilic as they consist of a superhydrophobic part, PDMS, as well as a water-soluble part, polyNAM. It is anticipated that there would be many advantages of these types of structures in personal care and cosmetic formulations, and that control of molecular weight and polydispersity index (PDI) would allow optimization and understanding of performance in a future niche application.

1.3.2   Secondary objectives

In order to synthesize the desired novel PDMS-*b*-polyNAM copolymers, using RAFT polymerization, it was important that the initial PDMS macroCTA used was as pure as possible in order to prevent any unwanted side reactions. Optimization of the esterification

reaction to produce this macroCTA was thoroughly investigated. Further investigation into the use of this PDMS macroCTA with styrene was tested in order to validate its effectiveness in RAFT systems. It was considered important to first test effectiveness of synthesizing a model PDMS/PSt copolymer before attempting to copolymerize PDMS with NAM. Finally, a series of homopolymerizations of NAM were performed in order to work towards identifying a possible optimal reaction system for the synthesis of novel PDMS-*b*-polyNAM copolymers.

References

(1)   Brash, J. L. *Ann NY Acad Sci,* 1977, *283,* 356.

(2)   Leininger, R. I.; Falb, R. D.; Grode, G. A. *Ann NY Acad Sci,* 1968, *146,* 11.

(3)   Lyman, D. J.; Metcalf, L. C.; Albo, D. J.; Richards, K. F.; Lamb, J. *Trans. Am. Soc. Artif. Organs,* 1974, *20,* 474.

(4)   Owen, M. J. *Chemtech,* 1981, *11,* 288.

(5)   Tang, L.; Sheu, M. S.; Chu, T.; Huang, Y. H. *Biomaterials,* 1999, *20,* 1365.

(6)   Torchillin, V. P.; Trubetskoy, V. S.; Whiteman, K. R.; Caliceti, P.; Ferruti, P.; Veronese, F. M. *J. Pharm. Sci.,* 1995, *84,* 1049.

(7)   Veronese, F. M.; Largajolli, R.; Visco, C.; Ferruti, P.; Miucci, A. *Appl. Biochem. Biotechnol.,* 1985, *11,* 269.

(8)   D'Agosto, F.; Charreyre, M.-T.; Mellis, F.; Pichot, C.; Mandrand, B. *J. Appl. Polym. Sci.,* 2003, *88,* 1808.

(9)   de Lambert, B.; Chaix, C.; Charreyre, M.-T.; Laurent, A.; Aigoui, A.; Perrin-Rubens, A.; Pichot, C. *Bioconjugate Chem.,* 2005, *16,* 265.

(10)   de Lambert, B.; Charreyre, M.-T.; Chaix, C.; Pichot, C. *Polymer,* 2007, *48,* 437.

(11)   Epton, R.; Goddard, P. *Polymer,* 1980, *21,* 1367.

Chapter 2

Historical and theoretical background: Radical polymerizations

Abstract

The 'new' generation of LRP, making use of either reversible termination or reversible transfer processes, yield polymers with characteristics resembling those obtained with the 'older' generation of living polymerization techniques such as anionic and cationic polymerizations. These newer techniques have many advantages above the 'older' generation techniques. It is therefore the basis of this chapter to provide the reader with a background on how the 'older' techniques developed as well as how the development of these techniques led to the development of their new counterparts. Comparisons between conventional radical polymerizations with the new breed of LRP will be made with regards to their differences as well as similarities. Finally, this chapter will end off with a brief discussion of an important feature of RAFT polymerizations – the removal of terminal or internal thiocarbonylthio functionalities that can ultimately be reduced to provide a wide range of chain end functionalities on the polymer chain.

2.1   Introduction

Since the 'birth' of living polymerization systems in the 1950s scientists have been able to synthesize polymers with predictable molecular weights, control the PDI, as well as achieve a desirable molecular structure (composition, functionality, topology *etc.*).[1-4] The earliest accounts of living polymerization systems were based on ionic processes.[5-8] The beauty of living systems is that a variety of architectures may be synthesized including linear,[9,10] star,[11-18] graft (comb),[19-27] cyclic,[28,29] core-shell particle[30-32] and dendritic architectures,[33,34] with various compositions, including homopolymers,[35-37] statistical/random,[38-41] block,[37,39,42-50] alternating[51,52] and gradient[38,53] copolymers which cannot be easily synthesized by other techniques.

The development of LRP techniques during the 1990s was considered an improvement upon the original living systems as it allowed a more facile synthesis, *e.g.* under less rigorous conditions, of well-defined polymeric materials from a larger variety of monomers. LRP ideally represents a situation in which all chains are initiated at the start of a reaction,

they all grow at the same rate, and active radical chains are not active long enough for such species to undergo chain transfer or termination reactions to produce dead polymer chains.[54] If these conditions are satisfied, the results from SEC would show that the molecular weights of such chains increase linearly with conversion according to predetermined molecular weights as well as display narrow PDIs (typically, $\overline{}, M_W/\overline{}, M_n <$ 1.5). Some advantages of radical systems include their compatibility with a large variety of functional groups (*e.g.*, amino, hydroxyls, carboxyls, *etc.*) that were previously unable to be polymerized using living ionic techniques, as well as the facile synthesis of the initiators used in such systems.[55] Compared to other forms of non-radical living polymerizations, such as anionic,[56,57] cationic,[58-63] group transfer polymerization,[64,65] olefin,[3] coordination[66,67] and ring-opening metathesis polymerizations (ROMP),[68] LRP is not as synthetically demanding as the former and does not require as complicated and extreme reaction conditions such as very high/low temperature. In addition, LRP does not show the same sensitivity to acidic and protic monomers as anionic techniques do; LRP does not require the same level of inert atmosphere and high purity (and expensive) reagents as is required in anionic systems and is tolerant to water (thereby allowing reactions to be performed in aqueous media). These factors make LRP suitable for use in industrial syntheses and applications. A disadvantage of LRP processes is the side reactions resulting from active radical species which may either undergo transfer or termination reactions, thereby forming various side products.[69]

2.2   Chain polymerizations

Radical polymerizations, either conventional or LRP, are a form of chain polymerization. Compared to other forms of polymerization, such as condensation (step) polymerization, a chain polymerization produces high molecular weight polymers early on in the reaction which allows a shorter reaction time to be more common in radical chain polymerizations. In condensation polymerization, high molecular weight polymers are only obtained at very high conversions. An anionic, cationic or radical reactive species will add monomer units in a chain reaction and grow to relatively high molecular weights. It is important to note that not all monomers will react with either of these reactive centers. Monomers are usually specific for anionic, cationic or radical species as these forms of initiation do not work for all monomers. The carbon-carbon double bond in vinyl monomers and the carbon-oxygen double bond in aldehydes and ketones are the two main types of linkages that undergo chain polymerizations, although the former is by far more important. The carbonyl group is not readily prone to polymerization by radical initiators because of its polarized nature.[70]

2.2.1   Conventional radical polymerization mechanism

Conventional radical chain polymerizations (from here on referred to only as conventional radical polymerizations) are an important class of techniques as more than 50% of industrially produced polymers are nowadays produced via free radical processes.[71] These types of polymerizations are more tolerant of functional groups and impurities compared to techniques such as anionic and cationic chain polymerization. Therefore, there was a drive to develop techniques that would combine the simplicity of radical techniques with the ability to produce living polymers. These reactions are involved in a sequence of four steps, namely, initiation, propagation, transfer and termination. The active species in radical polymerizations are organic (free) radicals, either electrophilic or nucleophilic in nature, and are stabilized either by resonance or polar effects, or both.

2.2.1.1   Initiation reactions

Initiation takes place by means of a radical species. Compounds such as 2,2'-azobis(isobutyronitrile) (AIBN) undergo dissociation by means of thermal, photochemical or redox methods in order to produce radical species. These radicals are then used as the reactive center to which monomer units are added. Generally, the lower the initiator concentration, the higher the molecular weight of the polymer and the lower the conversion.[72] This can be explained by imagining that if only five initiator chains are initiated, then the monomer will be used to grow only five chains. But, if ten initiator chains were initiated, then the monomer will be used to propagate ten chains. It can be understood that in the last scenario, provided the same amount of monomer was added to both examples, less monomer will be available to the ten chains instead of the five chains.

Initiation involves two steps: the first step (2.1) is the homolytic dissociation of the initiator species to produce two radicals, where k_d is the rate coefficient for initiator decomposition and R· is the primary radical (the value for AIBN is *ca.* $6.2 \times 10^{-5}\,\text{s}^{-1}$ in dimethylformamide at $71.2\,^\circ\text{C}$); the second step (2.2), which is usually faster in most polymerizations, involves the addition of the primary radical to the first monomer molecule (M) to produce the first monomer-adduct, which is the chain-initiating radical (M_1·), where k_i is the rate coefficient for initiation. Conventional radical polymerizations usually follow steady-state conditions. Under steady-state conditions, the rate of initiation is the same as the rate of termination, which is approximately 1000 times slower than the rate of propagation. Slow initiation can occur in radical polymerizations as a result of using initiators with very long half-lifetimes. Due to the fact that termination is a second-order reaction with respect to radical concentration, to ensure that high molecular weight chains are produced, very small amounts of initiator must be used.

$$I \xrightarrow{k_d} 2\,R\text{\textbullet} \tag{2.1}$$

$$R\text{\textbullet} + M \xrightarrow{k_i} M_1\text{\textbullet} \tag{2.2}$$

$$R\text{\textbullet} + H_2C=\underset{\underset{H}{|}}{\overset{\overset{Y}{|}}{C}} \xrightarrow{k_i} R-CH_2-\underset{\underset{H}{|}}{\overset{\overset{Y}{|}}{C}}\text{\textbullet}$$
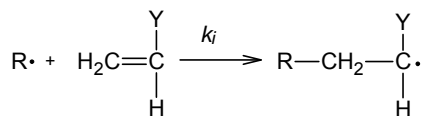
When transfer reactions can be neglected, the instantaneous degree of polymerization, DP_{inst}, is, according to equation (2.3) reciprocally dependent on the square root of the initiator concentration at time t, $[I]_t$, where k_p is the rate coefficient of propagation, $[M]_t$ is monomer concentration at time t, f is the initiator efficiency factor and $\langle k_t \rangle$ is the average rate coefficient of termination.[73]

$$DP_{inst} = k_p [M]_t \sqrt{f k_d [I]_t \langle k_t \rangle} \tag{2.3}$$

There are different classes of compounds which may be used as initiating species, for instance, the class of peroxy compounds (benzoyl peroxide (BPO), acetyl peroxide) and the class of azo-compounds (*e.g.* AIBN) (Figure 2.1). The rate of initiator loss, $-d[I]/dt$, as expressed by equation (2.4), is proportional to k_d and the initial initiator concentration ($[I]_0$). For most initiators, k_d varies from 10^{-4}–10^{-9} s^{-1}, depending on the initiator and temperature.

$$\frac{-d[I]_0}{dt} = k_d [I] \tag{2.4}$$

The rate of producing primary radicals by thermal homolysis, R_d, is given by

$$R_d = 2 f k_d [I]_0 \tag{2.5}$$

which in turn is the rate determining step in initiation, and subsequently the rate of initiation is given by

$$R_i = 2 f k_d [I]_0 \tag{2.6}$$

The variable f is the initiator efficiency. It is more clearly defined as the fraction of radicals produced from homolysis that is successful in initiating polymer chains. $(1-f)$ is equal to the wastage factor, therefore, for a reaction in which only 40% of the chains are successfully initiated from primary radicals, R\text{\textbullet}, f would equal 0.4, and $(1-f)$ would equal 0.6. The initiator efficiency would never be unity (equal to 1), due to side reactions that

take place to produce stable products that do not undergo propagation with monomer. Solomon and Moad[74] showed that the initiator efficiency of AIBN varies between 20% and 76% depending on monomer conversion. The decomposition of initiator within the solvent cage is the most predominant reaction that decreases the efficiency of f.[70] Reactions such as these are referred to as the *cage effect*,[75,76] and this effect is observed in almost all initiation systems. When the radical diffuses out of the solvent cage, then the reaction of the primary radical with monomer is the predominant reaction, and f increases very rapidly. As the concentration of monomer increases so does f, but it does eventually reach a limiting value. At low concentrations of monomer, the initiator concentration is higher, leading to higher rates of initiation. This subsequently leads to more radical species which combine with each other to form stable species which do not undergo propagation with monomer. f will also decrease as the viscosity of the medium increases. The time the radicals spend in the solvent cage increase as a result of a more viscous medium, which in turn increases the probability of radical combination.
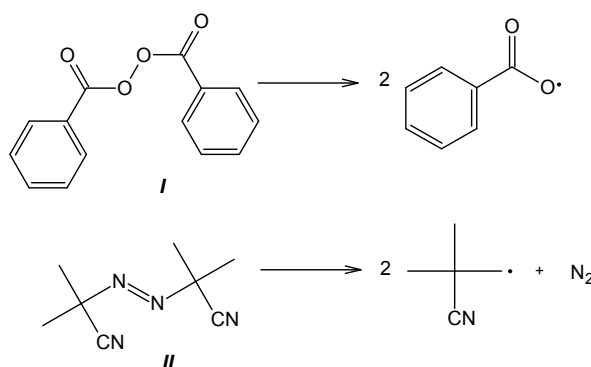
Figure 2.1   **Structures of initiator species and their corresponding radicals: (*I*) benzoyl peroxide (BPO); (*II*) 2,2'-azobis(isobutyronitrile) (AIBN).**

2.2.1.2   Propagation reactions

There are two manners in which the propagating radical can attach to the monomer species; the first is when the propagating radical attaches to the unsubstituted carbon, and the second is when the propagating radical attaches to the substituted carbon. The former is a more favorable approach as a more stable species is formed due to the stabilization of the radical through resonance effects of the substituents. Additionally, this approach results in less steric hindrance when the propagating radical attaches to the unsubstituted carbon. In the case of the second approach, the substituents cannot assist in stabilizing the radical as they are not attached directly to it. It is also more likely that additional monomer units will attach in the same sequential sequence as proposed by the first method (also referred to as a *head-to-tail (HT) addition, or 1,3-placement)*. The reasons for this can be based on steric and resonance grounds. HT addition is the

predominant mode of propagation in chain polymerization. The other forms of addition are referred to as *HH (head-to-head)* or *TT (tail-to-tail)*.
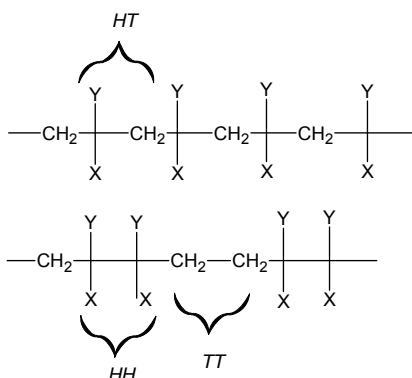
The propagation step consists of the growth of successive monomer units to chain-initiating species ($M_1\cdot$). k_p for most monomers is very high. The value of k_p for most monomers is in the range of 10^2–10^4 $M^{-1}s^{-1}$.
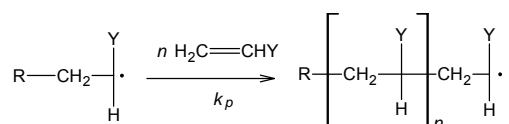
The rate of polymerization (or alternatively, the rate of monomer disappearance) is given by equation (2.7), but since the number of molecules that react in the initiation step is far less than that for propagation when producing high molecular weight polymer the term R_i can be neglected, to yield equation (2.8).

$$\frac{-d[M]}{dt} = R_i + R_p \tag{2.7}$$

$$\frac{-d[M]}{dt} = R_p \tag{2.8}$$

The rate of propagation involves many individual propagation steps, all of which essentially have the same rate coefficients, therefore the rate of propagation (or alternatively, the rate of polymerization) is given by

$$R_p = k_p [P\cdot][M]_t \tag{2.9}$$

where $[M]_t$ is the monomer concentration, and $[P\cdot]$ is the total concentration of all chain-radicals larger than size $M_1\cdot$. Since the concentration of radicals present at any point is

usually very low (~10^{-8}M), it is difficult to measure, and therefore, to make things a little less complicated, a steady-state concentration of radicals is assumed to exist during the course of polymerization. A steady-state implies that

$$R_i = R_t = 2\langle k_t \rangle [P \cdot]^2 \qquad (2.10)$$

After substituting equation (2.10) into equation (2.9) one obtains an equation for the rate of polymerization (2.11).

$$R_P = k_p [M] \left(\frac{R_i}{2\langle k_t \rangle} \right)^{\frac{1}{2}} \qquad (2.11)$$

In conventional radical polymerizations it is not possible to manipulate molecular structure, add chain-end functionalities, or incorporate the addition of a second monomer since the average life of a propagating chain is very short-approximately 1 second (constituting approximately 1000 acts of propagation with a frequency of approximately 1 millisecond).[73]

2.2.1.3   Transfer reactions

Transfer reactions in conventional radical polymerizations require higher activation energy than propagation reactions; therefore transfer reactions are not the main cause of chain-breaking reactions (as in the case of carbocationic polymerizations). The higher the temperature, the more pronounced the effect of transfer reactions.

Chain transfer reactions result in an effective decrease of the size of the propagating polymer chain due to transfer of an atom from a compound (monomer, catalyst, solvent, polymer, or initiator) to the growing polymeric radical chain, resulting in the radical activity being transferred to a smaller molecule. This forms a dead polymer chain and a radical that is released which is free to engage in further propagation with monomer if sufficiently reactive. The consequence of chain transfer reactions is the occurrence of lower molecular weight polymers than otherwise predicted and an additional fraction of dead chains. Transfer agents are added to polymerizations to reduce average molecular weights and assist in controlling the distribution of chain lengths. Solvents such as acids, carbonyl compounds, amines, alcohols, *etc.* have high chain transfer constants, C_s, much higher than aliphatic hydrocarbons.[70] The reason for this is that the radicals are easily stabilized by the adjacent N, O or C=O atoms. In addition to this, the higher the bond strength between two atoms, the weaker is the ability of the compound to act as a chain

transfer agent. Hydrocarbons with their strong C-H bond strength are poor chain transfer solvents, but compounds with weak S–S, S–H or C–X (X = halogen) bonds are very good chain transfer compounds. In the case of monomers, the more reactive the propagating radical is, the better they act as chain transfer agents, *e.g.* vinyl acetate.
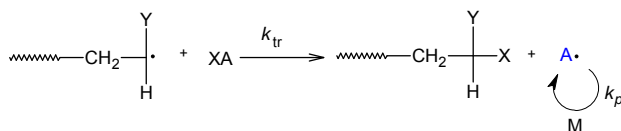
The rate of chain transfer, R_{tr}, can be expressed by

$$R_{tr} = k_{tr}[M\cdot][XA] \tag{2.12}$$

where [XA] is the concentration of chain transfer agent, such as a solvent molecule, a monomer molecule or a thiocarbonylthio moiety.

2.2.1.4   Termination reactions

Bimolecular termination, a diffusion-controlled process, between two radicals can take place by means of either coupling (resulting in one polymer molecule) or disproportionation (resulting in two polymer molecules). The former is the predominant means of bimolecular termination when chain transfer reactions are minimized or non-existent. Disproportionation reactions take place more commonly when the temperature is increased, the propagating radical is sterically hindered or it has many β-hydrogens available for transfer (as in the case of methyl methacrylate). Chain-breaking reactions, such as bimolecular termination and chain transfer reactions, will always occur in conventional radical polymerizations due to the type of propagating radicals that are present, and as a result thereof, the lifetime of the propagating radical species is short. Typical $\langle k_t \rangle$ values range from 10^6–10^8 M^{-1}s^{-1} (much larger than k_p). However, this does not prevent propagation from taking place, due to the low concentration of radicals present (low radical flux) as well as the fact that (classically) R_p is only dependent on the square root of $\langle k_t \rangle$.[70] The termination rate coefficients are influenced by initiator concentration (*i.e.* radical flux) and polymer concentration (*i.e.* degree of conversion and degree of polymerization *i.e.* chain length).[77] The higher the radical flux, the more likely radicals will find each other and terminate. Also, the greater the polymer conversion, the slower the movement of active chain ends and the slower the rate of radicals terminating by this mechanism. Compared to ionic polymerizations, termination rate coefficients are much higher as the electrostatic repulsions between two anions or cations prevent termination reactions from taking place. Termination is a second-order reaction with respect to radical

concentration, therefore, at low radical concentrations, the rate of termination becomes much slower than that of propagation, which is a first-order reaction.
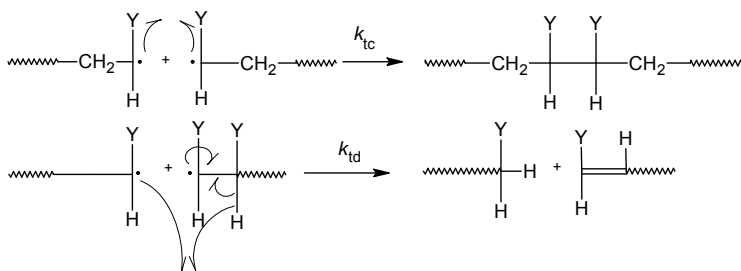
2.2.2   Conventional radical polymerization process conditions

All monomers that undergo radical polymerization are able to be processed in homogeneous or heterogeneous conditions, although there are usually only one or two process conditions which are preferable when it comes to commercial applications. The various process conditions in which monomers can be polymerized via conventional radical polymerization (and subsequently LRP) include bulk,[78,79] solution,[80,81] suspension,[82,83] emulsion, [30,78,84] precipitation and dispersion[85] polymerization.

2.2.2.1   Bulk polymerization

Essentially, this is a homogenous system in which an organic initiator is used. This process has the advantage of potentially containing the least amount of contaminants since it does not involve any solvent. As no solvent is present, the viscosity increases quite rapidly and large amounts of heat which cannot dissipate are generated as a result. It is the viscosity increase that results in the gel effect. Broad PDIs are also a common result due to chain transfer to polymer taking place. Commercially, this method of polymerization is not commonly used for chain polymerizations, although styrene, ethylene and methyl methacrylate are polymerized in bulk up to low conversions to avoid the problems associated with bulk polymerizations. Step polymerizations are more commonly seen using bulk conditions rather than chain polymerizations.

2.2.2.2   Solution polymerization

This process overcomes many of the viscosity and exothermic problems associated with bulk polymerizations. The solvent acts as a diluent and aids in the transfer of the heat of polymerization. Three disadvantages however include (1) solvent which needs to be removed, which can be a costly and difficult process, (2) the possibility of additional chain transfer reactions and (3) molecular weights and polymerization rates are lower as compared to emulsion polymerization.

2.2.2.3   Suspension polymerization

Monomer, the dispersant (oil phase), is suspended as droplets (50–500µm diameter) in water, the continuous phase. A two-phase system exists, which is maintained by agitation and the presence of stabilizers. If agitation should stop, droplet coalescence could result. Two types of stabilizers are commonly used, namely water-soluble polymers (such as polyvinyl alcohol), or water-insoluble inorganic compounds (such as talc, barium sulfate, kaolin, magnesium carbonate). Stabilizers are usually used at 0.1wt% of the water phase. This concentration is much lower than that used in emulsion polymerizations (1–5%). The low concentration of stabilizers results in the large size of monomer droplets. In addition to this, the presence of a low concentration of stabilizers prevents (or minimizes) the existence of micelles. In suspension polymerizations, an oil-soluble initiator is used, which is soluble in the monomer droplets. Each monomer droplet is considered to be a miniature bulk polymerization system and the smaller size of these droplets compared to a bulk system renders the kinetics in this system much quicker. An advantage includes the fact that separation of the polymer is much easier than in solution polymerizations.

Inverse suspension and *micro suspension* techniques are also used. The former makes use of an organic solvent that acts as the continuous phase and a water-soluble monomer (dispersant). The latter technique follows the same principle as suspension polymerizations, except that the sizes of the droplets are much smaller (1µm).

2.2.2.4   Emulsion polymerization

This process makes use of a heterogeneous medium that consists of two insoluble phases, namely the continuous phase (usually water) and the dispersing phase (non, –or slightly, water-soluble monomer). The advantages of this technique are that the thermal and viscosity issues described for bulk conditions are avoided. Compared to solution polymerization, one can obtain high molecular weight polymers without sacrificing polymerization rates. This can be achieved by increasing the number of particles in which polymerization is taking place, whilst maintaining a constant initiation rate. The use of higher surfactant concentrations will increase the number of polymer particles in which polymerization can take place, which in turn increases the degree of polymerization. A further manner in which smaller particle sizes may be obtained is by making use of sonication methods.

2.2.2.5   Precipitation polymerization

With this process, the monomer and initiator are initially soluble in the reaction medium and, as conversion increases, the polymer becomes insoluble in either the solvent used or the monomer used. After the polymer has precipitated out of solution, polymerization is maintained by absorbing the monomer and initiator into the polymer particles.

2.2.2.6   Dispersion polymerization

In this process the monomer, organic solvent, initiator and stabilizer form a homogeneous reaction medium (one homogeneous continuous phase), but as conversion increases, the medium becomes heterogeneous as the polymer becomes insoluble in the solvent. The polymer particles remain stabilized by the stabilizer and polymerization continues by the absorption of monomer from the continuous phase into the polymer particles. The size of the polymer particles formed are in the range 1–10µm, somewhat between those formed in emulsion and suspension polymerizations.

2.3   Is it "living", "controlled" or both?

To date there has been much debate as to whether or not it is technically correct to refer to the LRP techniques such as RAFT polymerization, ATRP and stable free radical polymerization (SFRP) as *living* polymerization techniques.[86] The earliest account and description of a living polymerization was provided by Szwarc in 1956.[6,7] He defined ''living polymerization'' as a polymerization that proceeds ''without chain transfer or termination''. Szwarc eliminated termination and transfer reactions by the development of special high vacuum techniques to eliminate any traces of moisture or oxygen from the reactions of non-polar vinyl monomers.[6,87] Later, this process was used on an industrial scale for the synthesis of well-defined block copolymers capable of performing as thermoplastic elastomers.[88] According to definition, by Szwarc, living techniques would then describe a situation in which:

- polymerization proceeds to full conversion and, upon further addition of monomer, polymerization continues to occur, thereby allowing the synthesis of copolymers. The requirement for this is that the polymer chains are able to reversibly terminate or deactivate. (Note that this is not necessary for ionic techniques, *e.g.* two anions will not terminate since they repel each other.)
- the number of polymer chains is constant during polymerization
- the PDI is narrow
- functional chain-ends can be obtained quantitatively
- molecular weight can be controlled stoichiometrically

In the RAFT process the polymer is referred to as *living* as it is end-capped with a thiocarbonylthio moiety, which undergoes reversible chain transfer processes between active and dormant chains. The CTA has a very high effective chain transfer constant, which allows rapid exchange between dormant and active chains. This rapid exchange allows all of the polymer chains to grow at the same rate, thereby "controlling" the amount of monomer inserted with each cycle to produce very narrow PDIs compared to conventional free radical polymerizations. There are other factors which can be "controlled", or fine-tuned, in RAFT polymerizations, such as the macromolecular architecture, the degree of polymerization as well as the chain-end functionality. From the above it can be seen that the CTA used in RAFT polymerization fulfils both the requirements for producing a "living" as well as a "controlled" polymerization. For the purposes of this dissertation, the RAFT process is considered to be both *living* and "controlled", although the term *living* will be used in order to adhere to the same terminology as that used by Szwarc. For more detail on the RAFT process, refer to Section 2.8

2.4 Living anionic polymerization

In the past *living* polymerization processes were typically reserved for anionic polymerization processes, but as already mentioned, these processes are limited with respect to the choice of monomer and require very stringent reaction conditions, making wide-scale commercial application not viable. Anionic polymerizations fulfil each of the seven requirements proposed by Szwarc[6,7] to be considered a living technique. The mechanism of living anionic polymerization involves the rapid dissociation of an initiator such as alkyl lithium in non-polar solvents (although some polar solvents may be used in the case of very hydrophobic materials) to produce anions (in pairs or aggregates) which are able to undergo propagation with the monomer. Unlike in cationic polymerization, halogenated solvents are avoided due to their facile nature of nucleophilic substitution with carbanions.[70] The associated ion pairs (the anion and counter ion that are closely associated with each other) are considered to be dormant species as their reactivities are several orders of magnitudes smaller than that of free ions in solution.[89] A rapid equilibrium exists between the active and dormant species, thereby ensuring a narrow PDI.[90] Since it is essential for living systems that initiation takes place rapidly, all polymer chains have an equal chance of growing from the same point in time and monomer units are incorporated at the same rate, allowing all the polymer chains to reach the same degree of polymerization. It is possible to target a specific degree of polymerization by adjusting the monomer to initiator ratio as all of the monomer that is converted can be equally divided amongst all the initiator-derived polymer chains. Transfer reactions can

occur in anionic polymerization by way of the proton transfer from the solvent or a deliberately added chain transfer agent, but bimolecular termination does not occur as the chains carry the same anionic charge.

2.5   Iniferters

The work by Otsu *et al.*[91] in the early 1980s formed the basis for understanding the general mechanisms for the reversible termination/transfer reactions we know today, such as nitroxide-mediated polymerization (NMP), ATRP and RAFT polymerization. This group made some interesting observations when they added certain compounds to a radical polymerization. When compounds such as dithiocarbamates and disulfides were added to a radical polymerization reaction, the polymers exhibited a certain amount of living behaviour. They termed these compounds *iniferters* as they acted as an initiator, transfer agent and termination agent. The structure of an iniferter is such that, upon dissociation, it forms an active radical (A·) and a stable radial (B·) (refer to Figure 2.2). The species (A·) initiates polymerization to form an active growing species, whilst the species (B·) acts as the deactivating (controlling) agent to deactivate the active species to its dormant counterpart (in NMP (B·) would be equivalent to the stable nitroxide radical species). The stable free radicals (B·) formed are too stable to initiate propagation. As with the other LRP techniques, the activation/deactivation between the active and dormant species is a reversible process. Although this system presented certain living characteristics,[91] it did not show very high control due to side reactions (such as transfer to iniferter) that took place, resulting in broad PDIs.[92] This method was therefore not considered as another possible approach to LRP.
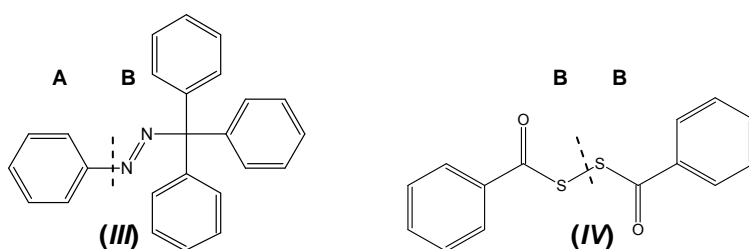
Figure 2.2   **Structures of iniferters: triphenylphenylazomethane *(III)*; dibenzoyl disulfide (*IV*).**

2.6   Versatile and efficient living radical polymerization (LRP)

A new class of LRP techniques has been developed which would overcome all, if not many, of the limitations set forth in anionic and cationic polymerizations. They include SFRP,[93-95] ATRP,[47,96-102] and RAFT,[25,103-108] degenerative transfer polymerization (DT) with alkyl iodides[109,110] and cobalt-mediated radical polymerization (CMRP),[111,112] although the last two will not be discussed in detail in this chapter. An example of SFRP is NMP.[55,69,93,113-119] One can now synthesize (co)polymers with well-defined macromolecular architectures and molecular weights (as seen in LRP) by using the simple and convenient chemical reagents and methods as used in free radical chemistry. These advantages render these processes suitable in commercial applications. The main difference between SFRP/ATRP and RAFT is that the former are considered **reversible termination (deactivation)** processes involving deactivation of the growing radical chains which are trapped by a stable free radical (deactivating agent). Only a single polymer chain interacts with the deactivating agent at any one point in time. RAFT polymerization on the other hand is not a termination process, but rather (effectively) a **chain transfer (degenerative exchange)** process involving the transfer of the CTA (deactivating agent) between growing radical chains. More than one polymer chain (at any one point in time) is involved in the chain transfer process between active and dormant polymer chains.

All of these methods rely on the establishment of a dynamic equilibrium between active radicals and dormant species.[120,121] In the case of NMP and ATRP, this self-regulation/dynamic equilibrium is based on the persistent radical effect (PRE).[121-124] Degenerative transfer processes such as RAFT polymerization do not obey the PRE. Compared to conventional radical polymerizations and RAFT polymerizations, in NMP and ATRP, a steady-state is achieved through the activation/deactivation cycle and not through initiation and termination.

Successful LRP is determined by the amount of control that the polymers display. The variables that affect the degree of control are typically: (1) the efficiency and speed of initiation, (2) the speed in which the exchange processes take place, and (3) the presence of termination or transfer reactions. Fast initiation, rapid exchange processes and absent/negligible termination and transfer reactions result in polymers of uniform chain length with predetermined molecular weights.

Target number average molecular weights, $\bar{M}_n$, in LRP systems may be determined by using equation (2.13)[125] in which $[M]_0$, $[CTA]_0$ and $[AIBN]_0$ are the concentrations of

monomer, CTA and AIBN respectively at the start of the reaction, and M_M and M_{CTA} are the molecular weights of the monomer and CTA respectively.

$$-, M_{n\,Theor} = \frac{[M]_0}{[CTA]_0 + 2f[AIBN]_0\,(1 - e^{-k_d t})} \times M_M \times conversion + M_{CTA} \qquad (2.13)$$

Since the k_d value is usually small, the second term in the denominator in equation (2.13) often becomes negligible, even when f has a maximum value (f=1). If we follow the usual assumption that direct initiation is minimal, this equation may be rewritten as

$$-, M_{n\,Theor} = \frac{[M]_0}{[CTA]_0} \times M_M \times conversion + M_{CTA} \qquad (2.14)$$

An important difference between LRP and other living techniques is that, in the case of the former, termination reactions are unable to be completely avoided, although, if the correct components are chosen, termination becomes a negligible aspect in LRP.

2.6.1   Reversible termination processes

These systems involve the reversible deactivation of a growing polymeric radical chain. The persistent radical, which was first coined by Szwarc in 1962,[126] acts as a deactivator, and if chosen correctly will allow rapid deactivation of the active radical species to form the dormant species. Such systems obey the PRE in which an irreversible accumulation of the persistent radical takes place due to irreversible termination reactions. Subsequently, this build-up results in a reduction of the active radical concentrations, and hence termination reactions, by assisting in rapid deactivation through shifting the equilibrium towards the dormant species side. Through this deactivation process, few (ideally one) monomer units undergo propagation, hereby contributing to the narrow PDIs as monomer conversion increases. The deactivator assists in keeping the radical flux very low at all times, allowing termination to still take place yet make it a *negligible* part of the process. The persistent radical cannot terminate with itself, only reversibly with the propagating radical in the deactivation step.

The equilibrium constant, K_{eq} (in the absence of termination or transfer reactions), determines the polymerization rate. If K_{eq} is too small, too low a propagating radical species concentration will exist and polymerization will not occur at all, or very slowly. If K_{eq} is too large, the propagating radical concentration would be very high and result in an increase of $<k_t>$ due to bimolecular terminations. Polymerization would slow down as a result. The deactivating species contributes to ensuring an adequate equilibrium constant

by reducing the active radical concentration in LRP systems to very low levels so that control is achieved by all chains growing at the same/similar rate. In the case of NMP this agent is a nitroxide; in ATRP this agent is a transition metal catalyst. Only SFRP (NMP) and ATRP will be discussed under this section.

2.6.1.1   Stable free radical polymerizations (SFRP) and nitroxide-mediated polymerization (NMP)

As previously mentioned, NMP is an example of SFRP. This technique was developed in the early 1980s by Solomon *et al.*[127,128] and Rizzardo[95] who did the pioneering work using TEMPO (2,2,6,6-tetramethylpiperidin-1-oxyl) (*V*) as a nitroxide (Scheme 2.1). Georges *et al.*,[129] in 1993, were the first to successfully report on the LRP of styrene using TEMPO that resulted in a linear evolution of molecular weights with conversion and narrow PDIs (PDI<1.3). They made some important advances in the area of LRP when they realized that nitroxides could function as thermally transient adducts, similar in manner to that in which the iniferters functioned,[130] although with many added advantages. Nitroxides were well-known as inhibitors of polymerizations,[131] therefore there was no concern that they would initiate polymerization, and nitroxides were shown to assist in the decomposition of peroxide initiators,[132] thereby contributing to the majority of polymer chains being initiated at the same point in time.

NMP uses a nitroxide, a stable free radical, plus other nitroxides as its counter radical, and therefore has the advantage of being free of any metal compounds.[133] Compared to other forms of SFRP, the use of a nitroxide in NMP as a stable free radical is generally more efficient than the other types of compounds commonly employed, *e.g.* dithiocarbamates,[134,135] triazolinyl,[136] *etc*. Various other types of compounds such as nitrones[137,138] and nitroso compounds[139] have been investigated as possible reagents in controlled NMP. In SFRP, non-radical traps can also be used, such as thioketone[140] or phosphate,[141] in addition to using radical trapping species. The equilibrium constant in SFRP ($K_{eq}=k_{act}/k_c$, where k_c is the cross-coupling rate coefficient of the propagating radical species P· and the deactivating species) is generally very small (K_{eq} for styrene at 120 °C ~1.5 x 10^{-11}M).[121] Due to the fact that the values of the equilibrium constants are so low, when an excess of nitroxide is used, the equilibrium is strongly shifted to the dormant species and the polymerization rate is significantly decreased. In theory, the polymerization rate could be increased in NMP if the concentration of the deactivator, such as TEMPO, was decreased. This can be achieved by the addition of certain additives or initiating radicals to the system.[142-144] In the case of styrene (the monomer for which the first reactions of NMP were successful), the slow polymerization rate was never

a problem due to the thermal self-initiation of styrene, which subsequently contributed to the decrease of the deactivator species concentration.
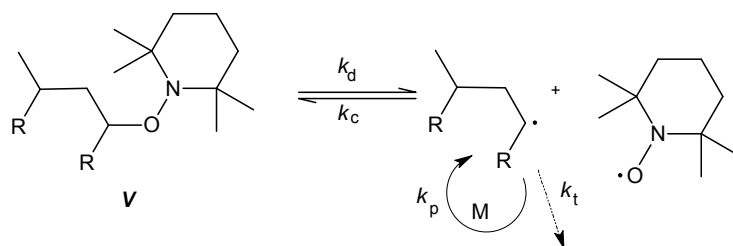
Scheme 2.1 **Nitroxide-mediated polymerization (NMP) using TEMPO (nitroxide) (*V*) as capping agent.**

Nitroxide radicals confer controlled behaviour on the system through rapid deactivation of propagating radicals, thereby shifting the equilibrium towards the dormant polymer chain. There are generally two mechanisms by which initiation is carried out. The first one generally provides better control over polymer molecular weight and architecture,[145] whilst the second is not successful in the polymerization of block copolymers. The two initiating mechanisms are either:

- through thermal decomposition (k_d) of an alkoxyamine such as TEMPO (or many of its derivatives) into a reactive radical and a stable radical – often referred to as unimolecular initiation,[145,146] or

- through the use of a radical source such as AIBN, BPO or γ-rays, as well as a radical trapping species (*e.g.* nitroxide radical) – often referred to as bimolecular initiation.

The kinetics are governed by the so-called "persistent radical effect" as explained by Fischer[147] (refer to Scheme 2.2). Once the initiating species (R$_0$-X) (*e.g.* alkoxyamine or conventional radical initiator) has dissociated (a), the reactive (transient) radical (R$_{i-1}$·) adds to monomer to start propagation (b). Initiation reactions in SFRP are slower than in ATRP and RAFT polymerization reactions. This leads to higher molecular weights than the expected theoretical molecular weights at lower conversions.[133] All transient radicals combine reversibly with the stable (persistent) radical (X·) which in turn reduces the concentration of propagating radicals in the system. The dormant species (R$_i$-X) is formed (c). The nitroxide species (X·) (persistent radical) is not sufficiently reactive to participate in propagation or termination, therefore as irreversible termination occurs between growing polymeric radicals (transient radicals) amongst themselves, the concentration of the persistent radical (nitroxide) progressively increases with time. Chain transfer reactions do not readily occur in NMP; instead the transient radicals undergo irreversible

23

self termination to form polymer products that are unable to react further (d). As a result of this self-termination of the transient radical, the nitroxide concentration builds up and causes the reaction to proceed via a single pathway, namely that of the coupling between the nitroxide and a polymeric radical.[71] This bimolecular termination between the persistent and transient radicals results in an excess of deactivating persistent radicals (nitroxides), which shifts the equilibrium in favour of the dormant species, resulting in a reduction of the polymerization rate, but a concurrent increase in the control of the molecular weight distribution of the polymer chains.

In terms of the structure of the nitroxide species, it is important that the C–O bond in the dormant nitroxide end-capped species be labile enough to easily dissociate and undergo propagation. A drawback to NMP is that, in many cases, high temperatures (T>100 °C) are required for polymerization to take place,[113] due to the high stability of the C–O bonds. It was for this reason that a search was carried out for alternative nitroxides; compounds with more labile C–O bonds were required so that lower temperatures could be used. Bulkier nitroxides provide lower dissociation energies, resulting in more radicals being produced and hence faster propagation rates.[73] The controlled polymerization of poly(butylacrylate) (PBA) at temperatures as low as 70°C has been made possible with the synthesis of a new type of bulky nitroxide.[71,148] Although, in general, bulky nitroxides seem to be more efficient at controlling various monomers, it is not so in the case of methacrylates.[149,150] Only the TEMPO nitroxide is readily available. Although, many nitroxide derivatives have been synthesized, the synthesis itself is not always facile and the derivatives may undergo many potential side reactions.[151]

$$R_0\text{-}X \underset{}{\overset{k_d}{\rightleftharpoons}} R^{\bullet}_{i\text{-}1} + X^{\bullet} \qquad (a)$$

$$R^{\bullet}_{i\text{-}1} + M \xrightarrow{k_p} R^{\bullet}_i \qquad (b)$$

$$R^{\bullet}_i + X^{\bullet} \underset{}{\overset{2k_t}{\rightleftharpoons}} R_i\text{-}X \qquad (c)$$

$$R^{\bullet}_i + R^{\bullet}_j \xrightarrow{2k_t} P_i + P_j \qquad (d)$$
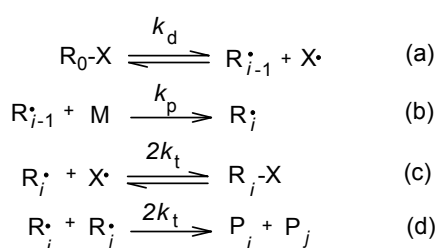
Scheme 2.2   **Reaction mechanisms for NMP based on the persistent radical effect (PRE).**

Many other nitroxide derivatives have been introduced since the advent of NMP and the list is very long, although the reader is encouraged to read a comprehensive review on this topic.[71] However, some selected nitroxides will be mentioned in this text. Nitroxide derivatives such as α-hydrido derivatives based on 2,2,5-trimethyl-4-phenyl-3-azahexane-3-oxy skeleton, (*VI*), have been reported for the controlled polymerizations of styrene,

acrylates, acrylamides and acrylonitrile.[152] Another α-hydrido-based alkoxyamine, (*VII*), derivative has been reported by Benoit *et al.*[153] in the successful controlled copolymerization of styrene and maleic anhydride in which they used 4-oxo-TEMPO (*VIII*) as the additional nitroxide-mediating agent. This compound, (*VIII*), has also been used for polymerizing acrylates at temperatures above 145°C .[94] The use of this nitroxide (*VIII*) was a significant improvement on the traditional TEMPO that was used, but PDIs were still quite broad (1.4–1.67).[154] The same group also reported that the use of reducing additives such as hydroxyacetone can be used to control the concentration of free nitroxide in systems using acrylates as the monomer.[155] This led to a significant increase in the rate of polymerization, however PDIs were still broad (1.4–1.95). Various authors[118,144,156-158] have reported on the successful LRP of various monomers using N-*tert*-butyl-*N*-(1-diethylphosphonate-2,2-dimethylpropyl) nitroxide (named SG1) (*IX*), a phosphonate derivative. For example, Benoit *et al.*[159] reported on the controlled LRP of acrylates in which they used SG-1 to give a PDI of about 1.11. The same compound (*IX*) was used by Phan *et al.*[160] in the synthesis of PBuA as well as gradient copolymers of methyl methacrylate (MMA)/*N,N*-dimethyl acrylamide (DMA). Not only did SG-1 provide control over the polymers that were synthesized, but this nitroxide led to faster propagation than any other nitroxide used thus far.[118]

Advances in SFRP and NMP have allowed a wider scope of monomers to be polymerized in a controlled manner, particularly *di*-substituted alkenes such as methyl methacrylate. In a recent article by Nicolas *et al.*,[161] the successful LRP synthesis of MMA was reported in which a small amount of styrene was added to the contents.[162] Styrene homopolymers and copolymers,[113,151,163-165] as well as methacrylic derivatives[166] and 4-vinylpyridine,[167-169] have shown living polymerization features.[93] Generally, disadvantages associated with using SFRP or NMP are the difficulty in introducing chain-end functionalities and the need to use equimolar quantities of the nitroxide species or its precursor. Future work in NMP is still important, as nitroxides which would allow polymerizations to occur at lower temperatures would be a great advantage. Also, monomers such as methyl methacrylate and vinyl acetate, can to date, not yet be polymerized in a controlled manner by NMP. Certainly, the search for new nitroxides which can control the polymerization of these types of monomers will be an invaluable success.[124]
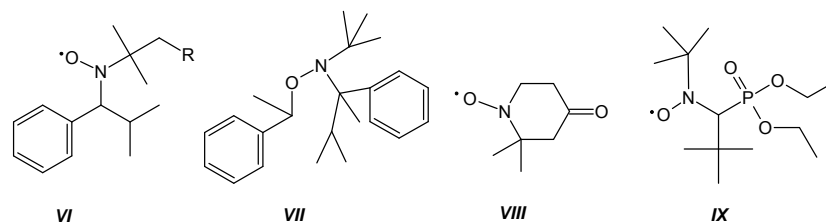
Figure 2.3   Nitroxide derivatives used in NMP techniques.

2.6.1.2   Atom transfer radical polymerization (ATRP)

ATRP (Scheme 2.3) is defined as the reversible abstraction of a halogen atom between the active (radical) and dormant (temporarily halogen end-capped) functional chain ends.[133] It has its roots in the organic synthesis reaction atom transfer radical addition (ATRA).[170] ATRP was discovered independently in 1995 by two scientists, namely, Matyjaszewski[101,171] and Sawamoto,[172] who preferred to call it by different names (although the same mechanism was involved); Matyjaszewski referred to it as ATRP, whilst Sawamoto referred to it as transition metal-catalyzed radical polymerization. Compared to the other forms of LRP, ATRP is more complex due to the transition metal complex, often a heterogeneous catalytic system, which is used.[173] Initiation may take place by means of thermal, chemical or photochemical stimuli of the dormant initiator species (typically an alkyl halide species) after which the transition metal catalyst abstracts the halogen atom from the initiator (*R-X*). Typical metals that have been investigated include copper,[174-176] ruthenium,[177] nickel,[178] palladium,[179] rhodium,[180] rhenium[181] and iron.[182,183] The catalyst is oxidized when the halogen is transferred and a radical is generated, thereby allowing the polymer chain to grow.

To achieve controlled polymers, the process of initiation, as well as deactivation, must be fast to keep the PDI narrow. For rapid deactivation there must be a drastic reduction in the concentration of the active radicals at any given moment. In ATRP, kinetics is governed by the PRE as well as the transition metal complex (TM(I)/L). The polymerization rate increases as the amount of activator increases and is dependent on the ratio of [activator]:[deactivator].[73] As the number of radicals in the system increases, so the concentration of the oxidized metal-containing halide (deactivator) increases, the equilibrium is shifted to the dormant species and the catalyst is regenerated by reduction of the oxidized transition metal complex. This activation/deactivation cycle is reversible. Molecular weights are dependent on the initiator concentration and not on the transition metal concentration.[73] Reverse ATRP has also been reported for the successful synthesis of polymers using copper-based homogeneous[184] and heterogeneous[185] systems in solution and emulsion[186] as well as with iron complexes.[187] Reverse ATRP makes use of a conventional radical initiator, such as AIBN, with the transition metal in its higher oxidation

state (*e.g.* CuBr$_2$(dNbpy)$_2$). The advantage of this type of system is that the components used are not extremely sensitive to oxygen (compared to ATRP), therefore they can easily be prepared, stored *etc*. The disadvantage of reverse ATRP is that (high purity) block copolymers cannot be synthesized, although this can be overcome with the use of both conventional radical initiators as well as halogen-transferable initiators. This process is referred to as simultaneous normal and reverse initiation ATRP.[188,189]

ATRP has proved to be a more accessible technique than NMP with regards to the range of monomers that has been polymerized.[173] It is however restricted with regard to protonated monomers and those with anhydride functionalities, although some acidic monomers have been reported to show good living behaviour.[190] A disadvantage of the ATRP system is that a metal catalyst is used in the polymerization process. It is often essential that this metallic species be removed from the final product prior to end-use of the polymer in consumer products. This has posed numerous problems, although some success has been achieved in removing the metal.[173,191-193] ATRP is moderately sensitive to oxygen and will not necessarily reduce target molecular weights as small amounts of oxygen will be scavenged by the catalyst, which is present in a much higher concentration than the propagating radical.[194] However, it has been reported that trace amounts of oxygen can have a negative effect on the polymerization rate compared to conventional radical polymerization.[195] This is most probably due to the oxidation of the catalyst, thereby decreasing its concentration and subsequent polymerization rate. [173] The advantages of ATRP include the wide range of temperatures that can be used, the possibility of creating end-group functionality, the ability to produce block copolymers in any order (compared to RAFT polymerizatioin in which certain monomer combinations require a selective first block), as well as the absence of the Trommsdorf effect.[73]

Scheme 2.3   **ATRP mechanism. (R-X) = alkylhalide initiator; TM = transition metal, ((I) and (II) represent the different oxidation states of the transition metal)).**

2.6.2   Degenerative transfer processes

Systems operating under degenerative transfer processes do not obey the PRE and, unlike those systems that do, the formal equilibrium constant should be unity. The kinetics of degenerative transfer systems follows that of radical polymerization (where a steady-state is achieved through initiation and termination reaction rates being identical). The polymerization rate is (classically) proportional to the square root of the initiator concentration. Control of the polymer is provided by the transfer agent, in which the rate of exchange (k_{ex}) ($k_{ex}=k_{add}/k_{-add}$) must be faster than k_p in order for there to be good control. The growing radical undergoes exchange processes with the transfer agent via either atom/group transfer (*e.g.* alkyl iodides),[84,110,109] via addition-fragmentation with unsaturated poly(methacrylates),[196,197] or via dithioesters and related compounds (known as the RAFT process). The latter approach is used more frequently than both of the former processes, due to the fact that the polymers produced via this approach generally display narrower PDIs. In the case of using alkyl iodide transfer, the reasons for its poorer success is due to the fact that these transfer agents have smaller rate coefficients of addition relative to the rate coefficients of propagation, which results in polymers with broad PDIs.[109] Only the RAFT process will be discussed under degenerative LRP mechanisms.

2.6.2.1   Reversible addition-fragmentation chain transfer (RAFT) polymerization

RAFT (refer to Schemes 2.4 and 2.5) polymerization makes use of a thiocarbonylthio moiety, which reversibly transfers itself between the active growing polymeric radical end-capped chains, however the concentration of these radicals is very low at any point. The process involves the insertion of monomer units between the weak C–S bonds. Initiator radicals are formed after the decomposition of the initiator, which can either add to monomer (step I in Scheme 2.5), or undersirably to the CTA ((2) in Schemes 2.4 and 2.5). Polymeric radicals formed from the initiator species can then add to CTA (2) with rate coefficient k_{add} to form an intermediate radical species ((3) in Schemes 2.4 and 2.5). In RAFT polymerization, it is desirable to achieve fast rates for addition of a given radical species to the C=S double bond. This can be achieved by ensuring the chosen Z group has a stabilizing effect on the intermediate radical. This intermediate radical (3) can then either fragment to form the original polymeric radical (1) (with rate coefficient k_{-add}, or undergo β-scission to produce the first polymeric CTA ((4) in Schemes 2.4 and 2.5) whilst at the same time releasing the leaving group radical (R·) ((5) in Schemes 2.4 and 2.5) (rate coefficient $k_{-β}$) (step II). Fast fragmentation of the intermediate radical species (producing R·) relative to the rate of propagation is desired in RAFT polymerization systems and can be achieved when choosing a R group that is inherently a good free

radical leaving group and is efficient at reinitiating polymerization. If the leaving group radical (5) is a good re-initiator of monomer, a polymeric radical species ((6) in Scheme 2.5) will be formed (step III in Scheme 2.5) which can in turn add to the first polymeric CTA agent ((4) in Schemes 2.4 and 2.5) to form another type of intermediate radical ((7) in Scheme 2.5). After all the original CTA (2) is consumed (step II in Scheme 2.5), the main equilibrium (step IV in Scheme 2.5) in RAFT processes is reached. This self-regulating process continues for the life of the monomer (or for as long as radicals are present). The rate coefficients of addition (k_{add}) and fragmentation ($k_{-\beta}$) depend on the chemical nature and chain length of the radicals.[198]

The CTA (simple or macroCTA) that is used plays the role of the dormant species (the oxidized transition metal complex and the nitroxide in the case of ATRP and NMP respectively).[73] The concentration of CTA is much larger than that of the radical initiators to avoid the possible termination of initiator derived radicals, hereby ensuring that the majority of chains contain the thiocarbonylthio moiety and undergo activation/deactivation processes. The final polymeric product contains the thiocarbonylthio moiety, and it is this functionality which allows the polymer to act as a dormant CTA that can participate further in the synthesis of block copolymers. The disadvantages of polymers containing the thiocarbonylthio moiety include a characteristic sulfur odour as well as discolouration of the product (ranging from violet to red to pale yellow). For these reasons, several methods for the removal of the thiocarbonylthio end-group have been attempted.[199-202] Further disadvantages of the RAFT process include the cumbersome synthesis and stability of the transfer agent, as well as the possibility of the intermediate radical species undergoing side reactions. See Section 2.8 for a detailed description of the RAFT process.
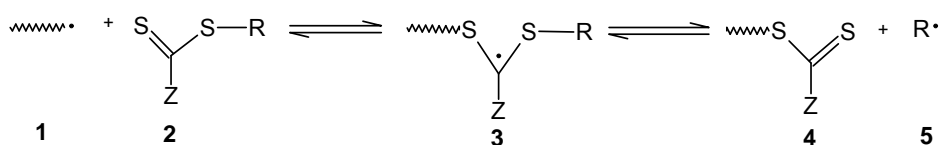
Scheme 2.4   **RAFT mechanism - simplified (Z = stabilizing group, R = leaving group).**

2.7   Comparison of LRP to conventional radical polymerization

As is the case with LRP, conventional radical polymerizations are chain reactions involving radical species which are responsible for the steps common to both systems, namely initiation, propagation, transfer and termination. In addition to this, the same solvents, initiators, temperatures, and monomers may be used.[203] LRP and conventional

radical polymerizations proceed via the same radical mechanism and, for both types of systems, bulk, solution, suspension and emulsion reaction systems may be used. The major difference between these types of systems is that with LRP systems a thiocarbonylthio chain transfer agent is used, which allows control over the molecular weights targeted, the PDI as well as the macromolecular architecture of the polymer chains.[54,103,204] This transfer agent is responsible for the deactivation of the active radical into the dormant state, hereby allowing the chains to still remain 'alive' after the reaction is completed. Although similar conditions, monomers and processes may be used for both LRP and conventional radical polymerizations, the mechanisms of these systems are quite different. Conventional radical polymerizations involve slow initiation and lots of termination reactions, producing many dead chains at any point in the reaction, whilst in all LRP there is virtually a negligible amount of termination reactions, producing chains that remain 'alive' after they have undergone propagation.

Conventional radical polymerizations are considered to be non-living due to irreversible termination reactions and chain transfer reactions. This implies that once radicals have terminated with each other they have no means of being reinitiated to further chain growth. One also does not have accurate control over the macromolecular structure obtained. With conventional radical polymerizations, depending on the system, the PDI becomes broader over time and usually the $\overline{M}_n$ is very high during the beginning stages of the polymerization and decreases as monomer is consumed. Another drawback to conventional radical polymerization systems is that one cannot control chain-end functionality.

Conventional radical polymerization reactions are tolerant to many impurities, including oxygen. Compared to LRP, initiation is relatively slow with regards to propagation, and propagating species react with each other, leading to termination reactions throughout the polymerization. Due to the short lifetime of radicals, the growing polymeric chains too have short lifetimes, resulting in a broadening of the distribution of chain lengths. Also, with radical polymerization, one is able to achieve very high molecular weights in a relatively short time compared to LRP. In LRP systems, the cumulative lifetime over which the polymer chains remain in their active state ($P_n\cdot$) is far shorter than for those found in radical systems.[54] In LRP, molecular weight is directly proportional to the conversion of monomer since all chains are growing at the same rate. The initiation rate is almost instantaneous and is usually much faster or similar to the propagation rate, hereby allowing control over the oligomeric chains fairly early on in the reaction. If the rate of initiation is much slower compared to propagation then polymers with broad molecular

weight distributions will result.[205] The relatively fast process of deactivation in LRP leads to a low concentration of active radical species (low radical flux) which in turn contributes to the longer polymerization times compared to radical polymerization. This regulated growth is due to the presence of the CTA which allows the polymer chains to grow simultaneously. In radical systems the concentration of radicals at any one point in time is very high (high radical flux), ultimately increasing the chances of radicals finding each other and terminating to form single chains, which may effectively double the size in molecular mass. Similarly, because of the high concentration of radical species in conventional radical polymerization systems, propagation and termination steps occur rather rapidly, allowing polymerizations to reach high conversions quickly in comparison to LRP. Also, since conventional radical polymerization systems are active and do not have to be "reactivated", as a LRP system does, polymerization times are reduced.

The description of LRP as *living* implies that termination is negligible, thus allowing the growing chain ends to remain active after polymerization is complete. In other words, these polymers can be used in chain extension reactions or as precursors for the formation of block copolymers upon addition of further monomer.[43,47,105,107,206-208] Bimolecular termination is minimized as a result of the low radical flux brought about by the introduction of dormant states for the growing polymeric species. These dormant states can be achieved by either reversible termination or reversible transfer processes. With LRP systems, a narrow PDI can be obtained by the presence of a deactivating agent and the number-average molecular weight, which increases with time, can be predetermined. In order to further ensure control of the polymerization it is important that the initiation step is fast compared to propagation and termination so that all the chains can be initiated at the same point and have a better chance of growing at the same rate. Due to the fact that in LRP the entire propagation step takes approximately 1 second, chain-end functionality may be introduced into the polymer chains and various macromolecular structures may be synthesized.[209] These structures can also be synthesized by radical polymerizations, but not with the same degree of control or degree of functionality as can be achieved with the living techniques. Carboxyls, amines, double bonds and halogens are examples of functional groups that can be incorporated into the polymer either at the beginning, in the middle, or at the end(s) of the chain, between blocks, or evenly spaced along the polymer backbone.

2.8   The RAFT process

The RAFT process is one of the most versatile LRP methods by which polymers with well-controlled architectures can be made. Compared to the other LRP techniques, RAFT is

the most versatile LRP technique[54,86] as it is tolerant to a wider range of monomers such as acids (*e.g.* acrylic acid),[210] acid salts,[211,212] tertiary amino groups (*e.g.* 2-(dimethylamino)ethyl methacrylate)[213] as well as hydroxy groups (*e.g.* hydroxyethyl methacrylate). [214] The difference between RAFT polymerization and that of the other two LRP described earlier, namely SFRP and ATRP, is that in degenerative transfer systems such as RAFT polymerization, the PRE does not exist. A steady state of radicals is produced via initiation and termination reactions, as in conventional radical polymerizations. The first work described using this type of system involved xanthate esters and was referred to as macromolecular design by interchange of xanthate (MADIX). MADIX and RAFT polymerization follow the same mechanism and differ only in the polymerization mediator used.[106] The first time that RAFT polymerization was referred to as a *living* system was seen in the patent of Le *et. al.* published in 1998.[104]

The mechanism of RAFT polymerization (Scheme 2.5) involves the same steps as conventional radical polymerizations, namely initiation, propagation, transfer and termination, although in RAFT polymerization the propagation step is more detailed compared to that in conventional radical systems. RAFT polymerization has two additional steps, the pre-equilibrium and core equilibrium steps, in order to slow down the polymerization and produce controlled architectures.[215] The pre-equilibrium step is responsible for the transformation of the CTA into a macroCTA compound, whilst the core equilibrium is responsible for the sequential and uniform addition of monomer units to the macroradical CTA in order to control the PDI of all the chains. These two processes are independent of each other. The various steps are described below (refer to Scheme 2.5 for label designations):

Step I: Initiation involves the decomposition of an external source of radicals, such as 1,1'-azobis(isobutyronitrile) or 2,2'-azobis(isobutyronitrile) (AIBN), which are commonly used initiators in RAFT polymerization systems. These radicals then add monomer units to form a propagating polymeric radical (P_n·) (1), or, which is undesirable, replace the R group (5) on the CTA (*i.e.* the initiator radicals may also react directly with the CTA before reacting with the monomer).

Step II. The propagating radical species (P_n·) (1) undergoes a reversible chain transfer step with the CTA (2). During this step an intermediate radical is formed (3). It is important that the leaving group (R) be chosen as to be easily displaced in favour of forming the polymeric thiocarbonylthio compound (4) ($k_{-\beta} > k_{add}$), *e.g.* R must be a good homolytic leaving group.

Step III. The leaving group (R·) (5) should be able to reinitiate polymerization (k_{ri}) with further monomer units to form a new propagating radical ($P_n·$) (or, when all monomer is consumed, reversibly react with the polymeric thiocarbonylthio compound) (4) (step IV).

Step IV. This is the main equilibrium phase in which the polymeric thiocarbonylthio compound (4) is the only CTA species present (initial CTA has been completely consumed). Rapid activation (k_{-add}) and deactivation (k_{add}) of polymeric radicals between active and dormant chains allows regular additions of monomer units to growing polymer chains (k_p), ensuring a narrow PDI.

Step V. Termination reactions will always be present in free radical systems, either by combination (k_c) or disproportionation (k_d). However, since the concentration of radical species in controlled systems is kept to a minimum, the vast majority of chains are initiated by the CTA re-initiating group (R·) and end-capped with the thiocarbonylthio group. The termination constant $<k_t>$ is chain length dependent and decreases during the polymerization to reach a steady rate of polymerization. As the monomer concentration decreases with conversion, the propagation rate will decrease, but termination and other side reactions may still persist at the same rate, and depends on both the initiator conversion to radicals as well as the efficiency of these radicals to add monomers.

Step I. Initiation

Step II. Pre-equilibrium: Formation and fragmentation of Intermediate radical species

Step III. Re-initiation

Step IV. Pre-equilibrium

Step V. Termination
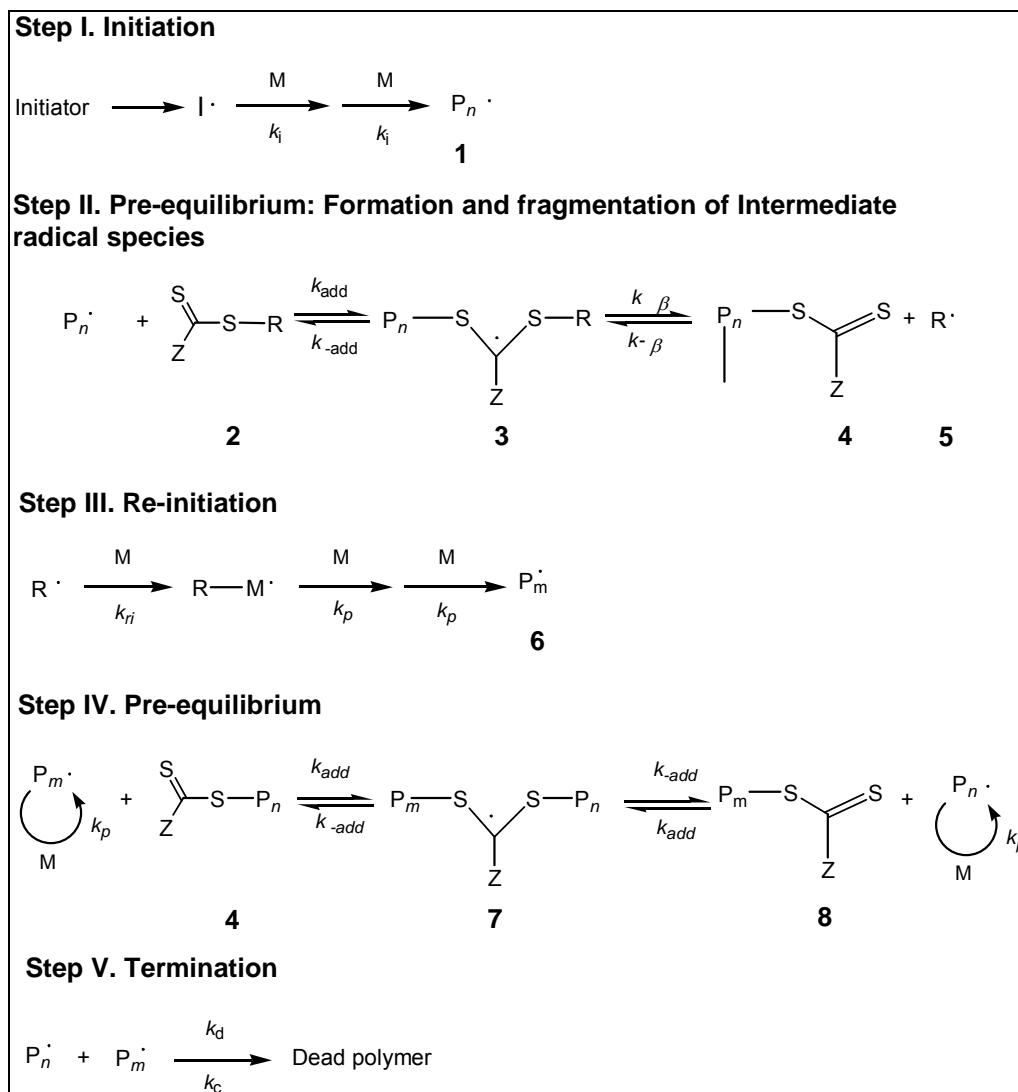
Scheme 2.5. Mechanism of RAFT polymerization (Z = stabilizing group; R = leaving group).

2.8.1 Variables to consider in RAFT

The most important variables to consider when using RAFT polymerization include choice and molar ratio of initiator, CTA and monomer.

2.8.1.1 Initiator

In RAFT polymerization, the initiator is very important for contributing to theoretical and experimental molecular weights corresponding. Essentially, every initiation event results in a termination event. The greater the concentration of initiator used in comparison to the concentration of CTA used, the lower the experimental molecular weight of the chains compared to the theoretical molecular weight (equation (2.13)). This is due to a higher rate of termination taking place as a result of the higher concentration of radicals present.

This would result in termination reactions being favoured in comparison to reactions involving only one radical species (propagation or addition-fragmentation reactions).[107] In addition, a higher initiator concentration would broaden the molecular weight distribution (due to the higher radical flux which could result in termination and transfer reactions). On the other hand, higher initiator concentrations lead to faster rates of polymerization[216,217] (dependent on the square root of initiator concentration). Multifunctional initiators or CTAs hold the key to the synthesis of a variety of macromolecular architectures, such as stars.

2.8.1.2   Chain transfer agent (CTA)

A wide variety of CTAs have been used to date, namely dithioesters (C-functional Z groups),[35,36,103,105,108,218-220] trithiocarbonates (S-functional Z groups),[16,43,219,221,222] dithiocarbamates (N-functional Z groups)[44,223-225] and xanthates (O-functional Z groups)[44,226-230]. Trithiocarbonate and aliphatic dithioester CTA agents have greater hydrolytic stability that their dithiobenzoate counterparts and are also known to contribute to less retardation in the system.[107,231] The choice of CTA depends on the monomer being used; the functionality can allow some to be more effective than others. This is mainly due to the type of substituents found on the CTA, namely the leaving group and the stabilizing group. Z and R groups are important for the effectiveness of the RAFT process and should therefore be carefully selected in order to provide control.[232]

A large variety of R and Z groups have been used interchangeably, to form CTAs that are applicable to a wide variety of monomers, hereby making RAFT polymerization a more versatile polymerization method than the other LRP techniques.[106] Control of the polymer is generally provided by the CTA. In order to ensure that most of the polymer chains are end-capped with the thiocarbonylthio moiety it is important to use a large concentration of CTA relative to initiator.[107] A high concentration of CTA will prevent a large amount of radicals, particularly early on in the reaction, from bimolecular termination, which would lead to fewer chains containing the thiocarbonylthio moiety than expected. The polymerization rate can however be retarded by the concentration of CTA used,[107,217] and is heavily dependent on the nature of the Z group.[233] A greater percentage of thiocarbonylthio-terminated chains may also be achieved when using CTAs with a high chain transfer constant, C_{tr}. This ensures that the CTA is consumed fairly early on in the reaction, ensuring that the majority of chains are grown from these initiating species, rather than from radicals as a result of initiator decomposition. This would further ensure a narrower PDI due to the fact that there is not an extended period over which initiator chains are produced and propagating with monomer instead of CTA. The C_{tr} for various thiocarbonylthio compounds span more than five orders of magnitude depending on the Z and R groups as well as the monomer being polymerized.[234] It is generally believed that

in order to obtain low PDIs, transfer agents with transfer constants greater than 2 should be used.[235,236]

Inhibition can also occur in RAFT polymerizations and is also influenced by the nature of the CTA, particularly the R group. It is important that the leaving group be a good homolytic leaving group so that the intermediate radical (3) favours fragmentation in the direction of the product (4). In other words, the choice of leaving group (R group) should be one which is easily fragmented yet is able to re-initiate polymerization.[107] Generally, steric factors, radical stability and polar factors all play an important role in determining the leaving group ability of the R group (the more stable, bulky and electrophilic, the better it performs as a leaving group).[237] The S-R bond is generally a very weak bond therefore it is fairly labile. Examples of effective R groups include cyanoisopropyl and cumyl functionalities. Numerous research groups have studied the effect of the R group on a variety of monomers.[36,107,125,206,216,238] Chong *et al.*[237] performed a study on the effect of the R group on several monomers including methyl methacrylate, styrene, methyl acrylate and butyl acrylate, and they were able to find evidence supporting the theory that certain radical species do not have a high enough C_{tr}, in the case of certain monomers in order to promote a narrow PDI, characteristic of a living polymerization system. They found that in the case of methyl methacrylate, the R group of the CTA plays a very strong role in determining the effectiveness of the system.

Retardation has been observed in many dithioester-mediated polymerizations, and there are two main, yet opposing, explanations provided for this phenomenon. The CAMD research group,[239] assumes that slow fragmentation of the intermediate radical is the reason for rate retardation as this radical is stable enough to cause no termination with P• (no cross-termination). The other school of thought on this subject matter was proposed by Monteiro *et al.*[207] who noted the production of a tripled molecular weight species in a monomer-free model experiment with a UV-irradiated polystyryl dithiobenzoate. These authors[240] then assumed that the reason for retardation is that the macroCTA radical ((7) in reaction step IV in Scheme 2.5) may undergo self-termination and termination with free macroradicals, thus slowing down the rate of polymerization at enhanced levels of initial RAFT agent (*i.e.* cross-termination). Numerous studies have also been performed on the effect of the stabilizing group [107,221,231,238,241,242] and it has been determined that it affects the rate of addition of radicals to the reactive C=S bond on the CTA. The Z group should activate the C=S bond towards radical addition. The Z group also plays a role in modifying the fragmentation rates and stabilizes the intermediate radicals ((3) and (7) in Scheme 2.5) formed when the propagating radical is added to the CTA (2). Generally it is more acceptable for certain applications to include the desired functionalities within the

R group rather than the Z group due to the labile nature of the C–S bond of the latter end-group.[202]

At this point it is important to consider the equilibrium between the active propagating radical species ($P_m \cdot$ and $P_n \cdot$) and the dormant polymeric thiocarbonylthio compounds (8). In order to ensure a narrow PDI it is important that there is a rapid deactivation between the active propagating radicals and the dormant polymeric thiocarbonylthio compounds. There is the possibility of retardation occurring when the intermediate radical species ((3) and (7)) is formed. If k_{add} is fairly small or if re-initiation of polymerization is slow relative to propagation, then there is a likelihood that side reactions, between the intermediate and/or re-initiating radical occurs, thus retarding the rate of polymerization.[237] This is more likely to occur when higher concentrations of CTA are used, or monomer concentration is very low.[107]

Retardation and inhibition are important processes that occur in numerous polymerization systems and the extent of research into the mechanism behind these processes is vast.[107,239,240,243] Certain CTAs, such as cumyl dithiobenzoate (CDB) and *tertiary*-butyl dithiobenzoate (*t*BDB), are known to show high levels of retardation during the polymerization of certain monomers such as butyl[244] and methyl acrylate,[245] methacrylates and styrene.[107,216] The latter two are particularly more prone to retardation in polymerization rates when higher concentrations of CDB are used.[216] When lower concentrations of CTA are used an inhibition period may be observed, which is due to the consumption of the initial CTA. Inhibition periods are more notable with CTA that have low C_{tr}, such as benzyl dithiobenzoate.[237]

2.8.1.3   Monomer

Each monomer has its own chain transfer constant (k_{tr}). Impurities in monomers can act as inhibitors or retarders which in turn can retard and inhibit the reaction and cause irreproducible polymerization rates amongst identical reactions. If this is/was the case then excess initiator may be used to compensate for these impurities which act as radical scavengers. Monomers with groups that confer resonance and/or polarity (*e.g.* vinyl chloride, vinyl acetate, styrene, (meth)acrylamides, *etc.*) are more reactive than those that do not possess such groups. The reason for this is that the driving force is in the direction to expel the radical as it is very stable in this form due to the resonance or polarity directed upon it. These monomers generally require lower temperatures to undergo radical polymerizations.

2.8.2 Removal of thiocarbonylthio end-groups in RAFT polymers

Various methods for the removal of the thermally and photochemically unstable dithioester moiety (C=S) end-group in RAFT synthesized polymers have been investigated to varying degrees of success. The removal of this unstable moiety from the polymer chain end allows the introduction of a wide range of chain-end functionalities to the polymers.

There are generally three accepted methods which include:

1) radical-induced reduction (to provide a hydrocarbon end-group)
2) thermal elimination (to provide an unsaturated end-group)
3) reaction with a nucleophile, such as a hydroxide (to provide a thiol end-group)

2.8.2.1 Radical-induced reactions

The ease with which thiocarbonylthio groups undergo radical reactions through addition-fragmentation (via formation of an intermediate radical species) makes this method of end-group removal possible. A hydrogen donor (H–X) compound is used, which transfers a hydrogen atom to the propagating polymeric radical released after fragmentation of the polymeric CTA agent. Work by Postma *et al.*[201] involved the removal of the trithiocarbonate end-group to produce inert hydrocarbon PSt chain ends. They used a series of reducing agents which included (trimethylsilyl)silane, AIBN and tributylstannane. They showed that only the latter acted as an effective reducing agent as the former displayed characteristics of a high molecular mass shoulder on the SEC chromatograms. These high molecular mass shoulders were attributed to either incomplete reduction or competition between the silane reduction of the intermediate polystyryl radicals and that of other radical-radical coupling reactions that may have led to termination reactions. Other authors have published similar results in which the trithiocarbonate or dithiobenzoate end-group was successfully removed from PSt,[202] PMMA[202] and poly(acenaphtalene)[246,247] using tributylstannane as reducing agent. Other reducing agents have also been reported to be as effective in the removal of thiocarbonylthio end-groups, namely hypophosphite salts, in particular *N*-ethylpiperidine hypophosphate.[199] The advantage of these above the stannane and silane H-donors is that they are less toxic and the by-products produced from these reactions are water-soluble therefore they can easily be removed when using hydrophobic polymers such as PSt and PMMA.

Perrier *at al.*[200] proposed the use of a large excess of AIBN to the thiocarbonylthio end-capped polymer in which a radical exchange process takes place in order to remove the end-group. It was found that this process worked much better for PMMA than for PSt as the PMMA propagating radical is a very good leaving group, approximately 100 fold better than for the PSt propagating radical. For both acrylic and styrene polymers a very large excess of AIBN is required and end-group removal is still difficult to achieve.

2.8.2.2 Thermolysis

Thermolysis of thiocarbonylthio terminated polymers leads to olefinic products as well as derivatives of the CTA used. The advantage of thermolysis compared to other processes in which these end-groups can be removed is the fact that no chemical treatment is involved. The only requirement is that the polymer and its functionality are stable under thermolysis conditions.[201] The thermolysis of trithiocarbonate PBuA and PSt was achieved at temperatures between 210°C–250°C by Davis *et al.*[248] They concluded that this method would work equally well for other CTA functionalities such as xanthates and dithioesters. Postma *et al.*[201] investigated the thermolysis of trithiocarbonate end-capped PSt at 200°C, under nitrogen, in which they concluded effective removal of the end-groups. The thermal decomposition of a series of dithioester compounds was investigated by Xu *et al.*,[249] amongst them a PMMA end-capped dithioester. It was concluded that thermal decomposition of PMMA end-capped with this dithioester functionalities resulted in decomposition temperatures (120°C, according to DSC onset at 65°C) far below the usual thermolysis temperatures reported in the literature (210°C–250°C). Therefore, the thermal

decomposition of living chains in PMMA RAFT polymerizations cannot be ignored as this would result in rate retardation, polymers with higher molecular weights than predicted as well as broader molecular weight distributions. However, the same authors found that the polymerization of styrene did not display the same problems as with MMA at temperatures of 90°C, although at 60°C the styrene polymerizations mediated with cumyl dithiobenzoate (CDB) displayed the same retardation and molecular weight distribution broadening effects as did PMMA mediated with CDB. Further work by other research groups included the successful thermolysis of a PSt chain containing a *bis*-RAFT agent that was successfully cleaved in half, indicating that both of the trithiocarbonate functionalities reacted equally during the polymerization.[202]
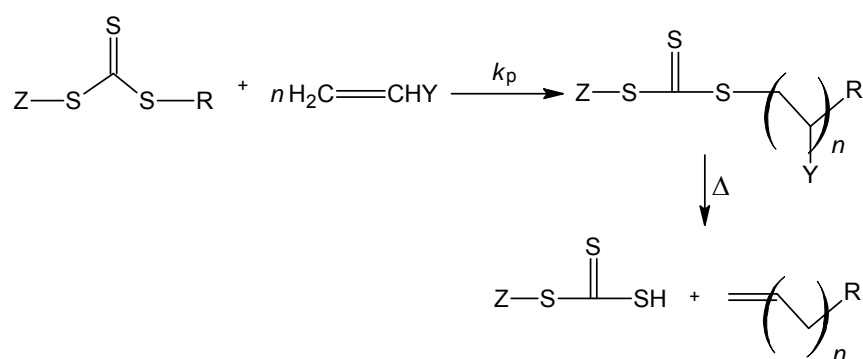
2.8.2.3   Reaction with nucleophiles

Nucleophiles are compounds that have an affinity towards protons. Various amines [43,250256] (via aminolysis), hydroxides[224,252,257] (via hydrolysis) and borohydride[258-260] have been successfully used to cleave the thiocarbonylthio bond in various polymers synthesized via RAFT polymerization. Unsuccessful cleavage of a polystyrene chain containing a *bis*-RAFT agent was reported by Moad *et al.*,[202] using piperidine as the nucleophile. A bimodal distribution appeared in the SEC with a small peak on the high molecular weight side. It was suspected that oxygen had entered the reaction flask, causing the initially formed thiol to undergo oxidative coupling to produce a disulfide compound.
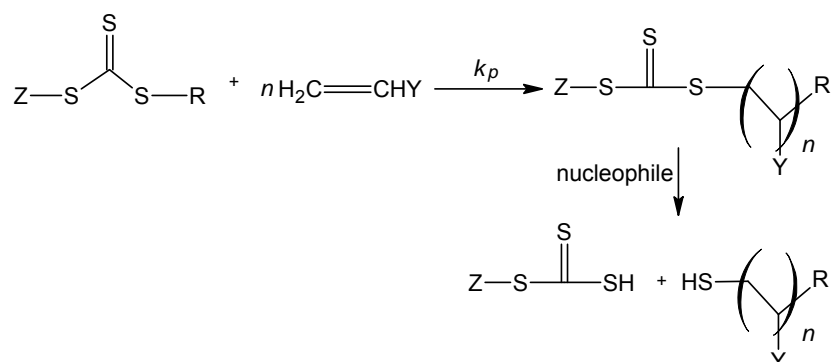
2.9 Conclusion

The author introduced this chapter by providing the reader with a brief history and summary of radical polymerizations, followed by three steps that take place in chain polymerizations (conventional radical polymerizations and LRP), namely, initiation, propagation, transfer and termination. In addition to this, various process conditions in which conventional polymerization, as well as LRP, which may be used with these techniques were detailed, *e.g.* suspension, bulk *etc.* After bringing it to the attention of the reader that there is an on-going debate amongst scientists in the LRP field as to whether or not such techniques should be referred to as either "living", "controlled", or both, the author proceeded to describe living anionic polymerization. The remainder of the chapter focused on explaining and comparing the mechanism of three LRP techniques, namely, NMP, ATRP and RAFT polymerization, with the most emphasis placed on the latter technique as this was the choice of polymerization for the syntheses in the following chapters. Finally, the chapter concluded with a short summary of three techniques in which the thiocarbonylthio end-groups in polymers, synthesized by RAFT polymerization, can be removed.

References

(1) Bielawskia, C. W.; Grubbs, R. H. *Prog. Polym. Sci.,* **2007**, *32,* 1.

(2) Webster, O. W. *Science,* **1991**, *251,* 887.

(3) Domskia, G. J.; Rosea, J. M.; Coatesa, G. W.; Boligb, A. D.; Brookhart, M. *Prog. Polym. Sci.,* **2007**, *32,* 30.

(4) Leibler, L. *Prog. Polym. Sci.,* **2005**, *30,* 898.

(5) Dreyfuss, M. P.; Dreyfuss, P. *Polymer,* **1956**, *6,* 93.

(6) Swarzc, M. *Nature,* **1956**, *176,* 1168.

(7) Swarzc, M.; Levy, M.; Milkovich, R. M. *J. Am. Chem. Soc.,* **1956**, *78,* 2656.

(8) Bawn, C. E. H.; Bell, R. M.; Ledwith, A. *Polymer,* **1965**, *6,* 95.

(9) Boschetti-de-Fierro, A.; Muller, A. J.; Abetz, V. *Macromolecules,* **2007**, *40,* 1290.

(10) Stewart, I. C.; Lee, C. C.; Bergman, R. G.; Toste, F. D. *J. Am. Chem. Soc.,* **2005**, *127,* 17616.

(11) Chaffey-Millar, H.; Stenzel, M. H.; Davis, T. P.; Coote, M. L.; Barner-Kowollik, C. *Macromolecules,* **2006***,* 6406.

(12) Baek, K.-Y.; Kamigaito, M.; Sawamoto, M. *J. Polym. Sci. Part A: Polym. Chem,* **2002**, *40,* 2245.

(13) Lord, H. T.; Quinn, J. F.; Angus, S. D.; Whittaker, M.; Stenzel, M. H.; Davis, T. P. *J. Mat. Chem.,* **2003**, *13,* 2819.

(14) Stenzel, M. H.; Davis, T. P. *J. Polym. Sci. Part A: Polym. Chem.,* **2002**, *40,* 4498.

(15) Stenzel-Rosenbaum, M.; Davis, T. P.; Chen, V.; Fane, A. G. *J. Polym. Sci. Part A: Polym. Chem.,* **2001**, *39,* 2777.

(16) Boschmann, D.; Vana, P. *Macromolecules,* **2007**, *40,* 2683.

(17) Bosman, A. W.; Vestberg, R.; Heumann, A.; Frechet, J. M. F.; Hawker, C. J. *J. Am. Chem. Soc.,* **2003**, *125,* 715.

(18) Yang, J. C.; Mays, J. W. *Macromolecules,* **2002**, *25,* 3433.

(19) Baum, M.; Brittain, W. J. *Macromolecules,* **2001**, *35,* 610.

(20) Barner, L.; Li, C. e.; Hao, X.; Stenzel, M. H.; Barner-Kowollik, C.; Davis, T. P. *J. Polym. Sci. Part A: Polym. Chem,* **2004**, *42,* 5067.

(21) Baskar, G.; Landfester, K.; Antonietti, M. *Macromolecules,* **2000**, *33,* 9228.

(22) Matyjaszewski, K.; Teodorescu, M.; Miller, P. J.; Peterson, M. L. *J. Polym. Sci., Part A: Polym. Chem,,* **2000**, *38,* 2440.

(23) Sedjo, R. A.; Mirous, B. K.; Brittain, W. J. *Macromolecules,* **2000**, *33,* 1492.

(24) Pyun, J.; Kowalewski, T.; Matyjaszewski, K. *Macromol. Rapid Commun.,* **2003**, *24,* 1043.

(25) Bernard, J.; Favier, A.; Davis, T. P.; Barner-Kowollik, C.; Stenzel, M. H. *Polymer,* **2006**, *47,* 1073.

(26) Cheng, C.; Khoshdel, E.; Wooley, K. L. *Nano. Lett.,* **2006**, *6,* 1741.

(27) Cheng, C.; Powell, K. T.; Koshdell, E.; Wooley, K. L. *Macromolecules,* **2007**, *40,* 7195.

(28) Oike, H.; Mouri, T.; Tezuka, Y. *Macromolecules,* **2001**, *34,* 6592.

(29) Takeuchi, D.; Inoue, A.; Osakada, K.; Kobayashi, M.; Yamaguchi, K. *Organometallics,* **2006**, *25,* 4062.

(30) Smulders, W.; Monteiro, M. J. *Macromolecules,* **2004**, *37,* 4474.

(31) Aqil, A.; Detrembleur, C.; Gilbert, B.; Jerome, R.; Jerome, C. *Chem. Mat.,* **207**, *19,* 2150.

(32) van Zyl, A. J. P.; Sanderson, R. D.; de Wet-Roos, D.; Klumperman, B. *Macromolecules,* **2003**, *36,* 8621.

(33) Lecolley, F.; Waterson, C.; Carmichael, A. J.; Mantovani, G.; Harrisson , S.; Chappell, H.; Limer, A.; Williams, P.; Ohno, K.; Haddleton, D. M. *J. Mat. Chem.,* **2003**, *13,* 2689.

(34) Leduc, M. R.; Hawker, C. J.; Dao, J.; Frechet, J. M. J. *J. Am. Chem. Soc.,* **1996**, *118,* 11111.

(35) D'Agosto, F.; Hughes, R.; Charreyre, M.-T.; Pichot, C.; Gilbert, R. G. *Macromolecules,* **2003**, *36,* 621.

(36) Favier, A.; Charreyre, M.-T.; Chaumont, P.; Pichot, C. *Macromolecules,* **2002**, *35,* 8271.

(37) Schmitt, B.; Muller, A. H. E. *Macromolecules,* **2001**, *34,* 2115.

(38) Davis, K. A.; Matyjaszewski, K. *Adv. Polym. Sci.,* **2002**, *159,* 1.

(39) Sumerlin, B. S.; Lowe, A. B.; Thomas, D. B.; McCormick, C. L. *Macromolecules,* **2003**, *36,* 5982.

(40) Vosloo, J. J.; Tonge, M. P.; Fellows, C. M.; D'Agosto, F.; Sanderson, R. D.; Gilbert, R. G. *Macromolecules,* **2004**, *37,* 2371.

(41) Heise, A.; Nguyen, C.; Malek, R.; Hedrick, J. L.; Frank, C. W.; Miller, R. D. *Macromolecules,* **2000**, *33,* 2346.

(42) Cianga, I.; Hepuzer, Y.; Sehatli, E.; Yagci, Y. *J. Polym. Sci. Part A: Polym. Chem,* **2001**, *40,* 2199.

(43) Mayadunne, R. T. A.; Rizzardo, E.; Chiefari, J.; Krstina, J.; Moad, G.; Postma, A.; Thang, S. H. *Macromolecules,* **2000**, *33, 243.*

(44) Lai, J. T.; Shea, R. *J. Polym. Sci. Part A: Polym. Chem.,* **2006**, *44,* 4298.

(45) Lacroix-Desmazes, P.; Delair, T.; Pichot, C.; Boutevin, B. *J. Polym. Sci. Part A: Polym. Chem,,* **2000**, *38,* 3845.

(46) Matyjaszewski, K.; Shipp, D. A.; Mcmurtry, G. P.; Gaynor, S. G.; Pakula, T. *J. Polym. Sci., Part A: Polym. Chem.,* **2000**, *38,* 2023.

(47) Davis, K. A.; Charleux, B.; Matyjaszewski, K. *J. Polym. Sci. Part A: Polym. Chem.,* **2000**, *38,* 2274.

(48) Burguiere, C.; Pascual, S.; Bui, C.; Vairon, J.-P.; Charleux, B.; Davis, K. A.; Matyjaszewski, K.; Betremieux, I. *Macromolecules,* **2001**, *34,* 4429.

(49) Neugebauer, D.; Matyjaszewski, K. *Macromolecules,* **2003**, *36,* 2598.

(50) Mizuno, N.; Satoh, K.; Kamigaito, M.; Okamoto, Y. *Macromolecules,* **2006**, *39,* 5280.

(51) Lutz, J.-F.; Kirci, B.; Matyjaszewski, K. *Macromolecules,* **2003,** *36*, 3136.

(52) Kirci, B.; Lutz, J.-F.; Matyjaszewski, K. *Macromolecules,* **2002**, *35,* 2448.

(53) Matyjaszewski, K.; Ziegler, M. J.; Arehart, S. V.; Greszta, D.; Pakula, T. *J. Phys. Org. Chem.,* **2000**, *13,* 775.

(54) Moad, G.; Rizzardo, E.; Thang, S. H. *Aust. J. Chem.,* **2005**, *58,* 379.

(55) Gotz, H.; Harth, E.; Schiller, S. M.; Frank, C. W.; Knoll, W.; Hawker, C. J. *J. Polym. Sci. Part A: Polym. Chem.,* **2002**, *40,* 3379.

(56) Moingeon, F.; Masson, P.; Mery, S. *Macromolecules,* **2007**, *40,* 55.

(57) Hsieh, H. L.; Quirk, R. P. *Anionic polymerization: principles and practical applications*, Marcel Dekker: New York, 1996.

(58) Faust, R.; Kennedy, J. P. *J. Polym. Sci. Part A: Polym. Chem.,* **2003**, *25,* 1847.

(59) Wang, Y.; Wang, L.-S.; Goh, S.-H.; Yang, Y.-Y. *Biomacromolecules,* **2007**.

(60) Kanazawa, A.; Kanaoka, S.; Aoshima, S. *J. Am. Chem. Soc.,* **2007**, *129,* 2420.

(61) Penczek, S.; Kubisa, P. *Polym. Sci.,* **1985**, *68,* 1.

(62) Sawamoto, M. *Prog. Polym. Sci.,* **1991**, *16,* 111.

(63) Matyjaszewski, K.; Sigwalt, P. *Polym. Int.,* **1994**, *35,* 1.

(64) Georgiou, T. K.; Patrickios, C. S. *Macromolecules,* **2006**, *39,* 1560.

(65)   Georgiou, T. K.; Vamvakaki, M.; Patrickios, C. S. *Biomacromolecules,* **2004**, *5,* 2221.

(66)   Taguchi, M.; Tomita, I.; Yoshida, Y.; Endo, T. *Macromol. Chem. Phys.,* **2000**, *201,* 1025.

(67)   Wang, J.; Tomita, I. *Macromolecules,* **2001**, *34,* 4294.

(68)   Connor, E. F.; Nyce, G. W.; Myers, M.; Mock, A.; Hedrick, J. L. *J. Am. Chem. Soc.,* **2002**, *126,* 914.

(69)   Farcet, C.; Belleney, J.; Charleux, B.; Pirri, R. *Macromolecules,* **2002**, *35,* 4912.

(70)   Odian, G. *Principles of Polymerization*, 4th ed., Wiley Interscience: New York, 2004.

(71)   Studer, A.; Schulte, T. *Chem. Rec.,* **2005**, *5,* 27.

(72)   Jing, Y.; Sheares, V. V. *Macromolecules,* **2000**, *33,* 6255.

(73)   Braunecker, W. A.; Matyjaszewski, K. *Prog. Polym. Sci.,* **2007**, *32,* 93.

(74)   Solomon, D. H.; Moad, G. *Makromol. Chem. Macromol. Symp.,* **1987**, *10,* 109.

(75)   Bamford, C. H. "Radical Polymerization", in *Encyclopedia of Polymer Science and Engineering*; 13, eds. Mark, H. F.,Bikales, N. M.,Overberger, C. G.,Menges, G.; Wiley-Interscience: New York, 1988, 708.

(76)   Koenig, T.; Fischer, H. "Cage Effects", Chap. 4, in *Free Radicals*; I, eds. Kochi, J. K.; Wiley: New York, 1973.

(77)   Van Berkel, K. Y.; Russel, G. T.; Gilbert, B. *Macromolecules,* **2005**, *38,* 3214.

(78)   Rivera, M. R.; Rodriguez-Hernandez, A. A.; Hernandez, N.; Castillo, P.; Saldivar, E.; Rios, L. *Ind. Eng. Chem. Res.,* **2005**, *44,* 2792.

(79)   Kazmaier, P. M.; Daimon, K.; Georges, M. K.; Hamer, G. K.; Veregin, R. P. N. *Macromolecules,* **1997**, *30,* 2228.

(80)   Favier, A.; Charreyre, M.-T.; Pichot, C. *Polymer,* **2004**, *45,* 8661.

(81)   He, L.; Read, E. S.; Armes, S. P.; Adams, D. J. *Macromolecules,* **2007**, *40,* 4429.

(82)   Fuji, Y.; Ando, T.; Kamigaito, M.; Sawamoto, M. *Macromolecules,* **2002**, *35,* 2949.

(83)   Nishikawa, T.; Kamigaito, M.; Sawamoto, M. *Macromolecules,* **1999**, *32,* 2204.

(84)   Lansalot, M.; Farcet, C.; Charleux, B.; Vairon, J.-P. *Macromolecules,* **1999**, *32,* 7354.

(85)   Song, J.-S.; Winnik, M. A. *Macromolecules,* **2006**, *39,* 8318.

(86)   Darling, T. R.; Davis, T. P.; Fryd, M.; Gridnev, A. A.; Haddleton, D. M.; Ittel, S. D.; Matheson, R. R. J.; Moad, G.; Rizzardo, E. *J. Polym. Sci. Part A: Polym. Chem.,* **2000**, *38,* 1706.

(87)   Szwarc, M. *Carbanions, living polymers and electron transfer processes*, Interscience Publishers: New York, 1968.

(88)   Holden, G.; R.;, K. H.; Quirk, R. P. *Thermoplastic elastomers*, 3rd ed., Hanser: Munich, 2004.

(89)   Szwarc, M. *Ions and ion pairs in organic reactions.*, Wiley: New York, 1972.

(90)   Litvinenko, G.; Mueller, A. H. E. *Macromolecules,* **1997**, *30,* 1253.

(91)   Otsu, T.; Tazaki, M. *Makromol. Chem., Rapid Commun.,* **1982**, *3,* 133.

(92)   Endo, K.; Murata, K.; Otsu, T. *Macromolecules,* **1992**, *25,* 5554.

(93)   Fischer, A.; Brembilla, A.; Lochon, P. *Eur. Polym. J.,* **2000**, *37,* 33.

(94)   Keoshkerian, B.; Macleod, P. J.; Georges, M. K. *Macromolecules,* **2001**, *34,* 3594.

(95)   Rizzardo, E. *Chem. Aust.,* **1987**, *54,* 32.

(96)   Patten, T. E.; Matyjaszewski, K. *Acc. Chem. Res.,* **1999**, *32,* 895.

(97)   Matyjaszewski, K.; Xia, J. *Chem. Rev.,* **2001**, *101,* 2921.

(98)   Kamigaito, M.; Ando, T.; Sawamoto, M. *Chem. Rev.,* **2001**, *101,* 3689.

(99)   Angiolini, L.; Benelli, T.; Giorgini, L.; Salatelli, E. *Polymer,* **2005**, *46,* 2424.

(100)   Rademacher, J. T.; Baum, M.; Pallack, M. E.; Brittain, W. J. *Macromolecules,* **2000**, *33,* 284.

(101)   Wang, J.-S.; Matyjaszewski, K. *J. Am. Chem. Soc.,* **1995**, *117,* 5614.

(102)   Tsarevsky, N. V.; Sarbu, T.; Gobelt, B.; Matyjaszewski, K. *Macromolecules,* **2002**, *35,* 6142.

(103)   Chiefari, J.; Chong, Y. K. B.; Ercole, F.; Krstina, J.; Jeffery, J.; Le, T. P. T.; Mayadunne, R. T. A.; Meijs, G. F.; Moad, C. L.; Moad, G.; Rizzardo, E.; Thang, S. H. *Macromolecules,* **1998**, *31,* 5559.

(104)   Le, T. P.; Moad, G.; Rizzardo, E.; Thang, S. H. PCT Int Appl WO 9801478A1, 1998; *Chem Abstr* **1998**, *128*, 115390.

(105)   Chong, B. Y. K.; Le, T. P. T.; Moad, G.; Rizzardo, E.; Thang, S. H. *Macromolecules,* **1999**, *32,* 2071.

(106)   Perrier, S.; Takolpuckdee, P. *J. Polym. Sci. Part A: Polym. Chem.,* **2005**, *43,* 5347.

(107)   Moad, G.; Chiefari, J.; Chong, B. Y.; Krstina, J.; Mayadunne, R. T.; Postma, A.; Rizzardo, E.; Thang, S. H. *Polym. Int.,* **2000**, *49,* 993.

(108)   Fournier, D.; Hoogenboom, R.; Thijs, h. M. L.; Paulus, R. M.; Schubert, U. S. *Macromolecules,* **2007**, *40,* 915.

(109)   Gaynor, S. G.; Wang, J.-S.; Matyjaszewski, K. *Macromolecules,* **1995**, *28,* 8051.

(110)   Iovu, M. C.; Matyjaszewski, K. *Macromolecules,* **2003**, *36,* 9346.

(111)   Wayland, B. B.; Poszmik, G.; Mukerjee, S. L.; Fryd, M. *J. Am. Chem. Soc.,* **1994**, *116,* 7943.

(112)   Kaneyoshi, H.; Matyjaszewski, K. *Macromolecules,* **2005**, *38,* 8163.

(113)   Hawker, C. J.; Bosman, A. W.; Harth, E. *Chem. Rev.,* **2001**, *101,* 3661.

(114)   Schierholz, S.; Givehchi, M.; Fabre, P.; Nallet, F.; Papon, E.; Guerret, O.; Gnanou, Y. *Macromolecules,* **2003**, *36,* 5995.

(115)   Veregin, R. P. N.; Georges, M. K.; Kazmaier, P. M.; Hamer, G. K. *Macromolecules,* **1993**, *26,* 5316.

(116)   Georges, M. K.; Veregin, R. P. N.; Kazmaier, P. M.; Hamer, G. K. *Macromolecules,* **1993**, *26,* 2987.

(117)   Fukuda, T.; Terauchi, T.; Goto, A.; Tsujii, Y.; Miyamoto, T.; Shimuzu, Y. *Macromolecules,* **1996**, *29,* 3050.

(118)   Benoit, D.; Grimaldi, S.; Robin, s.; Finet, J.-P.; Tordo, P.; Gnanou, Y. *J. Am. Chem. Soc.,* **2000**, *122,* 5929.

(119)   Brinkmann-Rengel, S.; Niessner, N. *ACS Symp. Ser.,* **2000**, *768,* 394.

(120)   Greszta, D.; Mardare, D.; Matyjaszewski, K. *Macromolecules,* **1994**, *27,* 638.

(121)   Goto, A.; Fukuda, T. *Prog. Polym. Sci.,* **2004**, *29,* 329.

(122)   Fischer, H. *Chem. Rev.,* **2001**, *101,* 3581.

(123)   Tang, W.; Tsarevsky, N. V.; Matyjaszewski, K. *J. Am. Chem. Soc.,* **2006**, *128,* 1598.

(124)   Fischer, H. *J. Polym. Sci. Part A: Polym. Chem.,* **1999**, *37,* 1885.

(125)   Thomas, D. B.; Convertine, A. J.; Myrick, L. J.; Scales, C. W.; Smith, A. E.; Lowe, A. B.; Vasilieva, Y. A.; Ayres, N.; McCormick, C. L. *Macromolecules,* **2004**, *37,* 8941.

(126)   Khanna, S. N.; Levy, M.; Szwarc, M. *Trans. Faraday. Soc.,* **1962**, *58,* 747.

(127)   Solomon, D. H.; Rizzardo, E.; Cacioli, P. European Patent 135280A2, 1985, U.S. Patent 4581429, 1985; *Chem. Abstr.* **1985**, *102*, 221335q.

(128)   Solomon, D. H. *J. Polym. Sci. Part A: Polym. Chem.,* **2005**, *43,* 5748.

(129)   Georges, M. K.; Veregin, R. P. N.; Kazmaier, P. M.; Hamer, G. K. *Macromolecules,* **1993**, *26,* 2987.

45

(130) Soloman, D. H.; Rizardo, E.; Cacioli, P. Stable free radicals have been used to form adducts with monomer which can initiate "living" chains for the synthesis of oligomers. U.S.Patent 4,581,429, 27 March, 1985; Rizzardo, E. *Chem. Aust.* 1987, 54, 32.

(131) Moad, G.; Rizzardo, E.; Soloman, D. H. *Polym. Bull.,* **1982**, *6,* 589 and references cited therein.

(132) Moad, G.; Rizzardo, E.; Soloman, D. H. *Tetrahedron Lett.,* **1981**, *22,* 1165.

(133) Shipp, D. A.; Matyjaszewski, K. *Polym. Prep.* **1999**, *40,* 450.

(134) Otsu, T.; Yoshida, M.; Tazaki, T. *Makromol Chem Rapid Comm,* **1982**, *3,* 133.

(135) Otsu, T.; Matsunaga, T.; Doi, T.; Matsumoto, A. *Eur. Polym. J.,* **1995**, *31,* 67.

(136) Steenbock, M.; Klapper, M.; Muellen, K. *Macromol. Chem. Phys.,* **1998**, *199,* 763.

(137) Janzen, E. G. *Acc. Chem. Res.,* **1971**, *4,* 3126.

(138) Detrembleur, C.; Sciannamea, V.; Koulic, C.; Claes, M.; Hoebeke, M.; Jérôme, R. *Macromolecules,* **2002**, *35,* 7214.

(139) Chalfont, G. R.; Perkins, M. J. *J. Am. Chem. Soc.,* **1967***, 89,* 3054.

(140) Ah Toy, A.; Chaffey-Millar, H.; Davis, T. P.; Stenzel, M. H.; Izgorodina, E. I.; Coote, M. L. e. a. *Chem. Commun.,* **2006***,* 835.

(141) Gaynor, S.; Greszta, D.; Mardare, D.; Teodorescu, M.; Matyjaszewski, K. *J. Macromol. Sci. Pure Appl. Chem,* **1994**, *A31,* 1561.

(142) Greszta, D.; Matyjaszewski, K. *J. Polym. Sci. Part A: Polym. Chem.,* **1997**, *35,* 1857.

(143) Goto, A.; Fukuda, T. *Macromolecules,* **1997**, *30,* 4272.

(144) Bertin, D.; Chauvin, F.; Marque, S.; Tordo, P. *Macromolecules,* **2002**, *35,* 3790.

(145) Hawker, C. J.; Barclay, G. G.; Orellana, A.; Dao, J.; Devonport, W. *Macromolecules,* **1996**, *29,* 5245.

(146) Hawker, C. J. *J. Am. Chem. Soc.,* **1994**, *116,* 11186

(147) Fischer, H. *Macromolecules,* **1997**, *30,* 5666.

(148) Studer, A.; Harms, K.; Knoop, C.; Mueller, C.; Schulte, T. *Macromolecules,* **2004**, *37,* 27.

(149) Bertin , D.; Gigmes, D.; Le Mercier, C.; Marque, S. R. A.; Tordo, P. *J. Org. Chem.,* **2004**, *69,* 4925.

(150) Chauvin, F.; Dufils, P.-E.; Gigmes, D.; Guillaneuf, Y.; Marque, S. R. A.; Tordo, P.; Bertin, D. *Macromolecules,* **2006**, *39,* 5238.

(151) Chong, Y. K.; Ercole, F.; Moad, G.; Rizzardo, E.; Thang, S.-H. *Macromolecules,* **1999**, *32,* 6895.

(152) Benoit, D.; Chaplinski, V.; Braslau, R.; Hawker, C. J. *J. Am. Chem. Soc.,* **1999**, *121,* 3904.

(153) Benoit, D.; Hawker, C. J.; Huang, E. E.; Lin, Z.; Russell, T. P. *Macromolecules,* **2000**, *33,* 1505.

(154) Keoshkerian, B.; Georges, M. K.; Quinlan, M.; Veregin, R. P. N.; Goodbrand, R. *Macromolecules,* **1998**, *31,* 7559.

(155) Colombani, D.; Steenbock, M.; Klapper, M.; Mullen, K. *Macromol. Rapid Commun.,* **1997**, *18,* 243.

(156) Grimaldi, S.; Finet, J. P.; Zeghdaoui, A.; Tordo, P.; Benoit, D.; Gnanou, Y.; Fontanille, M.; Nicol, P.; Pierson, J. F. *Polym. Prepr.,* **1997**, *38,* 651.

(157) Robin, S.; Gnanou, Y. *Polym. Prepr.,* **1999**, *40,* 387.

(158) Qiu, J.; Charleux, B.; Matyjaszewski, K. *Prog. in Polym. Sci,,* **2001**, *26,* 2083.

(159) Benoit, D.; Grimaldi, S.; Finet, J. P.; Tordo, P.; M.;, F.; Gnanou, Y. *Polym. Prepr.,* **1997**, *38,* 729.

(160) Phan, T. N. T.; Maiez-Tribut, S.; Pascault, J.-P.; Bonnet, A.; Gerard, P.; Guerret, O.; Bertin, D. *Macromolecules,* **2007**, *40,* 4516.

(161) Nicolas, J.; Dire, C.; Mueller, L.; Belleney, J.; Charleux, B.; Marque, S. R. A.; Bertin , D.; Magnet, S.; Couvreur, L. *Macromolecules,* **2006**, *39,* 8274.

(162) Nicolas, J.; Dire, C.; Mueller, L.; Belleney, J.; Charleux, B.; Marque, S. R. A. e. a. *Macromolecules,* **2006**, *39,* 8274.

(163) Hutchison, J. B.; Stark, P. F.; Hawker, C. J.; Anseth, K. S. *Chem. Mat.,* **2005**, *17,* 4789.

(164) Charleux, B.; Nicolas, J.; Guerret, O. *Macromolecules,* **2005**, *38,* 5485.

(165) Narumi, A.; Matsuda, T.; Kaga, H.; Satoh, T.; Kakuchi, T. *Polymer,* **2002**, *43,* 4835.

(166) Higaki, Y.; Otsuka, H.; Takahara, A. *Macromolecules,* **2004**, *37,* 1696.

(167) Diaz, T.; Fischer, A.; Jonquières, A.; Brembilla, A.; Lochon, P. *Macromolecules,* **2003**, *36,* 2235.

(168) van der Veen, M. H.; de Boer, B.; Stalmach, U.; van de Wetering, K. I.; Hadziioannou, G. *Macromolecules,* **2004**, *37,* 3673.

(169) Fischer, A.; Brembilla, A.; Lochon, P. *Macromolecules,* **1999**, *32,* 6069.

(170) Gossage, R. A.; van de Kuil, L. A.; van Koten, G. *Acc. Chem. Res.,* **1998**, *31,* 423.

(171) Wang, J.-S.; Matyjaszewski, K. *Macromolecules,* **1995**, *28,* 7901.

(172) Kato, M.; Kamigaito, M.; Sawamoto, M.; Higashimura, T. *Macromolecules,* **1995**, *28,* 1721.

(173) Matyjaszewski, K.; Xia, J. *Chem. Reviews,* **2001**, *101,* 2921.

(174) Goodwin, J. M.; Olmstead, M. M.; Patten, T. E. *J. Am. Chem. Soc. (Communication),* **2004**, *126,* 14352.

(175) Xia, J.; Matyjaszewski, K. *Macromolecules,* **1999**, *32,* 2434.

(176) Yu, Q.; Zeng, F.; Zhu, S. *Macromolecules,* **2001**, *34,* 1612.

(177) Peter, K.; Thelakkat, M. *Macromolecules,* **2003**, *36,* 1779.

(178) Moineau, G.; Minet, M.; Teyssie, P.; Jerome, R. *Macromolecules,* **1999**, *32,* 8277.

(179) Lecomte, P.; Drapier, I.; Dubois, P.; Teyssie, P.; Jerome, R. *Macromolecules,* **19997**, *30,* 7631.

(180) Moineau, G.; Granel, C.; Dubois, P.; Jerome, R.; Teyssie, P. *Macromolecules,* **1998**, *31,* 542.

(181) Kotani, Y.; Kamigaito, M.; Sawamoto, M. *Macromolecules,* **1999**, *32,* 2420.

(182) Zhu, S.; Yan, D. *Macromolecules,* **2000**, *33,* 8233.

(183) Matyjaszewski, K.; Wei, M.; Xia, J.; McDermott, N. E. *Macromolecules,* **1997**, *30,* 8161.

(184) Xia, J.; Matyjaszewski, K. *Macromolecules,* **1999**, *30,* 7692.

(185) Xia, J.; Matyjaszewski, K. *Macromolecules,* **1999**, *32,* 5199.

(186) Qiu, J.; Gaynor, S.; Matyjaszewski, K. *Macromolecules,* **1999**, *32,* 2872.

(187) Moineau, G.; Dubois, P.; Jerome, R.; Senninger, T.; Teyssie, P. *Macromolecules,* **1998**, *31,* 545.

(188) Gromada, J.; Matyjaszewski, K. *Macromolecules,* **2001**, *34,* 7664.

(189) Li, M.; Jahed, N. M.; Min, K.; Matyjaszewski, K. *Macromolecules,* **2004**, *37,* 2434.

(190) Ashford, E. J.; Naldi, V.; O'Dell, R.; Billingham, N. C.; Armes, S. P. *Chem. Commun.* **1999,** 1285.

(191) Matyjaszewski, K.; Pintauer, T.; Gaynor, S. *Macromolecules,* **2000**, *33,* 1476.

(192) Hong, S. C.; Paik, H. P.; Matyjaszewski, K. *Macromolecules,* **2001**, *34,* 5099.

(193) Liou, S.; Rademacher, J. T.; Malaba, D.; Pallack, M. E.; Brittain, W. J. *Macromolecules,* **2000**, *33,* 4295.

(194) Matyjaszewski, K.; Coca, S.; Gaynor, S. G.; Wei, M.; Woodworth, B. E. *Macromolecules,* **1998**, *31,* 5967.

(195) Chambard, G., in *Control of Monomer Sequence distribution (Ph. D. thesis)*, Technische Universiteit Eindhoven, Eindhoven, **2000**, p. 88-89

(196) Moad, C. L.; Moad, G.; Rizzardo, E.; Thang, S. H. *Macromolecules,* **1996**, *29,* 7717.

(197) Krstina, J.; Moad, G.; Rizzardo, E.; Winzor, C. L. *Macromolecules,* **1995**, *28,* 5381.

(198) Han, X.; Fan, J.; He, J.; Xu, J.; Fan, D.; Yang, Y. *Macromolecules,* **2007**, *40,* 5618.

(199) Chong, Y. K.; Moad, G.; Rizzardo, E.; Thang, S. *Macromolecules,* **2007**, *40*, 4446.

(200) Perrier, S.; Takolpuckdee, P.; Mars, C. A. *Macromolecules,* **2005**, *38,* 2033.

(201) Postma, A.; Davis, T. P.; Evans, R. A.; Li, G.; Moad, G.; O'Shea, M. S. *Macromolecules,* **2006**, *39,* 5293.

(202) Moad, G.; Chong, Y. K.; Postma, A.; Rizzardo, E.; Thang, S. H. *Polymer,* **2005**, *46,* 8458.

(203) Moad, G.; Solomon, D. H. *The Chemistry of Free Radical Polymerization*, Pergamon: Oxford, 1995.

(204) Destarac, M.; Taton, D.; Zard, S. Z.; Saleh, T.; Yvan, S. *ACS Symp. Ser.,* **2003**, *854,* 536.

(205) LJ., G. *J. Chem. Phys.,* **1958**, *28,* 91.

(206) Mitsukami, Y.; Donovan, M. S.; Lowe, A. B.; McCormick, C. L. *Macromolecules,* **2001**, *34,* 2248.

(207) De Brouwer, H.; Schellekens, M. A. J.; Klumperman, B.; Monteiro, M. J.; German, A. L. *J. Polym. Sci., Part A: Polym. Chem.,* **2000**, *38,* 3596.

(208) Gaillard, N.; Guyot, A.; Claverie, J. *J. Polym. Sci. Part A: Polym. Chem.,* **2003**, *41,* 684.

(209) Matyjaszewski, K. *Macromolecules,* **1999**, *32,* 9051.

(210) Muthukrishnan, S.; Pan, E. H.; Stenzel, M. H.; Barner-Kowollik, C.; Davis, T. P.; Lewis, D.; Barner, L. *Macromolecules,* **2007**, *40,* 2978.

(211) Yusa, S.; Shimada, Y.; Mitsukami, Y.; Yamamoto, T.; Morishima, Y. *Macromolecules,* **2004**, *37,* 7507.

(212) Yusa, S.; Shimada, Y.; Mitsukami, Y.; Yamamoto, T.; Morishima, Y. *Macromolecules,* **2003**, *37,* 7507.

(213) Krasia, T. C.; Patrickios, C. S. *Macromolecules,* **2006**, *39,* 2467.

(214) Albertin, L.; Stenzel, M.; Barner-Kowollik, C.; Foster, L. J. R.; Davis, T. P. *Macromolecules,* **2004**, *37,* 7530.

(215) Lovestead, T. M.; Theis, A.; Davis, T. P.; Stenzel, M. H.; Barner-Kowollik, C. *Macromolecules,* **2006**, *39,* 4975.

(216) Chong, B. Y. K.; Krstina, J.; Le, T. P. T.; Moad, G.; Postma, A.; Rizzardo, E.; Thang, S. H. *Macromolecules,* **2003**, *36,* 2256.

(217) Luo, Y.; Wang, R.; Yang, L.; Yu, B.; Li, B.; Zhu, S. *Macromolecules,* **2006**, *39,* 1328.

(218) Dureault, A.; Taton, D.; Destarac, M.; Leising, F.; Gnanou, Y. *Macromolecules,* **2004**, *37,* 5513.

(219) Baussard, J.-F.; Habib-Jiwan, J.-L.; Laschewsky, A.; Mertogluc, M.; Storsberg, J. *Polymer* **2004**, *45,* 3615.

(220) Thomas, D. B.; Sumerlin, B. S.; Lowe, A. B.; McCormick, C. L. *Macromolecules,* **2003**, *36,* 1436.

(221) Chiefari, J.; Mayadunne, R. T. A.; Moad, C. L.; Moad, G.; Rizzardo, E.; Postma, A.; Skidmore, M. A.; Thang, S. H. *Macromolecules,* **2003**, *36,* 2273.

(222) Lai, J. T.; Filla, D.; Shea, R. *Macromolecules,* **2002**, *35,* 6754.

(223) Destarac, M.; Charmot, D.; Franck, X.; Zard, S. Z. *Macromol. Rapid Comm.,* **2000**, *21,* 1035.

(224) Schilli, C.; Lanzendörfer, M. G.; Müller, A. H. E. *Macromolecules,* **2002**, *35,* 6819.

(225) Mayadunne, R. T. A.; Rizzardo, E.; Chiefari, J.; Chong, Y. K.; Moad, G.; Thang, S. H. *Macromolecules,* **1999**, *32,* 6877.

(226) Taton, D.; Wilczewska, A.; Destarac, M. *Macromol. Rapid Commun.,* **2001**, *22,* 1497.

(227) Jacquin, M.; Muller, P.; Lizarraga, G.; Bauer, C.; Cottet, H.; Theodoly, O. *Macromolecules,* **2007**, *40,* 2672.

(228) Quiclet-Sire, B.; Wilczewska, A.; Zard, S. Z. *Tetrahedron Letters,* **2000**, *41,* 5673.

(229) Monteiro, M. J.; de Barbeyrac, J. *Macromolecules,* **2001**, *34,* 4416.

(230) Monteiro, M. J.; de Barbeyrac, J. *Macromol. Rapid Comm.,* **2002**, *23,* 370.

(231) Chiefari, J.; Mayadunne, R. T. A.; Moad, C. L.; Moad, G.; Rizzardo, E.; Postma, A.; Skidmore, M. A.; Thang, S. H. *Macromolecules,* **2003**, *36,* 2273.

(232) Favier, A.; Charreyre, M.-T. *Macromol. Rapid Commun.,* **2006**, *27,* 653.

(233) Coote, M. L. *Macromolecules,* **2004**, *37,* 5023.

(234) Goto, A.; Sato, K.; Fukuda, T.; Moad, G.; Rizzardo, E.; Thang, S. H. *Polym Prepr,* **1999**, *40,* 397.

(235) Muller, A. H. E.; Zhuang, R.; Yan, D.; Litvinenko, G. *Macromolecules,* **1995**, *28,* 4326.

(236) Muller, A. H. E.; Litvenko, G. *Macromolecules,* **1997**, *30,* 1253.

(237) Chong, Y. K.; Krstina, J.; Le, T. P. T.; Moad, G.; Postma, A.; Rizzardo, E.; Thang, S. H. *Macromolecules,* **2003**, *36,* 2256.

(238) Lansalot, M.; Davis, T. P.; Heuts, J. P. A. *Macromolecules,* **2002**, *35,* 7582.

(239) Barner-Kowollik, C.; Quinn, J. F.; Morsley, D. R.; Davis, T. P. *J. Polym. Sci. Part A: Polym. Chem.,* **2001**, *39,* 1353.

(240) Monteiro, M. J.; de Brouwer, H. *Macromolecules,* **2000**, *34,* 349.

(241) D'Agosto, F.; Hughes, R. J.; Charreyre, M.-T.; Pichot, C.; Gilbert, R. G. *Macromolecules,* **2003**, *36,* 621.

(242) Barner-Kowollik, C.; Quinn, J. F.; Nguyen, T. L. U.; Heuts, J. P. A.; Davis, T. P. *Macromolecules,* **2001**, *34,* 7849.

(243) McLeary, J. B.; Calitz, F. M.; McKenzie, J. M.; Tonge, M. P.; Sanderson, R. D.; Klumperman, B. *Macromolecules,* **2004**, *37,* 2383.

(244) Chernikova, E.; Morozov, A.; Leonova, E.; Garina, E.; Golubev, V.; Bui, C.; Charleux, B. *Macromolecules,* **2004**, 6329.

(245) Ah Toy, A.; Vana, P.; Davis, T. P.; Barner-Kowollik, C. *MAcromolecules,* **2004**, *37,* 744.

(246) Chen, M.; Ghiggino, K. P.; Smith, T. A.; Thang, S. H.; Wilson, G. J. *Aust. J. Chem.,* **2004**, *57,* 1175.

(247) Chen, M.; Ghiggino, K. P.; Thang, S. H.; White, J.; Wilson, G. J. *J. Org. Chem.,* **2005**, *70,* 1844.

(248) Postma, A.; Davis, T. P.; Moad, G.; O'Shea, M. S. *Macromolecules,* **2005**, *38,* 5371.

(249) Xu, J.; He, J.; Fan, D.; Tang, W.; Yang, Y. *Macromolecules,* **2006**, *39,* 3753.

(250) Mayadunne, R. T. A.; Jeffery, J.; Moad, G.; Rizzardo, E. *Macromolecules,* **2003**, *36,* 1505.

(251) Favier, A.; Ladaviere, C.; Charreyre, M.-T.; Pichot, C. *Macromolecules,* **2004**, *37,* 2026.

(252) Thomas, D. B.; Convertine, A. J.; Hester, R. D.; Lowe, A. B.; McCormick, C. L. *Macromolecules,* **2004**, *37,* 1735.

(253) Patton, D. L.; Mullings, M.; Fulghum, T.; Advincula, R. C. *Macromolecules,* **2005**, *38,* 8597.

(254) Nakayama, M.; Okano, T. *Biomacromolecules,* **2004**, *6,* 2320.

(255) Qiu, X.-P.; Winnik, F. M. *Macromol. Rapid Commun.,* **2006**, *27,* 1648.

(256) Farinha, J. P. S.; Relogio, P.; Charreyre, M.-T.; Prazeres, T. J. V.; Martinho, J. M. G. *Macromolecules,* **2007**, *40,* 4680.

(257)   Llauro, M. F.; Loiseau, J.; Boisson, F.; Delolme, F.; Ladaviere, C.; Claverie, J. *J. Polym. Sci. Part A: Polym. Chem.,* **2004**, *42,* 5439.

(258)   Sumerlin, B. S.; Lowe, A. B.; Stroud, P. A.; Zhang, P.; Urban, M. W.; McCormick, C. L. *Langmuir,* **2003**, *19,* 5559.

(259)   McCormick , C. L.; Lowe, A. B. *Acc. Chem. Res.,* **2004**, *37,* 312.

(260)   Scales, C. W.; Convertine, A. J.; McCormick, C. L. *Biomacromolecules,* **2006**, *7,* 1389.

Chapter 3

PDMS macroCTA synthesis and characterization

Abstract

The synthesis of various ester-containing PDMS macroCTAs by means of activation of the carboxylic acid group on the CTA using 1,3-dicyclohexylcarbodiimide (DCC) is described. DCC is used widely in the synthesis of peptides[1,2] and esters[3-6] and produces good results. Two macroCTAs containing PDMS were synthesized via coupling of end-functionalized PDMS using DCC as the coupling agent and characterized extensively by means of SEC, proton and carbon nuclear magnetic resonance (^{1}H-NMR and ^{13}C-NMR respectively) spectroscopy and infrared spectroscopy (IR). Three variables were investigated, namely, (1) the influence of excess acid/DCC, (2) time of reaction and (3) use of 4-(dimethylamino)pyridine (DMAP) as catalyst, as well as catalyst concentration. Optimal reaction conditions, as determined by the author, resulting in complete conversion of PDMS into its ester counterpart included the use of excess acid/DCC as well as the use of catalytic amounts of DMAP at room temperature over a period of 10 hours.

3.1   Introduction

The aim of this work was to functionalize monohydroxy-terminated polydimethylsiloxane (PDMS-OH) (a dimethiconol) into a reactive intermediate by introduction of a thiocarbonylthio chain end-functionality. Through introducing the characteristic thiocarbonylthio functionality to the chain end of PDMS, this product can be classified as an ester-containing PDMS macroCTA. Refer to Figure 3.1 for the proposed PDMS modified material ((11a) or (11b)). This polymeric ester can be incorporated as block units when used to synthesize block copolymers of varying nature (as described in Chapters 4 and 6). Compared to homopolymerizations of the second block (monomer) used, due to the presence of the silicone content, along with the characteristic properties associated herewith (*e.g.* flame-retardation, bio-compatibility, hydrophobicity *etc.*), block copolymers containing the PDMS moiety will have modified material surface properties.[7-9] The influence of the properties associated with PDMS on the block copolymer can be modified by tailoring the lengths as well as the nature of the second polymer. Another important application of block copolymers containing PDMS is that, due to the incompatibility of PDMS with almost all other organic materials,[10] through copolymerizing silicone-

containing materials with organic materials, the compatibility of these silicone-containing materials can be increased.[11-17]
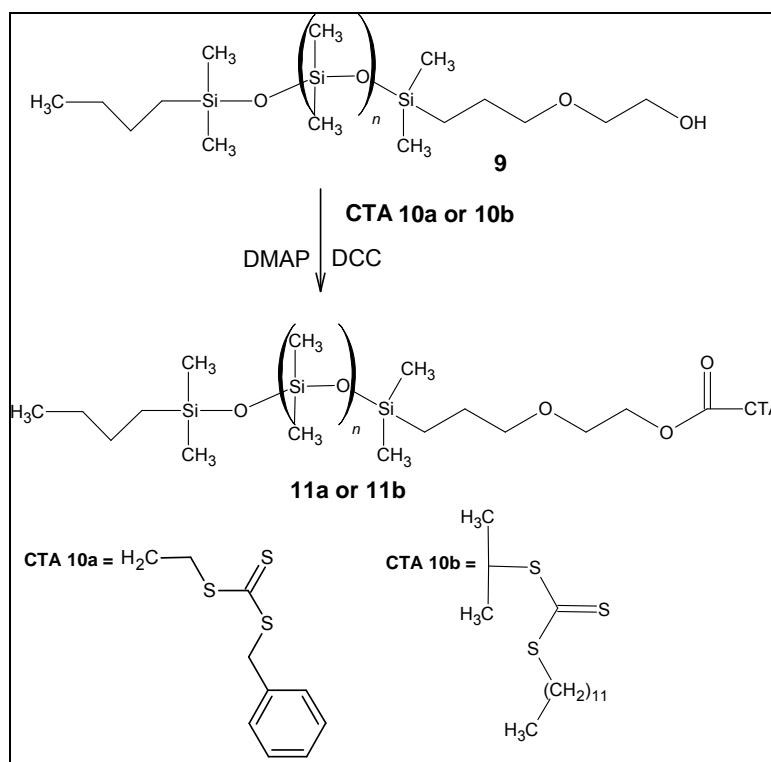
Figure 3.1   **Proposed chemical structure of PDMS macroCTA (11a or 11b) synthesized through modification of PDMS (9).**

Previous studies described the formation of a PDMS macroCTA based on dihydroxy-terminated PDMS[18] but minimal characterization results and evidence regarding the degree and purity of this polymeric compound were provided. The work described in this chapter covers a thorough description of the direct esterification procedure, namely the variables that had to be considered as well as characterization of the PDMS macroCTAs synthesized. Characterization techniques included NMR, IR and SEC.

3.2   Objectives

The two objectives for the successful synthesis of PDMS macroCTAs are to obtain a:

- High degree of conversion into the PDMS macroCTA
- Purified ester-containing PDMS macroCTA

3.2.1   Objective 1: Obtaining a high degree of conversion into the PDMS macroCTA

Due to the high cost of PDMS reagent and the labour intensive synthesis of the CTAs it was desirable to achieve a high degree of conversion of the PDMS into the PDMS macroCTA, which would be used further to form block copolymers with a hydrophobic monomer (Chapter 4) and a hydrophilic monomer (Chapter 6). The first objective was therefore to achieve the highest possible conversion for the PDMS macroCTAs synthesized. It was speculated that the high molecular weight of PDMS would be a potential problem in obtaining high degrees of conversion for this material.

3.2.2   Objective 2: Obtaining pure PDMS macroCTA

The second objective was to obtain a high degree of purity for the PDMS macroCTAs which could then be used in further polymerizations with various monomers. Therefore, a procedure had to be devised to separate the unreacted starting materials from the desired product. Initially there was concern about the large size of the PDMS macroCTA moving through the column, but this was overcome with relative ease as this compound moved through with the solvents of choice.

3.3   Why use silicones?

The family of "silicones" consists of a variety of compounds, namely (linear) PDMS (either dimethicone, or if terminated with a hydroxyl group–dimethiconol), cyclomethicones, polyether siloxanes, phenyl siloxanes, and amino alkyl siloxanes amongst others. Silicone materials have been in use in the medical and pharmaceutical industries for over 50 years.[19] They can be found as raw materials in catheters and pacemakers as well as transdermal delivery systems.[20]

PDMS is of interest to many chemists and formulators as there are a large number of silicon-type materials with vastly different physical properties. This versatility allows the formulator to pick and choose from a class of materials which can be slippery/sticky, volatile/non-volatile, liquid/elastomeric, gentle on skin/strongly adhesive. Probably the greatest benefits that silicon materials can bring to cosmetic formulations are better aesthetic and sensory profiles (*i.e.* act as skin-feel modifiers, water-barrier protectants, defoamers, desoapers (*i.e.* eliminators of creamy whitening of a cosmetic formulation during the initial running onto skin or hair) and conditioners and emollients), as well as a vehicle for the release of active ingredients.[21]

Dimethicone/PDMS is a linear organo-silicon polymer with a silicon-oxygen framework and is used in a variety of applications. The exceptionally low T_g (-125°C; T_m of -50°C)[22] of PDMS allows it to take on a liquid state at room temperature. In addition to this the flatter Si–O–Si bond angle (130–150°) versus C–O–C bond angle (105–115°),[21] and low bending force constant of Si–O–Si linkages, allows it to have high chain flexibility.[23] PDMS, as well as many other silicone products (*e.g.* cyclomethicone) are used in the formulations for the personal care industry.[21]

PDMS is a highly flexible, amorphous elastomeric hydrophobic material. It also displays good optical transparency, resistance to UV radiation and to ozone[24], flame-retardant properties[24], high gas permeability[24] and moldability, it is inert[24], non-toxic, and hemo-/bio-compatible [9,25-28], has a low curing temperature and easily seals with other materials.

Applications for which silicon-containing materials may be suitable include:
- electrical applications in which dielectric stability allows it to be used for power cable insulation
- mechanical applications requiring low and high temperature flexibility as well as chemical inertness, for example, acting as sealants for aircraft doors and windows, freezers and ovens. As a result of its high bond energy (106 kcal/mol),[29] PDMS is not highly susceptible to oxidative and thermal degradation (for dimethylsilicone fluids degradation begins at 350°C).[30] It is well known that the thermal degradation of PDMS in inert atmosphere and under vacuum results in depolymerization over the range of 400–650°C to produce cyclic oligomers.[31,32]
- shock absorbers and vibration damping applications as a result of the low intermolecular/intramolecular forces between siloxane molecules causing the material to provide low resistance when stressed
- water repellency, as it is a hydrophobic material. Most silicones are hydrophobic and dissolve in non-polar solvents. The highly open macromolecular structure of PDMS, as well as its flexibility, allow the siloxane backbone to spread out the methyl substitutions at an interface. This means that when PDMS comes into contact with a substrate the methyl substitutions shield the polar siloxane backbone to form a hydrophobic sheath, resulting in low surface tension and energy.[33]
- biomedical and cosmetic applications in which chemical inertness, nontoxicity or biocompatibility, optical transparency, gas permeability and oxidative and thermal stability are just a few of the desired characteristics. The most common types of silicon materials used in such formulations include dimethicones (linear) and cyclomethicones (cyclic). PDMS has good permeability to water vapour, gases

and oxygen, and has been used together with various materials to attain properties suitable for ophthalmic applications (artificial corneas,[34-37] contact lenses).[38,39] It has also been used as a vehicle for drug delivery applications.[37] Skin adhesives in which specific bio-materials or medical drugs are transported through the patch into the skin is another important area when using silicone materials.[40,41] Oxygen permeability of materials is enhanced by the addition of either fluoro- or siloxanyl-groups in the polymer design[18] and the copolymerzation of hydrophilic monomers and hydrophobic monomers can lead to the formation of self-reinforcing hydrogels.

There are many aesthetic benefits that silicone polymers can present for cosmetic applications, in either solid or liquid form, namely a silky smooth feel, gloss, improved substantivity, and rub-off or wash-off resistance (the latter is due to its hydrophobicity, which has been exploited in the area of sun screen applications), less tackiness, spreadability/wettability (due to less oiliness), lubricancy (more slippery), occlusivity and emolliency. Silicone polymers are generally odourless and colourless (with some exceptions).

PDMS has a low surface tension (PDMS, 20 dynes/cm; cf. benzene 28.9)[21] which allows it to spread easily over surfaces, and when coupled with other properties (*e.g.* low coefficient of friction) results in smooth, non-tacky aesthetic properties.[21] PDMS has lower surface tension than the skin, which causes it to wet, easily spread and adhere to skin. This property has resulted in silicon materials becoming an important consideration in the manufacture of pressure sensitive adhesives. Due to the fact that silicones are liquid at room temperature (except for silicone waxes) they can be processed fairly easily into a variety of forms, such as sticks for antiperspirants, creams for face, hands and body, as well as aerosols or foam formulations (pump systems). PDMS can also form thin films over substrates as well as spread over its own film. Of great importance in medical applications are silicone skin contact adhesives[33] which are gaining great attention as it is a means to gently attach adhesives to the skin that can deliver hydrophilic molecules to it. This ability is made possible by the mobile, open network of the dimethylsiloxane network which is hydrophobic and, in turn, can bind to skin. In addition, PDMS is relatively inert to non-aqueous materials as well as active ingredients used in pharmaceutical formulations. Studies have been performed on the release of the active ingredient ketoconazole from a polydimethylsiloxane environment showing that by the addition of certain ingredients (addition of 0.3–0.5% sodium bicarbonate-citric acid) to make the matrix less lipophilic, the ketoconazole will have less affinity for the hydrophobic siloxane and dissolve in the aqueous receptor medium.[33]

3.4   What are esters used for?

The polar nature of esters generally make them good products for detergents. They solubilize the oil products (grease or fats) deposited on a surface and remove them. In the personal care market a large variety of esters are used. Fats and oils are glyceryl esters of fatty acids and are found in animal and plant tissue. Examples include almond and avocado oil. Fatty esters (with a straight alkyl chain, *e.g.* C_8–C_{12}) are widely used as emollients, emulsifiers, surfactants, preservatives, conditioners and opacifiers. Polymers of acrylic esters (methyl-, butyl-, ethyl acrylate) are used in paints, coatings, textiles and adhesives. Other areas in which esters may be used include synthetic lubricants, plasticizers in medical vinyl gloves and children's toys (phthalate esters).

3.5   How do you synthesize esters?

Esterification (condensation reactions) are step polymerization reactions that proceed *via* a different mechanism to radical chain polymerizations. Esterification reactions are equilibrium reactions in which the use of a catalyst shifts the equilibrium towards product formation. There are numerous methods by which ester compounds can be synthesized, usually employing either acidic / basic conditions. If at all possible, the use of a catalyst-free reaction is preferable in order to follow a "green chemistry" protocol. The advantage of catalyst-free esterification is that, in the fields of food technology and cosmetics, the products may be introduced directly into formulations after synthesis. A disadvantage of using catalyst-free reactions is that a high yield usually requires high temperatures. When using catalysts, either acidic or basic, the use of lower temperatures, even room temperature, becomes viable. Various catalysts that may be used include Brønstead catalysts, Lewis acids, a mixture of diethyl azodicarboxylate (DEAD) and triphenylphosphine (The Mitsunobu reaction), 2-halo-1-methylpyridinium salts (*e.g.* *p*-toluenesulphonic acid), enzymes, as well as a mixture of DCC/DMAP. For more details on each of these types of catalytic methods, refer to the book by Otera.[42]

In its simplest terms, ester synthesis makes use of an alcohol functional compound. In the work described below, the direct esterification of PDMS-OH with a carboxylic acid CTA leads to coupling via the use of the dehydrating agent DCC, which shifts the equilibrium of the reaction towards product formation through complexation with the water byproduct that is formed in these types of reactions. Carbodiimides were reported in 1955 to represent an attractive route for the synthesis of peptides, and to date, the use of DCC[43] has been frequently reported in the literature as an attractive route for esterification reactions.[2-6,44-48] The advantages of using the DCC coupling agent include the ability to perform reactions under milder conditions compared to acid/base catalyzed reactions, as

well as the ease of performing reactions at room temperature. DCC catalyzed reactions are also not sensitive to the steric bulk of the reactants and hence they may be used to synthesize tertiary alcohols. [3] According to the known mechanism by which esterification takes place between alcohols and acids in the presence of DCC,[48] besides the main process, the competing side reaction of intramolecular rearrangement with formation of an *N*-acylurea occurs ((16) and (19) in Schemes 3.3 and 3.5 respectively).[1,6,42,47] After the reaction of excess carboxylic acid with excess DCC the very reactive *O*-acylurea ((15) and (18) in Schemes 3.3 and 3.5 respectively) reacts with the carboxylate, acting as a nucleophile, to form the predominantly symmetrical anhydride intermediate ((17) and (20) in Schemes 3.3 and 3.5 respectively). The side reaction referred to above is a base-catalyzed acyl migration from the isourea oxygen to nitrogen; the *N*-acylurea does not undergo further hydrolysis.[1] Its formation is driven presumably by the basic carbodiimide moiety. The catalyst DMAP ((21) in Scheme 3.6) reacts with the anhydride to form an acylpyridinium carboxylate ion pair (22), which in turn reacts with the alcohol to yield the ester compound ((11b) in Scheme 3.6), regenerated DMAP (21), insoluble DHU (which is insoluble in most organic solvents except alcohols)[49] and carboxylic acid ((10a) and (10b)) which is recycled by DCC to form more anhydride. The formation of the *N*-acylurea can however be suppressed by the use of catalytic amounts of *p*-aminopyridines (*e.g.* DMAP (21)).[42]

3.6   Synthesis of PDMS macroCTAs

3.6.1   Experimental

3.6.1.1   Materials

The following materials were used as received: polydimethylsiloxane [480355] (PDMS) (Aldrich, monohydroxy terminated, $\overline{},M_n \approx 4670$ g/mol), calcium chloride [10043-52-4] (Saarchem), 1,3-dicyclohexylcarbodiimide (DCC) [538-75-0] (Aldrich, 99%), magnesium [7439-95-4] (Aldrich, 98%), bromobenzene [108-86-11] (Acros, 99%), carbon disulphide [75-15-0] (CS_2) (Aldrich, 99.9%), 4,4'-Azobis(4-cyanovaleric acid) [2638-94-0] (Aldrich, +75%), HCl [7647-010] (Saarchem, 32%), diethylene glycol methyl ether [111-77-3] (Aldrich, 99%), 4-(dimethylamino)pyridine (DMAP) [1122-58-3] (Aldrich, 99%). Hexane [110-54-3] (Merck, 96%) and dichloromethane (DCM) [75-09-2] (Merck, 96%) were distilled prior to use. Chloroform [67-766-3] (Merck, >99.8%), dimethyl sulfoxide [67-68-5] (Merck, >99%), ethyl acetate [141-78-6] (Merck, 98%), pentane [109-66-0] (Merck, 75%), toluene [108-88-3] (Merck, 98.5%), acetone [67-64-1] (Merck, >96%), acetonitrile [75-05-8] (Merck, >99%), methanol [67-56-1] (Merck, 99%), ethanol [64-17-5] (Merck,

99%) and deuterated chloroform (C_6D_6, 99.6%, 0.1% TMS, Aldrich) were used as received. Silica packing material (Macherey-Nagel, Kieselgel 60) was used for column chromatography.

3.6.1.2 Esterification procedure

The following was a general method that was used for all esterification reactions performed in this study. All glassware used was dried in an oven overnight. The carboxylic acid (CTA), carbodiimide activator (DCC), alcohol (PDMS), and solvent were introduced into a 50mL round-bottom flask equipped with a magnetic stirrer. In addition to the above, a catalyst (DMAP) was added to the round-bottom flask. The contents were immediately sealed with an anhydrous calcium chloride tube and allowed to stir at room temperature. For the reactions performed above room temperature, the flask was fitted with a condenser. After the desired reaction time the solution was filtered to remove the unreacted 1,3-dicyclohexylurea (DCU) precipitate and the solvent removed *in vacuo* after which a sample was submitted for ^{1}H- and ^{13}C-NMR spectroscopy in order to determine the conversion. The product was a clear, bright yellow solution.

3.6.1.3 Analyses and sample preparation

Conversion: ^{1}H-NMR and ^{13}C-NMR spectra were recorded on a Varian VXR 300MHz and a Varian Unity Inova 400MHz NMR spectrometer, respectively, to measure the extent of conversion of the unreacted PDMS. The analyses were performed at room temperature using $CDCl_3$. The peaks used to identify the formation of the PDMS macroCTA ester bond in the NMR spectra were the methylene peaks of PDMS with chemical shifts at: PDMS macroCTA (11a) – (^{1}H, ref $CDCl_3$ at 7.26ppm) 4.25, 3.62 and 3.41ppm (A, B and C respectively in Scheme 3.1), (^{13}C, ref $CDCl_3$ at 77.0ppm) 64.1, 68.4 and 74.2ppm (A, B and C respectively in Scheme 3.1); PDMS macroCTA (11b) - (^{1}H, ref $CDCl_3$ at 7.26ppm) 4.25, 3.62 and 3.41ppm (A, B and C respectively in Scheme 3.4), (^{13}C, ref $CDCl_3$ at 77.0ppm) 65.1, 68.2 and 74.1ppm (A, B and C respectively in Scheme 3.4). The unreacted methylene peak counterparts in the NMR spectra for PDMS occur at: (^{1}H, ref $CDCl_3$ at 7.26ppm) - 3.72, 3.52 and 3.43ppm (A', B' and C' respectively in Schemes 3.1 and 3.4), (^{13}C) 61.9, 71.7 and 74.1ppm (A', B' and C' respectively in Schemes 3.1 and 3.4). Take note: impurities in the spectrum of PDMS (^{1}H, ref $CDCl_3$ at 7.26ppm) were identified at 6.1(s), 3.8 (t) and 3.48ppm. Refer to Appendix 1 for chemical shift values of PDMS. Usually, the most easily identifiable methylene peak in the ^{1}H-NMR spectrum was peak A as this chemical shift was far from its unreacted counterpart as well as other species. For these reasons, when overlapping of peaks B (B') or C (C') rendered

integration thereof an exhaustive exercise, peaks A and A' were used in determining conversion. Side reactions often cannot be completely avoided in many syntheses; therefore, the existence of relatively small unknown peaks was not a major concern for the author as they could possibly be removed in the purification step.

Infrared spectroscopy (IR): Infrared spectra were recorded on a Nexus™ Nicolet spectrometer from Thermo. Samples were analysed using NaCl windows and either CHCl$_3$ or THF as solvent. In order to determine specific IR absorption bands for the various samples the liquid or solid samples were dissolved in a solvent of choice (either THF or CHCl$_3$) and directly analyzed by IR spectroscopy (after subtracting the solvent as background).

Molecular weight analyses (relative). Molecular weights were determined using size exclusion chromatography (SEC). This chromatographic technique separates polymer molecules according to size, or more correctly hydrodynamic volume. Depending on whether the chromatographic medium is a gel or not, the technique is also referred to as gel permeation chromatography (GPC). Samples were prepared for SEC analysis by drying the liquid sample *in vacuo* for 12–18 hours and then weighing off ~10mg of the sample and dissolving in 3mL HPLC grade THF (0.012% BHT). The solution was then filtered through a 0.2µm filter and then submitted for SEC analysis. UV wavelengths used to analyze samples were 254nm and 320nm as the thiocarbonylthio moiety absorbs at these wavelengths. The SEC instrument consisted of a Waters 717 plus Autosampler controller, and a Waters 1515 Isocratic HPLC pump. A Waters 2414 differential refractometer detector as well as a dual λ absorbance detector were used at 30°C. The SEC was calibrated with ten narrow MWD Polymer Laboratories polystyrene (PSt) Easivial Standards, with a molecular weight range of 580 g/mol to 3 000 000 g/mol. HPLC THF (containing 0.012% BHT was used as mobile phase at a flow rate of 1mL/min. Separation was achieved using two PLgel (Polymer Laboratories) 5µm Mixed-C (300×7.5mm) columns connected in series along with a PLgel 5µm guard column (50×7.5mm). The columns were kept at a constant temperature of 30°C, the injection volume was 100µL and the analysis ran for 30 minutes per sample. Data processing was performed using Breeze Version 3.30 SPA (Waters) software.

3.6.1.4 Synthesis of chain transfer agents (CTAs)

CTA (10a): 3-(((Benzylthio)carbonothioyl)thio)propanoic acid was synthesized and purified according to a procedure described by Stenzel *et al.*[50] According to NMR, the yellow powder produced a yield of 65% and purity estimated to be >94%. ^{1}H-NMR (CDCl$_3$,

300 MHz, δ (ppm)): 7.31 (m, *Ar*), 4.61 (s, S-C*H₂*-Ar), 3.62 (t, CH₂-C*H₂*-S), 2.84 (t, C*H₂*-CH₂-S). ¹³C-NMR (CDCl₃, 300 MHz, δ (ppm)): 222.1 (C=S), 176.5 (C=O), 134.7 (Ph), 127.8–129.2 (Ph), 41.54 (CH₂-Ph), 32.90 (CH₂-CH₂), 30.82.

IR (NaCl) (CHCl₃, units = cm⁻¹): 2927, 1712, 1495, 1454, 1424, 1066; (THF): 2971, 1365.

CTA (10b): 2-(Dodecylsulfanyl)thiocarbonylsulfanyl-2-methyl propionic acid was synthesized according to the procedure described by Lai *et al.*[51] According to NMR, purity was estimated to be >88%.

¹H-NMR (CDCl₃, 300 MHz, δ (ppm)): 3.27 (t, S-C*H₂*), 1.71 (s, (C*H₃*)₂), 1.25 (m, (C*H₂*)ₙ), 0.87 (t, C*H₃*). ¹³C-NMR (CDCl₃, 300 MHz, δ (ppm)): 222.3 (C=S), 179.0 (C=O), 55.9 (C), 36.9 (S-*CH₂*), 31.7 (S-CH₂-*CH₂*), 29.5 (m, (*CH₂*)ₙ), 27.6 (S-CH₂-CH₂-*CH₂*), 25.1 (*CH₂*-CH₃), 22.5 ((*CH₃*)₂), 13.9 (*CH₃*).

IR (NaCl) (CHCl₃, units = cm⁻¹): 3430, 2926, 2854, 1705, 1653, 1467, 1284, 1175, 1130, 1067, 816, 768, (THF): 2972, 1459.

3.6.2 Results and discussion

3.6.2.1 Investigation of the stoichiometric <u>molar ratios</u> required for converting PDMS into the PDMS macroCTA (11a) with high conversion.

The following investigations were performed using CTA (10a) and all reactions were performed under reflux using anhydrous chloroform. Refer to Table 3.1 for a description of experimental conditions as well as Table 3.2 for ¹H- and ¹³C-NMR chemical shift and integration values. Scheme 3.1 is a simplified reaction scheme of experiments A–D indicating the peak labels that were used to identify specific chemical shifts in the NMR spectra.

Table 3.1 **Experimental conditions for experiments A–D. All reactions were performed using CTA (10a) in chloroform under reflux.**

Experiment	CTA (#)	OH:CTA:DCC	[OH] (mmol/L)	[CTA] (mmol/L)	[DCC] (mmol/L)	Solvent (wt%)	Time (h)	Conversion (%)
A	10a	1.0 : 1.1 : 1.1	26	29	29	87	72	< 40
B	10a	1.0 : 1.1 : 1.0	117	129	116	95	72	100
C	10a	1.0 : 2.9 : 2.9	49	139	138	80	72	62
D	10a	1.0 : 3.0 : 3.1	71	211	218	70	120	100

Hypothesis 1:

"A <u>similar</u> molar ratio of PDMS, CTA and DCC would be sufficient to produce a high degree of conversion for the PDMS macroCTA".

This was the starting point for the reactions to come. It was needed to know whether stoichiometric amounts, or an excess, would be necessary for the complete conversion of PDMS into an ester.

Experiment A

The experiment was refluxed for 72 hours after which the solution of the crude reaction product was passed through a vacuum filter. A sample was analyzed by ^{1}H- and ^{13}C-NMR spectroscopy in order to determine conversion. It was not reliable to integrate the methylene peaks in the ^{1}H-NMR spectrum as there was considerable overlapping. It could however be approximated in the ^{13}C-NMR spectrum, according to the heights of the relevant peaks (A (A'), B (B') and C (C') in Scheme 3.1) that only less than 40% of the PDMS reacted. Therefore, this hypothesis is false. It is not possible to obtain high conversions when using PDMS (9) and a similar molar ratio of CTA (10a).
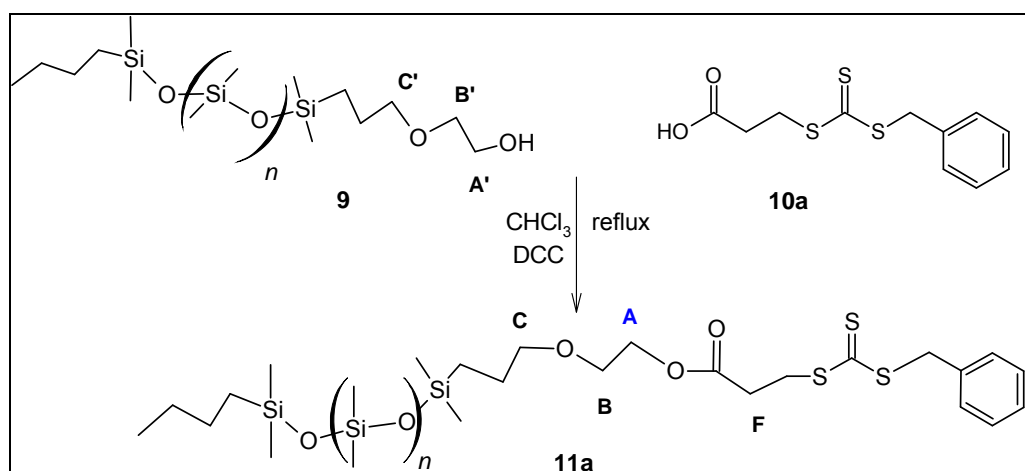
Scheme 3.1   **Simplified reaction scheme for esterification between PDMS (9) and CTA (10a) in the presence of DCC (12) (experiment A).**

Table 3.2   Specific chemical shift and integration values for experiments A–D.

Experiment		Signal (ref. Scheme 3.1)	Chemical shift (ppm)		Integration values[#]	
			Unreacted (')	Reacted	Unreacted (')	Reacted
A	^{13}C-NMR	A	*61.9*	**64.1**		
		B	*71.8*	**68.1**		
		C	*74.1*	**73.9**		
B	^{13}C-NMR	A	*61.1*	**63.9**		
		B	*72.3*	**69.0**		
		C	*69.8*	**70.5**		
		D	*71.5*	**71.9**		
		E	*58.5*	**58.9**		
C	^{1}H-NMR	A	*3.73*	**4.25**	*121*	**200**
		B	*3.53*	**3.62**	*124*	******
D	^{13}C-NMR	A		**64.1**		
		B		**68.4**		
		C		**74.2**		

** difficult to integrate these values due to overlapping

only integration values for ^{1}H-NMR were determined and reported

Hypothesis 2:

"A <u>similar</u> molar ratio of diethylene glycol methyl ether (13), CTA and DCC would be sufficient to produce a high degree of conversion"

In order to substantiate the outcome of the previous hypothesis, a model reaction of a short chain alcohol was performed in order to determine whether the bulky nature of the PDMS would render steric effects a possible explanation for incomplete conversion to an ester. If the same reaction conditions are applied as reaction A, but this time using a shorter chain length alcohol, obtaining a higher conversion would lead us to believe that the large size of PDMS causes it to react more slowly than a shorter alcohol would during the esterification process.

Experiment B

The experiment was refluxed for 72 hours after which the solution of the crude reaction product was passed through a vacuum filter. A sample was analyzed by ^{1}H- and ^{13}C-NMR spectroscopy in order to determine conversion.

The ^{1}H-NMR spectrum displayed overlapping of the peaks, therefore integration values could not accurately be calculated. The ^{13}C-NMR spectrum indicated that there was no trace of any unreacted methylene peaks (refer to Table 3.1 for experimental conditions and Table 3.2 for specific chemical shift values) (Scheme 3.2, peaks A'–E'). In conclusion, the second hypothesis is true. The model reaction demonstrated that full conversion of the

alcohol is possible with a slight excess of CTA. The following experiment, reaction C, investigates the use of an *excess* of CTA on the degree of PDMS conversion to an ester.
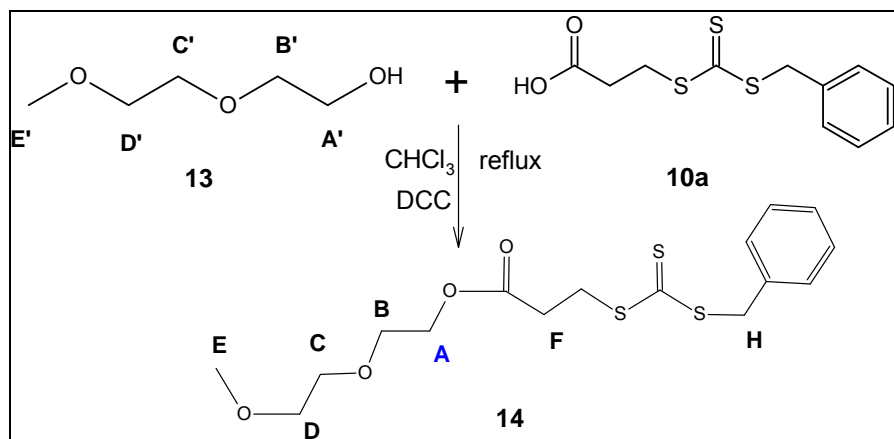
Scheme 3.2 **Simplified reaction scheme for esterification between diethylene glycol methyl ether (13) and CTA (10a) in the presence of DCC (12) (experiment B).**

Hypothesis 3:
 "Over a period of 72 hours, an <u>excess</u> molar ratio of CTA and DCC, with respect to the alcohol, is required when using PDMS as the starting alcohol in order to produce a high degree of conversion for the PDMS macroCTA".

Since experiment A showed signs of very little conversion, and experiment B indicated full conversion, it would appear that it is necessary, when using PDMS (9), that an excess of starting materials is necessary.

Experiment C

The experiment was refluxed for 72 hours after which the solution of the crude reaction product was passed through a vacuum filter. A sample was analyzed by ^{1}H- and ^{13}C-NMR spectroscopy in order to determine conversion. The ^{1}H- and ^{13}C-NMR spectra produced the chemical shifts as depicted in Table 3.2 (refer to Table 3.1 for experimental conditions). The average value determined for the conversion of PDMS (9) to its ester counterpart was 62%, and was determined as follows: the integration values obtained for methylene peak A' (representing the unreacted counterpart) and methylene peak B' (representing the unreacted counterpart) were averaged, thereby providing an integration value of 122.5. The reacted methylene signal (peak A) was set to a value of 200 which was divided by itself as well as the average value of the unreacted counterparts (refer to equation (3.1)).

$$\left[\frac{\int A' + \int B'}{2}\right] = \frac{121 + 124}{2} = 122.5$$

$$\frac{\int A}{\int A + [ave \int A' \& \int B']} = \frac{200}{200 + 122.5} = \frac{200}{322.5} = 62\% \qquad (3.1)$$

Compared to experiment A, in which similar molar ratios were used, a much higher degree of conversion was obtained in experiment C. In conclusion, the hypothesis tested is true. The molar ratio used was dependent on the size of the alcohol used. The reasons for this can be attributed to steric effects. It is postulated that due to the bulky nature of PDMS, it would render the esterification process slow, or incomplete, compared to when using shorter chain alcohols which can easily 'find' the CTA. Therefore, it is advisable to use an excess of CTA (10a) when attempting to esterify PDMS (9).

Even though an excess of CTA (10a) was used, full conversion of PDMS (9) was not yet achieved. The next section investigates the effects of *time* on the esterification of PDMS.

3.6.2.2   Investigation of the <u>time</u> required for converting PDMS into the PDMS macroCTA (11a) with high conversion.

As described in Section 3.6.2.1 (hypothesis 3), when using a large compound such as PDMS (9) an excess of CTA/DCC is required to obtain a high yield of ester when performing the esterification reaction over a period of 72 hours. The effect of time on a PDMS esterification was therefore thought to perhaps also play a role. Refer to Table 3.1 for experimental conditions as well as Table 3.2 for specific chemical shift and integration values in the ^{1}H- and ^{13}C-NMR spectra.

Hypothesis 4:
"Even when using an <u>excess</u> of CTA, a <u>longer reaction time</u> is still required when using PDMS as starting material than when using a shorter alcohol".

Experiment D

The experiment was refluxed for 120 hours after which the solution of the crude reaction product was passed through a vacuum filter. A sample was analyzed by ^{1}H- and ^{13}C-NMR spectroscopy in order to determine conversion. The ^{1}H-NMR spectrum showed the shifts as depicted in the Table 3.2. Scheme 3.3 provides an illustration of the proposed reaction mechanism when using PDMS (9), CTA (10a) and DCC (12).

It was not possible to use the ^{1}H-NMR spectrum to determine conversion as there was significant overlapping of reacted and unreacted counterpart methylene peaks. However, the ^{13}C-NMR spectrum showed no signs of any unreacted species, which allows the author to conclude that this reaction proceeded to 100% conversion. It is therefore concluded that this hypothesis is true. Even when an excess of CTA (10a) is used with PDMS (9) (as was proven necessary in the previous section), a longer time is still deemed necessary. The reason can be the bulky nature of PDMS, which would cause the esterification reaction to proceed at a slower rate compared to smaller alcohols.

3.6.2.3   Summary of variables investigated with respect to optimization of esterification reaction conditions when using PDMS.

Table 3.3 summarizes the focus of the previous four experiments (A–D). A model experiment using similar molar ratios of starting materials was performed using a smaller alcohol, diethylene glycol methyl ether (13), which produced an ester compound with full conversion. This was not the case when using PDMS (9). It is postulated that due to the large size and nature of PDMS, steric effects could play a role in the efficient formation of the ester. Therefore, when using PDMS (9) the use of excess acid/DCC is required if high yields are desired. In addition to using excess reagents, a reaction time of 120 hours was found to be required when using PDMS (9) as the alcohol.

Table 3.3   Description of each hypothesis and the results from the experiments performed using PDMS (9), CTA (10a) and DCC (12) in order to synthesize PDMS macroCTA (11a).

Hypothesis	Description	% Conversion of PDMS	Accept hypothesis	Reject hypothesis
1	A similar molar ratio of PDMS, CTA and DCC would be sufficient to produce a PDMS macroCTA in high yield.	<40		X
2	A similar molar ratio diethylene glycol methyl ether, CTA and DCC would produce a PDMS ester compound in high yield.	100	X	
3	Over a period of 72 hours, an excess molar ratio of CTA and DCC is required when using PDMS as the starting alcohol in order to produce a PDMS macroCTA in high yield.	62	X	
4	Even when using an excess of CTA, a longer reaction time is still required when using PDMS as starting material than when using a shorter alcohol.	100	X	
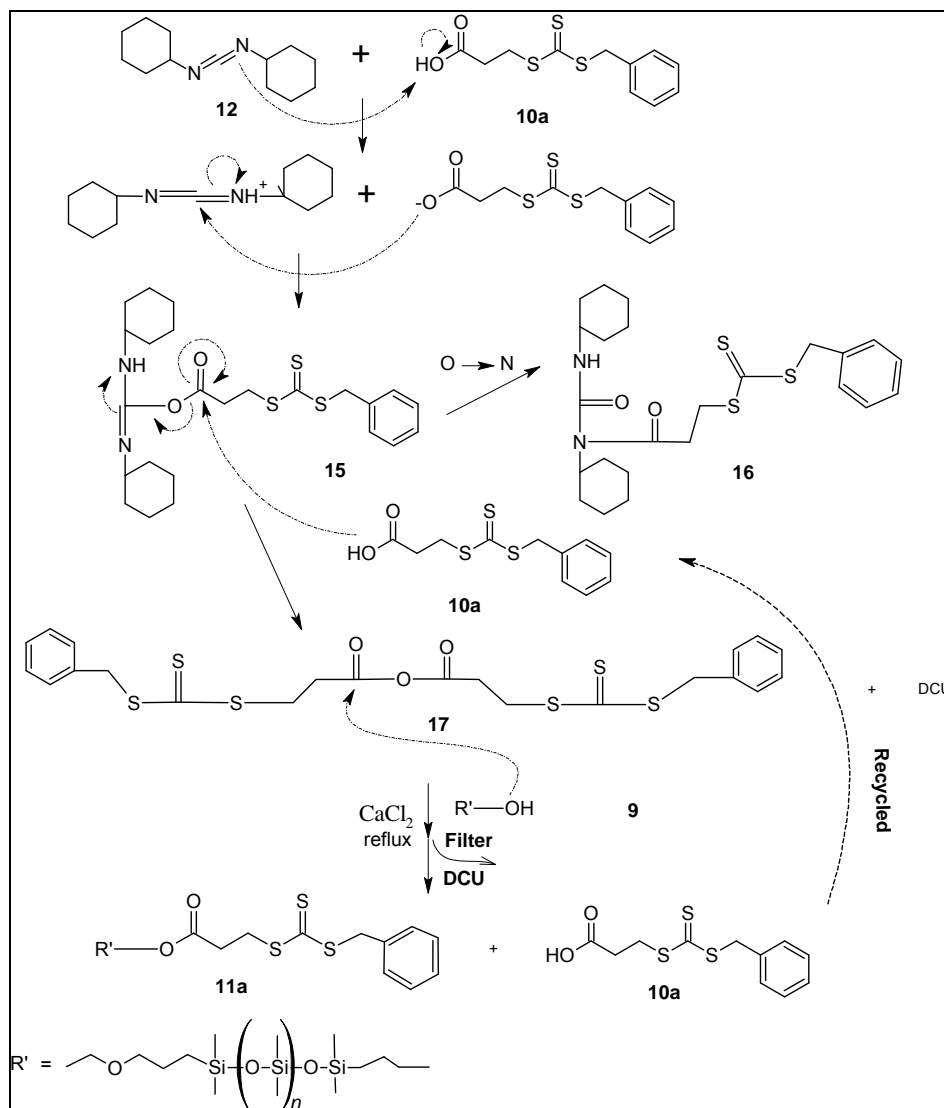
Scheme 3.3. Reaction mechanism for esterification between PDMS (9) and CTA (10a) in the presence of DCC (12) (experiment C).

3.6.2.4   Synthesis of a second trithio-PDMS macroCTA

Having established that excess CTA/DCC and longer reaction times (120 hours) are required when synthesizing the PDMS macroCTA (11a), it was desirable to repeat conditions in order to synthesize another trithio-PDMS macroCTA (11b). Refer to Table 3.4 for experimental conditions as well as Table 3.5 for specific chemical shift and integration values in the ^{1}H- and ^{13}C-NMR spectra of experiment E.

Experiment E

This experiment involved the esterification of CTA (10b) with PDMS (9). The reaction was refluxed for 120 hours in CHCl$_3$, after which the solution of the crude reaction product was passed through a vacuum filter. A sample was analyzed by ^{1}H- and ^{13}C-NMR spectroscopy in order to determine conversion. Refer to Scheme 3.4 for NMR peak labels.

Scheme 3.5 provides an illustration of the proposed reaction mechanism when using PDMS (9), CTA (10b) and DCC (12). Figure 3.2 compares the ^{1}H-NMR spectra of unreacted PDMS with that of its reacted ester counterpart. There does appear to be unreacted methylene peaks B' and A' present at 3.53 and 3.73ppm respectively.

Table 3.4   Experimental conditions for experiments E–I.

E	CTA (#)	OH:CTA:DCC:DMAP	[OH] mmol/L)	[CTA] (mmol/L)	[DCC] (mmol/L)	[DMAP] (mmol/L)	S*	S	Time (h)	T (^{o}C)	C (%)
E	10b	1.0 : 3.0 : 3.1 : 0	71	212	218	-	69	CHCl$_3$	120	reflux	96
F	10b	1.0 : 1.8 : 1.8 : 0.1	65	118	118	6.5	71	DCM	30	30	100
G	10b	1.0 : 1.8 : 1.8 : 0.5	65	117	118	19	71	DCM	5	30	74
H	10b	1.0 : 1.8 : 1.8 : 0.1	65	117	117	6.5	71	DCM	8	30	98
I	10b	1.0 : 1.8 : 1.8 : 0.1	65	117	117	6.5	71	DCM	10	30	100

E = experimental

S* = solvent wt%

S = solvent

T = temperature

C = conversion
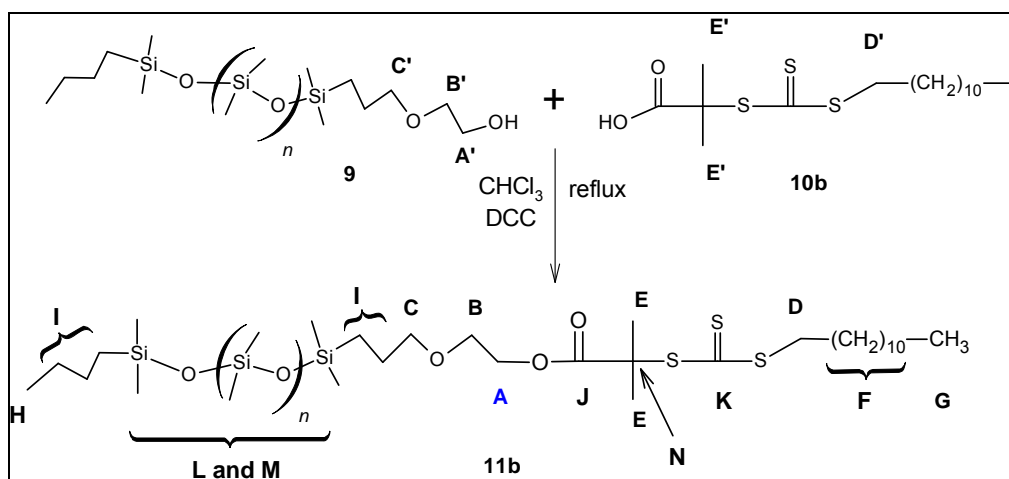
Scheme 3.4   Structure of PDMS macroCTA (11b).

67
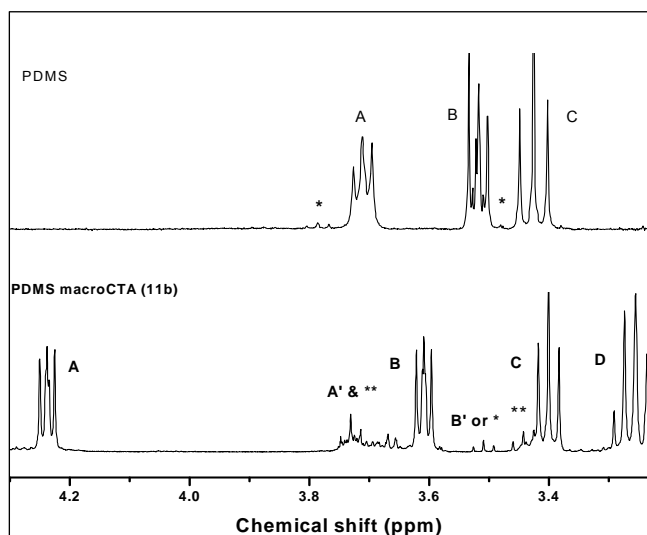
Figure 3.2 **¹H-NMR spectra of unreacted PDMS (9) and the PDMS macroCTA (11b) of reaction E. Reference signal is CDCl₃ at 7.26ppm. (* impurity as found in PDMS, ** unknown side product peaks.)**

In both the ¹H- and ¹³C-NMR spectra there was a clear indication of unreacted peaks. Refer to Table 3.1 for a list of unreacted methylene peaks found to be present. According to the author, the conversion of PDMS into ester was 96%. Equation (3.2) shows how this value was calculated. In this case, integrals A and B' were used in the same equation as an assumption was made that methylene peaks A and B would undergo the same extent of reaction.

$$\frac{\int A}{\int A + \int B'} = \frac{200}{200+9} = \frac{200}{209} = 96\% \tag{3.2}$$

The ¹H-NMR (Figure 3.2) and ¹³C-NMR (not shown) spectra indicate that the conversion of PDMS (9) to its ester counterpart was at least 96%. Reacted ester proton and carbon signals (peak A, B and C) are present at (¹H) 4.25, 3.63 and 3.42ppm, and (¹³C) 74.1, 68.2 and 65.1ppm, respectively.
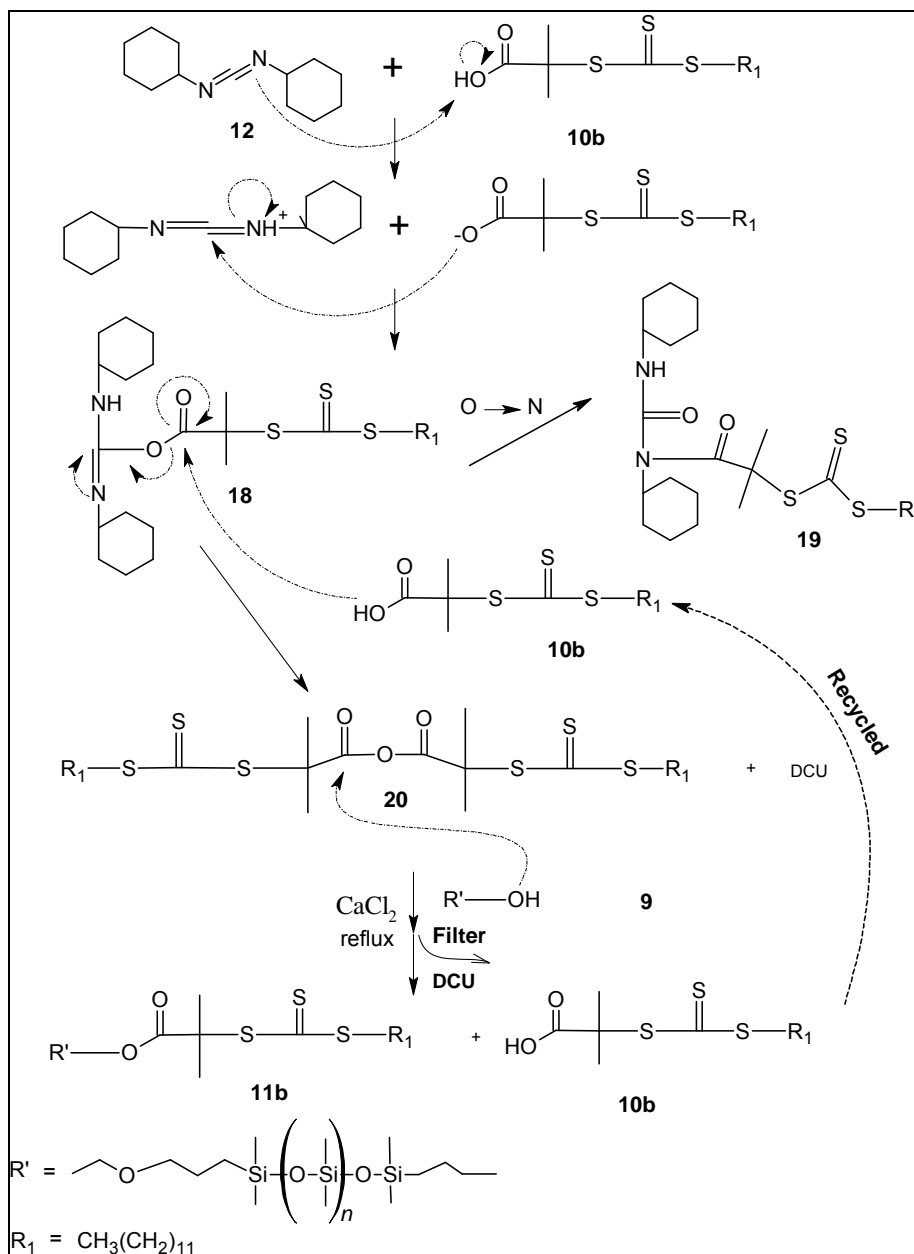
Scheme 3.5 **Reaction mechanism for esterification between PDMS (9) and**

CTA (10b) in the presence of DCC (12) (experiment E).

Table 3.5   **Specific chemical shift and integration values for experiments E–I.**

Reaction		Signal (ref. Scheme 3.4)	Chemical Shift (ppm)		Integration values		Final conversion (%)
			Unreacted (')	Reacted	Unreacted (')	Reacted	
E	^{1}H-NMR	A		4.25		200	96
		B	*3.52*	3.62	*9*	200	
		C		3.41		**	
		D		3.26		**	
	^{13}C-NMR	A		74.1			
		B		68.2			
		C		65.1			
F	^{1}H-NMR	A	*3.73*	4.25	*2.8*	200	100
		B		3.62		201	
		D		3.27		360*	
	^{13}C-NMR	A		65.1			
		B		68.2			
		C		74.1			
G (5 h)	^{1}H-NMR	A	*3.72*	4.24	*69*	200	74
		B	*3.52*	3.61	**	**	
		C		3.41	**	**	
		D		3.26	**	470*	
	^{13}C-NMR	A	*61.9*	65.1			
		B	*71.6*	68.2			
		C	*74.1*	74.1			
H (7.5h)	^{1}H-NMR	A	*3.73*	4.25	*3.8*	200	98
		B		3.62	**	200	
		C		3.41	**		
		D		3.26			
	^{13}C-NMR	A	*61.5*	65.1			
		B	*71.8*	68.2			
		C	*74.1*	74.1			
I (10h)	^{1}H-NMR	A		4.25		200	>99
		B		3.62		204	
		C		3.41		338	
	^{13}C-NMR	A		65.1			
		B		68.2			
		C		74.1			

* this value accounts exactly for unreacted as well as reacted species.

**difficult to integrate due to overlapping of peaks.

3.6.2.5 Improved procedure for synthesizing PDMS macroCTAs

A value of greater than 96% for the conversion of PDMS (9) to the PDMS macroCTA ((11a) and (11b)) described in Sections 3.6.2.1, 3.6.2.2 and 3.6.2.4 was not reproducible with successive attempts. Conversion of unreacted alcohol varied between 30% and 100% on numerous occasions. A simple, convenient and reliable procedure was desired. The following reactions make use of the widely used nucleophilic base catalyst DMAP, often used as a catalyst in esterification reactions.[52-54] The following reactions had

significantly improved reaction yields (≥96%) with ensured repeatability, compared to those reactions performed without the use of DMAP. DMAP was essential in this reaction system in order to reduce reaction times and temperatures. Synthesis by DCC/DMAP coupling under the reaction conditions employed as described in this section resulted in the PDMS ester-containing macroCTA as the main product.

Experiment F

Compared to the reactions described in the previous sections (Sections 3.6.2.1–3.6.2.4), this reaction makes use of the nucleophilic base catalyst DMAP. It has been reported that diimides can react directly with amines (such as DMAP), but the coupling reaction of the DMAP to the carbonyl ((18) in Scheme 3.7) is typically much faster.[49] Directly coupling of the amine may occur when an excess of amine is used. Reaction time is expected to decrease significantly, even when only using catalytic amounts of DMAP.

The reaction was run for 30 hours at room temperature after which a solution of the crude reaction product was passed through a vacuum filter in order to remove the insoluble white urea precipitate (DCU). A sample was analyzed by ^{1}H- and ^{13}C-NMR in order to determine conversion. Refer to Table 3.4 for experimental conditions. Scheme 3.6 provides an illustration of the proposed reaction mechanism when using PDMS (9), CTA (10b) and DCC (12). The ^{1}H-NMR spectrum produced the shifts as depicted in Table 3.5. Figure 3.3 compares the ^{1}H-NMR spectra of unreacted PDMS with that of its reacted ester counterpart.
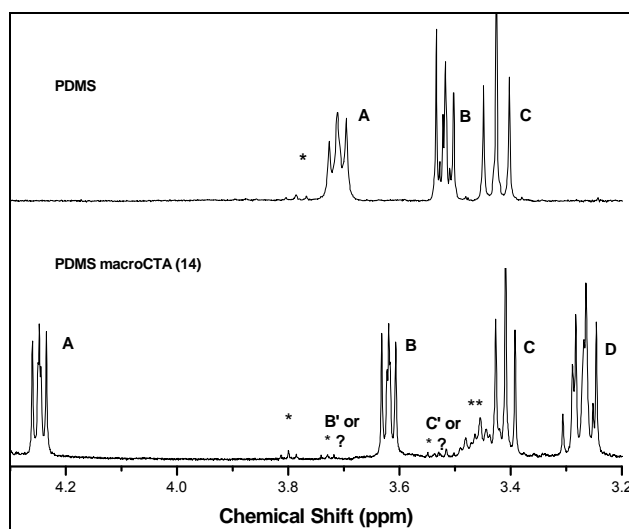
Figure 3.3   [1]**H-NMR spectra of unreacted PDMS (9) and the PDMS macroCTA (11b) of experiment F. Reference signal is CDCl₃ at 7.26ppm. (* impurity as found in PDMS, ** unknown side product peaks.)**
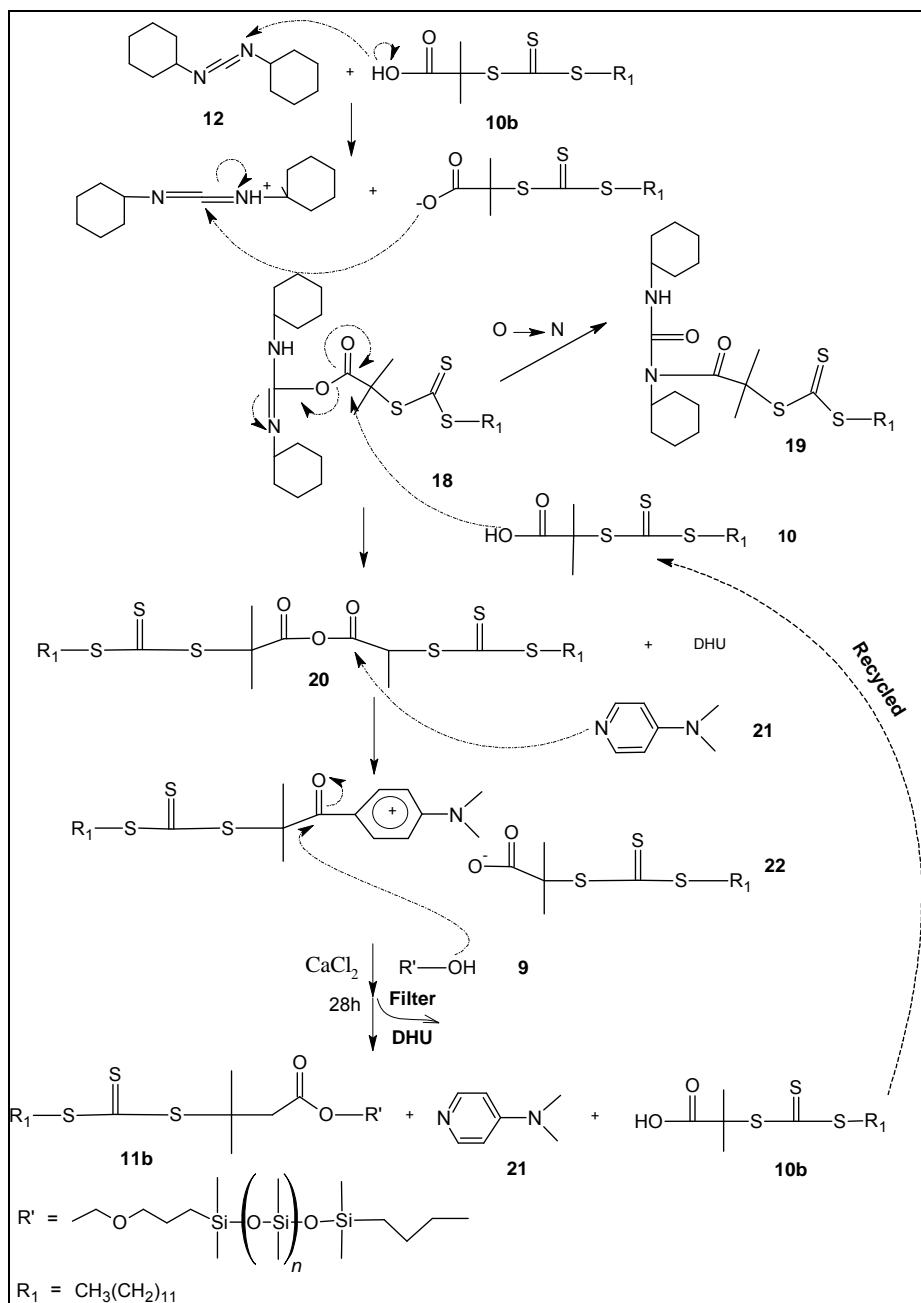
Scheme 3.6 **Reaction mechanism for esterification between PDMS (9) and CTA (10b) in the presence of DCC (12) and DMAP (21) (catalytic amount) (experiment F).**

There appears to be species present at 3.53 and 3.73ppm. These values are approximating that of unreacted methylene peaks B' and A' respectively, although it is possible that these peaks could be due to impurities or side products belonging to the PDMS (9) starting material (Sigma claimed the purity of the material to be ~85%). The ^{13}C-NMR of the unreacted PDMS and PDMS macroCTA (11b) is compared in Figure 3.4. There is no clear indication of any unreacted methylene peaks present in the PDMS macroCTA (11b), although it must be taken into consideration that the sensitivity of ^{13}C-NMR is not as sensitive as that of ^{1}H-NMR.

At a conservative approach, when considering the species corresponding to the peaks at 3.53 and 3.73ppm to be the unreacted methylene peaks B' and A', the conversion of PDMS would then be ≥96%.
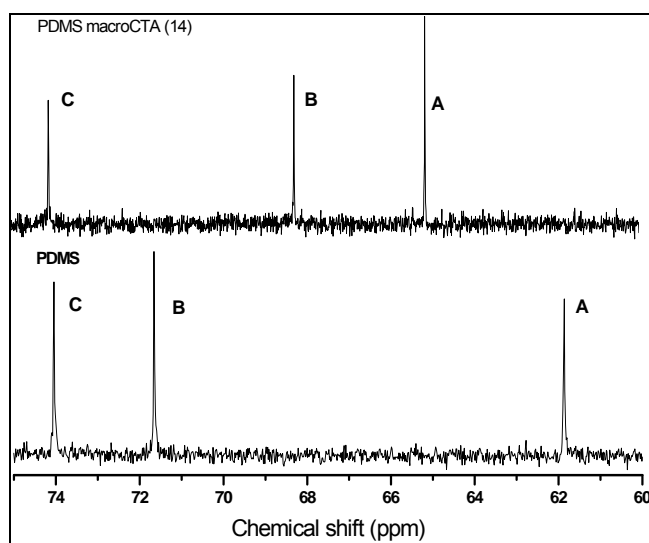
Figure 3.4   **^{13}C-NMR spectra of unreacted PDMS (9) and the PDMS macroCTA (11b) of experiment F. Reference signal is CDCl$_3$ at 77.0ppm.**

3.6.2.6   Investigation of the [DMAP]

According to the literature, when an excess of DMAP is used, the ester is formed in greater yield compared to when catalytic amounts are used.[47] It was therefore important to investigate the effect of a higher concentration of DMAP (reaction G).

Refer to Scheme 3.6 for the designation labels of the relevant compounds. It is known that a larger concentration of DMAP (21) accelerates the acylation of the alcohol by the acylpyridinium-dicyclohexyl uronium ion pair (22). In addition, use of a higher concentration of DMAP will facilitate the direct attack of DMAP (21) on the *O*-acylurea (18), bypassing the anhydride formation and resulting in the acylpyridinium carboxylate ion pair (23). Both these processes should contribute to increasing the yield of the ester compared to the *N*-acylurea (19).[47] Hence, the following reaction was carried out which employs the same molar ratios and temperature as the previous reaction (reaction F), but makes use of a larger concentration (5 times more) of DMAP. A larger catalyst concentration should allow the reaction to proceed at a faster rate, therefore, this reaction was run for 5 hours.

Experiment G

The experiment was run for 5 hours after which the solution of the crude reaction product was passed through a vacuum filter. A sample was analyzed by ^{1}H- and ^{13}C-NMR spectroscopy in order to determine conversion. Refer to Scheme 3.4 for NMR peak labels and Tables 3.4 and 3.5 for experimental conditions and specific chemical shift values respectively. Scheme 3.7 is a proposed reaction mechanism for the esterification process when an excess of DMAP is used. Take note: the reaction proceeds slightly differently to when a catalytic amount of DMAP is used (Scheme 3.6).

From the ^{13}C-NMR spectra (not shown), there was clear evidence of unreacted methylene peaks (Scheme 3.5, peaks A'–C') belonging to PDMS (9). The ^{1}H-NMR spectrum (not shown) also showed signs of unreacted methylene peak (1H, 3.72 (t), peak A'). From the integral values in the ^{1}H-NMR spectrum, equation (3.3) was used to calculate the conversion of PDMS (9) into its ester counterpart (11b).

$$\frac{\int A}{\int A + \int A'} = \frac{200}{200 + 69} = \frac{200}{269} = 74\% \tag{3.3}$$

3.6.2.7   Investigation of time using catalytic amounts of DMAP

The author wanted to determine whether experiment F, which made use of catalytic amounts of DMAP and running the reaction at room temperature for 30 hours, could be optimized. The following reactions look at the effects of time on the esterification of PDMS into its ester counterpart.

Experiment H

The experiment was run for 7.5 hours at room temperature after which a solution of the crude reaction product was passed through a vacuum filter in order to remove the insoluble white urea precipitate (DCU). A sample was analyzed by ^{1}H- and ^{13}C-NMR specctroscopy in order to determine conversion. Refer to Table 3.4 for experimental conditions. The NMR spectra produced the shifts as depicted in Table 3.5. There was clear evidence of unreacted methylene peaks (A'-C') present in the ^{13}C-NMR spectrum, and from the ^{1}H-NMR spectrum it could be calculated from the unreacted methylene peak A' that there was approximately only 98% conversion of the PDMS into its ester counterpart. This value was calculated according to equation (3.4).

$$\frac{\int A}{\int A + \int A'} = \frac{200}{200 + 3.8} = \frac{200}{203.8} = 98\% \qquad (3.4)$$
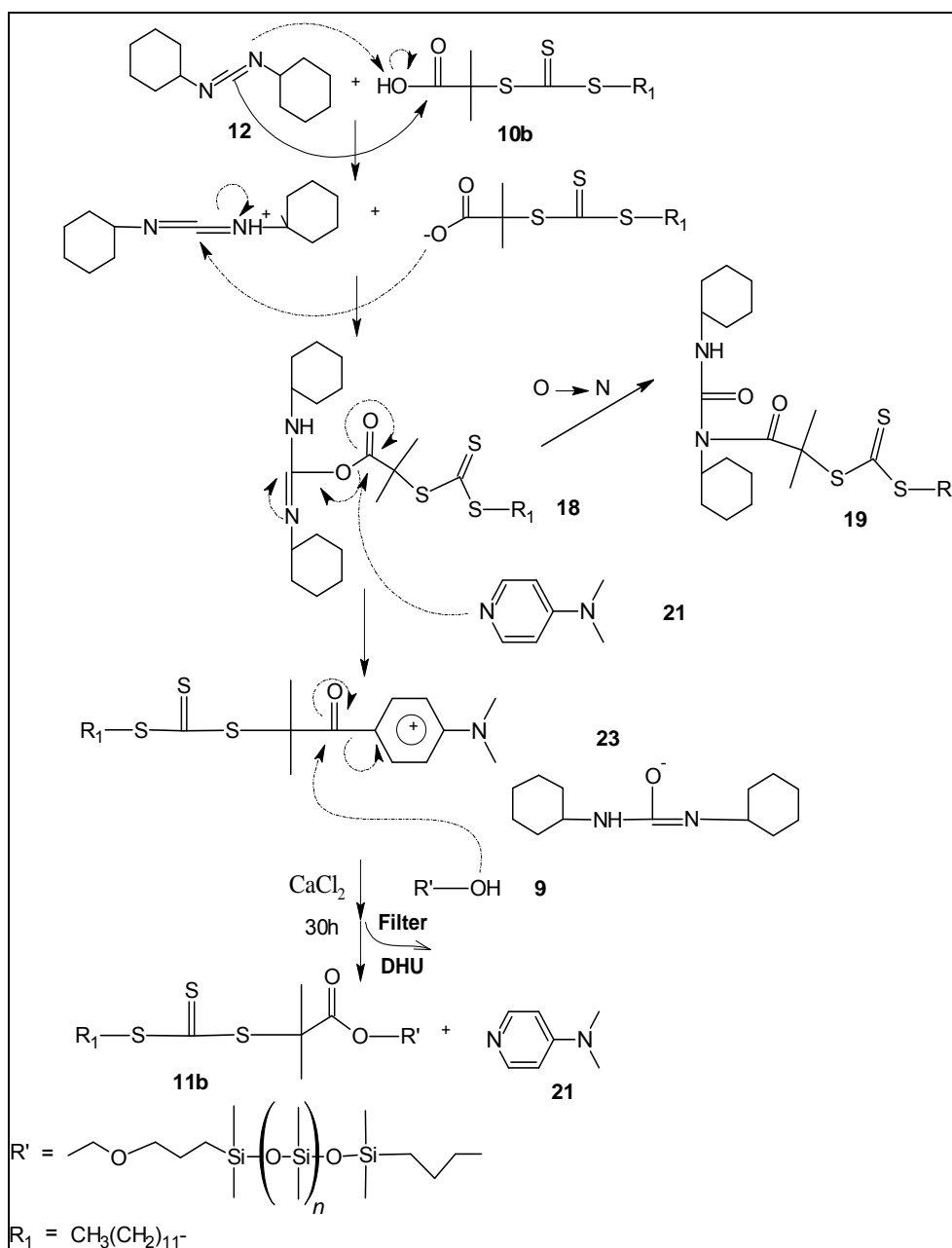
Scheme 3.7 **Reaction mechanism for the esterification between PDMS (9) and CTA (10b) in the presence of DCC (12) and DMAP (21) (excess) (experiment G).**

Experiment I

The experiment was run for 10 hours at room temperature after which a solution of the crude reaction product was passed through a vacuum filter in order to remove the insoluble white urea precipitate (DCU). A sample was analyzed by ^{1}H- and ^{13}C-NMR in order to determine conversion. Refer to Table 3.4 for experimental conditions. The NMR

spectrum produced the shifts as depicted in Table 3.5. From the ^{13}C-NMR spectrum, there was no evidence of unreacted methylene peaks (A'-C'), and in the ^{1}H-NMR spectrum, there was no evidence of unreacted methylene peak A' at 3.72ppm (the presence of peaks B' and C' could not be easily distinguished due to overlapping). Therefore, it can be concluded that reaction I was an improvement upon experiment F in that almost complete conversion of PDMS into its ester counterpart could now be achieved under the same mild conditions as reaction F except running it for 10 hours instead of 30 hours.

3.7   Purified PDMS macroCTAs

The second objective was to obtain pure PDMS macroCTAs which could then be used in further polymerizations with various monomers. A procedure was devised to separate the unreacted starting materials.

3.7.1   Purification procedure

The crude product (±2mL) was diluted with hexane (100mL) and extracted three times with acetonitrile (100mL). After the solvent was evaporated, the crude product was purified by silica gel chromatography with a 1:1 (v/v) hexane/ethyl acetate mixture as eluent to obtain a bright yellow oil. Refer to Appendix I for an illustration of the species present on thin layer chromatography (TLC) plates.

3.7.1.1   Analysis of PDMS macroCTA (11a)

Yield: 57%.
Purity: According to NMR spectroscopy, the purity was 96%.

^{1}H-NMR (ref CDCl$_3$ at 7.26, δ (ppm), 400MHz): 7.6–7.32 (BSTCP, m, Ar-H), 4.60 (BSTCP, s, CH_2), 4.25 (PDMS, m, CH_2), 3.63 (m, PDMS and BSTCP, CH_2), 3.42 (PDMS, t, CH_2), 2.81 (BSTCP, t, CH_2), 1.58–1.68 (PDMS, m, CH_2), 0.53 (PDMS, m, Si-CH_2), 0.23 (PDMS, s, Si-CH_2), 0.075 (PDMS, broad m, (Si-(CH_3)$_2$)$_n$. Impurities at (δ (ppm)): 6.5, 5.33, 5.2, 4.17, 3.78, 3.71, 3.52, 3.03, 2.08, 1.85, 1.45, 1.2, 0.85.

^{13}C-NMR (ref CDCl$_3$ at 77.0ppm, δ (ppm), 400MHz): 14.14 (PDMS, CH_3), 23.41 (PDMS, CH_2), 31.31, 33.08, 41.52 (BSTCP, CH_2), 64.13, 68.40, 74.17 (PDMS, CH_2), 127.8–129.2 (Ph-C), 134.82 (BSTCP, C_4), 171.38 (C=O), 222.88 (C=S).
IR (units = cm^{-1}): C=O (1734), PDMS (2963, 2905, 1417, 1260, 1093, 1020, 865, 800, 662), BSTCP (2927, 1740, 1454, 1424, 1066).

3.7.1.2   Analysis of PDMS macroCTA (11b)

IR, SEC and NMR spectroscopy were used to characterize the compound. The respective results can be seen in Figures 3.5–3.7. Refer to Scheme 3.4 to identify peak label references. Analysis hereof follows:

Yield: Varies between 57–63%.

Purity: According to ^{1}H-NMR, the purity was very high (~99%).

^{1}H-NMR (ref CDCl$_3$ at 7.26, δ (ppm), 400 MHz): 4.25 (PDMS, t, CH_2-O-C=O), 3.62 (PDMS, t, CH$_2$-O-CH_2-CH$_2$-O-C=O), 3.41 (PDMS, t, -CH_2-O-CH$_2$-), 3.27 (DIBTC, t, -S-CH_2-), 1.70 (DIBTC, s, (CH_3)$_2$), 1.40–70 (PDMS, m, (CH_2)$_n$), 1.26 (DIBTC, m, (CH_2)$_n$), 0.88 (DIBTC, t, CH_3), 0.53 (PDMS, m, Si-CH_2), 0.23 (PDMS, s, Si-CH_2), 0.075 (PDMS, broad m, (Si-(CH_3)$_2$)$_n$). Impurities at (δ (ppm)): 8.4 (s), 6.1 (s), 4.26 (m), 3.8 (t), 3.72 (t), 3.7 (s), 3.5 (m), 1.95 (s).

^{13}C-NMR (ref CDCl$_3$ at 77.0ppm, δ (ppm), 400MHz): 221.4 (C=S), 172.9 (C=O), 74.1, 68.2, 65.1 (PDMS, CH_2), 55.9 (DIBTC, C), 36.9 (DIBTC, (S-CH_2)), 31.9 (DIBTC, (CH_2)), 29 (m, DIBTC, (CH_2)$_n$), 27.9 (DIBTC, CH_2), 25.3 (DIBTC, CH_2), 23.5 (PDMS, CH_2), 22.7 (DIBTC, (CH_3)$_2$), 14.16 (PDMS, CH_3), 14.1 (DIBTC, CH_3).

IR (units = cm^{-1}): C=O (1740), PDMS (2963, 2905, 1413, 1261, 1094, 1020, 864, 801, 663).

The IR (Figure 3.5) spectrum of the PDMS macroCTA (11b) shows the characteristic bands of the PDMS segment at 800, 865, 1260, 1020, 1093cm^{-1} as well as the carbonyl stretch vibration at 1740cm^{-1}. The first three peaks belong to the Si–CH$_3$ deformation whilst the fourth and fifth one is as a result of the Si–O–Si asymmetric stretching vibration in PDMS.
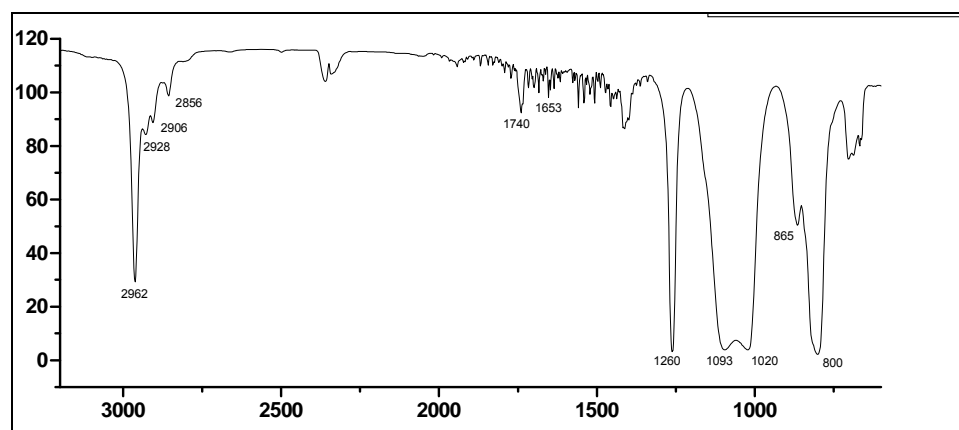
Figure 3.5   Infrared spectrum of PDMS macroCTA (11b).

SEC (Figure 3.6) indicates the incorporation of the thiocarbonylthio moiety in the ester as seen by the absorption of UV at 254nm and 320nm. PDMS (9) does not have any UV absorbance.

M_{nSEC} = 4 900g/mol
M_{pSEC} = 5 200g/mol
PDI = 1.15
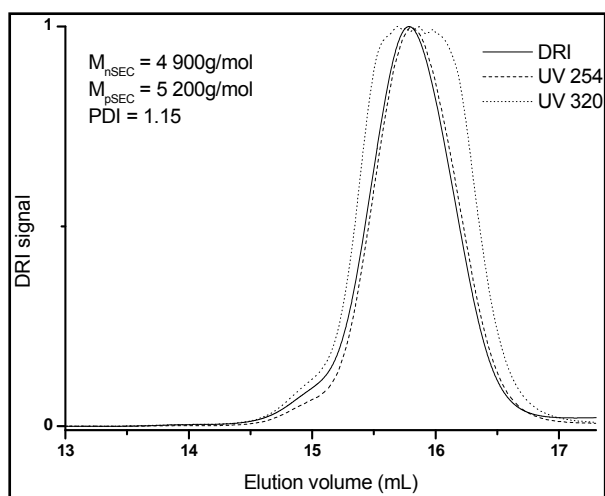
Figure 3.6 **SEC chromatogram of PDMS macroCTA (11b) showing UV (254nm and 320nm) and DRI detector signal overlays.**

Finally, Figure 3.7 presents the ^{13}C- and ^{1}H-NMR spectra of the purified product. Refer to Scheme 3.4 for peak identification.
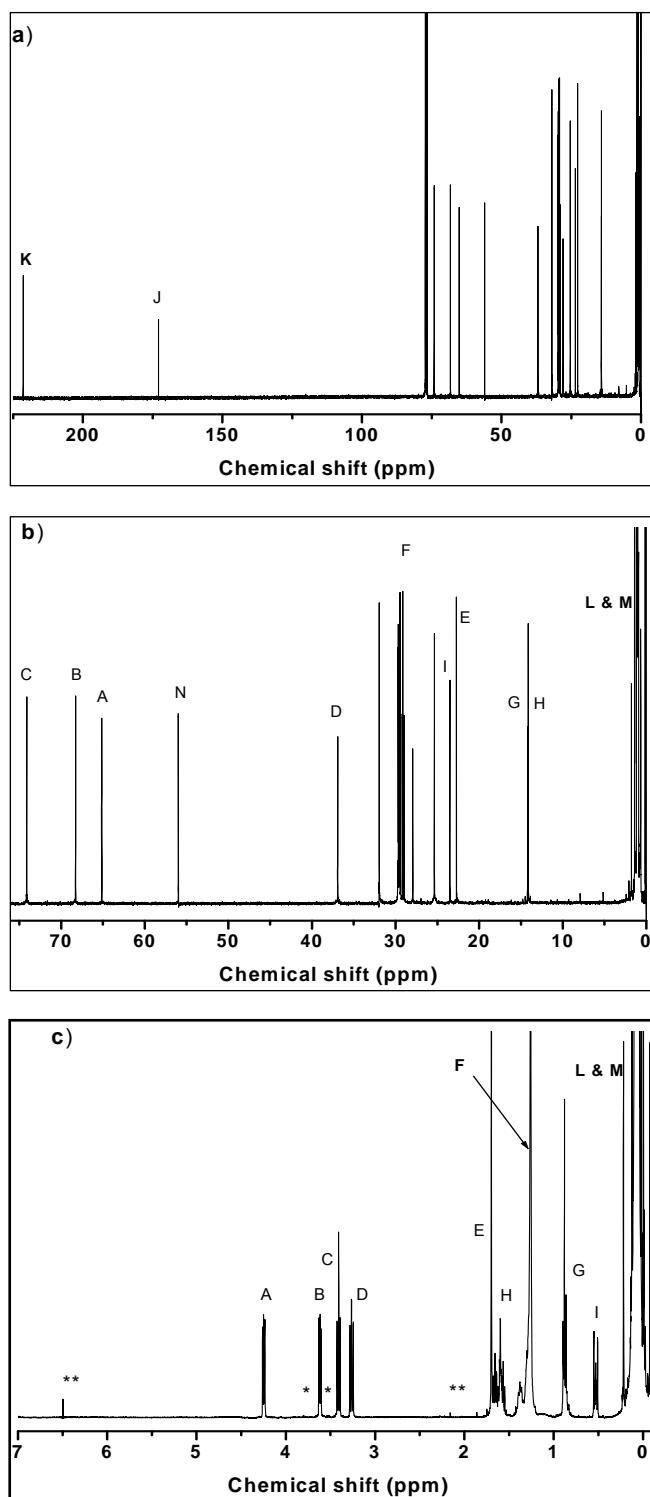
Figure 3.7   (a) and (b) ^{13}C-NMR spectrum for purified PDMS macroCTA (11b). No presence of detectable impurities or unreacted starting materials; (c) ^{1}H-NMR spectrum for purified PDMS macroCTA (11b). *presence of impurity from PDMS (9) and ** presence of unknown impurities.

3.8   Conclusion

The objectives of this work were achieved, namely those of obtaining:

1.   A high degree of conversion ($\geq$96%) of PDMS into the PDMS macroCTA

2.   A high degree of purity (~99%) of the ester-containing PDMS macroCTAs

As seen in Section 3.6.2.7, improved experimental conditions for the synthesis of a PDMS macroCTA were used compared to those described in the article by Pai *et al.* [18] Improved reaction conditions using DMAP as catalyst involved:

- A reduction in reaction time from 72 hours to 10 hours
- A reduction in temperature from reflux conditions to room temperature
- Slightly lower excess molar ratios of acid/DCC were used (1.8 versus 2)
- Extensive characterization of PDMS macroCTAs using ^{1}H-NMR, ^{13}C-NMR, IR spectroscopy and SEC.

3.9   Future Scope

Initial reaction conditions to attain 100% conversion of the abovementioned PDMS macroCTAs included the use of a three-fold excess of CTA and DCC and using reflux temperatures over a period of 120 hours. Through the process of investigations, the author improved reaction conditions significantly, showing that 100% conversion could be obtained within 5 hours. Although purification of the PDMS macroCTA when using this approach turned out to be slightly challenging, it is in the opinion of the author that this can be achieved. As already mentioned, this was not a core objective of this work, and the author was satisfied with the improvements that were reached.

References

(1)   Sewald, N.; Jakubke, H.-D. *Peptides: Chemistry and Biology*, WILEY-VCH Verlag GmbH: Weinheim, 2002.

(2)   Zalipsky, S.; Gilon, C.; Zilkha, A. *Eur. Polym. J.,* **1983**, *19.*

(3)   Hassner, A.; Alexanian, V. *Tetr. Lett.,* **1978**, *46,* 4475.

(4)   Putnam, D.; Langer, R. *Macromolecules,* **1999**, *32,* 3658.

(5)   Besheer, A.; Hause, G.; Kressler, J.; Mader, K. *Biomacromolecules,* **2007**, *8,* 359.

(6)   Cameron, N. S.; Eisenberg, A.; Brown, G. R. *Biomacromolecules,* **2002**, *3,* 116.

(7)   Yilgor, E.; Yilgor, I.; Suzer, S. *Polymer,* **2003**, *44,* 7271.

(8)   Yilgor, I.; Steckle, W. P. J.; Yilgor, E.; Freelin, R. G.; Riffle, J. S. *J. Polym. Sci., Part A: Polym. Chem.,* **1989**, *27,* 3673.

(9)   Tang, L.; Sheu, M. S.; Chu, T.; Huang, Y. H. *Biomaterials,* **1999**, *20,* 1365.

(10)   Voronkov, M. G.; Mileshkevich, V. P.; Yuzhelevskii, Y. A. *The siloxane bond*, Consultants Bureau: New York, 1978.

(11)   Karal, O.; Hamurcu, E. E.; Baysal, B. M. *Polymer,* **1997**, *38,* 6071.

(12)   Lovinger, A. J.; Han, B. J.; Padden, J. F. J.; Mirau, P. A. *J. Polym. Sci., Part B: Polym. Phys.,* **1993**, *31,* 115.

(13)   Yilgor, I.; McGrath, J. E. *Adv. Polym. Sci.,* **1988**, *86,* 1.

(14   Lelah, M. D.; Cooper, S. L. *Polyurethane in Medicine.*, Boca Raton:CRC Press: 1986.

(15   Kawakami, Y.; Yamashita, Y. Ring-opening polymerization., in *ACS symposium series No. 286*; eds. McGrath, J. E.; Washington DC: American Chemical Society: Washington, 1985, Chapter 19.

(16)   Kumaki, T.; Sisido, M.; Imanishi, Y. *J. Biomed. Mater. Res.,* **1985**, *19,* 785.

(17)   Yilgor, I.; Steckle, W. P. J.; Yilgor, R.; Freelin, G.; Riffle, J. S. *J. Polym. Sci., Part A: Polym. Chem.,* **1989***,* 3673.

(18)   Pai, T. S. C.; Barner-Kowollik, C.; Davis, T. P.; Stenzel, M. H. *Polymer,* **2004**, *45,* 4383.

(19)   Starch, M. S. Using silicones in topical products, in *Drugs and the pharmaceutical sciences*; 42, eds. Amman, A. H.; 1990, Chapter 19.

(20)   Colas, A.; Aguadisch, L. *Chimie Nouvelle,* **1997**, *15,* 1779.

(21)   Schueller, R.; Romanowski, P. *Conditioning Agents for Hair and Skin*, Cosmetic Science and Technology Series/Volume 21, Dekker: New York, 1999.

(22)   Batra, A.; Cohen, C.; Kim, H.; Winey, K. I.; Ando, N.; Gruner, S. M. *Macromolecules,* **2006**, *39,* 1630.

(23)   Grigoras, S.; Lane, T. H. Conformation Analysis of Substituted Polysiloxanes Polymers, in *Silicon-Based Polymer Science: A Comprehensive Resource*; eds. Zeigler, J. M., Fearon, F. W. G., Eds.; Adv. Chem. Ser. 224; American Chemical Society: Washington, DC, 1990, Chapter 7, p.125.

(24)   Tomanek, A. *Silicones and Industry*, Hanser (Wacker Chemie): Munich, 1991.

(25)   Lyman, D. J.; Metcalf, L. C.; Albo, D. J.; Richards, K. F.; Lamb, J. *Trans. Am. Soc. Artif. Organs,* **1974**, *20,* 474.

(26)   Brash, J. L. *Ann. NY Acad. Sci.,* **1977**, *283,* 356.

(27)   Leininger, R. I.; Falb, R. D.; Grode, G. A. *Ann. NY Acad. Sci.,* **1968**, *146,* 11.

(28)   Owen, M. J. *Chemtech,* **1981**, *11,* 288.

(29)   Brook, M. A. *Silicon in Organic, Organometallic and Polym. Chem.*, John Wiley and Sons: New York, 2000.

(30)   Noll, W. *Chemistry and Technology of Silicones*, Academic Press: New York, 1968.

(31) Thomas, T. H.; Kendrick, T. C. *J. Polym. Sci., Part A-2: Polym Phys.,* **1969**, *7,* 537.

(32) Grassie, N.; MacFarlane, J. *Eur. Polym. J.,* **1978**, *14,* 875.

(33) Thomas, X., 2003. *Silicone Adhesives in Healthcare Applications*, Dow Corning Healthcare Industry.

(34) Hsuie, G. H.; Lee, S. D.; Wang, C. C.; Shiue, M. H. I.; Chang, P. C. T. *Biomaterials,* **1994**, *15,* 163.

(35) Aucoin, L.; Grifith, C. M.; Pleizier, G.; Deslandes, Y. *J. Biomater. Sci. Polym. Edn.,* **2002**, *13,* 447.

(36) Merrett, K.; Griffith, M.; Duble, M. A.; Sheardown, H. E. *J. Biomed. Mat. Res.,* **2003**, *67A,* 981.

(37) Liu, L.; Sheardown, H. E. Opthalmic Biomaterials and preparation thereof. US 2004/0258727 A1, 28 May 2004.

(38) Lai, Y. C.; Valint Jr, P. L. *J. Appl. Polym. Sci.,* **1996**, *61,* 2051.

(39) Lai, Y. C.; Friends, G. D. *J. Biomed. Mat. Res.,* **1997**, *35,* 349.

(40) Paranjape, M.; Garra, J.; Brida, S.; Schneider, T.; White, R.; Currie, J. *Sensors and Actuators A: Physical,* **2003**, *104,* 195.

(41) Dow Corning® Silicones for transdermal drug delivery systems brochure, Dow Corning Corp., Healthcare Industries, Product Information Form No. 51-978C-01,10-11).

(42) Otera, J. *Esterification: Methods, Reactions and Applications*, Wiley-VCH Verlag GmbH & Co.: Weinheim, 2003.

(43) Sheehan, J. C.; Hess, G. P. *J. Am. Chem. Soc.,* **1955**, *77,* 1067.

(44) Tsarevsky, N. V.; Sarbu, T.; Gobelt, B.; Matyjaszewski, K. *Macromolecules,* **2002**, *35,* 6142.

(45) Kataka, R.; Kobayashi, K.; Yamada, K.; Oku, H.; Emori, N. *Biopolymers,* **2004**, *73,* 641.

(46) Yoshimura, T.; Matsuo, K.; Fujioka, R. *J. Appl. Polym. Sci.,* **2005**, *99,* 3251.

(47) Tsvetkova, B.; Tencheva, J.; Peikov, P. *Acta. Pharm.,* **2006**, *56,* 251.

(48) Wiener, H. *J. Molec. Cat.,* **1986**, *37,* 45.

(49) Bodansky, M. *Principles of Peptide Synthesis*, 2nd. ed., Springer-Verlag: New York, 1993.

(50) Stenzel, M. H.; Davis, T. P.; Fane, A. G. *J. Mater. Chem.,* **2003**, *13,* 2090.

(51) Lai, J. T.; Filla, D.; Shea, R. *Macromolecules,* **2002**, *35,* 6754.

(52) Klemenc, S. *Foren. Sci. Int.,* **2002**, *129,* 194.

(53) Shiels, R. A.; Jones, C. W. *J. Molec. Cat.:Chem.,* **2006**, *261,* 160.

(54) Spivey, A. C.; Arseniyadis, S. *Angew. Chem. Int. Ed.,* **2004**, *43,* 5436.

Chapter 4

Block copolymer synthesis with poly(styrene) (PSt) using a PDMS macroCTA

Abstract

Mono-functional PDMS macroCTA was used to prepare an AB type block copolymer. The work that follows describes the synthesis of block copolymers using styrene and a trithiocarbonyl-capped PDMS compound as macroCTA using RAFT polymerization in both solution and emulsion media. To the best of our knowledge, this is the first report of synthesizing a block copolymer of PDMS-*b*-PSt ((24a) and (24b) in Scheme 4.1) in miniemulsion using RAFT polymerization.

4.1   Introduction

This part of the research was used as a stepping stone, or model reaction, in order to demonstrate the principle of using a thiocarbonyl end-capped PDMS material as a macroCTA in the synthesis of block copolymers. Styrene was considered an appropriate monomer of choice for copolymerizing with the PDMS macroCTA in order to facilitate an easy choice of solvent when polymerizing in solution to ensure the solubility of all the reaction components. Another important consideration why styrene was chosen to perform these model reactions is that the block copolymer of PDMS-*b*-PSt is soluble in THF which is the mobile phase used for in-house SEC analysis.

One of the advantages of solution polymerization over emulsion polymerizations is that the former overcomes many of the viscosity and exothermic problems associated with bulk polymerizations. The solvent acts as a diluent and aids in the transfer of the heat of polymerization. There are however many disadvantages to solution/bulk polymerizations: processing or sampling can become problematic as the medium can become very viscous; initiator efficiency can effectively decrease to zero at high conversions as diffusion of radicals becomes slower in the medium; impurities can be present in the solvent; chain transfer to solvent can occur; the monomer concentration in solution polymerizations are somewhat lower than in emulsions which contributes to a lowering of the rates of polymerization. The advantages to using emulsion polymerization are well documented; good thermal control, fast kinetic rates, high molecular weights attainable and the use of

water as a dispersant instead of an organic solvent[1]. In emulsion polymerizations particles are present and the viscosity of the medium (water) is dominated by the concentration of these particles as well as the particle size. Reaction rates are significantly enhanced in emulsion systems due to compartmentalization. Refer to Section 4.5.1 for a further explanation on important theoretical concepts regarding emulsion/miniemulsion polymerizations.

It is of great value when opting to use RAFT polymerization that the CTA that is used fragments in such a way that upon addition of a polymeric radical species, the thiocarbonylthio moiety is placed at the terminal end of the block copolymer. The advantage of this is that if one needs to remove the thiocarbonylthio moiety with regard to the desired application, the removal hereof is easily performed without having to cleave the second block of the copolymer. One of the two previously synthesized PDMS macroCTAs (11b) (as described in Chapter 3) fragments in such a manner. Both of the PDMS macroCTAs ((11a) and (11b)) synthesized in the previous chapter were used in the experiments described in this chapter; the former resulting in the thiocarbonylthio moiety being placed at the core, with the latter resulting in it being placed at the terminal end of the block copolymer. Scheme 4.1 illustrates the reaction scheme for both types of block copolymers that are formed when using the two different PDMS macroCTAs ((11a) and (11b)) as starting blocks.

4.2   Objectives

At the onset of this study, there were two main objectives to be fulfilled:

- The successful synthesis of PDMS-*b*-PSt block copolymers with sufficiently high conversion rates, and GPC chromatograms which indicate that the block copolymers do indeed contain both the RAFT functionality as well as PSt.

- Using microscopy to study the phase segregation of these block copolymers.

4.2.1   Objective 1: Obtaining sufficient polymerization rates of PDMS-*b*-PSt block copolymer

As mentioned in the introduction, the experiments to follow are model reactions for further work involving the synthesis of amphiphilic block copolymers (Chapter 6). It was therefore necessary to first develop a system with two compatible polymers (PDMS and PSt) which could be analyzed to determine whether the PDMS macroCTAs can be successfully used as the starting blocks to synthesize the desired block copolymers. It was also important to ensure high and speedy conversion rates as the application of these block copolymers,

and future ones, would not see any application in industry if a major percentage of the monomer is not polymerized.
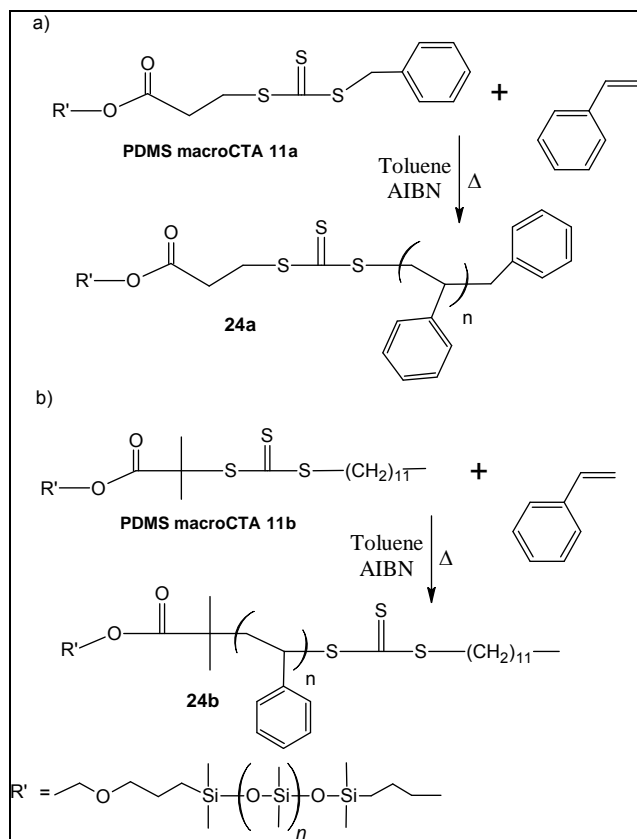
Scheme 4.1 **Reaction scheme using (a) PDMS macroCTA (11a) to produce PDMS-*b*-PSt block copolymers (24a), resulting in the thiocarbonylthio moiety placed at the core of the block copolymer and (b) PDMS macroCTA (11b) to produce PDMS-*b*-PSt block copolymers (24b), resulting in the thiocarbonylthio moiety placed at the terminal end of the block copolymer.**

4.2.2   Objective 2: Microscopy studies

In addition to the above objective, using a technique such as TEM to gather images of these materials would be one approach to identify whether these block copolymers undergo self-assembly to form one of many possible morphologies.

4.3   Experimental

4.3.1   Materials

Styrene [100-42-5] (Plascon Research Centre, University of Stellenbosch, estimated purity ~99%) was washed with 0.3M KOH and distilled under vacuum prior to use in order to

remove inhibitor and polymer. Toluene [108-88-3] (Merck, 98.5%), methanol [67-56-1] (Merck, 98%), hexadecane (HD) [544-76-3] (Sigma, 99%, GC), sodium dodecyl sulphate (SDS) [151-21-3] (Sigma, 99%, GC) were used as received and 2,2'-azobis(isobutyronitrile) [78-67-1] (AIBN, Riedel De Haen) was recrystallized twice from methanol. 1,3,5-Trioxane [110-88-3] (Aldrich, ≥99%) was used as internal reference in all solution polymerizations. Distilled deionized water was used in all miniemulsion reactions. PDMS macroCTAs (11a and 11b) were purified as described in Chapter 3, Section 3.7.1.

4.3.2   Solution polymerization procedure

All solution experiments were performed in the same manner. Toluene was used as solvent to ensure that temperatures were run at well below reflux conditions, and AIBN was used as initiator in all polymerizations. A typical experimental procedure is described. A solution of monomer (styrene), initiator (AIBN), CTA (PDMS macroCTA), and solvent (toluene) were introduced in a 250mL Schlenk tube equipped with a magnetic stirrer. The mixture was degassed by five freeze–evacuate–thaw cycles and then heated in a thermostated oil bath. Periodically, samples were withdrawn from the polymerization medium via a syringe for analyses. Polymers were purified by precipitation in an excess of methanol, filtered and washed several times using the same solvent, after which they were dried *in vacuo* to give a polymer powder with a slight yellow tinge. Trioxane (internal reference for ^{1}H-NMR determination of monomer consumption) was used in all reactions. In some reactions the trioxane was added directly to the rest of the contents in the flask prior to the start of polymerizations, whilst for others, an external tube containing trioxane was added to the NMR tube prior to analysis. The complete elimination of residual monomers was confirmed by ^{1}H-NMR spectroscopy.

4.3.3   Miniemulsion polymerization procedure

All miniemulsion experiments were performed in the same manner. A typical miniemulsion experimental procedure is described. A solution of monomer (styrene), CTA (PDMS macroCTA 11a or 11b), costabilizer (HD) and initiator (AIBN), as well as an aqueous solution of surfactant (SDS) were stirred overnight. Prior to ultrasonication, the organic and aqueous phases were premixed and subjected to a 45 minute ultrasonication cycle. The emulsions were subsequently transferred to a 250mL three-necked flask equipped with a magnetic stirrer and degassed for 15 minutes with nitrogen. Polymerizations were carried out at 75°C. Samples were periodically withdrawn from the reaction mixture and analyzed by gravimetric conversion, particle size and transmission electron microscopy (TEM).

4.3.4 Ultrasonication

Emulsification was carried out using ultrasonication (Ultrasonic Homogenizer, Nissei, US-600T, 12mm diameter tip, set at "Power 10") for 12 minutes at 0°C in a 30mL glass vial.

4.3.5 Analyses and sample preparation

Conversion - Solution. The extent of conversion was determined by means of both gravimetry and ^{1}H-NMR spectroscopy. Proton nuclear magnetic resonance (^{1}H-NMR) spectra were recorded on a Varian VXR 300MHz spectrometer and were performed at room temperature using deuterated chloroform (CDCl$_3$) (99.8%) as the solvent. For determination of conversion by means of gravimetry, the solution of the sample containing monomer was weighed after which it was dried to completion in a vacuum oven for 12 hours, and subsequently weighed again. In order to verify the gravimetric method, ^{1}H-NMR spectroscopy was also used to monitor the conversion of styrene. Trioxane (CDCl$_3$, 5.1ppm) was used in all reactions in order to monitor the conversion of the styrene monomer peaks at 5.26, 5.78 and 6.74ppm. In some reactions trioxane was added to the rest of the contents in the flask, whilst for others, an external trioxane reference tube was inserted into the NMR tube containing the sample to be analyzed. A ^{1}H-NMR spectrum was recorded at the beginning of the experiment, as well as at regular time intervals throughout the polymerization in order to determine the conversion. The study of the polymerization kinetics performed by ^{1}H-NMR spectroscopy gave a series of spectra showing the disappearance of the signals from the styrene double bond hydrogens as compared to either, the constant trioxane peak (5.1ppm) or those of the polymer backbone at 1.8ppm. In the case of using an external trioxane reference, a constant amount of sample (0.1g) was transferred to an NMR tube, deuterated chloroform added, after which the external trioxane reference tube was added prior to the analysis.

Conversion - Miniemulsion. The extent of conversion was determined by means of gravimetry. Aliquots of the aqueous solution containing monomer were weighed at regular time intervals after which it was dried to completion for 72 hours, and subsequently weighed again.

Molecular Weight Analyses - Solution. Molecular weights were determined using SEC. Samples were prepared for SEC analysis by precipitating each solution aliquot in methanol, washing it several times, and then drying it to completion in a vacuum oven for 12 hours. The dried polymers were weighed off (~10mg), and dissolved in 3mL HPLC

grade THF (containing 0.012% BHT), filtered through a 0.2µm filter and then submitted for SEC analysis. The SEC instrument specifications can be seen in Chapter 3.

Contact angle measurements were carried out on a GBX Digidrop Contact Angle Analyser using water as the wetting sample. The temperature of the system was kept constant at 25°C and a water droplet volume of 2.0µL was used for all analyses.

Particle Size measurements were performed on a Malvern Zetasizer Nano 2590 instrument fixed at 90 degrees at 25°C. The system was calibrated using nanosphere size standards of polymer microspheres (Malvern instruments) in water with a mean diameter of 60nm.

Morphology was determined using TEM. TEM was carried out at the University of Cape Town, Electron Microscope Unit A. The apparatus used was a Leo 912 TEM operating at 120KV attached to a digital camera. All the samples were analyzed on copper grids. All samples polymerized by miniemulsion techniques were diluted further with distilled deionized water. Some samples were analyzed without stain as well as with a 2% uranyl acetate solution stain before being mounted onto the copper grid. Samples polymerized by solution techniques were prepared in a variety of manners: some samples were first precipitated and diluted further with the respective reaction solvent(s) before being placed on the copper grid, whilst other samples prepared by solution polymerization were diluted further with reaction solvent and stained before being placed on the copper grid.

4.4   Synthesis of PDMS-*b*-PSt block copolymers in solution

Block copolymer synthesis was performed using RAFT polymerization in toluene. A homogenous solution was obtained throughout the polymerization.

4.4.1   Results and discussion

4.4.1.1   Effect of temperature

The detailed procedure for preparing the block copolymers is outlined in Section 4.3.2 and depicted in Scheme 4.1. Experimental data for both experiments performed are summarized in Table 4.1. The trithiocarbonyl PDMS macroCTA (11b) that was synthesized (as described in Chapter 3) was used in the AIBN-initiated RAFT polymerization of styrene at two different temperatures, namely 85°C (experiment 1) and 100°C (experiment 2). All other experimental parameters were kept constant except for the initiator concentration. In experiment 1, in which a lower temperature was used, a higher initiator concentration was

used in order to enhance the kinetics of the reaction. These polymerizations were carried out at their respective temperatures to produce block copolymers with a trithiocarbonyl group at the ω-terminal and a carboxylic group at the α-terminal (Scheme 4.1).

Table 4.1   **Experimental conditions for PDMS-*b*-PSt block copolymerizations using PDMS macroCTA (11a) (experiment 4) or (11b) (experiments 1–3), AIBN and styrene.**

Experiment	Temperature (°C)	[M]/[CTA]	[CTA]/[AIBN]	[M] (mol/L)	[AIBN] (mmol/L)	[PDMS macroCTA] (mmol/L)
1	85	1000	1.7	2.26	1.35	2.27
2	100	1000	3	2.26	0.76	2.27
3	100	1000	3	2.02	0.68	2.02
4	100	1000	3	2.02	0.68	2.02

Two experiments were performed, each at different temperatures, in order to determine whether faster polymerization rates would result when higher temperatures were used and to determine which system displays the best control. Samples were taken at regular intervals and analyzed by gravimetry as well as ^{1}H-NMR spectroscopy in order to determine conversion. There was good agreement between the ^{1}H-NMR and gravimetric conversion results, especially at lower conversions. There were some discrepancies at higher conversions, and this is most probably due to the overlapping of the polymer peaks in the proton spectra. Results for these experiments are shown in Figures 4.1–4.4 and Table 4.2 below.

Both these reactions have approximately the same polymerization rate up until 24 hours, after which the polymerization at the higher temperature increases at a faster rate (Figure 4.1). The reason for this is probably as a result of the assistance of the higher temperature towards the autopolymerization of styrene at higher temperatures via the most generally accepted mechanism for the spontaneous polymerization of styrene, the Mayo mechanism. This reaction proceeds via a Diels-Alder dimerization to produce a transient dimer which in turn reacts with styrene to generate two styrenic radicals that start the propagation with styrene. For a further discussion of this mechanism, the reader is referred to some in-depth articles.[2,3] Higher temperatures in turn also increase the decomposition rate of AIBN, and the rates of propagation, addition, and fragmentation of the RAFT intermediate radicals. The $\ln([M]_0/[M]_t)$ versus time plots, Figure 4.2, were considered linear during the polymerization at 85°C, confirming that the concentration of radical species remained constant. It must be noted that the curve does not intersect the graph at
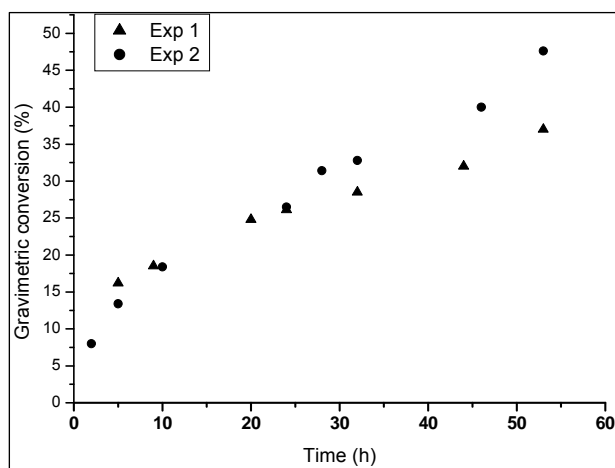
Figure 4.1   **Conversion data for PDMS-*b*-PSt block copolymers in toluene using PDMS macroCTA (11b); experiment 1 (▲) 85°C, [AIBN] = 1.35mmol/L; experiment 2 (●) 100°C, [AIBN] = 0.76mmol/L.**

zero. For the reaction run at 100°C, it was observed that there was a slight curving of the line indicating that the generation of primary radicals did no longer balance the loss of propagating radicals via irreversible termination reactions.

SEC analyses of aliquots taken from the polymerization indicated a series of unimodal curves and a monotonic increase in molecular weight with conversion (Figures 4.3 (a) and (c)). In addition to this, there appears to be good agreement between the UV signals at 254nm and 320nm with the differential refractive index (DRI) signal (Figures 4.3 (b), (d)). The choice of UV wavelengths can be explained by the fact that PSt has a dominant UV absorbance at 254nm and a minor absorbance at 320nm, however, the latter is considered negligible.

The thiocarbonyl functional group on the PDMS macroCTA has a strong UV absorbance at 320nm and a minimal absorbance at 254nm. Due to the fact that both UV signals overlap fairly well with the DRI signal, it allows one to deduce that the growing molecular weight species contain functionalities belonging to both the PDMS macroCTA and PSt. Therefore, one can infer that the maximum of the peak which is shifting corresponds with that of a living system consisting of a block copolymer of PDMS-*b*-PSt.
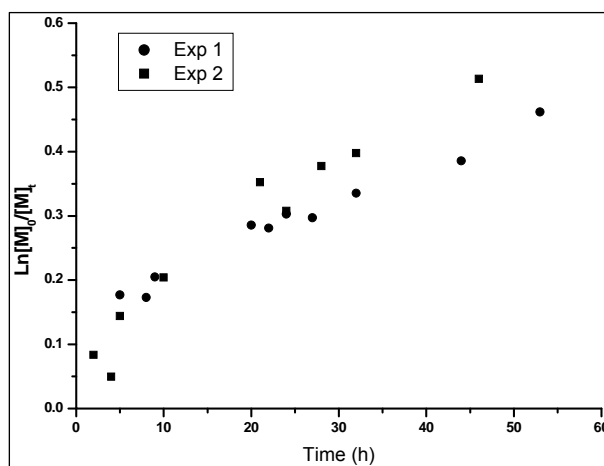
Figure 4.2   **1st Order kinetic plots for PDMS-*b*-PSt block copolymers in toluene using PDMS macroCTA (11b); experiment 1 (▲) 85°C, [AIBN] = 1.35mmol/L; experiment 2 (●) 100°C, [AIBN] = 0.76mmol/L.**

In addition to this, further analyses confirmed a relatively linear evolution in molecular weight with conversion (Figure 4.4 (a)), and PDIs remained relatively narrow throughout the polymerization (Figure 4.4 (b)), indicating that there was a fair amount of control in these polymerizations. However, the SEC data indicate somewhat lower $\overline{M}_n$ values (negative deviation) than those expected from the monomer to CTA (M:CTA) molar ratio throughout the polymerization. This can be as a result of either of the following reasons: (1) PSt calibration standards are not ideal for the analysis of PDMS-*b*-PSt block copolymers. Although one of the components of the block was that of PSt, the hydrodynamic volume of PDMS-*b*-PSt can be expected to be very different to that of homopolymer styrene (2) $\overline{M}_n$ theor was calculated from equation (2.14) without considering the number of radicals derived from the initiator,[4] which can be a possible cause of the negative deviation or (3) the possibility of oxygen entering the reaction flask and forming short molecular weight species. The next step is to investigate the difference in the PDIs between these two reactions. It is expected that the lower the temperature, the narrower the molecular weight distribution should be. Results for both reactions are summarized in Table 4.2.

The results in Table 4.2 indicate that in both experiments the molecular weight increased with conversion. The reason for using a lower initiator concentration at the higher temperature was to compensate for the larger amount of initiator radicals that would automatically be generated by the higher temperature alone. This should contribute to narrowing the PDI indices at higher temperatures by reducing the amount of irreversible termination that takes place. However, for the reaction performed at 85°C, the PDI remained fairly constant (PDI~1.3), but for the polymerization that was performed at 100°C, the polymer already displayed poor control (PDI~1.5) from the first sample even

91

though a lower initiator concentration was used (Figure 4.4 (b)). The reason for this can be explained through the fact that at higher temperatures, a larger amount of AIBN radicals are generated leading to a larger percentage of the chains to be initiated by AIBN radicals, which in turn would result in a larger amount of termination and increase the PDI. Also, at higher temperatures more radicals are created by the self initiation of styrene.
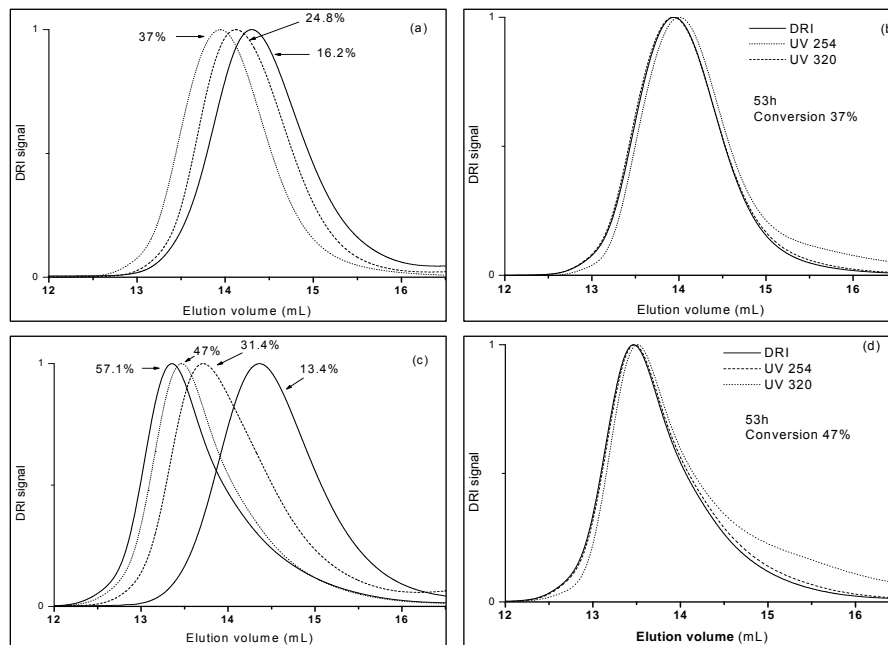
Figure 4.3 **SEC chromatograms of PDMS-*b*-PSt block copolymers for experiment 1 (a) increasing molecular weight for polymerization at 85°C (b) sample at 53h with 37% conversion for polymerization at 85°C showing UV 254nm and 320nm as well as DRI data; SEC chromatograms of PDMS-*b*-PSt for experiment 2 (c) increasing molecular weight for polymerization at 100°C (d) sample at 53h with 47% conversion for polymerization at 100°C showing UV 254nm and 320nm as well as DRI data.**
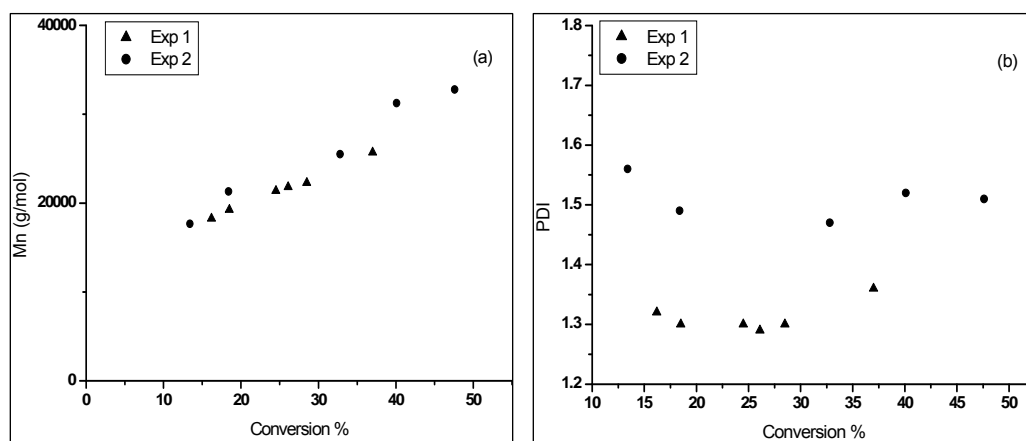
Figure 4.4 **(a) Number-average molecular weight ($\overline{},M_n$) and (b) PDI versus monomer conversion graphs for PDMS-*b*-PSt block copolymerizations at (1) 85°C, experiment 1 (▲) and (2) 100°C, experiment 2 (●).**

Table 4.2 **Experimental results for PDMS-*b*-PSt block copolymerizations at different temperatures and initiator concentrations using PDMS macroCTA (11b).**

Experiment	Time (h)	Gravimetric conversion (%)	^{1}H-NMR conversion (%) [#]	$\overline{},M_{n\,SEC}$ (g/mol)	PDI$_{SEC}$
1	5	16.2	16	18 262	1.32
	9	18.5	*na*	19 243	1.30
	20	24.8	22	20 188	1.31
	24	26.1	25	21 795	1.29
	32	28.5	*na*	22 293	1.30
	53	37.0	40	25 710	1.30
2	5	13.4	15	13 643	1.52
	10	18.4	19	17 677	1.49
	24	26.5	24	23 272	1.55
	32	32.8	*na*	25 500	1.47
	53	47.6	40	32 781	1.51

na = sample was not analyzed
as determined by using an external trioxane reference tube

For both experiments 1 and 2, there was no definite shoulder on the high molecular weight side of the SEC chromatograms, indicating that there was not a significant amount of termination of long molecular weight polymer chains taking place. The broadening of the UV signal on the low molecular weight side is not a concern as this can be explained to be due to the biased nature of the instrument towards the intensity of chromophore groups at low molecular masses. On the low molecular weight side there are fewer chromophore groups per chain (hence they are more concentrated and exaggerated by the instrument) than there are in higher molecular weight fractions. This behavior is typically seen throughout all the experiments that were analyzed.

The tailing seen in the DRI chromatograms on the lower molecular weight side however is a bit more complex to interpret, and can be explained to be most likely as a result of short chain termination involving initiator radicals. The question which arises from the broadening on the low molecular weight side is whether or not this is an indication of unreacted PDMS macroCTA, or whether this is as a result of the formation of short chain oligomers, also typically seen in radical polymerizations of this sort. The view of the author is that this effect is not as a result of unreacted PDMS macroCTA and can be explained as follows. The peak maximum for the PDMS macroCTA is found in the region of 15.6mL. If one looks at Figure 4.3 (b) and (d), one will notice that there is not a significant peak or any sort of broadening at around 15.6mL. If there were unreacted PDMS macroCTA on these systems, it would be clearly noticeable by the presence of a peak at 15.6mL. It is important to add, that it is understood that as the block (maximum point) increases in molecular weight, the concentration of the lower molecular weight species will decrease relative to it and it may be difficult to substantiate the previous claim. This argument would be greatly improved if the point at 15.6mL were to be part of the baseline, but due to the nature of these solution polymerizations, it is very difficult to obtain much higher molecular weights which would be shifted further from the point in question. Ideally, one needs to reach much higher molecular weights in order to shift the block copolymer peak far enough to be able to distinguish the presence of any unreacted material.

4.4.1.2 Study of different PDMS macroCTAs as effective and efficient first blocks for block copolymerization with styrene

Two experiments (experiments 3 and 4) were performed, each differing only in the type of PDMS macroCTA used. Table 4.1 summarizes the experimental conditions for each experiment and Table 4.3 provides the conversion and SEC results. Conversion was determined by ^{1}H-NMR spectroscopy using the ratio of the integration values of the polymer peak at 1.8ppm. Each of the PDMS macroCTAs ((11a) and (11b)) that were used are shown in Scheme 4.1. The leaving group of PDMS macroCTA (11a) is a primary benzyl radical, whilst that of PDMS macroCTA (11b) is a tertiary alkyl radical. According to theory, the benzyl radical is a poor leaving group as it is a primary radical, and it is probably going to be a poor homolytic leaving group with respect to the PSt propagating radical. The tertiary alkyl radical on the other hand is a relatively good leaving group and would probably be a good homolytic leaving group with respect to the PSt propagating radical. The fact that the tertiary alkyl radical in the case of PDMS macroCTA (11b) is a bulky macroradical could assist in the ability of it to act as a good leaving group due to steric hindrance factors. It would be interesting to note the effect these two macroCTAs will have on the kinetics as well as PDIs of the final polymers.
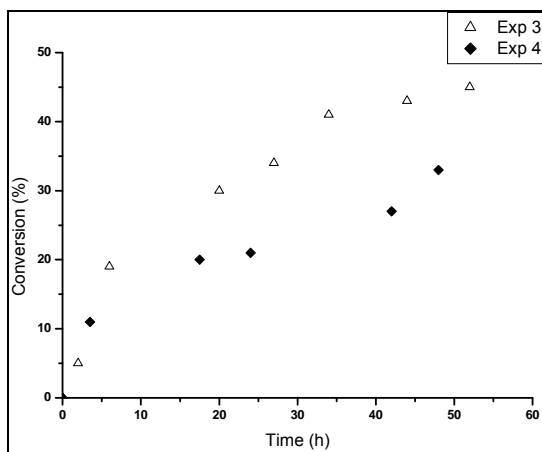
Figure 4.5   **Conversion data for PDMS-*b*-PSt block copolymers in toluene: experiment 3 (△), PDMS macroCTA (11b); experiment 4 (◆) PDMS macroCTA (11a).**

Figure 4.5 illustrates the difference in polymerization rates for experiments 3 and 4 and it can be seen that experiment 3 proceeded at a faster rate than that of experiment 4. According to theory, a primary radical is in a more active state than the tertiary radical, therefore it should probably act as a faster propagator than the stable tertiary radical. But, as can be seen from Figure 4.5 this was not the case. The author believes that there are a number of possible reasons for this, one of which could be due to some undetectable impurities present in the PDMS macroCTA that may retard polymerization. In experiment 4 there is evidence of an increase in polymerization rate after 30 hours. The author believes this is as a result of the autopolymerization mechanism of styrene (as explained in the previous section). The 1st order kinetic plots, Figure 4.6, were considered fairly linear for experiment 3, confirming that the concentration of radical species remained fairly constant during the polymerization. Experiment 4 indicated there to be a curving of the line implying that the generation of primary radicals did no longer balance the loss of propagating radicals via irreversible termination reactions. SEC analyses of aliquots taken from the polymerization indicated a series of unimodal curves and a monotonic increase in molecular weight with conversion (Figures 4.7 (a) and (c)). In addition to this, there appears to be good agreement between the UV signals at 254nm and 320nm with the DRI signal (Figures 4.7 (b), (d)). Table 4.3 indicates that both experiments showed a relatively linear evolution in molecular weight with conversion (Figure 4.8 (a)), although $\overline{M}_{n\text{SEC}}$ is somewhat lower than $\overline{M}_{n\text{theor}}$. The reasons for this is once again attributed to the use of PSt calibration standards, the possibility of oxygen entering the system during sampling, as well as the possibility of not accounting for initiator-derived chains in the molecular weight equation (2.13). For both reactions, PDIs did remain below 1.35 for the entire polymerization indicating that there was a fair amount of control in these polymerizations (Figure 4.8 (b)).

95
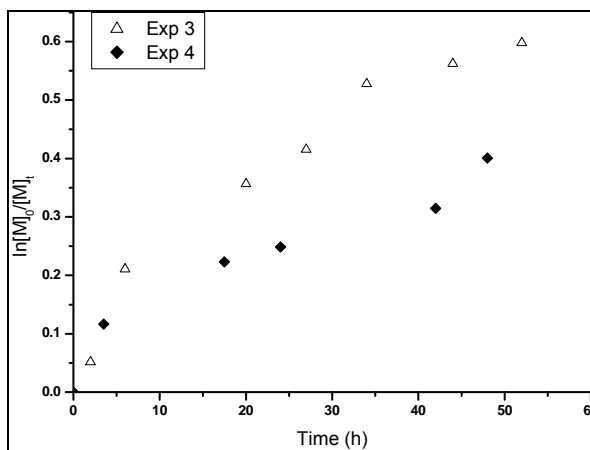
Figure 4.6   **1st Order kinetic plots for PDMS-*b*-PSt block copolymers in toluene using; PDMS macroCTA (11b) in experiment 3 (△) and PDMS macroCTA (11a) in experiment 4 (◆).**

Table 4.3   **Experimental results for PDMS-*b*-PSt block copolymerizations with AIBN and styrene using; PDMS macroCTA (11b) in experiment 3 (△) and PDMS macroCTA (11a) in experiment 4 (◆).**

Experiment	Time (h)	^{1}H-NMR conversion (%) #	$\overline{M}_{n_{SEC}}$ (g/mol)	PDI$_{SEC}$
3	2	5	18 400	1.27
	6	19	26 700	1.23
	20	30	41 600	1.28
	27	34	46 600	1.28
	34	41	59 600	1.30
	44	43	52 200	1.30
	52	45	55 200	1.34
4	3.5	11	21 000	1.32
	17.5	21	30 600	1.29
	21	*na*	31 900	1.31
	24	21	33 600	1.28
	42	27	38 000	1.28
	48	*33*	40 400	1.28

na = not analyzed

as determined by using an external trioxane reference tube
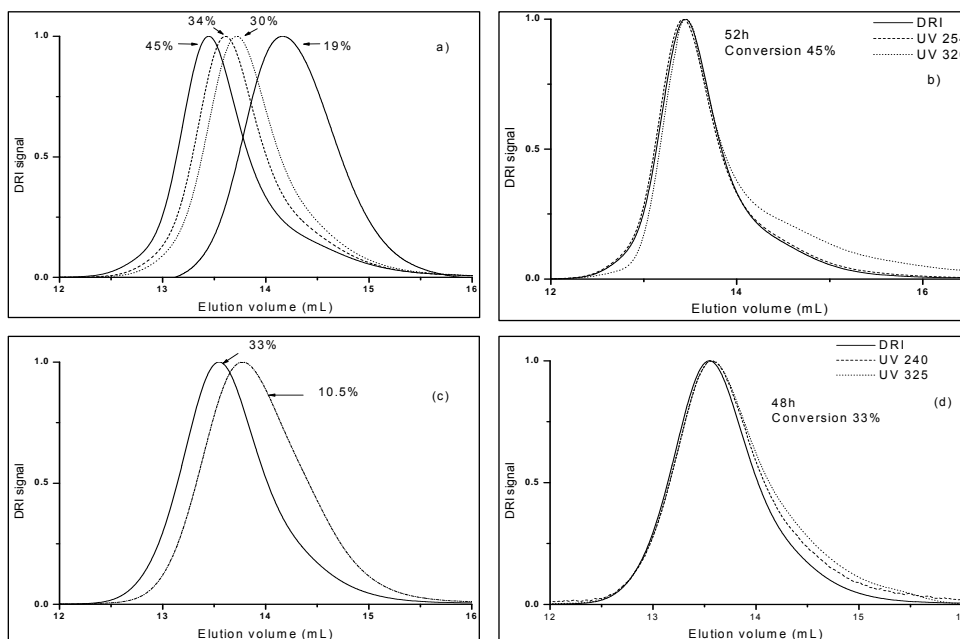
Figure 4.7 **SEC chromatograms of PDMS-*b*-PSt block copolymers for experiment 3 using PDMS macroCTA (11b) (a) increasing molecular weight for polymerization (b) sample at 52h with 45% conversion showing UV 254nm and 320nm as well as DRI data; SEC chromatograms of PDMS-*b*-PSt block copolymers for experiment 4 using PDMS macroCTA (11a) (c) increasing molecular weight for polymerization (d) sample at 48h with 33% conversion for polymerization showing UV 254nm and 320nm as well as DRI data.**
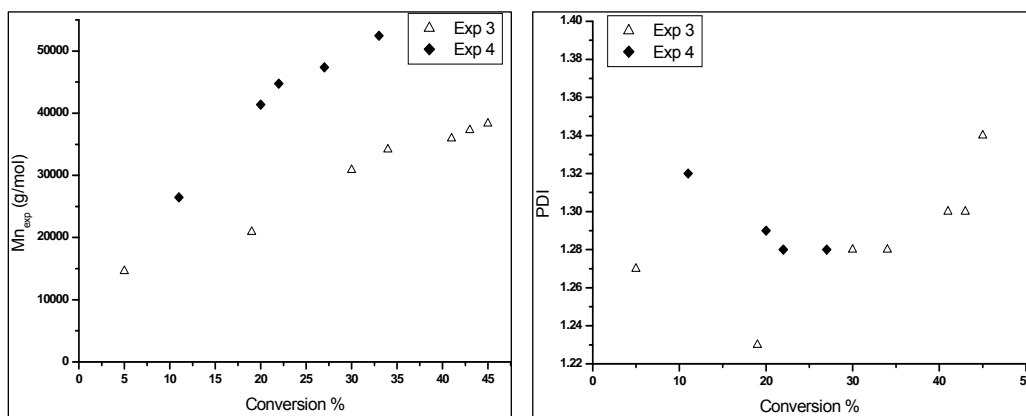
Figure 4.8 **(a) Number-average molecular weight ($\overline{}$,M_n) and (b) PDI versus monomer conversion graphs for PDMS-*b*-PSt block copolymerizations using: PDMS macroCTA (11b) in experiment 3 ($\triangle$) and PDMS macroCTA (11a) in experiment 4 ($\blacklozenge$).**

97

4.4.2 Characterization of PDMS-*b*-PSt block copolymers prepared by solution polymerization

4.4.2.1 Degree of hydrophobicity

The contact angle of a water droplet on a film of the PDMS-*b*-PSt block copolymers was measured using a contact analyzer. It is expected that the film would be relatively hydrophobic as PDMS is considered a superhydrophobic material, and PSt a relatively hydrophobic material. The percentage of PDMS relative to the entire final block in experiment 3 is ~10%, whilst that in experiment 4 is ~14%.

Table 4.4 **Contact angle measurements of PDMS-*b*-PSt block copolymers using water as solvent (experiments 3 and 4).**

Experiment	Contact Angle
3	106°
4	104.8°

4.4.2.2 TEM analysis

Two macroCTAs were used to synthesize block copolymers with styrene. These samples were subsequently analyzed by TEM in order to analyze the morphology. Figures 4.9 (a) and (b) compare the same sample, except the former is without stain and the latter is magnified and contains uranyl acetate stain. Even though stained images may sometimes produce better quality images, It is a worthy exercise to compare images with and without stain so that it becomes possible to identify whether or not the occurrence of possible multiplayer structures are not mistaken for the agglomeration of stain around the particles. Figures 4.9 (a) and (b) clearly show the existence of particles with a definite outerlayer. Many particles contain a sort of acorn-like structure, some even containing more than one acorn per particle. Figure 4.9 (c) is an image of the polymer from experiment 4 containing no stain in which, once again, an acorn-like structure is clearly identifiable with (the range of particle sizes were 140nm–270nm).

a)

b)

c)
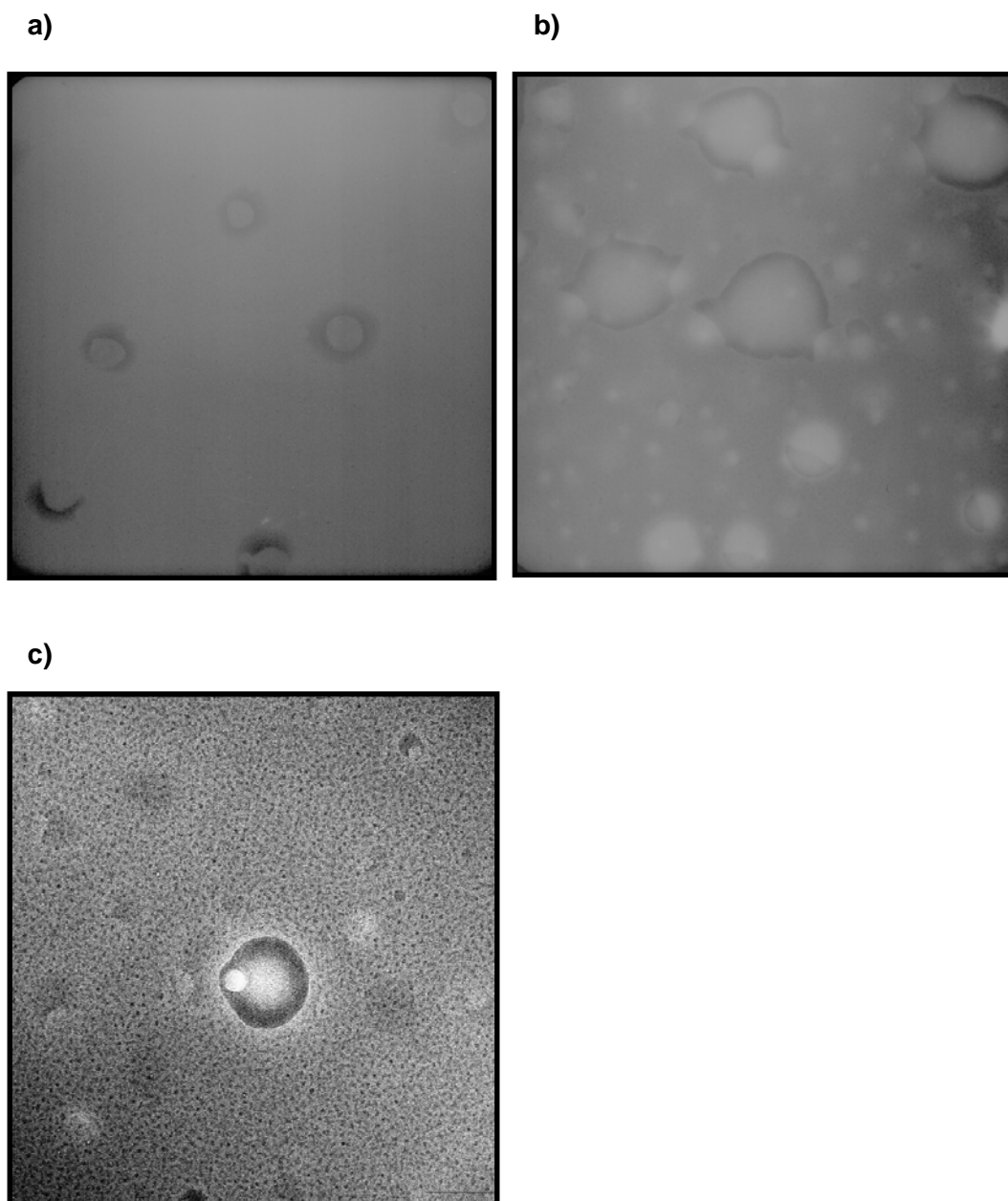
Figure 4.9   **TEM images of: PDMS-*b*-PSt block copolymer experiment 3 (a) no stain (b) uranyl acetate stain; (c) PDMS-*b*-PSt block copolymer experiment 4, no stain.**

4.5   Synthesis of PDMS-*b*-PSt block copolymers in miniemulsion

Due to the limitations set out in solution polymerizations (low conversion), it was decided that a much simpler method to achieve higher molecular weights and faster polymerization times would be through the use of miniemulsion polymerization systems. The work that follows describes the synthesis of a block copolymer of PDMS and PSt using RAFT-mediated miniemulsion polymerization. This work was essentially performed in order to prove the concept that PDMS can be used in miniemulsion polymerizations to synthesize block copolymers with sufficiently high polymerization rates and conversions. To the

knowledge of the author, this is the first report of the synthesis of a PDMS block copolymer using RAFT miniemulsion polymerization.

4.5.1   Emulsion/Miniemulsion theory

This area of chemistry has opened up a great potential for new applications and the reader is referred to a few recent reviews on the field of emulsion and miniemulsion polymerizations.[5-8] An important concept in emulsion/miniemulsion theory is the fact that polymerization takes place in small droplets (nano-droplets in the case of miniemulsion) which allow the system to benefit from all the advantages of conventional systems during polymerization *e.g.* high rates of polymerization and high molecular weights of the resulting polymers.[8] Compartmentalization refers to the segregation of active chains within different latex particles.[9] This phenomenon is primarily governed by the so-called 0–1 system in which only one radical is active within a particle at any given time therefore radical termination is minimized and polymerization rates enhanced. A simplified description of the radical emulsion process is described: monomer is dispersed in an aqueous solution of surfactant with a concentration above the critical micelle concentration (CMC); an initiator (almost always water-soluble) radical from the aqueous phase enters a particle (either a micelle in which case it would be called heterogeneous nucleation, or monomer droplets)[7] containing no other radicals; this radical is then allowed to propagate until a second radical enters the particle, at which point, the particles almost instantaneously terminate, resulting back to a particle containing zero radicals. An important consideration here is that the lengths of the two radicals can hardly be the same, in fact, the second radical to enter has hardly any time to propagate before it is terminated (instantaneous termination).[9] The result of compartmentalization is that faster reaction rates and higher molecular weights can be achieved.[10]

Since the surface area of the monomer-swollen micelles are usually orders of magnitude greater than that of the monomer droplets, radical entry into monomer droplets is very low.[7] Homogeneous nucleation, in which the growing oligomers precipitate out in the aqueous phase, is a third mechanism by which a polymeric latex may be formed.[7] After nucleation, polymer particles grow through the diffusion of monomer from monomer droplets through the aqueous phase by means of diffusion. This can be a limiting mechanism for highly hydrophobic monomers. In this case, monomer droplet nucleation is desired and this can often be achieved through the use of technique, such as ultrasonication, in which the sizes of the monomer droplets can be decreased to submicron size. This sort of emulsion process is coined miniemulsion.[7] Droplet nucleation is what makes miniemulsions unique compared to conventional emulsion systems. The stability of

submicron monomer droplets is achieved through the use of a surfactant as well as a costabilizer (alternative nomenclature is 'hydrophobe'). The role of the former is to stabilize oil and water dispersions by reducing the surface tension and hereby prevent destabilization of an emulsion by collision and coalescence processes, whilst the role of the latter is to reduce the interfacial energy between droplets and hereby prevent Ostwald ripening. An important consideration with regards to the concentration of surfactant is that, whilst it is true that the more surfactant present, the smaller the monomer droplets will be, it is not desirable to have too much free surfactant (that amount spared after every droplet has been stabilized by surfactant) as this would assist in micellar nucleation in addition to droplet nucleation.

Many successful miniemulsion polymerizations have already been carried out with various monomers using RAFT polymerization,[11,12] ATRP[13,14] and SFRP.[15-17] The propagating and intermediate radicals behave very differently in propagation and termination in a RAFT miniemulsion system compared to that of a conventional miniemulsion system. Zero-one kinetics are followed when the following two conditions are met:[18] (1) the rate coefficient of cross-termination between propagating and intermediate radicals is similar to that of self-termination of propagating radicals, or (2) the fragmentation rate coefficient is adequately high. In terms of a using a CTA in emulsion/miniemulsion polymerization systems, the active chain distribution is in fact governed by the same 0–1 system as in non-living emulsion systems [9,18] and the compartmentalization effect is still effective in RAFT polymerization systems.[19] It has been argued that the kinetics of RAFT miniemulsion polymerization is the same as that of conventional miniemulsion polymerization because no radicals are generated or disappear in the RAFT process.[20] The difference though, in the case of RAFT polymerization, is that the presence of the CTA allows the dormant chains to grow without appreciable terminations throughout the polymerization.[9] Equation (4.1) describes the effect of RAFT polymerization addition on miniemulsion polymerization kinetics under a 0-1 condition,

$$\bar{n}_{RAFT^{-1}} = \bar{n}_{blank^{-1}} + 2K_{eq}[CTA]_0 \tag{4.1}$$

where $\bar{n}_{RAFT^{-1}}$ is the average number of propagating radicals per particle in a RAFT miniemulsion system, $\bar{n}_{blank^{-1}}$ is the average number of radicals per particle in a RAFT-free miniemulsion polymerization system, K_{eq} is the RAFT equilibrium constant and $[CTA]_0$ is the CTA concentration at time zero (t=0).

4.5.2   Results and discussion

The reason why this is such a unique piece of work is that PDMS has to date not been able to be part of a block copolymer synthesized by emulsion/miniemulsion polymerization (Scheme 4.2). The PDMS used was functionalized with a thiocarbonylthio moiety by means of a condensation reaction and used as a macroCTA in a further step to produce block copolymers in aqueous media. The advantages over solution polymerizations which can be expected when employing miniemulsion techniques include faster polymerization rates and higher conversions as initiator efficiency in these types of systems is effectively 100%.
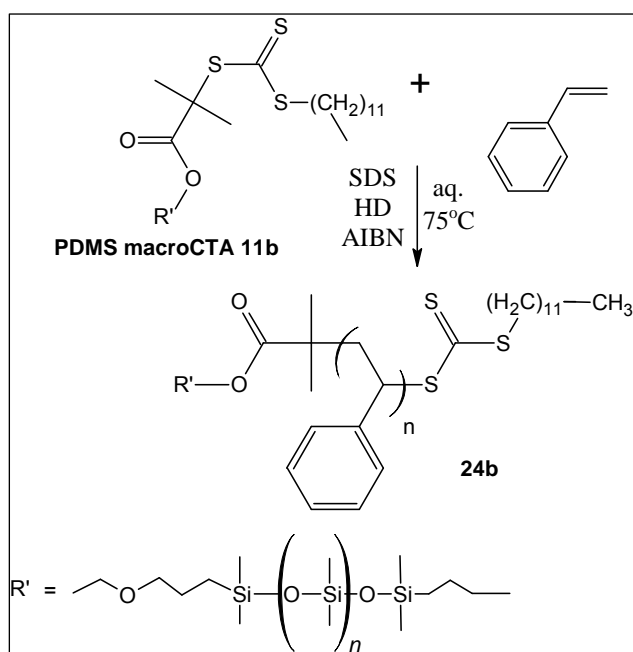
Scheme 4.2   Reaction scheme for miniemulsion polymerizations using PDMS macroCTA (11b) and styrene.

Two miniemulsion (experiments 5 and 6) polymerizations were performed at 75°C, each differing in the targeted molecular weight. Experimental data for both experiments performed are summarized in Table 4.5. The living nature of the system was controlled by using the trithiocarbonyl PDMS macroCTA (11b) that had previously been synthesized (as described in Chapter 3). Conversion data for both experiments are shown in Figure 4.10. Experiment 6 proceeded to complete conversion within six hours, whilst experiment 7 only reached around 50% in that time. The reason for this is that experiment 7 was targeted for a molecular weight of ~125 000g/mol, which is ten times more than that of experiment 6. A longer reaction time is usually required for higher molecular weights.

Table 4.5   **Experimental conditions for PDMS-*b*-PSt miniemulsion copolymers.**

E	T (°C)	[M]/ [CTA]	Theor (g/mol)	[CTA] /[AIBN]	[M] (mol/L)	[AIBN] (mmol/L)	P	[HD] *	[SDS] *	Water wt%	Styrene wt%	P %	HD wt%	SDS wt%
5	75	200	25 900	10	1.46	0.73	7.28	20	15.8	79	17	3.8	3.0	3.0
6	75	1150	124 700	10	1.73	0.15	1.50	21	16.3	79	20	~0.01	2.6	2.6

E = experiment   P % = PDMS macroCTA wt%

T = temperature   * (mmol/L)

P = [PDMS macroCTA] (mmol/L)
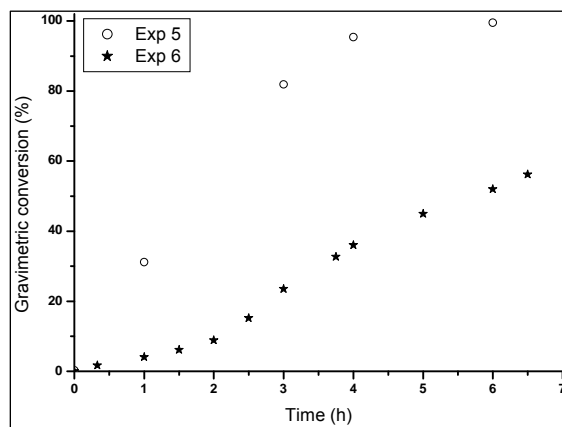
Figure 4.10   **Conversion data for PDMS-*b*-PSt miniemulsion block copolymers in aqueous solution using PDMS macroCTA (11b): experiment 5 (○), experiment 6 (★).**

Table 4.6   **Results for PDMS-*b*-PSt block copolymers synthesized by RAFT in miniemulsion.**

Experiment	Particle size (nm) *		$\overline{M}_n$ target (g/mol)	Conversion	
	First latex	Final latex		Time (h)	%
5	106	106	25 900	1	31
				3	82
				4	95
				6	>99
6	117	147	125 000	0.33	1
				1	3
				1	6
				2	8
				2.5	15
				3	23
				3.75	32
				4	36
				5	45
				6	52
				6.5	56

• as determined by dynamic light scattering

The 1st order kinetic plots for both experiment 5 and 6 are shown in Figure 4.11. Although both graphs seemed to show a slight negative deviation in the early stages of the reaction, they were considered to be fairly linear for the rest of the polymerization, confirming that the concentration of radical species remained fairly constant during the polymerization.
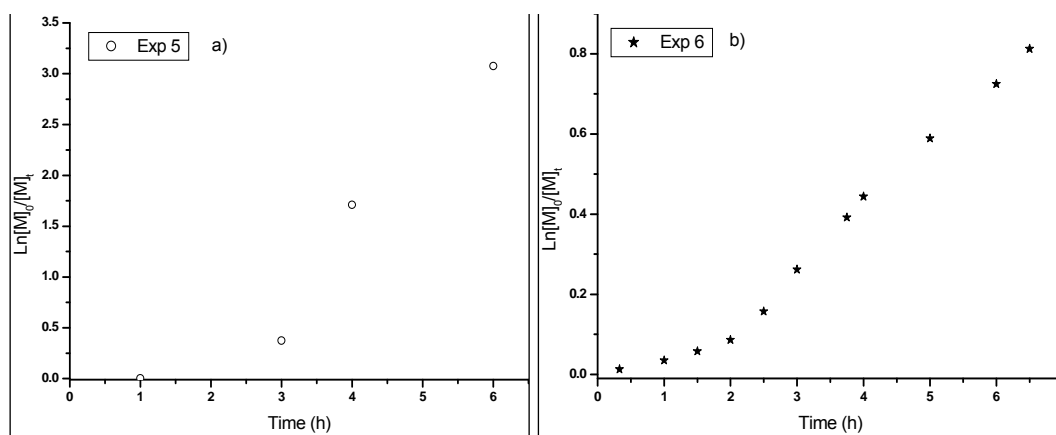
Figure 4.11   **1st Order kinetic plots for PDMS-*b*-PSt block copolymers in aqueous media using PDMS macroCTA 11b; a) experiment 5 (○); b) experiment 6 (★).**

4.5.3   Characterization of PDMS-*b*-PSt block copolymers prepared by miniemulsion polymerization

The PDMS-*b*-PSt block copolymers that have been synthesized are expected to produce self-assembled nanostructures. Diblock copolymers, with their rich phase behaviour and ordering transitions, are ideally studied to study structural transitions arising from confinement.[21] Various authors have undertaken experimental, theoretical and simulation studies to report on the various types of morphologies that can be expected when block copolymers are confined to either one-, two- or three-dimensional systems. In two dimensional systems (2D) morphologies such as concentric-cylindrical lamella,[22-25] stacked-disk or toroid,[23] porous (mesh) lamellae,[25] parallel lamellae and helices[26] have been observed. An important consideration in terms of specific morphology patterns in the degree of confinement (*i.e.* 1D, 2D or 3D) of the block copolymers as well as the surface preference for the segments of the block. Three-dimensional confined self-assembly of block copolymers has resulted in many more novel morphologies not seen in the 2D systems.[27,28] Concentric-spherical lamellae were predicted in these studies, amongst a host of novel morphologies such as perforated concentric-spherical lamellae, segments in which one segment forms struts embedded in the holes of the other segments domains, acorn-shaped particles *etc.* The reason for the 3D systems producing a host of novel morphologies is that in a 3D space the block copolymers have a much greater freedom to orient themselves and rearrange into new patterns. Jeon *et al.*[29] have recently reported on

the blending of PSt-*b*-poly(butadiene) and PSt homopolymer in emulsion polymerization. A variety of morphologies, such as concentric shells, perforated lamellae *etc.*, were observed for different weight fractions of homopolymer to that of the block and the ratio of the diameter of the emulsion drop to the feature spacing of the phase-separated domains. Recent experimental studies performed by the group of Russell *et al.* [22] also studied PSt-*b*-poly(butadiene) diblock copolymers and observed cylindrical and concentric lamellar domains in the pore. Concentric lamellae were also seen in the experimental studies performed by Sun *et al.*[30] on PSt-*b*-poly(methyl methacrylate) symmetric block copolymers.

4.5.3.1   TEM analysis

Figure 4.12 depicts the TEM images taken from the miniemulsion polymerization experiments 5 and 6. Figure 4.12 (a) is the image of the reaction which ran to complete conversion (experiment 5) and there is a clear evidence of multiple concentric rings (onion-like structures) in the particles. According to a recent simulation study,[27] these sorts of 3D images would be expected when there is medium to strong surface preference of one of the segments for a larger range of pore sizes. Figures 4.12 (b) and (c) are images of the miniemulsion polymerization which ran to 56% conversion (experiment 6). These particle images differ to those seen in experiment 5 and more closely resemble those of core-shell or acorn-like particles. According to the same simulation study[27] previously referred to, acorn-like structures are expected when there is low to medium surface preference of one of the segments and rather small pores. The author believes that a possible reason for the difference in the morphology between experiment 5 and 6 is that, in experiment 5, the final latex sample was lower molecular weight than the final sample in experiment 6. Different ratios of the different domains should influence the orientation behaviour of the material. Also, in experiment 6, a lower surfactant and costabilizer concentration was used, which is a possible reason for the particle sizes being larger than those in experiment 5. According to the simulation studies mentioned earlier on, different particle sizes will affect the morphology of the block copolymer.

Attached in Appendix 2 are further TEM images of PDMS-*b*-PSt block copolymers prepared by RAFT using miniemulsion (same as above). Since only TEM images were used to characterize these samples, no further details of these experiments are included in the main body of this dissertation. It can be said that these images are similar to those seen in Figure 4.12 (a), in which a series of multiple concentric rings (onion-like structures) were consistently observed for all the experiments performed.

a)

b)

c)
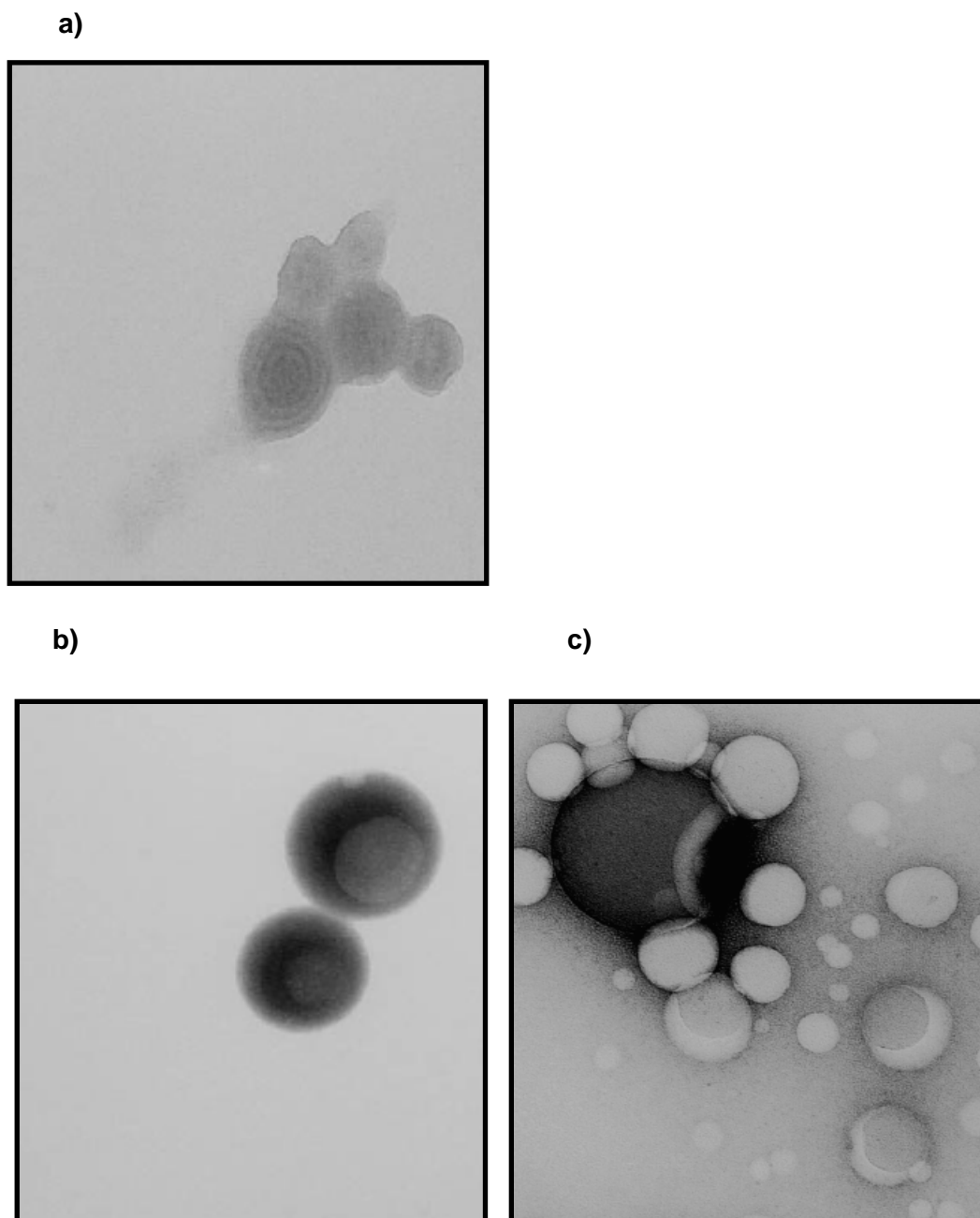
Figure 4.12 **TEM images of: (a) PDMS-*b*-PSt block copolymer experiment 5, no stain; PDMS-*b*-PSt block copolymer experiment 6 (b) no stain, (c) uranyl acetate stain.**

4.6   Conclusion

The first objective was to successfully synthesize PDMS-*b*-PSt block copolymers with sufficiently fast polymerization rates and conversion. The kinetics of the four experiments performed in solution polymerization were quite low- most of them could not reach above 45% within 50 hours. The 1st order kinetic plots did not give an indication of excessive radical loss during the polymerization and the SEC chromatograms showed an increasing

$^-$,M_n with conversion. PDIs were relatively low for most of the time. It could be concluded from the SEC chromatograms through the good UV overlays that there was a thiocarbonylthio moiety present in the increasing molecular weight block copolymers. However, the author was not content with the restricted conversion obtainable from solution polymerizations. It was then decided to try the same system in miniemulsion in which initiator efficiency is essentially 100% throughout the polymerization therefore higher kinetics and molecular weights should be able to be obtained. This was exactly what was observed. Conversion rates were dramatically improved using miniemulsion polymerization techniques compared to solution polymerization. In addition to this, this was the first report of using PDMS as a macroCTA in the synthesis of a block copolymer in miniemulsion polymerization.

Morphology studies revealed that these materials do in fact form self-assembled structures as a result of phase segragation. This observation is consistent with the formation of diblocks. The majority of images revealed acorn-like, or onion-like, structures which have been observed in the literature for many other types of block copolymers.

References

(1) Gilbert, R. G. *Emulsion Polymerization: A Mechanistic Approach*, Academic Press: London, 1995.

(2) Mayo, F. R. *J. Am. Chem. Soc.,* **1968**, *90,* 1289.

(3) Kothe, T.; Fischer, H. *J. Polym. Sci., Part A: Polym. Chem.,* **2001**, *39,* 4009.

(4) Moad, G.; Rizzardo, E.; Thang, S. H. *Aust. J. Chem.,* **2005**, *58,* 379.

(5) Tang, P. L.; Sudol, E. D.; Adams, M. E.; Silebi, C. A.; El-Aasser, M. S. *Polymer Latexes*; eds. Daniels, E. S.,Sudol, E. D.,El-Aasser, M. S.; American Chemical Society: Washington, DC, 1992, 72.

(6) Sudol, E. D.; El-Aasser, M. S. *Emulsion Polymerization and Emulsion Polymers*; eds. Lovell, P. A.,El-Aasser, M. S.; John Wiley & Sons Ltd.: Chichester, 1997, 699.

(7) Asua, J. *Prog. Polym. Sci.,* **2002**, *27,* 1283.

(8) Landfester, K. *Macromol. Rapid Comm.,* **2001**, *22,* 896.

(9) Butte´, A.; Storti, G.; Morbidelli, M. *Macromol. Theory Simul.,* **2002**, *11,* 37.

(10) Ghielmi, A.; Storti, G.; Morbidelli, M.; Ray, W. H. *Macromolecules,* **1998**, *31,* 7172.

(11) Moad, G.; Chiefari, J.; Chong, B. Y.; Krstina, J.; Mayadunne, R. T.; Postma, A.; Rizzardo, E.; Thang, S. H. *Polym. Int.,* **2000**, *49,* 993.

(12) De Brouwer, H.; Tsavalas, J. G.; Schork, F. J.; Monteiro, M. J. *Macromolecules,* **2000**, *33,* 9239.

(13) Matyjaszewski, K.; Qui, J.; Shipp, D. A.; Gaynor, S. *Macromol. Symp.,* **2000**, *155,* 15.

(14) Oh, J. K.; Tang, C.; Gao, H.; Tsarevsky, N. V.; Matyjaszewski, K. *J. Am. Chem. Soc.,* **2006**, *128,* 5578.

(15) Macleod, P. J.; Barber, R.; Odell, P. G.; Keoshkerian, B.; Georges, M. K. *Maromol. Symp.,* **2000**, *155,* 31.

(16) Prodpran, T.; Dimonie, V.; Sudol, E. D.; El-Aasser, M. S. *Macromol. Symp.,* **2000**, *155,* 1.

(17) Georges, M. K.; Lukkarila, J. L.; Szkurhan, A. R. *Macromolecules,* **2004**, *37,* 1297.

(18) Luo, Y.; Wang, R.; Yang, L.; Yu, B.; Li, B.; Zhu, S. *Macromolecules,* **2006**, *39,* 1328.

(19) Tonge, M. P.; McLeary, J. B.; Vosloo, J. J.; Sanderson, R. D. *Macromol. Symp.,* **2003**, *193,* 289.

(20) Butte´, A.; Storti, G.; Morbidelli, M. *Macromolecules,* **2001**, *34,* 5885.

(21) Bates, F. S.; Frederickson, G. H. *Annu. Rev. Phys. Chem.,* **1990**, *41,* 525.

(22) Xiang, H.; Shin, K.; Kim, T.; Moon, S. I.; McCarthy, T. J.; Russell, T. P. *Macromolecules,* **2004**, *37,* 5660.

(23) Xiang, H.; Shin, K.; Kim, T.; Moon, S. I.; McCarthy, T. J.; Russell, G. T. *J. Polym. Sci., Part B: Polym. Phys.,* **2005**, *43,* 3377.

(24) Li, W.; Wickham, R. A.; Garbary, R. A. *Macromolecules,* **2006**, *39,* 806.

(25) Feng, J.; Riuckenstein, E. *J. Chem. Phys.,* **2006**, *125,* 164911.

(26) Yu, B.; Sun, P.; Chen, T.; Jin, Q.; Ding, D.; Li, B.; Shi, A.-C. *J. Chem. Phys.,* **2007**, *127,* 114906.

(27) Yu, B.; Li, B.; Jin, Q.; Ding, D.; Shi, A.-C. *Macromolecules,* **2007**, *40,* 9133.

(28)   Li, W.; Wickham, R. A. *Macromolecules,* **2006**, *39,* 8492.

(29)   Jeon, S.-J.; Yi, G.-R.; Koo, C. M.; Yang, S.-M. *Macromolecules,* **2007**, *40,* 8430.

(30)   Sun, Y.; Steinhart, M.; Zschech, D.; Adhikari, R.; Michler, G. H.; Gosele, U. *Macromol. Rapid Commun.,* **2005**, *26,* 369.

Chapter 5

RAFT homopolymerizations using n-acryloylmorpholine (NAM)

Abstract

The RAFT polymerization of NAM was studied in order to establish reaction conditions which would provide optimal rates of monomer conversion and to determine experimental molecular weights. To our knowledge these are the first examples of homopolymerizations of NAM reported using 2-(dodecylsulfanyl)thiocarbonylsulfanyl-2-methyl propionic acid (DMP) (10b) as chain transfer agent (CTA) by means of RAFT polymerization. This CTA was chosen due to its facile preparation as well as the fact that it appeared to the author that the nature of its substituents should make for a good choice of CTA. DMP is a trithiocarbonate with very high chain transfer efficiency[1,2] and polymerizations were performed to mimic expected kinetics in Chapter 6 as the macro CTA (synthesized in Chapter 3) used in the following chapter is functionalized with CTA (10b). Fast polymerization rates following first order kinetics as well as the presence of UV 325nm absorption due to the thiocarbonylthio moiety with increasing molecular weights result from these polymerizations. In addition to this, PDIs<1.5 were achieved for all RAFT polymerizations carried out. Comparisons were made using a second CTA, 2-((2-phenyl-1-thioxo)-thio)propanoic acid (PTP) (10c), for the homopolymerizations with NAM. This CTA has been used previously with NAM and is presented in this work merely for comparative reasons. The work carried out in this section of the research was performed with the aim of obtaining optimal conditions for the work in the forthcoming chapter, namely that of block copolymerizations by RAFT polymerization with PDMS and NAM.

5.1   Introduction

Poly(acrylamides) are polar compounds that contain a nitrogen as well as an oxygen atom in their structure. This class of polymer is biocompatible as well as hydrophilic. NAM is an amphiphilic, water-soluble bi-substituted acrylamide derivative that has been used extensively to synthesize cross-linked networks for gel-phase synthesis of peptides,[3] semipermeable membranes for plasma separation,[4,5] polymeric supports for gel chromatography[6] and (capillary)[7] electrophoresis,[8] and has been used in photocurable products such as inks,[9] as well as for molecular biology[10-14] and biomedicine and drug

delivery applications.[15-20] This monomer (and corresponding polymer) is soluble in a wide range of organic solvents (chloroform, dichloromethane, dioxane, isopropanol, dimethylforamide, tetrahydrofuran (THF)) as well as aqueous media, making it very versatile with regards to analytical techniques. PolyNAM chains can reach high molecular weights and have shown to display a low incidence of provoking immunological reactions *in vivo*[15,21-23] with a virtual lack of toxicity,[18] making it a suitable material for many biological applications.[24,25]

5.2   Objectives

The three objectives for this part of the research are to be able to:

- be the first to report on the successful RAFT polymerization of NAM using CTA (10b).
- deduce from a comparative study of CTAs with different stabilizing and leaving (Z and R respectively) groups whether the CTA (10b) is a good choice of CTA for RAFT polymerizations of NAM.
- be able to report on molecular weight data of the homopolymerizations performed with NAM using multiangle light scattering (MALS).

5.3   Living radical (meth)acrylamide polymerizations

Acrylamide derivatives have been synthesized by conventional free radical techniques but there has been some difficulty with regards to using some of the controlled radical techniques. Controlled NMP has been obtained for the acrylamide *bi*-substituted derivative *N,N*-dimethylacrylamide (DMA) and *N-tert*-butyl-2-methyl-1-phenylpropyl nitroxide (TIPNO)[26] as the controlling agent, but was uncontrolled when using 2,2,6,6-tetramethyl-1-piperdinyloxy nitroxide (TEMPO)[27] as the controlling agent. NMP has also been used to synthesize block copolymers of DMA-*b*-butyl acrylate (DMA-*b*-BA),[28] DMA-*b*-4-vinylpyridine,[29] DMA-*b*-*N*-hexadecyl-4-vinylpyridinium bromide.[30]

The first papers using NMP to synthesize poly(*N*-isopropylacrylamide) (PNIPAM) dates back to 2001 in which Hawker *et al.*[31] synthesized NIPAM polymers using α -hydrogen-containing nitroxides such as 2,2,5-trimethyl-3-(phenylethoxy)-4-phenyl-3-azahexane (TIPNO-styryl).[32] Recent success of telechelic PNIPAM via NMP initiated by functional nitroxides on the basis of TIPNO derivatives has been reported by Binder *et al.*[33] in which PDIs remained below 1.2 for conversions above 80%. In addition to this, styrene, acrylate, acrylamide and acrylonitrile-based monomers have also been polymerized with these nitroxide derivates. It has been shown that with nitroxides such as TIPNO-styryl, there has been a dramatic increase in the range of monomers that can be polymerized

under controlled conditions and many of the limitations associated with the living NMP free radical procedures has been overcome.[26] Although the use of NMP to synthesize polyacrylamides and their derivatives may follow a controlled polymerization, it is not as common as the use of RAFT polymerization.

Using ATRP, once again, not a wide range of (meth)acrylamide derivatives have been successfully synthesized. Work by Rademacher *et al.*[34] as well as Teodorescu[35,36] indicated that ATRP is not an appropriate method for the living radical polymerizations of (meth)acrylamides. This was based on broad PDIs and poor agreement between theoretical and experimental number average molecular weights ($\overline{M}_n$) which were obtained for the polymerization of DMA. Rademacher *et al.*[34] concluded that the reason for the poor control was due to the complexation of the copper salts with the amide group of the chain ends which stabilizes the radical and hereby retards the deactivation step in ATRP. Since the deactivation step of the activated acrylamide polymer chains are slow, this results in a high concentration of radicals leading to an increase in spontaneous termination reactions. Huang *et al.*[37] have claimed a living polymerization of acrylamide using ATRP with surface-immobilized initiators, however, they did not determine whether this polymer system is capable of reinitiating further monomer.

There has been some success with the ATRP of DMA and other acrylamides when 2-chloropropionate was used as initiator and CuCl/Me$_6$TREN as catalyst.[36] The $\overline{M}_n$ of these polymers were restricted to approximately 10 000g/mol despite a narrow PDI (1.2).[36] Neugebauer *et al.*[38] managed to improve conditions in order to produce (co)polymers of DMA and butyl acrylate with $\overline{M}_n$ in the range of 50 000g/mol and maintaining PDIs at approximately 1.2. Polymerizations by other groups include using again, DMA, as well as diethylacrylamide (DEA) and NIPAM. Low molecular weights (below 20 000g/mol) were obtained with a PDI of around 1.6 for DMA and DEA, whilst the polymerization of NIPAM was uncontrolled.[39] NAM has been synthesized as a graft copolymer from cellulose using cellulose chloroacetate (Cell-ClAc) as a macro-initiator,[40] as well as from poly(styrene-*co*-*p*-chloromethylstyrene) (62/38) as the macroinitiator in the presence of CuBr/1,2-dipiperidinoethane.[41] ATRP has been used to synthesize homopolymers of DMA as well as copolymers of DMA-*b*-BA using methyl 2-chloropropionate/CuCl/Me$_6$TREN as the initiating/catalyst,[38] and *N*-(2-hydroxypropyl)methacrylamide-*b*-BA.[42] Although the above groups have managed to report successful results using ATRP for mostly DMA, it is usually not the method of choice when wanting to synthesize controlled polyacrylamides and their derivatives.

The newest LRP technique, RAFT, appears to be the most versatile of the living polymerization approaches for controlling the homo- and copolymerization of a wide range of (meth)acrylamide derivatives, even to high molecular weights.[1,43-52] The first controlled polymerization of an acrylamide derivative by RAFT polymerization, reported by Le *et al.*,[53] used DMA as the monomer and benzyl dithiobenzoate as the CTA and resulted in a PDI lower than 1.2 for molecular weights exceeding 100 000g/mol. Work by several other groups on the RAFT polymerization of DMA have also been reported.[46-48] Acrylamide itself has been polymerized by RAFT polymerization in aqueous media using a xanthate[54] or dithioester[55] CTA producing molecular weights in the range of 30 000g/mol and PDIs below 1.3. Other water-soluble, non-ionic acrylamide derivatives that have been polymerized by the RAFT process include NIPAM,[56-59] dimethylaminoethylmethyl acrylamide (DMAEMAm)[60] and NAM (see Section 5.4 for a summary of these reactions). Water-soluble, ionic acrylamide derivatives, such as sodium 3-acrylamido-2-methylpropanesulfonate (AMPS) and sodium 3-acrylamido-3-methyl butanoate (AMBA), have also been polymerized as homopolymers[45] and block/statistical copolymers[61] by RAFT polymerization in aqueous media in the presence of 4-cyanopentanoic acid dithiobenzoate. The PDI remained below 1.3 for molecular weights of the homopolymers close to 30 000g/mol, whilst for the block copolymers, the PDI remained below 1.21 for molecular weights reaching 35 000g/mol. Sulfobetaine monomers are another class of ionic acrylamide derivatives for which the controlled synthesis by RAFT has been reported.[49] Several hydrophobic mono-substituted acrylamide derivatives have been polymerized by the RAFT process as well, such as *N-tertiary*-butylacrylamide (TBAm), the *N*-octadecylacrylamide (ODAm) and *N*-diphenylmethylacrylamide (DPMAm).[62] Using *tert*-butyl dithiobenzoate (*t*BDB) as CTA, only TBAm and ODAm exhibited a well controlled polymerization allowing conversion to reach up to 70% with PDIs remaining below 1.3 for molecular weights in the 30 000g/mol range. Using the same conditions, DPMAm only reached 20% conversion, mainly due to steric hindrance.

5.4 Literature review of NAM polymerizations

The conventional free radical homopolymerization of NAM, as well as the conventional free radical copolymerization of NAM with *N*-acryloxysuccinimide (NAS), were published in 1994 by Ranucci *et al.*[16] and in 2001 by D'Agosto *et al.*,[63] respectively. Over the past few years there have been many successful attempts of the living polymerization of NAM. NAM was polymerized using the RAFT process for the first time in 2002 by Favier *et al.*[64] in which a range of dithioester CTAs were investigated. According to the SEC results, of the range of dithioester CTAs tested, *t*BDB appeared to be the best suited for NAM polymerization ($\bar{\ },M_n$ increased linearly with conversion and PDI<1.1). Further work by

some of the members in this group included the investigation of experimental parameters[65] (temperature, monomer concentration, CTA to initiator molar ratio ([CTA]/[AIBN]), monomer to CTA molar ratio(M]/[CTA])) of polyNAM, using *t*BDB as CTA, as well as reporting on matrix-assisted laser desorption ionization time-of-flight mass spectrometry (MALDI-TOF MS) analysis.[66] Controlled polyNAM chains in the range from 2000–80 000g/mol and PDIs less than 1.1 were obtained and the lower molecular weight chains were successfully analyzed by MALDI-TOF MS. Work by D'Agosto *et al.*[67] investigated the effect of the Z group on NAM polymers using a CTA with the same R group, namely a propionic acid functionality, hereby giving rise to secondary reinitiating radicals. The two CTAs had a benzyl and phenyl Z group respectively, and results indicated that the former gave lead to improved molecular weight control and PDI (<1.2), indicating the process of a living polymerization. Recently, a study was carried out to determine the suitability of polyNAM as a poly(ethyleneglycol) (PEG) replacement in biological applications[68]. In this study, the homopolymerizations and block copolymerizations of NAM, *N*-acryloylpiperidine (AP), and *N*-acryloylazocane (AH) were carried out by means of RAFT polymerization. Results from this study revealed that polyNAM showed similar behaviour to PEG with respect to the size of aggregates and segregation behaviour.

Copolymers of NAM have been attempted by D'Agosto *et al.*[67] who successfully synthesized amphiphilic PNAM-*b*-PSt. Ferruti *et al.*[69] claimed to have synthesized polymers of NAM with acrylic and methacrylic esters of NAS, although they failed to provide precise molecular weight data. In other work published,[70] NAM was copolymerized by means of RAFT polymerization with the activated ester monomer NAS to yield water and organic soluble copolymers that may provide a range of biological and pharmaceutical applications. Also, NAM/NAS copolymer has been copolymerized by free radical polymerization to produce blocks for application in molecular biology.[11] Further block copolymers using NAM/RAFT polymerization can be found in the literature such as the amphiphilic poly(*N*-tert-butyl acrylamide-*b*-*N*-acryloylmorpholine) copolymer reported by de Lambert *et al.*[10], as well as the triblock copolymer of *tert*-poly(*N*-*tert*-butyl acrylamide-*b*-(*N*-acryloylmorpholine-*co*-*N*-acryloxysuccinimide)) which was a support for oligonucleotide (ODN) synthesis, to elaborate polymer-oligonucleotide conjugates.[13] Thermosensitive poly(*n*-isopropylacrylamide-*b*-*n*-acryloylmopholine)(PNIPAM-*b*-polyNAM) copolymers have been synthesized by Eeckman *et al.*[71] via conventional free radical polymerization for the application in oral controlled drug delivery systems. As to date, the most recent report of the synthesis of amphiphilic block copolymers in which one component was NAM was reported in 2008 by Li *et al.*[72] in which poly(methylacrylate)-*b*-poly(*N*-(acryloyloxy)succinimide-co-(*N*-acryloylmorpholine)) (PMA-*b*-P(NAS-*co*-NAM)) was

synthesized by RAFT polymerization and then was supramolecularly assembled into micelles in aqueous solution.

5.5 Experimental

5.5.1 Materials

N-Acryloylmorpholine (NAM) (Aldrich, 97%), 1,4-dioxane [123-91-1] (Merck, 99+%), diethyl ether [60-29-7] (Merck, 98%) and trioxane [110-88-3] (Riedel De Haen) were used as received. 2,2'-azobis(isobutyronitrile) [78-67-1] (AIBN) (Riedel De Haen) was purified by recrystallization from methanol. 2-(dodecylsulfanyl)thiocarbonylsulfanyl-2-methyl propionic acid (DMP) (10b)[2] and 2-((2-phenyl-1-thioxo)-thio)propanoic acid (PTP) (10c)[67] were synthesized according to the methods found in the literature.

5.5.2 Polymerization procedure

All solution experiments were performed in the same manner. 1,4-dioxane and AIBN were used as solvent and initiator for all polymerizations. A typical experimental procedure is described. A solution of monomer (NAM), initiator (AIBN), CTA (10b or 10c), trioxane (internal reference) and solvent (1,4-dioxane) were introduced in a 250mL Schlenk tube equipped with a magnetic stirrer. The mixture was degassed by freeze–evacuate–thaw cycles until no more oxygen was present and then heated in a thermostated oil bath. Periodically, samples were withdrawn from the polymerization medium via a syringe for analyses. Polymers were purified by precipitation in an excess of diethyl ether, filtered and washed several times using the same solvent, after which they were dried *in vacuo* to give a polymer powder. Trioxane (internal reference for ^{1}H-NMR determination of monomer consumption) was used in all reactions.

5.5.3 Analyses and sample preparation

Conversion. As a result of the high boiling point of the monomer (257°C at 1atm (760mm)), conversion had to be determined by an analytical method. ^{1}H-NMR was used to monitor the conversion of NAM. Proton nuclear magnetic resonance (^{1}H-NMR) spectra were recorded on a Varian VXR 300MHz spectrometer and were performed at room temperature using deuterated chloroform (CDCl$_3$) (99.8%) as the solvent. Approximately 120mg of sample was transferred to an NMR tube and deuterated chloroform added. A ^{1}H-NMR spectrum was recorded at the beginning of the experiment, as well as at regular time intervals throughout the polymerization. The conversion of polymer was determined

by monitoring the depletion of the monomer peaks (CDCl$_3$, 5.68, 6.28 and 6.53ppm, ref. trioxane 5.1ppm) in the ^{1}H-NMR spectra relative to trioxane.

Molecular weight analyses (relative). Molecular weights were determined using SEC. Samples were prepared for SEC analysis by precipitating each solution aliquot in diethyl ether, washing it several times, and then drying it to completion in a vacuum oven for 12 hours. The dried polymers were weighed off (~10mg), dissolved in 3mL HPLC grade THF (0.012% BHT), filtered through a 0.2μm filter and then submitted for SEC analysis. UV wavelengths used to analyze samples were 240nm and 320nm. These wavelengths were chosen due to the fact that the maximum absorption of polyNAM is at 240nm and the thiocarbonylthio functionality absorbs at 320nm. The SEC instrument specifications can be seen in Chapter 3.

Molecular weight analyses (absolute). The absolute molecular weights of the polymers were determined by multiangle light scattering (MALS) in THF containing 0.012% BHT at 30°C on a Dawn-F DSP instrument (Wyatt Technology; He-Ne laser operating at 632.8nm). The dried polymers were weighed off, dissolved in the solvent, filtered through a 0.2μm filter and then submitted for analysis. The column specifications and sample procedure were the same as that for determining relative molecular weights (as above). Data processing was performed using Astra (V4.73.04) software.

Measuring differential refractive increments (*dn/dc*)*.* The (dn/dc) of polyNAM was determined with the same eluent used in SEC and MALS - namely THF (concentration (c) <10.0mg/mL) - using a ScanRef (NFT) differential refractometer equipped with a filtered light source at 632.8 nm. Solutions were filtered through a 0.2μm filter. Data sampling and evaluation of the raw data were performed using Data Labview 4 Run-Time (National Instruments). No external thermostat was used. This was of no major concern as the response of the interferometric refractometer is independent of the refractive index of the reference solvent, η_r, as indicated by equation (5.1). Duplicate measurements were performed in all cases. This type of instrument is based on a wave front shearing (rotation) technique. Two coherent and linearly polarized beams of light pass, respectively, through two parallel flow cells, one containing the reference solvent, and the other the sample with the same solvent. Any difference in refractive index ($\Delta\eta$) between the two cells results in a phase shift of one beam relative to the other, which in turn is directly proportional to the refractive index difference of the fluids in the two cells.[73] Compared to conventional DRI detectors, this type of instrument allows one to directly measure $\Delta\eta$ ($\Delta\eta = \eta_s - \eta_r$), where η_s is the refractive index of the sample, which is

independent of the refractive index of the solvent (η_r) by measuring the phase difference φ which is calculated by

$$\varphi = \frac{2\pi l \Delta \eta}{\lambda_0}$$

(5.1)

where l is the length of the cell and λ_0 is the vacuum wavelength of the incident light. For more information on this analytical technique, the reader is referred to the specified reference.

5.6 Chromatographic characterization theory

5.6.1 Size exclusion chromatography (SEC)

Chromatographic analysis is a very important tool that has been used extensively in polymer material analysis. SEC (or alternatively gel permeation chromatography (GPC)) is a separation that is based on differences in molecular dimensions. The mechanism of this technique is the passing of a solute (sample) through a bed of cross-linked material (stationary phase/matrix) by means of an eluent (mobile phase/free liquid) of choice. The simple gel chromatography model proposed by Flodin[74] explains the relationship for many substances between elution volume and molecular weight. Flodin proposed that the partition coefficient of the solute between the stationary and mobile phase is governed exclusively by steric effects. Large molecules cannot penetrate into the large area occupied by the porous spaces between cross-links in the gel matrix (stationary phase) as easily as the smaller molecules can. Consequently, small molecules have access to a much wider accessible area between these pore walls of the gel matrix and will consequently be partitioned fairly evenly between the gel matrix and free liquid whilst the larger molecules will be partitioned in favour of the free liquid rather than that of the gel matrix. Hereby, the stationary phase retards different substances at different velocities to provide a separation of the various components of a material (*i.e.* according to molecular weight). Large molecules will be eluted at a smaller volume compared to smaller molecules.

The PDI is another property of the macromolecule which can be determined when using SEC. This property provides information on the amount of variation of polymer chains with different molecular weights present in the macromolecule. In order to determine molecular weights of polymers, one way is to have a calibration curve made up of standards with known molecular weights and very narrow PDIs. For well-fabricated columns, there is an approximate linear relationship over a wide range between the logarithm of molecular size

or weight and the elution volume.[73] Hence, molecular weight can be deduced by the time it takes for a sample to elute. Since columns are calibrated with well-defined standards (*e.g.* PSt), if the molecular configuration of the sample is very different to that of the PSt, very large errors in determining molecular weights can occur.

There are various types of detectors that can be used in conjunction with SEC, such as evaporative light scattering detectors (ELSD), ultraviolet (UV) detectors and differential refractive index (DRI) detectors. For the purposes of this study, only UV and DRI detectors will be discussed under this section. DRI detectors are concentration detectors which determine the concentration of the particular eluent (solution) through the relation

$$\eta_s = \eta_r + \left(\frac{dn}{dc} \right) \Delta c \tag{5.2}$$

where η_r is the refractive index of the pure solvent (reference), η_s is the solution refractive index, and (*dn/dc*) is determined by calibration of the unit for each sample and solvent.[73] Therefore,

$$\Delta c = \frac{(\eta_s - \eta_r)}{(dn/dc)} \tag{5.3}$$

When using a DRI detector as a concentration detector, it can be seen that the displacement of the incident light beam (*d*) is

$$d = \alpha \left(\frac{dn}{dc} \right) \frac{\Delta c}{\eta_r} \tag{5.4}$$

Where Δc is the concentration increment relative to the pure solvent and α is a geometrical constant related to the cell. The voltage output (ΔV) of the DRI is proportional to *d* (displacement distance of the split beams) which in turn is proportional to $\Delta \eta$. Equation (5.4) can be rewritten as

$$d = \frac{\Delta V}{\beta} = \alpha \frac{\Delta \eta}{\eta_r} \tag{5.5}$$

or

$$\Delta V = \gamma \Delta \eta \tag{5.6}$$

where β is a constant relating displacement to voltage change and $\gamma = \frac{\beta \alpha}{\eta_r}$. Rewritten in terms of concentration, equation (5.6) may be expressed as

$$\Delta c = \frac{\Delta V}{\gamma \, dn/dc}$$ (5.7)

From the above equation, it is important to ensure that the (*dn/dc*) of the separated sample is constant throughout to prevent incorrect concentration measurements.

5.6.2   Multiangle light scattering (MALS)

Compared to SEC, which is a *relative* method for molecular weight determination, light scattering (LS) is one of the few *absolute* methods available for determining polymer molecular weights. This implies that no calibration of the columns with accurate pre-synthesized standards is required. This type of measurement makes use of a laser beam as a light source which is directed upon the sample at several angles. Although LS is a tremendously powerful technique, essential to the characterization of polymers by means of this technique requires that the concentration of each eluting fraction be known, as well as measurement of a differential refractive index increment, (*dn/dc*). The (*dn/dc*) value is the change of solution refractive index with respect to a change in concentration of the molecular species being measured. This may not be problematic when it comes to analyzing homogenous (co)polymers as this value would remain fairly constant over a wide range of molecular weights. For a homopolymer it is generally accepted that the (*dn/dc*) value is almost entirely dependent on the monomer and weakly dependent on (or even independent of) molecular weight.[75] Therefore, for a given polymer-solvent system it is a characteristic constant dependent on the temperature, *T*, and the light wavelength, λ.[76] However, when analyzing heterogeneous copolymers, or polymers with molecular weights below several thousand g/mol, this value can change significantly with molecular weight, therefore it may become necessary to measure this quantity at each elution slice since it may be a function of molecular weight.[73] Often it may be sufficient to use mean (*dn/dc*) values when determining weight average molecular weights ($\bar{M}_W$) of bulk samples.[73]

The basic principle of light scattering is that the intensity of the scattered light (Rayleigh scattering) is directly proportional to the product of the polymer $\bar{M}_W$, c and square of (*dn/dc*) as given by

$$I_{scattered} \propto \bar{M}_W * c * (dn/dc)^2$$ (5.8)

119

This equation (5.8) is usually rewritten as

$$\frac{K*c}{R_\Theta} = \frac{1}{M_w P(\Theta)} + 2A_2 c$$

(5.9)

where A_2 is the second virial coefficient and $P(\Theta)$ is the normalized intensity distribution function, or "scattering function", which relates the angular variation in scattering intensity to the mean square radius (r_g) of the particle. When Θ is zero, $P(\Theta)$ is zero. Usually in SEC, concentrations are very dilute therefore the second term on the right hand side of equation (5.9) can be omitted if the following relation holds: $2A_2cM \ll 1$.[77] Therefore, equation (5.9) becomes

$$\frac{K*c}{R_\Theta} = \frac{1}{M_w}$$

(5.10)

The physical constant K* for vertically polarized incident light is given by

$$K* = \frac{4\pi^2 \eta_0^2}{N_A \lambda_0^4} \left(\frac{dn}{dc}\right)^2$$

(5.11)

where N_A is Avogadro's number. From the above equations, it can be learned that the molecular weight is inversely proportional to the square of (*dn/dc*).

According to Zimm,[78] the probability of finding the center of some segment within the volume element $d\tau$ at a distance τ from another reference segment in its vicinity is defined by

$$\frac{\eta N \rho(r) d\tau}{V}$$

(5.12)

where, N is the molecular concentration, η is number of segments of each molecule, $\rho(r)$ is the radial distribution function of the segments in the molecule and V refers to the total volume of the scattering molecules.

The second principle of light scattering is that the angular variation of scattered light is directly proportional to the related size of the molecule. Equation (5.13),[73] the Rayleigh-Gans-Debye (RGD) *approximation*, embodies the two principles of light scattering. The scattering of the light from a dilute suspension of molecules (as described by equation (5.12)), referred to as the excess Rayleigh ratio (R_Θ) (that is, excess of

scattering of the molecular solution above that scattered by the solvent alone divided by the incident intensity) is given by

$$I_{\text{scattered}} \propto R_{\Theta} = \frac{K^* \eta^2 N^2}{V^2} \int \rho(r) \exp(2\pi i s \, {}^{r}\!/_{\lambda}) d\tau \tag{5.13}$$

where Θ is the angle between the incident and scattered light, r is the distance between two segments, s is the vector difference between unit vectors in the directions of the incident and scattered light rays (*i.e.* s = i - j, refer to Figure 5.1), and λ is the wavelength of the incident light in the solvent of refractive index η_r ($\lambda = \lambda_0/\eta_r$). The integration is over all orientations as well as magnitudes of r at constant s. The magnitude of s is found to be $2\sin\left({}^{\Theta}\!/_{2}\right)$. Equation (5.13) is considered an approximation as it is only valid when the molecular refractive index is almost indistinguishable from the refractive index of the solvent and the total phase shift of the incident light wave as it passes through the molecule is negligible. For most molecules in solution, these conditions are generally satisfied.[73]
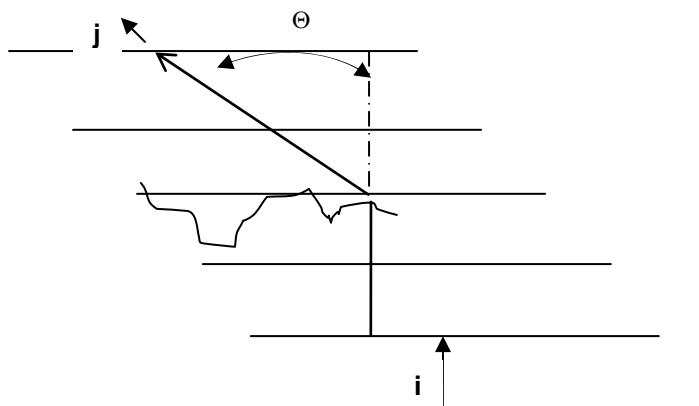
Figure 5.1   **Illustration of incident (i) and scattered (j) light wave from a large macromolecule in the RGD approximation.**

According to Zimm,[78] and equation (5.12), this is the probability of finding a segment in the vicinity of another reference segment, however, it is important that this probability be divided to include the *internal* and *external* probability of finding a segment at a distance r from another reference segment in its vicinity. The internal probability refers to the two segments being in the same molecule, while the external probability refers to the segments being in two separate molecules *i.e.*

$$\frac{\eta N \rho(r) d\tau}{V} = \left[\rho_1(r) + \frac{N \rho_2(r)}{V} \right] \eta d\tau \tag{5.14}$$

where ρ_1 is the internal part and ρ_2 is the external part. These two parts contribute to the Rayleigh ratio (5.13) defined earlier. ρ_1 may be represented in terms of $P(\Theta)$, defined by

$$P(\Theta) = \int \rho_1(r) \exp(2\pi i s \, {}^r\!/_\lambda) d\tau \tag{5.15}$$

The larger r_g, the larger the angular variation ($P_\Theta{}^0 = 1$). For more detail on the above derivations the reader is referred to the specified authors' work.[73,78] Substituting equation (5.15) (and an equation derived for ρ_2 not shown but referred to) into equation (5.13), the following fundamental light scattering equation is derived,

$$R_\Theta = K * cMP(\Theta)[1 - 2A_2 MP(\Theta)c] \tag{5.16}$$

to order c^2 (c is in g/mL) and noting that the second virial coefficient, which accounts for solvent/solute interaction, $A_2 = \dfrac{-N_A \eta^2 X}{(2M^2)}$. X is an integral representing the short range interaction between pairs of segments and M is the molecular weight of the sample. If the solution has a heterogeneous collection of molecular weights, then it is best to use $\overline{},M_W$. Rewriting equation (5.16) leads to the reciprocal of the intensity of scattered light

$$\frac{K * c}{R_\Theta} = \frac{1}{M_w P(\Theta)} + 2A_2 c \tag{5.17}$$

which is usually a good approximation to the true state of affairs at much higher concentrations than its reciprocal (5.16). This equation holds when $2A_2 cM \ll 1$. Therefore, as $\Theta \rightarrow 0, P(\Theta) \rightarrow 0$ and

$$\frac{K * c}{R_\Theta} \rightarrow \frac{K * c}{R_0} = \frac{1}{M_w} + 2A_2 c \tag{5.18}$$

And solving for $\overline{},M_W$,

$$M_w = \frac{1}{K * c/R_0 - 2A_2 c} \tag{5.19}$$

5.7   Homopolymerizations of NAM using CTA (10b)

The following section presents experimental and characterization data for homopolymerizations performed using a trithiocarbonate CTA (10b), with a tertiary leaving group, and NAM. The effect of temperature as well as [CTA]/[AIBN] ratio were investigated. For all experiments the monomer to chain transfer agent ratio (M:CTA) was such that a theoretical molecular weight of 49 700g/mol at 100% conversion was expected.

(10b)   NAM
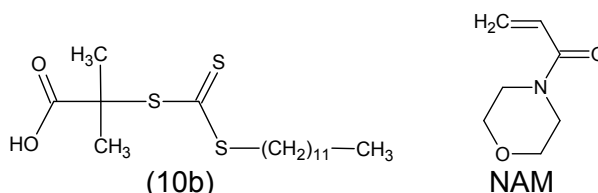
5.7.1   Results

5.7.1.1   Influence of temperature

The kinetics at two reaction temperatures, namely 80°C (experiment 1) and 90°C (experiment 2), were investigated. All other parameters were kept constant and the experimental conditions are shown in Table 5.1. Figure 5.2 (a) presents the conversion of both these experiments according to time. The kinetics follow the expected course with the higher temperature (90°C) polymerization proceeding at a faster rate than the polymerization at 80°C, which could be attributed to the decomposition rate of AIBN, and the rates of propagation, addition, and fragmentation of the RAFT intermediates which should all increase at higher temperatures. In the experiment performed at 90°C, 85% conversion was reached within 12 minutes (0.2h), whilst for the experiment conducted at 80°C, 88% conversion was reached within 45 minutes (0.75h). The $\ln([M]_0/[M]_t)$ versus time plots (Figure 5.2 (b)) were fairly linear for both reactions. For the reaction performed at 80°C, the $\ln([M]_0/[M]_t)$ plot was fairly constant throughout the polymerization, confirming that the concentration of radical species remained almost constant throughout. For the reaction performed at 90°C, initially the $\ln([M]_0/[M]_t)$ plot was fairly linear, afterwards which the observed curving indicated that generation of primary radicals did no longer balance the loss of propagating radicals via irreversible termination reactions.

Table 5.1 **Experimental conditions for the RAFT polymerization of polyNAM (experiments 1–4).**

Experiment	[M] / [CTA]	[CTA] / [AIBN]	[M]$_o$ (mol\L)	[AIBN] (mmol\L)	[CTA] (mmol\L)	Temperature (°C)
1	350	10	2	0.56	5.6	80
2	350	10	2	0.56	5.6	90
3	350	5	2	1.12	5.6	80
4	350	20	2	0.29	5.6	90
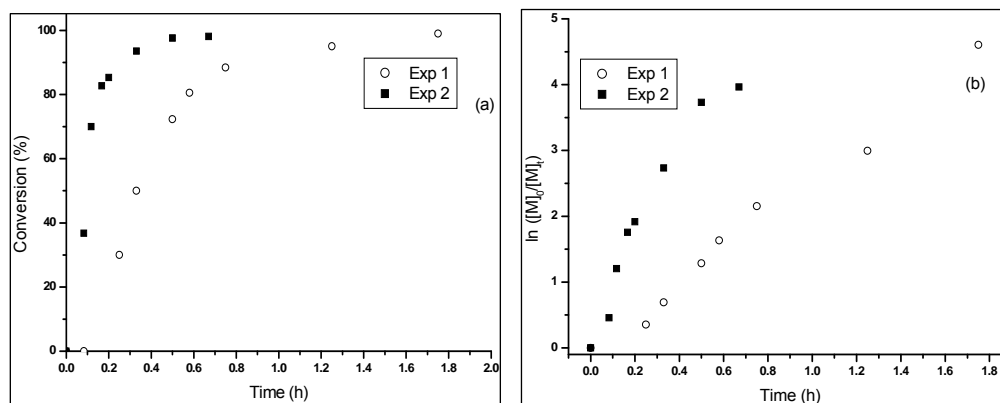
Figure 5.2 **Kinetic results for polyNAM in 1,4-dioxane using CTA (10b) and [AIBN] = 0.56mmol/L; experiment 1 (○) 80°C; experiment 2 (■) 90°C; (a) Conversion data (b) 1st Order kinetic plots.**

Apart from achieving high molecular weights in a reasonable amount of time, molecular weight control is yet another important consideration if one wants to synthesize living polymers. Figures 5.3 and 5.4 present the SEC graphs with DRI and UV overlays for experiment 1 and experiment 2 respectively. Figure 5.3 (a) represents the DRI signals for all the samples taken in experiment 1 in which the peaks were regularly shifted towards higher molecular weights as conversion increased. Figures 5.3 (b) and (c) compare the SEC traces of the polymeric samples precipitated at different time intervals. In all samples, there was a good agreement between the overlays of the DRI and UV 240nm signals, whilst at 325nm there is a slight deviation of the signal which is possibly due to the expected occurrence in such reactions of low molecular weight species (it is known that the UV detector signal is very sensitive to the low molecular weight range end). Because the UV signal sees a single group, it needs a molecular mass correction (while the DRI detector is not mass sensitive), this means that in this case a better fit on the low molecular mass side at high conversions would be produced. Within 20 minutes (0.33h), 50% conversion was reached whist maintaining a narrow PDI (1.12). As conversion increased, the molecular weight distribution became slightly broader with the final sample after 105 minutes (1.75h, 99% conversion) having a PDI of 1.20.
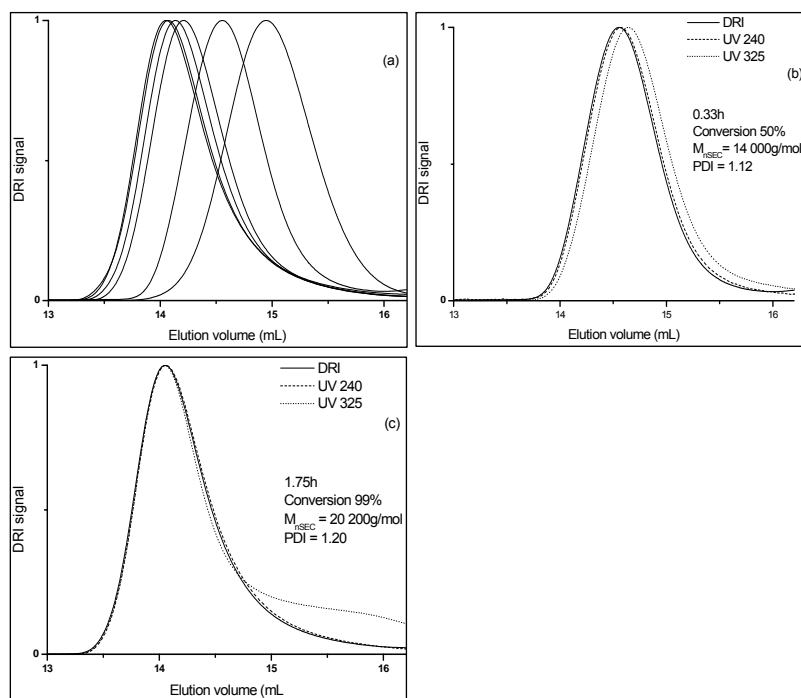
Figure 5.3 **SEC chromatograms of polyNAM for experiment 1 (a) DRI data showing increasing molecular weight for polymerization at 80°C (b) sample at 0.33h with 50% conversion showing UV 254nm and 320nm as well as DRI data (c) sample at 1.75h with 99% conversion showing UV 254nm and 320nm as well as DRI data.**

Figure 5.4 (a) represents the DRI signals for all the samples taken in experiment 2 whilst Figures 5.4 (b) and (c) displays the SEC graphs for samples precipitated at different time intervals. The SEC traces show that the peaks were regularly shifted towards higher molecular weights as conversion increased. The sample at 10 minutes (0.17h) indicates a fairly narrow PDI (1.19) with high conversion (83%), whilst the final sample at 40 minutes (0.67h) indicates a slightly broader PDI (1.24) at almost complete conversion (98%).

Figure 5.5 illustrates the theoretical molecular weight ($\overline{M}_{n\,Theor}$) values versus the observed molecular weight by means of SEC ($\overline{M}_{n\,SEC}$) values for experiments 1 (a) and 2 (b) obtained with polystyrene (PSt) calibration standards in THF. The $\overline{M}_n$ is defined as follows:

$$\overline{M}_{n\,Theor} = \frac{[M]_0}{[CTA]_0} \times M_M \times conversion + M_{CTA} \qquad (5.20)$$

where $[M]_0$ and $[CTA]_0$ are the initial concentrations of monomer and CTA that were added, and M_M and M_{CTA} is the molecular weight of the monomer and CTA respectively. It

should be noted that $\bar{M}_{n\,Theor}$ was calculated from equation (5.20) without considering the number of radicals derived from the initiator[79], which can be a possible cause of the negative deviation (more about this in Section 5.7.1.2).[80] It is also possible that the SEC standard calibration samples of PSt may be another cause for the negative deviations from the theoretical values.
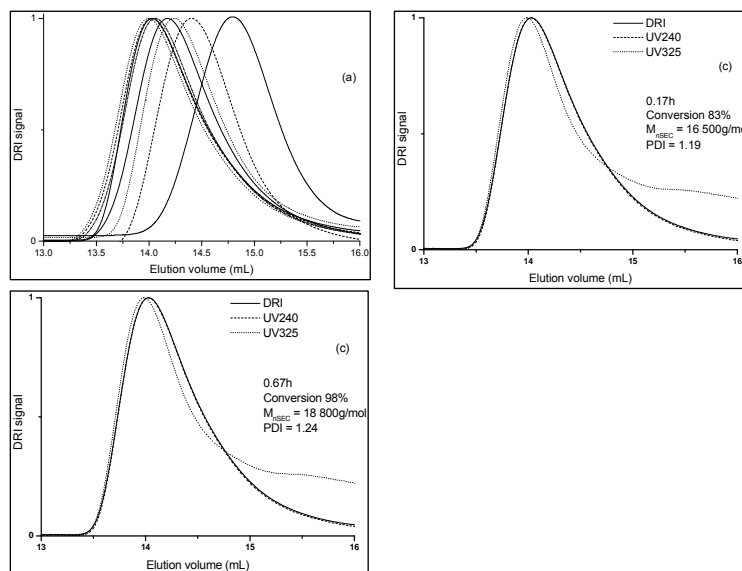

Figure 5.4   **SEC chromatograms of polyNAM for experiment 2 (a) DRI data showing increasing molecular weight for polymerization at 90°C (b) sample at 0.17h with 83% conversion showing UV 240nm and 325nm as well as DRI data (c) sample at 0.67h with 98% conversion showing UV 240nm and 325nm as well as DRI data.**

The author believes that PSt calibration standards are not ideal for the analysis of polyNAM polymers. Ideally in SEC, one would like to use polymer standards of the same polymer being analyzed. Unfortunately there were no polyNAM standards (or of similar hydrodynamic volume) available at the time of SEC analysis, therefore PSt standards were used as the relative calibration. Since SEC separates molecules according to their molecular dimensions, and it is highly likely that polyNAM polymers have different dimensions to that of PSt, the molecular weights are likely to be incorrect.
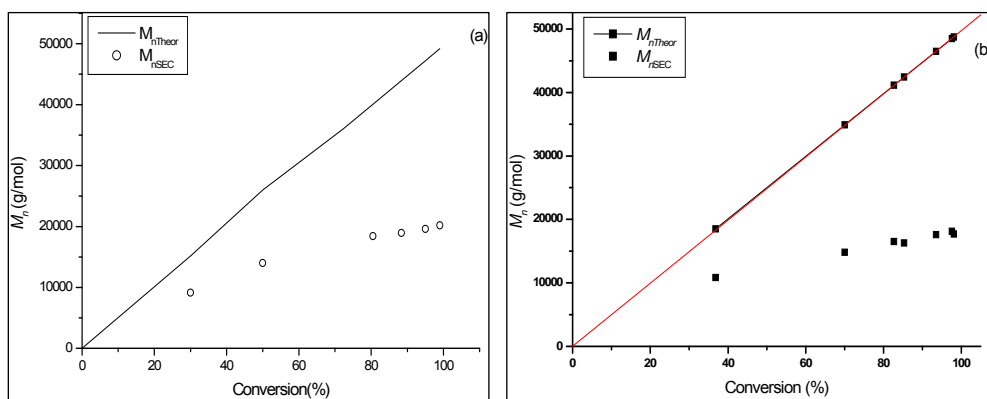
Figure 5.5 **Number-average molecular weight ($\bar{}$, M_n) versus monomer conversion graphs for: (a) experiment 1 (○) 80°C; (b) experiment 2 (■) 90°C.**

Figure 5.6 illustrates that the PDI for both experiments are fairly low, keeping in line with what is expected from a LRP. Refer to Table 5.2 for the results of these reactions.
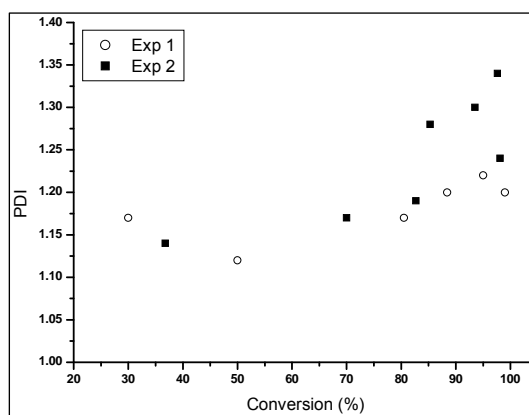
Figure 5.6 **PDI versus monomer conversion graphs for: experiment 1 (○) 80°C; experiment 2 (■) 90°C.**

As has been pointed out in Section 5.6.2, the use of MALS is an *absolute* method for determining polymer molecular weights in which no calibration standards are required. A series of polyNAM samples were analyzed using MALS. The results are reported in Section 5.9. The remainder of Sections 5.7 and 5.8 are concerned with homopolymerizations of NAM performed in the laboratory using two different CTAs. The results of these polymerizations were performed with SEC. In light of the fact that MALS should provide more accurate correlations between $\bar{}$, $M_{n\text{SEC}}$ and $\bar{}$, $M_{n\text{Theor}}$, the SEC results still provide valuable information in terms of the shape of the SEC peaks, the UV overlays, the PDI as well as the fact that there are increases in molecular weights of the polymers with conversion.

5.7.1.2 Influence of [CTA]/[AIBN]

Two sets of comparable reactions at different temperatures were compared with each other. In both instances, all experimental conditions were the same, except for the [CTA]/[AIBN] ratio. Comparisons were made between reactions performed at 80°C with a $[CTA]_o/[AIBN]_o$ of 5 and 10 (experiments 3 and 1 respectively), as well as between reactions performed at 90°C with a $[CTA]_o/[AIBN]_o$ of 10 and 20 (experiments 2 and 4 respectively). Refer to Table 5.1 for experimental conditions and Table 5.2 for results.

Figure 5.7 (a) is a plot of conversion versus time for experiments 1 and 3. Kinetics follows the expected course with a higher initiator concentration resulting in faster polymerization rates. In experiment 1, 95% conversion was reached within 75 minutes (1.25h), whilst for experiment 3, 96% conversion was reached within 30 minutes (0.5h). The $\ln([M]_0/[M]_t)$ versus time plots (Figure 5.7 (b)) for both reactions increased linearly, confirming that the concentration of radical species remained constant throughout.

Table 5.2   **Conversion and SEC results for the RAFT polymerization of polyNAM (experiments 1–4).**

| Experiment	Time (h)	Conversion % (^{1}H-NMR)	$\overline{M}_{n\,SEC}$ (g/mol)	$\overline{M}_{n\,Theor}$ (g/mol)	PDI$_{SEC}$
1	0.25	30	9 200	15 100	1.17
	0.33	50	14 000	25 000	1.12
	0.58	81	18 400	40 000	1.17
	0.75	88	18 900	44 000	1.20
	1.25	95	19 600	47 200	1.22
	1.75	99	20 200	49 200	1.20
2	0.08	37	10 900	18 500	1.14
	0.12	70	14 800	34 900	1.17
	0.17	83	16 500	41 100	1.19
	0.20	85	16 300	42 400	1.28
	0.33	94	17 600	46 500	1.30
	0.50	98	18 100	48 500	1.34
	0.67	98	18 800	48 700	1.24
3	0.17	54	15 200	27 000	1.17
	0.25	80	17 300	39 800	1.24
	0.33	90	18 600	44 800	1.26
	0.42	94	18 900	46 700	1.27
	0.50	96	19 900	47 700	1.28
	0.67	99	20 600	49 200	1.27
4	0.25	60	15 300	30 000	1.19
	0.33	75	17 400	37 200	1.21
	0.42	78	18 300	38 700	1.25
	0.58	86	18 900	42 800	1.28
	0.75	95	18 600	47 100	1.30
	1.50	97	20 000	48 400	1.28
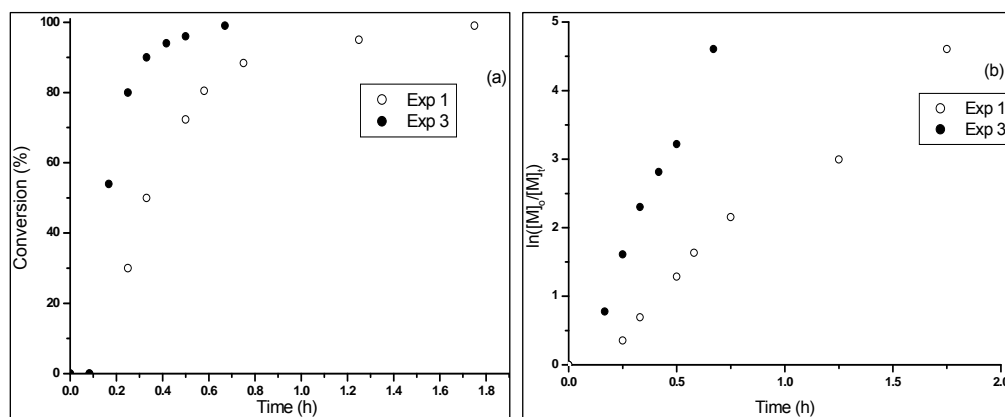
Figure 5.7   **Kinetic results for polyNAM in 1,4-dioxane using CTA (10b) at 80°C: experiment 1 (○), [AIBN] = 0.56mmol/L; experiment 3 (●), [AIBN] = 1.12mmol/L (a) Conversion data (b) 1ˢᵗ Order kinetic plots.**

Figure 5.3 (a) is a SEC graph of experiment 1, which was performed at 80°C, showing the DRI signals for all of the samples increasing in molecular weight as the conversion increases. A fairly lower initiator concentration was used compared to experiment 3 (half the concentration). The SEC chromatograms indicate that molecular weights increased linearly with conversion. Figure 5.3 (b) is the SEC graphs, including both DRI and UV data, for the sample taken after 20 minutes (50% conversion) indicating a fairly narrow PDI of 1.12. Figure 5.3 (c) is the SEC graph of the final precipitated sample taken after 105 minutes (99% conversion). The PDI for this sample is 1.20. The PDI did however increase slightly after 80% conversion, although it still remained fairly narrow until the last sample. It is expected that when a lower [AIBN]$_o$ is used, the PDI of the polymer should remain narrower. Along similar lines, Figure 5.8 (a) is a SEC graph of experiment 3 showing the DRI signals for all of the samples taken during the reaction. Molecular weights increased with increasing conversion. Figure 5.8 (b) is the SEC graph, including DRI and UV, for the sample taken after 10 minutes (54% conversion) indicating a fairly narrow PDI (1.17). Figure 5.8 (c) is the SEC graph of the final precipitated sample indicating both DRI and UV overlays. The PDI increased consistently throughout the polymerization with the final sample having a PDI of 1.27 (99% conversion).
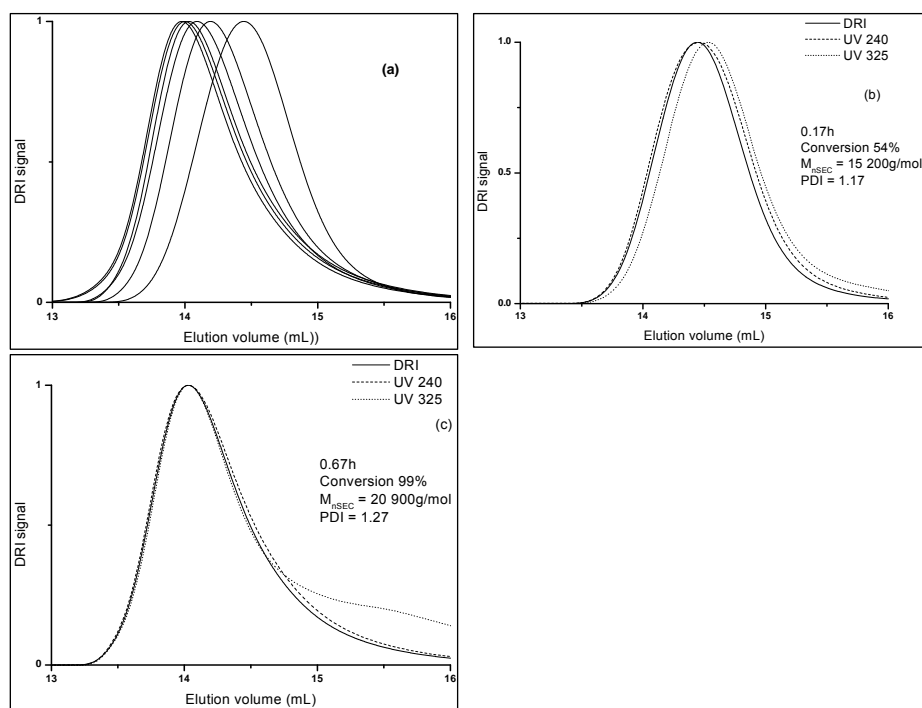
Figure 5.8   **SEC chromatograms of polyNAM for experiment 3 with [AIBN] = 1.12mmol/L: (a) DRI data showing increasing molecular weight for polymerization; (b) sample at 0.17h with 54% conversion showing UV 240nm and 325nm as well as DRI data (c) sample at 0.67h with 99% conversion showing UV 240nm and 325nm as well as DRI data.**

However, as was highlighted with the first two experiments, the SEC data for experiment 3 indicate somewhat lower $\overline{M}_n$ values than those expected from the M:CTA ratio throughout the polymerization (Figure 5.9 (a)). It has been reported previously in literature that negative deviations of molecular weight for RAFT polymerization of *N*-alkyl-substituted acrylamides can be expected.[80-82] According to the classic RAFT polymerization mechanism, the negative deviations may be an indication of the existence of other sources of radicals than the CTA-derived ones, such as initiator-derived chains.[79] In order to determine whether AIBN-derived radicals could be a possible explanation (or part thereof) for the negative deviations experienced in the above reactions (experiments 1 and 2), a lower initiator concentration was used to try and prove this theory. The molecular weight versus conversion graphs for experiments 1 and 3 (double [AIBN] used compared to experiment 1) are shown in Figure 5.9 (a). There appears to be very little, if any, difference between these values. Therefore, in these experiments, using a lower initiator concentration failed to correct the negative deviations and initiator-derived radicals can not be taken as the main cause of molecular weight deviations. The effect of a lower temperature in which a lower number of radicals will be formed was also considered a possibility for negative deviation of these polymers. There was a slight improvement in the molecular weights matching the theoretical values however, this alone was also not the

main cause of negative deviation (experiments 1 and 2 were compared with each other – graph not shown).
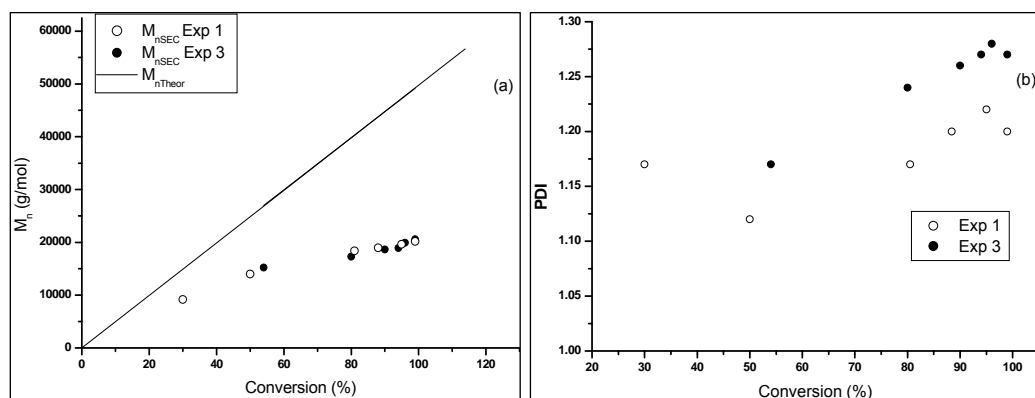
Figure 5.9 **(a) Number-average molecular weight ($\overline{}$, M_n) versus monomer conversion graphs for experiment 3 (●); (b) PDI versus monomer conversion graphs for: experiment 1 (○); experiment 3 (●).**

Comparisons of $[CTA]_o/[AIBN]_o$ were also performed at 90°C. Refer to experiments 2 and 4 in Tables 5.1 and 5.2. Figure 5.10 (a) presents the conversion of both these experiments according to time. The kinetics follows the expected course with the higher initiator concentration (experiment 2) polymerization proceeding at a faster rate than the polymerization in which a lower initiator concentration was used (experiment 4). In the experiment performed with a lower initiator concentration, 95% conversion was reached within 45 minutes (1.25h), whilst for the reaction performed with higher initiator concentration, 94% conversion was reached within 20 minutes (0.33h). The $\ln([M]_0/[M]_t)$ versus time plots (Figure 5.10(b)) for both reactions increased linearly during the initial stages of the reaction, confirming that the concentration of radical species remained constant although there was a negative deviation towards the last samples which is as a result of initiator decomposition.
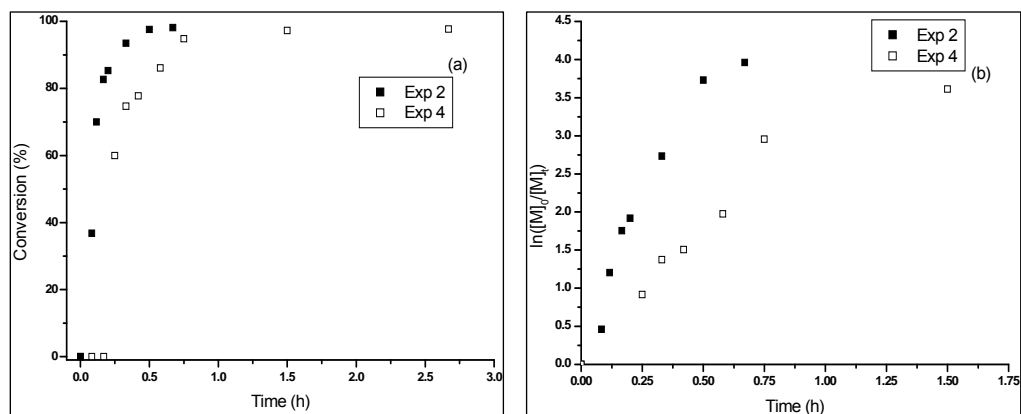
Figure 5.10 **Kinetic results for polyNAM in 1,4-dioxane using CTA (10b) at 90°C: experiment 2 (■), [AIBN] = 0.56mmol/L; experiment 4 (□), [AIBN] = 0.29mmol/L (a) Conversion data (b) 1st Order kinetic plots.**

131

Figure 5.4 is the SEC results for experiment 2 performed with a $[CTA]_o/[AIBN]_o$ of 10, whilst Figure 5.11 is the SEC results for experiment 4 performed with a lower initiator concentration ($[CTA]_o/[AIBN]_o = 20$). The SEC chromatograms of experiment 4 indicate that molecular weights increased linearly with conversion (Figure 5.11 (a)). Figure 5.11 (b) is the SEC graphs, including both DRI and UV data, for the sample taken after 15 minutes (0.25h, 60% conversion) indicating a fairly narrow PDI (1.19). Figure 5.11 (c) is the SEC graph of the final precipitated sample taken after 90 minutes (1.5h, 97% conversion). The PDI increased throughout the polymerization, although it still remained fairly narrow until the last sample (1.28).

However, as was highlighted with all of the previous experiments, the SEC data for experiment 4 indicate somewhat lower $\overline{M}_n$ values than those expected from the M:CTA molar ratio throughout the polymerization (Figure 5.12 (a)). We have learned from the previous experiments that initiator-derived radicals and temperature effects, although they may still play a slight contribution, are not the main cause of this significant negative deviation that occurs. It is believed that these negative deviations of the molecular weight of NAM can be attributed to the use of PSt standars for calibration purposes. A recent article reported on similar negative deviations of molecular weights observed for a series of disubstituted and monosubstituted acrylamide monomers.[80] Disubstituted acrylamide monomers have higher reactivity than their mono- subtituted counterparts, and as a result hereof, form more stabilized radicals and exhibit better control due to the electon donating conjugative effect of the substituents. This results in high polymerization rates and high monomer conversions for disubstituted derivatives. The radicals of monosubstituted monomers are more aggressive than those of their disubstituted counterparts and probably have higher addition rate coefficients. Results from SEC and MALDI indicated that it was easier for chain transfer to monomers to occur for monosubstituted acrylamides.

From the results presented in this study, the experiments performed with NAM seem to resemble the significant amount of negative deviation of molecular weights as reported for monosubstituted acrylamide derivatives in the above literature reference. The reason for this is, at the moment, unclear, as one would expect that the ring substituent of NAM would, like the disubstitued acrylamides, provide a strong electron donating conjugative effect and result in more stable radicals compared to a monosubstituted acrylamide derivative.
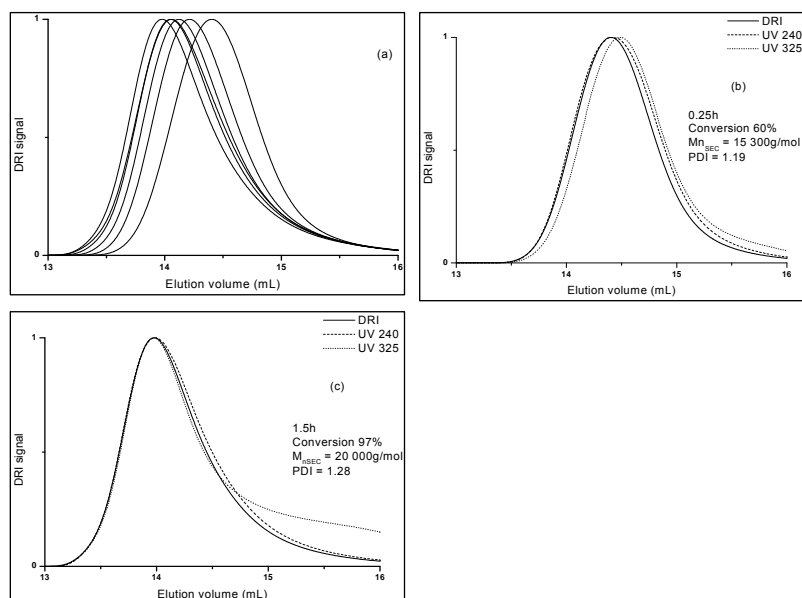
Figure 5.11 **SEC chromatograms of polyNAM for experiment 4 with [AIBN] = 0.29mmol/L: (a) DRI data showing increasing molecular weight for polymerization; (b) sample at 0.25h with 60% conversion showing UV 240nm and 325nm as well as DRI data (c) sample at 1.5h with 97% conversion showing UV 240nm and 325nm as well as DRI data.**
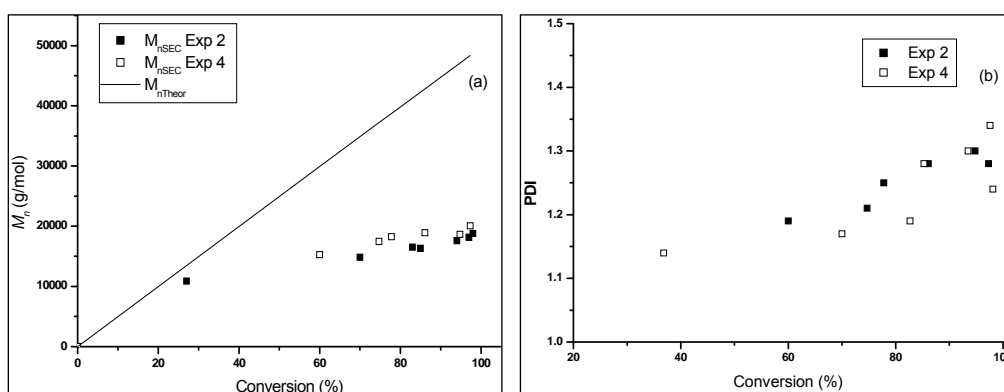
Figure 5.12 **(a) Number-average molecular weight ($\overline{\ }, M_\mathrm{n}$) for experiment 2 (■), [AIBN] = 0.56mmol/L and experiment 4 (□), [AIBN] = 0.29mmol/L and (b) PDI versus monomer conversion graphs for polyNAM polymerization at 90°C: experiment 2 (■) and experiment 4 (□).**

5.7.2   Discussion

Experiments 1–4 were performed using a trithiocarbonate CTA with a tertiary leaving group. Refer to Scheme 5.1 for a brief illustration of the reactant and products involved in these polymerizations. Tertiary radicals are superior leaving groups and are thus more favourable for efficient fragmentation (k_β) when attached to an intermediate radical (4) than their respective poly(acryloylmorpholine) adducts ($P_n^\cdot$) (k_{add}). Poly(acrylamide)

radicals are generally not good leaving groups[83], and it can be assumed that poly(acryloylmorpholine) radicals will inherently also be poor leaving groups.

The kinetic results of the above reactions followed suit with the reactions performed at higher temperatures, and those performed with a higher initiator concentration, showing faster rates of polymerization. The inherent rate of monomer conversion during CTA-mediated RAFT polymerization is usually determined from the slope (equal to $k_p[P_n \cdot]$) of the first-order plot of $\ln([M_0]/[M]_t)$ versus time.[44,57,84] Thomas *et al.*[83] reported on a study that for a given Z group at the same CTA/initiator ratio, the slope of $\ln([M_0]/[M]_t)$ plots will increase when the temperature is increased. Through experimental evidence they also could show that as the initiator concentration increased, an increasing slope of $\ln([M_0]/[M]_t)$ is expected and can be attributed to an increased number of active kinetic chains participating in the RAFT process.

Enhanced kinetics is not the only concern when wanting to use a controlled/living radical technique. Among the other concerns are the linearity of the logarithmic plots, the presence of a UV signal which can be attributed to the CTA, the linear increase in molecular weight with conversion as well as the PDI.
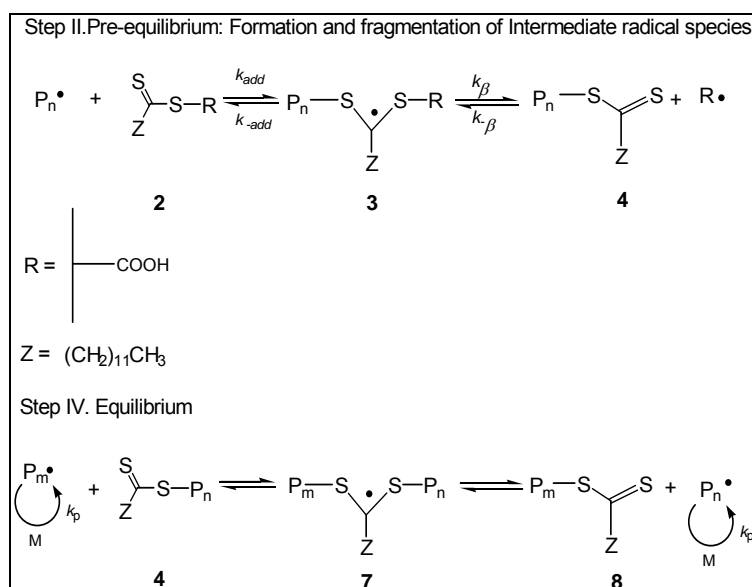
Scheme 5.1   Two steps in the mechanism of RAFT polymerization using CTA (10b).

Conversions for the above polymerizations were fairly fast with less inhibition and retardations as opposed to reactions using more Z-stabilized CTAs. For all reactions, there appeared to be a relatively linear increase in the 1st order kinetic plots to high conversion which is indicative of a fairly constant radical species concentration throughout the polymerizations. For a few of them, however, the final conversion samples did show a negative deviation which is likely as a result of initiator decomposition.

In all of the SEC chromatograms shown, there is a good overlay between the DRI and UV signals. Of particular concern would be the UV 325nm signal as this signal is attributed to the presence of CTA (polyNAM does not absorb at 325nm, however, it does absorb at 240nm). This signal is consistently shifting with the DRI signal as molecular weight increases.

When determining the linear increase of molecular weight with conversion, no meaningful comparison can be made between the observed and theoretical $\overline{M}_n$ because of the lack of absolute molecular weights. However, it was observed that the molecular weight did increase with conversion. The author believes that in order to make a befitting judgment of the degree of control, it is advantageous to consider the PDI data.

According to theory, in order to have optimal control of the polymers synthesized (PDI<1.5) it is necessary that C_{tr} of the thiocarbonyl compounds used in RAFT be greater than 2.[44,85,86] As for conventional chain transfer, the chain transfer constant in RAFT systems (C_{tr}) is given by the ratio of the rate constant for chain transfer to that for propagation (k_{tr}/k_p) (equation (5.21)). However, in the case of reagents that react by addition fragmentation, k_{tr} is a composite term which depends on the rate constant for addition to the thiocarbonyl group k_{add} and the partitioning of the intermediate radical formed between starting materials and products as shown in equation (5.22).[87]

$$C_{tr} = \frac{k_{tr}}{k_p} \qquad (5.21)$$

$$k_{tr} = k_{add} \frac{k_\beta}{k_{-add} + k_\beta} \qquad (5.22)$$

The transfer constants of various thiocarbonylthio compounds have been found to span more than five orders of magnitude (<0.01 to >1000) depending on the Z and R groups and the particular monomer(s) being polymerized.[88] It is desirable to achieve fast rates for both addition of a given radical species to the C=S double bond and fragmentation of the intermediate radical species (3) (producing R·) relative to the rate of propagation. As can be seen from equation (5.21), a high C_{tr} can be achieved by increasing your rates of addition and fragmentation which in turn can be achieved by fine-tuning the design of the CTA. Fast rates of addition can be achieved when the Z species has a stabilizing effect on the intermediate radicals, such as a phenyl group. Generally, a high C_{tr} can be achieved when the Z group in these thiocarbonylthio compounds consist of an (decreasing in the order) aryl>alkyl~alkylthio~pyrrole>acryloxy>amido>alkoxy>dialkylamino.[44]

Unlike the Z group, the R group affects the rate of fragmentation (k_β). The R group must be a good free radical leaving group and efficient at reinitiating polymerization. R should be a good free radical leaving group both in absolute terms and relative to the propagating species derived from the monomer being polymerized. Steric and polar factors also play an important part in determining leaving group ability (and subsequently the C_{tr}).[44] Generally, the bulkier the R group, the higher the C_{tr}. Likewise, the more polar the R group, the higher the C_{tr}.

The stabilizing alkyl group of CTA (10b) should contribute to a fairly high C_{tr} which would imply that the addition step (k_{add}) (propagating radical to thiocarbonyl compound) is quite fast. In addition to this, the leaving group of CTA (10b) is a tertiary radical which is a more stabilized radical than the propagating poly(acryloylmorpholine) radical species (secondary radical) which would favour a fast fragmentation of the intermediate radical in the direction of the product materials. For these reasons, it is expected that the design of the CTA used in reactions 1–4 should not lead to retardation (not observed in any of the above cases) caused by either (1) inefficient reinitiation of the R· or (2) slow fragmentation of the intermediate radical. In all experiments, the PDI of the final samples remained well within the limits of what would be considered a controlled/living polymerization although it did appear to increase slightly towards the final samples. The reason for this is probably due to termination reactions taking place due to increased viscosity. Together with the fact that there is an increase in molecular weight with conversion, and that the UV 325nm signal overlapped fairly well with the shifting DRI signal, the author believes it is sound to conclude that the combination of CTA (10b) and NAM is an appropriate choice of CTA and monomer respectively for RAFT polymerizations. In light of this, in the possible case of some deviation from theoretical molecular weights occurring (due to irreversible termination), the author believes that according to the above theory that this deviation would not be significant.

5.8   Homopolymerizations of NAM using CTA (10c)

The following section presents experimental and characterization data for homopolymerizations performed using a dithioester CTA (10c), which gives rise to secondary reinitiating radicals, and NAM. In each experiment, the data were compared to identical experiments performed with CTA (10b). For all experiments the M:CTA was such that a theoretical molecular weight 49 600g/mol at 100% conversion was expected. Polymerizations using CTA (10c) with NAM have been previously reported in the literature.[67] The results presented below show a slight improvement in the PDI results previously reported.
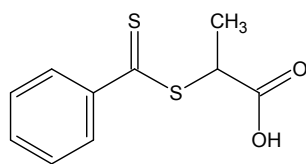
CTA (10c)

5.8.1 Results

5.8.1.1 Comparison of dithioester and trithiocarbonate CTAs

A few of the previous reactions, in which a trithiocarbonate CTA was used, were repeated using another type of CTA, namely 2-((2-phenyl-1-thioxo)-thio)propanoic acid (10c). Refer to Table 5.3 for a summary of the reaction conditions. The kinetics and PDIs of the polymers synthesized in Section 5.7, using CTA (10b), were compared to those synthesized with CTA (10c) (this section) (in all comparisons, identical reaction conditions were employed except for the choice of CTA). It was hoped that by the outcome of these results that the author would be able to elucidate any differences, if any, which could be due to the nature of the structural differences of these two CTAs. Refer to Table 5.4 for a summary of the results.

Table 5.3   Experimental conditions for the RAFT polymerization of polyNAM (experiments 5–7).

Experiment	[M] / [CTA]	[CTA] / [AIBN]	$[M]_0$ (mol\L)	[AIBN] (mmol\L)	[CTA] (mmol\L)	Temperature (°C)
5	350	10	2	0.57	5.7	80
6	350	5	2	1.33	5.72	80
7	350	10	2	0.57	5.72	90

Firstly, experiment 5, using CTA (10c), was a repeat of the experimental conditions of experiment 1. Figure 5.13 (a) presents the conversion of both these experiments according to time. The results indicate that the kinetics differed significantly when using CTA (10c). In experiment 1, 95% conversion was reached within 75 minutes (1.25h), whilst for experiment 5, 85% conversion was only reached after 10h. The $\ln([M]_0/[M]_t)$ versus time plot for experiment 5 (Figure 5.13 (b)) was fairly linear during the initial and middle stages of the polymerization although it did seem to taper off towards the end which allows the observer to believe that the generation of primary radicals did no longer balance the loss of propagating radicals via irreversible termination reactions.

137
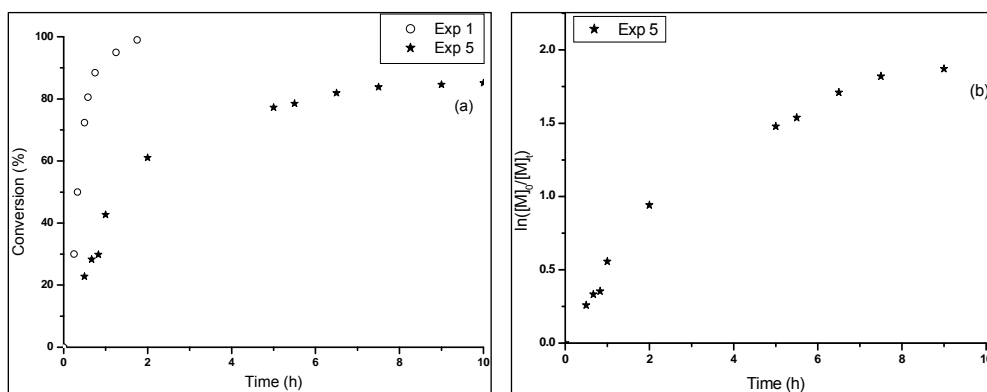
Figure 5.13 **Kinetic results for polyNAM in 1,4-dioxane at 80°C: experiment 1 (○), using CTA (10b); experiment 5 (★), using CTA (10c) (a) Conversion data (b) 1st Order kinetic plots.**

In order to compare the PDI of the two experiments, samples were taken at regular time intervals and analyzed by SEC. Figures 5.3 and 5.14 present the SEC graphs with DRI and UV overlays for experiment 1 and experiment 5 respectively. Within 20 minutes (0.33h), 50% conversion was reached in the polymerization of experiment 1 whilst maintaining a narrow PDI (1.12). As conversion increased, the PDI became slightly broader with the final sample after 105 minutes (1.75h, 99% conversion) having a PDI of 1.20. For experiment 5, 61% conversion was only reached after 2h whilst still maintaining a narrow PDI (1.14). The final sample (10h, 85% conversion) still maintained a narrow PDI (1.22).
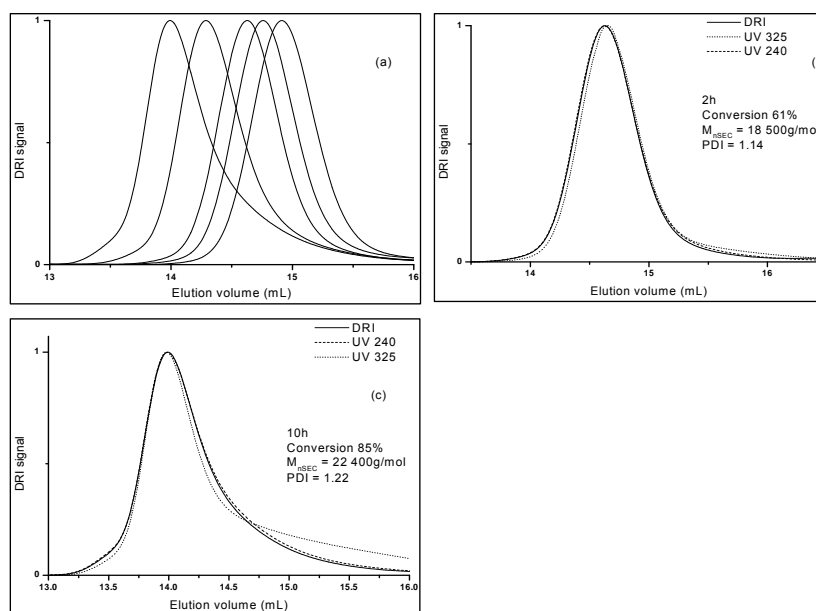
Figure 5.14 **SEC chromatograms of polyNAM for experiment 5 at 80°C using CTA (10c): (a) DRI data showing increasing molecular weight for polymerization; (b) sample at 2h with 61% conversion showing UV 240nm and 325nm as well as DRI data (c) sample at 10h with 85% conversion showing UV 240nm and 325nm as well as DRI data.**

138

However, as was highlighted with experiments 1–4, the SEC data for experiment 5 also indicate that somewhat lower $\bar{,}M_n$ values than those expected from the M:CTA molar ratio occurred throughout the polymerization (Figure 5.15 (a)). This is presumably due to the same reason provided earlier in the previous section, namely that the PSt calibration standards are not ideal for the analysis of polyNAM. Figure 5.15 (b) illustrates that the PDI for both experiments are fairly low, keeping in line with what is expected from a controlled polymerization system.

Compared to the results previously reported,[67] experiment 5 was performed at a lower temperature (85°C compared to 80°C), and a lower CTA concentration was used (11.4mmol/L compared to 5.7mmol/L). The same monomer concentration (2mol/L) CTA:AIBN ratio was used (10:1) in both the literature and experiment 5. Conversion was slower for experiment 5 (after 10h, 85%) than in the literature (2h, 80%) but experiment 5 showed a PDI of 1.14 at approximately the same conversion. This is an improvement upon the PDI value of 1.4 reported in the literature using CTA (10c).
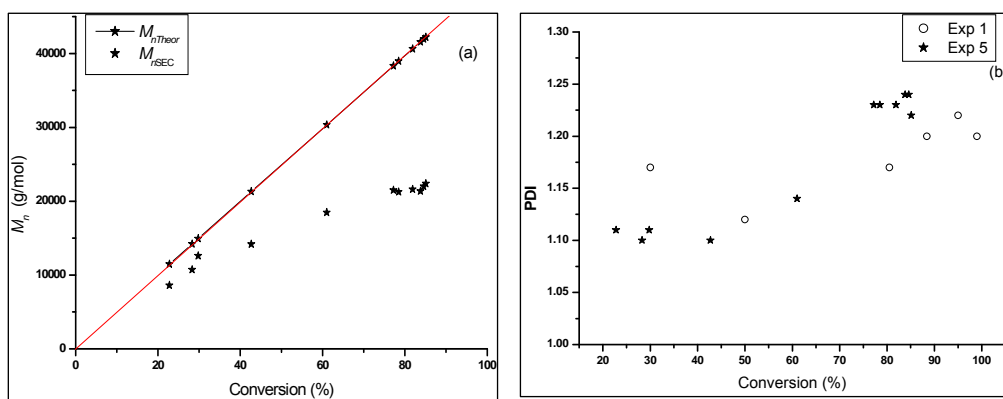
Figure 5.15 **(a) Number-average molecular weight ($\bar{,}M_n$) for experiment 5 (★) and (b) PDI versus monomer conversion graphs for polyNAM polymerization at 80°C: experiment 1 (○), experiment 5 (★).**

A second comparison was made between CTA (10b) and CTA (10c). Reaction conditions for experiment 3 were repeated using CTA (10c) (experiment 6). Figure 5.16 (a) presents the conversion of both these experiments according to time. As can be seen, once again the experiment using the dithioester CTA (experiment 6) polymerized at a significantly slower rate than that using the trithiocarbonate CTA (experiment 3). The $\ln([M]_0/[M]_t)$ versus time plot for experiment 6 (Figure 5.16 (b)) indicates that the generation of primary radicals was balanced with the loss of propagating radicals during the initial stages of the polymerization although it did seem to taper off towards the end of the reaction.
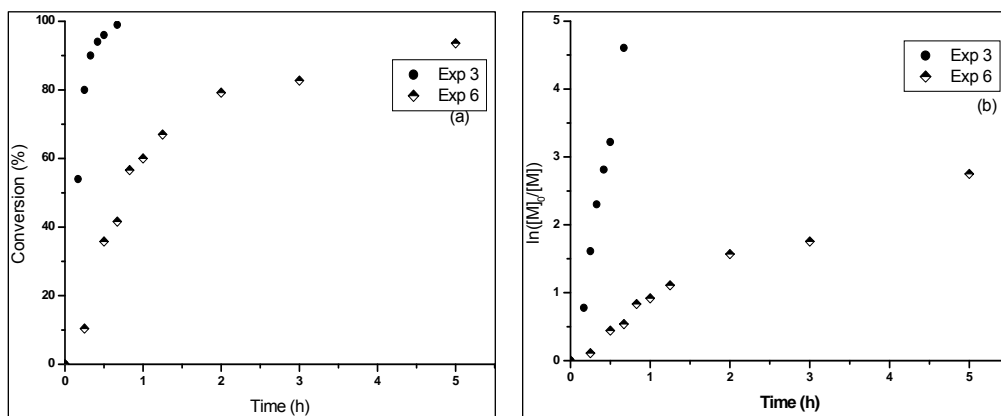
Figure 5.16   **Kinetic results for polyNAM polymers in 1,4-dioxane at 80°C: experiment 3 (●), using CTA (10b); experiment 6 (◇), using CTA (10c) (a) Conversion data (b) 1ˢᵗ Order kinetic plots.**

SEC analysis revealed that the molecular weights of the polymers for experiment 6 increased with conversion. Figures 5.8 and 5.17 present the SEC graphs with DRI and UV overlays for experiments 3 and 6 respectively. Within 10 minutes (0.17h), 54% conversion was reached in the polymerization of experiment 3 whist maintaining a fairly narrow PDI (1.17). As conversion increased, the molecular weight distribution became slightly broader with the final sample after 40 minutes (0.67h, 99% conversion) having a PDI of 1.27. For experiment 6, after 15 minutes (0.25h) only 10% conversion was obtained with the polymer displaying a very narrow PDI (1.11). The final sample (5h, 94% conversion) had a similar PDI (1.29) to that obtained with experiment 3.

Table 5.4 **Conversion and SEC results for the RAFT polymerization of polyNAM (experiments 5–7).**

| Experiment	Time (h)	Conversion % (NMR)	M_{nexp} (g/mol)	M_{ntheor} (g/mol)	PDI_{SEC}
5	0.50	23	9 000	11 400	1.11
	0.67	28	10 700	14 100	1.10
	0.83	30	12 600	14 900	1.10
	1.00	43	14 200	21 300	1.10
	2.00	61	18 500	30 300	1.14
	5.00	77	21 500	38 300	1.23
	5.50	79	21 300	38 900	1.23
	6.50	82	21 600	40 600	1.23
	7.50	84	21 400	41 500	1.24
	9.00	85	22 000	41 900	1.24
	10.00	85	22 400	42 200	1.22
6	0.25	10	4 900	5 300	1.11
	0.50	36	10 700	17 800	1.15
	0.83	57	15 500	28 000	1.16
	1.00	60	16 700	29 800	1.13
	1.50	67	18 000	33 200	1.23
	2.00	79	19 200	39 200	1.24
	3.00	83	20 000	41 000	1.28
	5.00	94	20 900	46 400	1.29
7	0.17	34	12 300	16 800	1.11
	0.33	44	14 500	21 800	1.12
	0.50	58	18 000	29 000	1.16
	0.67	67	19 400	33 200	1.20
	0.58	75	19 700	37 000	1.25
	1.25	78	21 200	38 400	1.26
	1.50	81	21 500	40 100	1.29
	2.00	85	21 900	42 300	1.30
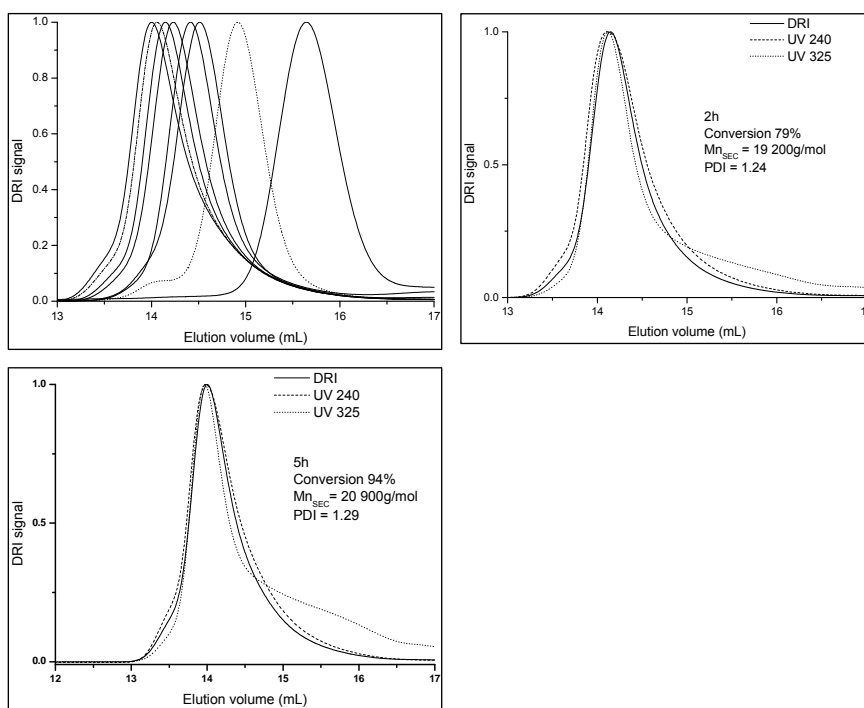
Figure 5.17   **SEC chromatograms of polyNAM for experiment 6 at 80°C using CTA (10c): (a) DRI data showing increasing molecular weight for polymerization; (b) sample at 2h with 79% conversion showing UV 240nm and 325nm as well as DRI data (c) sample at 5h with 94% conversion showing UV 240nm and 325nm as well as DRI data.**

However, as was highlighted with experiments 1–5, the SEC data for experiment 6 also indicate that somewhat lower $\bar{M}_n$ values than those expected from the M:CTA molar ratio occurred throughout the polymerization (Figure 5.18 (a)). This is presumably due to the same reason provided earlier in this section, namely that the PSt calibration standards are not ideal for the analysis of polyNAM polymers. Figure 5.18 (b) illustrates that the PDI for both experiments are fairly low, keeping in line with what is expected from a controlled polymerization system.

Compared to the results previously reported,[67] experiment 6 was performed at a lower temperature (85°C compared to 80°C), and a lower CTA concentration was used (11.4mmol/L compared to 5.7mmol/L). The same monomer concentration (2mol/L) was used in both the literature and experiment 6, but a higher CTA:AIBN ratio (5:1) was used in experiment 6 (compared to 10:1 in the literature). Conversion was the same after 2h for experiment 5 and the reaction reported in the literature but experiment 6 showed a PDI of 1.24 at this conversion. This is an improvement upon the PDI value of 1.4 reported in the literature using CTA (10c).
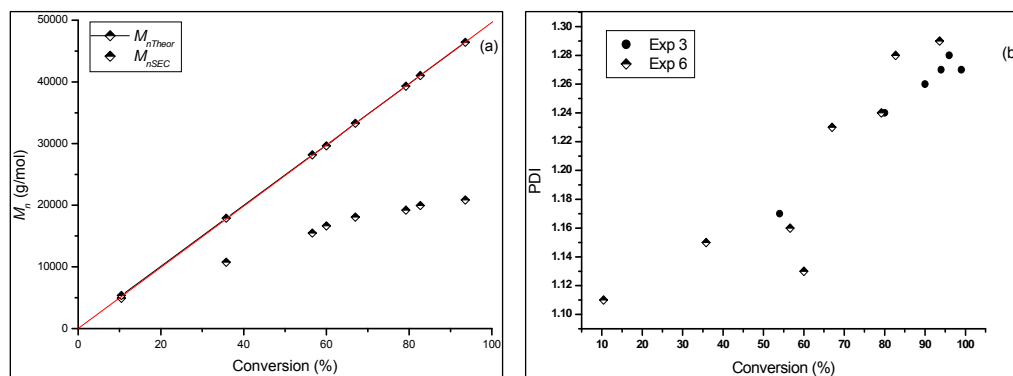
Figure 5.18 **(a) Number-average molecular weight ($\overline{}, M_n$) versus monomer conversion graphs for experiment 6 (◇), using CTA (10c) and (b) PDI versus monomer conversion graphs for polyNAM polymerization at 80°C: experiment 3 (●), using CTA (10b); experiment 6 (◇) using CTA (10c).**

A third comparison was made between CTA (10b) and (10c). In experiment 7, reaction conditions from experiment 2 were identical except for the CTA used. Figure 5.19 (a) presents the conversion of both these experiments according to time. Keeping in line with the previous two comparisons, the dithioester CTA polymerized at a slower rate than that of the trithiocarbonate CTA used. The $\ln([M]_0/[M]_t)$ versus time plot for experiment 7 (Figure 5.19 (b)) indicates that the generation of primary radicals was balanced with the loss of propagating radicals during the initial stages of the polymerization although it did seem to taper off towards the end of the reaction.
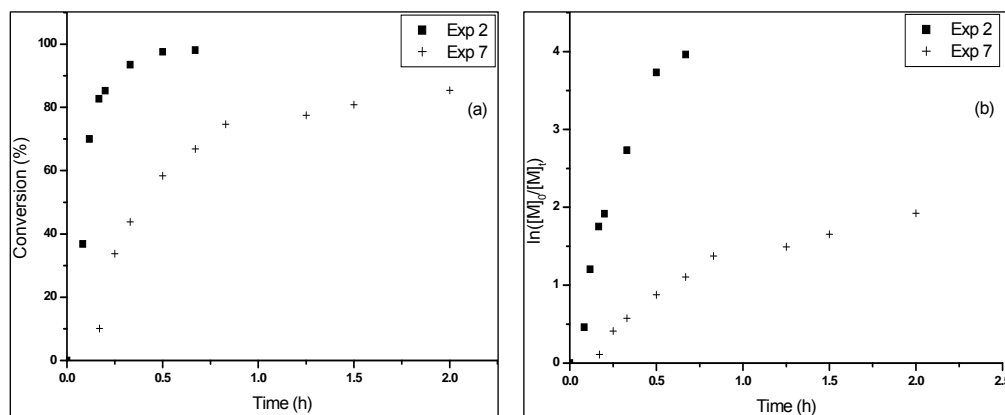
Figure 5.19 **Kinetic results for polyNAM in 1,4-dioxane at 90°C: experiment 2 (■), using CTA (10b) and experiment 7 (+), using CTA (10c) (a) Conversion data (b) 1st Order kinetic plots.**

SEC analysis revealed that the molecular weights of the polymers for experiment 7 increased with conversion. Figures 5.4 and 5.20 present the SEC graphs with DRI and UV overlays for experiments 2 and 7 respectively. Within 10 minutes (0.17h), 83% conversion was reached in the polymerization of experiment 2 whist maintaining a fairly narrow PDI

(1.19). As conversion increased, the PDI became slightly broader with the final sample after 40 minutes (0.67h, 98% conversion) having a PDI of 1.24. For experiment 7, after 10 minutes (0.17h) only 10% conversion was obtained with the polymer displaying a narrow PDI (1.17). The final sample (2h, 85% conversion) had a slightly broader PDI (1.3) to the final polymer sample obtained with experiment 2.

As with the previous experiments, and for similar reasons, the $\overline{M}_n$ values obtained in experiment 7 were much lower than the theoretical values (graph not shown). Refer to Table 5.4 for these results. Figure 5.21 illustrates that the PDI for experiments 2 were slightly higher than those for experiment 7 throughout the polymerization.
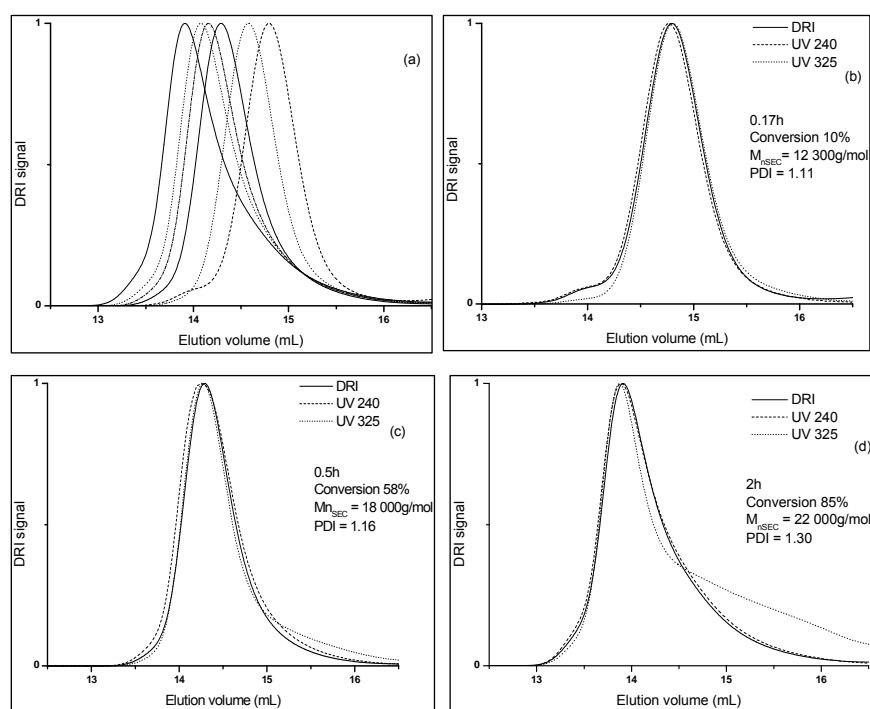
Figure 5.20   **SEC chromatograms of polyNAM for experiment 7 at 90°C using CTA (10c) (a) DRI data showing increasing molecular weight for polymerization; (b) sample at 0.17h with 10% conversion showing UV 240nm and 325nm as well as DRI data (c) sample at 30 minutes with 58% conversion showing UV 240nm and 325nm as well as DRI data (d) sample at 2h with 85% conversion showing UV 240nm and 325nm as well as DRI data.**

144
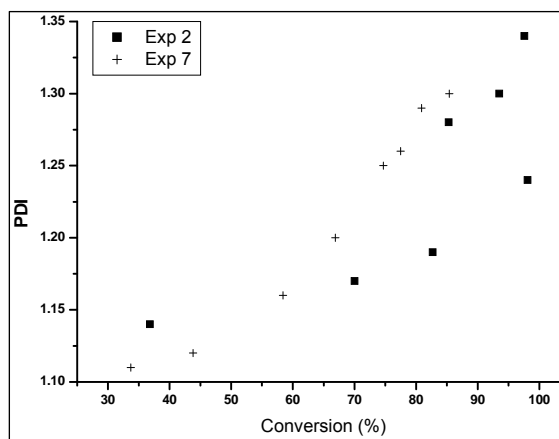
**Figure 5.21** **PDI versus monomer conversion graphs for polyNAM polymerization at 90°C: experiment 2 (■), using CTA (10b); experiment 7 (+), using CTA (10c).**

5.8.2   Discussion

The purpose of performing experiments 5–7 was to be able to compare the results obtained with those of experiments 1–3. The author believes that the observed difference between the behaviors of CTA (10b) and CTA (10c) could be related to the nature of their Z group (alkyl and phenyl respectively) as well as the R group. The results obtained in all three comparative experiments indicated that when using the dithioester CTA (10c) slower rate because of retardation was evident. In light of the slower kinetics, one would generally expect a narrowing of PDIs compared to faster kinetic reactions. This was the case during the initial stages of the polymerizations using the dithioester CTA (10c), although towards the final samples there was a slight increase in the PDIs compared to those polymerized with CTA (10b).

According to Moad,[44] and based on the mechanism shown in Scheme 5.2, several explanations for retardation may be envisaged. These include the following:

(1) Slow fragmentation of the adduct (3) formed from the initial CTA.

(2) Slow fragmentation of adduct (7) formed from the polymeric CTA.

(3) Slow reinitiation by the expelled radical (R·).

(4) Specificity for the expelled radical (R·) to add to the CTA rather than to monomer.

(5) Specificity for the propagating radical (P_n·) to add to the CTA rather than monomer (*i.e.* transfer constant too high!).
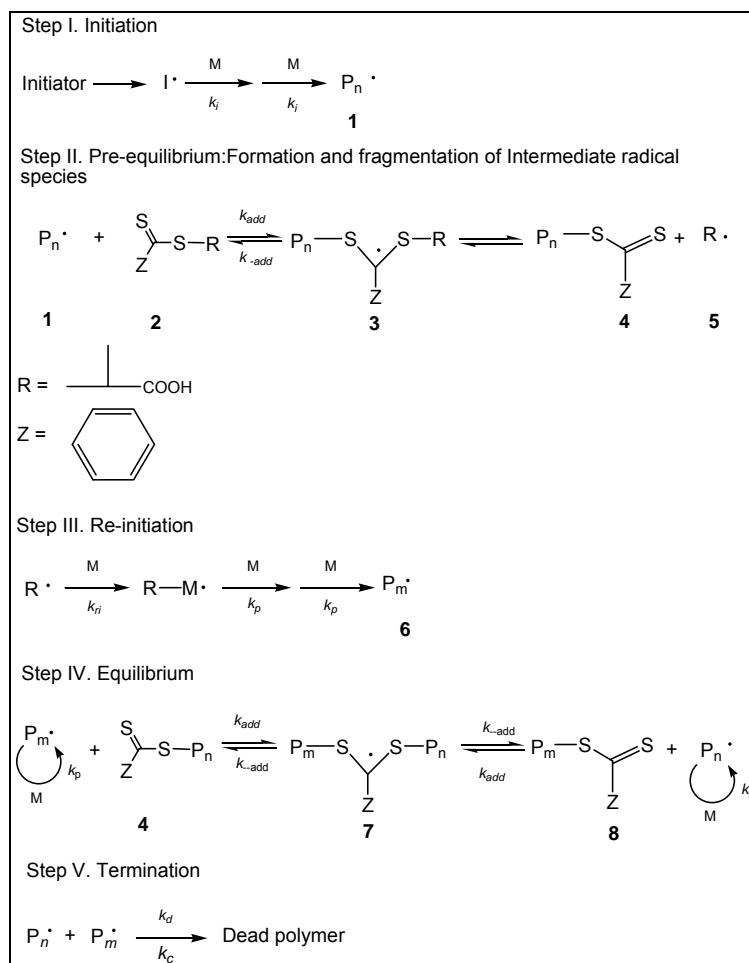
Scheme 5.2   Reaction mechanism of RAFT polymerization using CTA (10c).

It is apparent that there are significant differences in the efficiency of the two CTAs to mediate the RAFT polymerization of NAM. While the trithiocarbonate (using CTA (10b)) mediated RAFT polymerization yielded polyNAM to high conversions in relatively short times, the dithioester (using CTA (10c)) mediated NAM polymerizations never reached complete conversions as the reaction kinetics seemed to taper off towards the final samples. The kinetic plots for the dithioester mediated deviated significantly from what would be expected for first order kinetics. Interestingly, the molecular weight data, which are unimodal in all cases, are almost identical for the two polymerizations at final conversions, although the dithioester mediated RAFT polymerization appeared to show narrower PDI values during the initial stages of the reactions. The author believes that the differences can be rationalized by considering both the addition and fragmentation steps involving the intermediate radicals (3 and 7 in Schemes 5.1 and 5.2).

It is generally well known that tertiary radicals are superior leaving groups compared to secondary and primary radicals. Such a high polymerization rate with CTA (10b), which contains a better leaving group (tertiary radical) than CTA (10c) (secondary), can be

explained by a faster fragmentation of the corresponding intermediate radical species (3 and 7 in Schemes 5.1 and 5.2) due to a better tertiary radical stability which weakens the S–C bond. In the ground state, the S–R bond is weakened for CTA (10b) which means that a lower transition state energy is reached when R· is formed for CTA (10b) as compared to CTA (10c). Thus, kinetically, the rate of fragmentation of the intermediate radical to form the first polymeric CTA agent (4) for CTA (10b) should be faster than that for CTA (10c). It is also highly likely that the tertiary leaving group is also an efficient re-initiator of the NAM monomer which would imply that no marked retardation should take place. This was the case with the trithiocarbonate mediated NAM polymerizations (experiments 1–4).

Since secondary leaving groups are not as efficient as tertiary leaving groups, it is quite possible that some retardation would occur. Noticeable differences in kinetics during the early stages should be indicative of differences in the R group. Retardation was clearly evident from the beginning stages of polymerization in all the reactions involving the secondary CTA (10c) (experiments 5–7) and it appears to have resulted in a short apparent inhibition period. If there was clear evidence of long periods of inhibition at the start of the reactions, it would lead us to believe that the consumption of the CTA was slow and would subsequently result in molecular weights (and broad PDIs) above that expected from complete consumption of the CTA.[44] PDIs were particularly narrow for the dithioester mediated reactions during initial stages of the reaction. Therefore, the author does not believe a major cause of retardation to be due to the poorer secondary leaving group of CTA (10c) or the inability of this group to reinitiate polymerization (*i.e.* (1), (3) or (4) above) as this would have been evidenced by broad PDIs and significant inhibition times.

Since it is assumed that there was complete consumption of the CTA during the initial stages of the polymerization, retardation is therefore associated with the polymeric CTA intermediate (7), namely slow fragmentation hereof (*i.e.* (2) or (4) above). The opinion of the Barner-Kowollik *et al.*[89] is that if the CTA is very stabilized by for instance, a phenyl Z group, the equilibrium tends to shift to the macroCTA radical side (k_{add}) (compound 7 in Scheme 5.2) and its lifetime increases. CTA (10c) has a strong stabilizing phenyl group, which could result in too high a C_{tr} and subsequently slower fragmentation of the polymeric intermediate radical taking place.

The Z group affects the rate of free radical addition to the C=S bond and the R group affects the rates of fragmentation of the intermediate radicals. Therefore it can be seen that in the case where the one group is chosen to enhance the step that it affects, it would subsequently reduce the effectiveness of the other step (*i.e.* a stronger stabilizing group

would make the fragmentation step more difficult). For an efficient RAFT polymerization system both addition and fragmentation are required to be facile.

5.9   Characterization using SEC/LS

A series of reactions using CTA (10b) and NAM were performed with the objective of characterizing these samples by means of size exclusion chromatography in combination with light scattering (SEC/LS). A multiangle light scattering (MALS) instrument was used. The use of online light scattering, rather than standards, for the determination of molecular weight by SEC allows direct comparisons of experimental molecular weights with those predicted by theory. Details of this instrument can be seen in Section 5.5.3. Each sample analyzed was a separate reaction (*i.e.* no samples were taken during the polymerization). The (*dn/dc*) value of polyNAM in THF at 632nm wavelength could not be found in the literature therefore it had to be measured independently by means of an off-line refractometer. The (*dn/dc*) for polyNAM was 0.129mL/g.

5.9.1   Results and discussion

The same experimental procedure was followed as described in Section 5.5.2. For the following reaction (experiment 8) the M:CTA ratio was such that a theoretical molecular weight 49 600g/mol at 100% conversion was expected.

Table 5.5   **Experimental conditions for the RAFT polymerization of polyNAM (experiment 8).**

Experiment	[M] / [CTA]	[CTA] / [AIBN]	[M]$_o$ (mol\L)	[AIBN] (mmol\L)	[CTA] (mmol\L)	Temperature (°C)
8	350	10	2	0.6	6	80

Figures 5.22–5.24 present the kinetic and molecular weight data for experiment 8. As can be seen from these results, polymerization rates were relatively rapid following first order kinetics. Figure 5.24 shows that the molecular weights obtained by MALS match the theoretical molecular weights (based on ^{1}H-NMR conversion and equation (5.20)) very well until high conversion. Included in this figure are the results obtained by conventional SEC using PSt as calibration standards. It can be seen that there is a significant discrepancy between the relative and absolute results. According to the MALS results, the PDI remains narrow until high conversion.
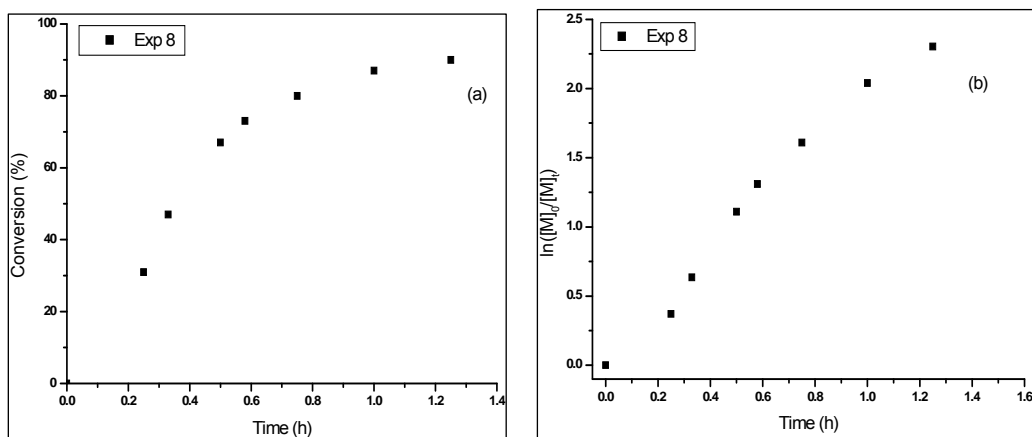
Figure 5.22   **Kinetic results for polyNAM in 1,4-dioxane at 80°C, [AIBN] = 0.6mmol/L and using CTA (10b); experiment 8 (a) Conversion data (b) 1st Order kinetic plots.**
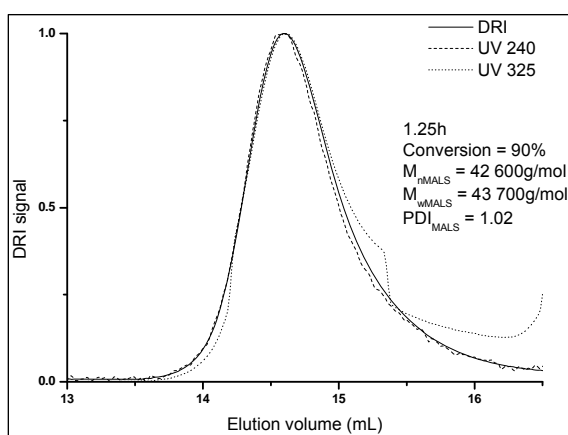
Figure 5.23   **SEC chromatogram of polyNAM for experiment 8 at 80°C using CTA (10b); sample at 1.25h with 90% conversion showing UV 240nm and 325nm as well as DRI data.**
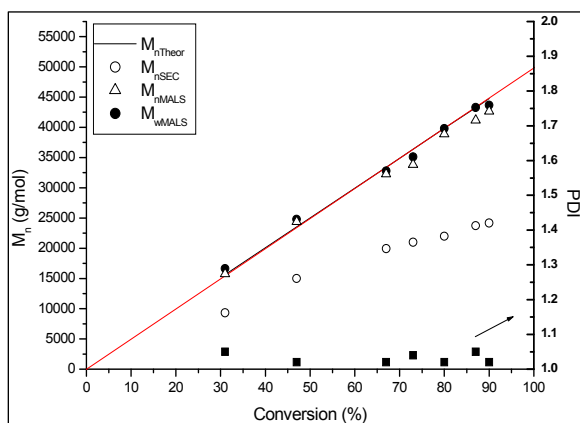
Figure 5.24   **Number-average molecular weight (‾,M_n) and PDI versus monomer conversion graphs for experiment 8 using CTA (10b) at 80°C.**

Table 5.6 **Conversion and MALS results for the RAFT polymerization of polyNAM (experiment 8).**

Experiment	Time (h)	Conversion % (^{1}H-NMR)	$\overline{M}_{n\,Theor}$ (g/mol)	$\overline{M}_{n\,MALS}$ (g/mol)	$\overline{M}_{w\,MALS}$ (g/mol)	PDI$_{MALS}$
8	0.25	31	15 600	15 800	16 600	1.05
	0.33	47	23 50	24 400	24 800	1.02
	0.50	67	33 400	32 300	32 800	1.02
	0.58	73	36 400	33 800	35 100	1.04
	0.75	80	39 800	38 900	39 800	1.02
	1.00	87	43 300	41 200	43 300	1.05
	1.25	90	44 800	42 600	43 700	1.02

Figure 5.25 is the ^{1}H-NMR spectrum of polyNAM. Unfortunately, molecular weights could not be confirmed through this technique as they were too high.
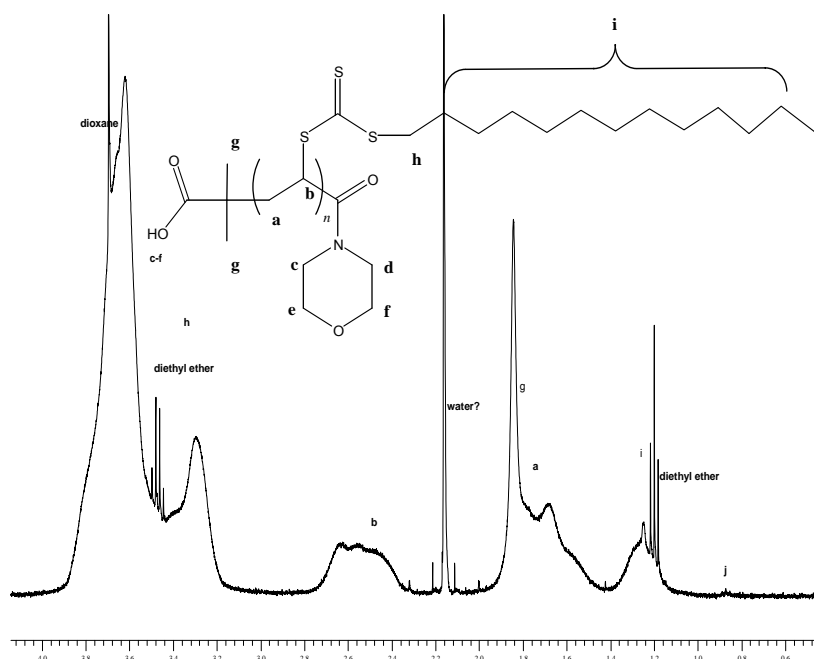
Figure 5.25 ^{1}**H-NMR spectrum of polyNAM synthesized in the presence of CTA (10b).**

5.10 Conclusions

Successfully homopolymerizations of NAM were performed in 1,4-dioxane at 80°C and 90°C using two different CTAs. Rates of polymerization in the present study show a marked dependence on the Z group and R group. Fast polymerizations and narrow PDIs were achieved using the trithiocarbonate CTA (10b), whilst the polymerizations using the dithioester CTA (10c), although also showing narrow PDIs, showed signs of retardation throughout the polymerization. The reasons for this can be attributed to the strong

stabilizing phenyl group of CTA (10c) which could cause the intermediate radical species to undergo slow fragmentation of the radical species. In addition to this, the leaving group of CTA (10c) is a secondary isopropyl radical which is not as good a leaving group as tertiary radicals, therefore, this too could slow down the fragmentation of the intermediate radical species. These improved results of CTA (10b) compared to CTA (10c) reinforce the use of PDMS macroCTA (11b) in the following chapter (block copolymerizations using NAM as second monomer). Conditions used in these homopolymerizations will be the starting point for the following chapter.

Very importantly, it was found that there was a significant difference in the results of SEC and MALS. This confirmed the importance of not using PSt standards to measure molecular weights for polyNAM. MALS results were performed on a series of polyNAM. The $\bar{M}_n$ and $\bar{M}_w$ values obtained from MALS corresponded very well with theoretical values as determined by ^{1}H-NMR spectroscopy.

References

(1)   Convertine, A. J.; Ayres, N.; Scales, C. W.; Lowe, A. B.; McCormick , C. L.
        Biomacromolecules, **2004**, *5,* 1177.

(2)   Lai, J. T.; Filla, D.; Shea, R. *Macromolecules,* **2002**, *35,* 6754.

(3)   Narrang, K.; Brunfeldt, K.; Norris, K. E. *Tetrahedron Lett.,* **1977**, *18,* 1819.

(4)   Onishi, M.; Fujii, T. PCT Int. Appl., WO 8900,878, 1989; Terumo Corp. *Chem. Abstr.* **1973**, *110*, 194367h.

(5)   Ishii, K.; Honda, Z. Ger. Offen 2,414,795,27, 1973; Daicel Ltd. *Chem. Abstr.* **1973**, *82*, 58534.

(6)   Epton, R.; Holding, S. R.; McLaren, J. *J. Chromatogr.,* **1975**, *110,* 327.

(7)   Gelfi, C.; de Besi, P.; Alloni, A.; Righetti, P. G. *J. Chromatogr.,* **1992**, *608,* 333.

(8)   Zewert, T.; Harrington, M. G. Acrylic polymer electrophoresis support media. United States Patent 5290411, 1994.

(9)   Takigami, M. Radiation-curable inks for ink-receiving layer formation, and printed products. JP Patent No. 2000034435, 2000.

(10)   de Lambert, B.; Charreyre, M.-T.; Chaix, C.; Pichot, C. *Polymer,* **2007**, *48,* 437.

(11)   D'Agosto, F.; Charreyre, M.-T.; Mellis, F.; Pichot, C.; Mandrand, B. *J. Appl. Polym. Sci.,* **2003**, *88,* 1808.

(12)   Epton, R.; Goddard, P. *Polymer,* **1980**, *21,* 1367.

(13)   de Lambert, B.; Chaix, C.; Charreyre, M.-T.; Laurent, A.; Aigoui, A.; Perrin-Rubens, A.; Pichot, C. *Bioconjugate Chem.,* **2005**, *16,* 265.

(14)   Minard-Basquin, C.; Chaix, C.; D'Agosto, F.; Charreyre, M.-T.; Pichot, C. *J. Appl. Polym. Sci.,* **2004**, *92,* 3784.

(15)   Torchillin, V. P.; Trubetskoy, V. S.; Whiteman, K. R.; Caliceti, P.; Ferruti, P.; Veronese, F. M. *J. Pharm. Sci.,* **1995**, *84,* 1049.

(16)   Ranucci, E.; Spagnoli, G.; Ferruti, P. *Macromol. Chem. Phys.,* **1994**, *195,* 3469.

(17)   Ranucci, E.; Bignotti, F.; Ferruti, P. *Macromol. Chem. Phys.,* **1995**, *196,* 2927.

(18)   Lim, D.; Kopecek, J.; Bazhilova, H.; Vacik, J. Hydrophilic acrylic copolymers containing N-heterocyclic compounds, Germany Patent No. 215190927, 1972; Ceskoslovenska Adademie Ved, invs. *Chem. Abstr.* **1972**, *77*, 491391f.

(19)   Veronese, F. M.; Largajolli, R.; Visco, C.; Ferruti, P.; Miucci, A. *Appl. Biochem. Biotechnol.,* **1985**, *11,* 269.

(20)   Torchillin, V. P.; Trubetskoy, V. S.; Whiteman, K. R.; Caliceti, P.; Ferruti, P.; Veronese, F. M. *J. Pharm. Sci.,* **1995**, *84,* 1049.

(21)   Sartore, L.; Peroni, I.; Ferruti, P.; Latini, R.; Bernasconi, R. *J. Biomater. Sci. Poly. Ed.,* **1997**, *8,* 741.

(22)   Caliceti, P.; Schiavon, O.; Veronese, F. M. *Bioconjugate Chem.,* **2001**, *12,* 515.

(23)   Torchillin, V. P.; Shtilman, M. I.; Trubetskoy, V. S.; Whiteman, K. R.; Caliceti, P.; Ferruti, P.; Veronese, F. M. *Biochim. Biophys. Acta,* **1994**, *1195,* 181.

(24)   Thomas, P. R.; Attfield, D. J. British Patent 914 780, 1954; British Nylon Spinners Ltd. *Chem Abstr* **1954**, *58*, 5810c.

(25)   Ham, G. E. U.S. Patent 2 683 703, 1954; Monsanto Chemical Co. *Chem. Abstr.* **1954**, *48*, 1184.

(26)   Benoit, D.; Chaplinski, V.; Braslau, R.; Hawker, C. J. *J. Am. Chem. Soc.,* **1999**, *121,* 3904.

(27)   Li, D.; Brittain, W. J. *Macromolecules,* **1998**, *31,* 3852.

(28)   Schierholz, S.; Givehchi, M.; Fabre, P.; Nallet, F.; Papon, E.; Guerret, O.; Gnanou, Y. *Macromolecules,* **2003**, *36,* 5995.

(29)   Fischer, A.; Brembilla, A.; Lochon, P. *Eur. Polym. J.,* **2000**, *37,* 33.

(30)   Fischer, A.; Brembilla, A.; Lochon, P. *Polymer,* **2000**, *42,* 1441.

(31)   Harth, E.; Bosman, A. W.; Benoit, D.; Helms, B.; Frechet, J. M. F.; Hawker, C. J. *Macromol. Symp.,* **2001**, *174,* 85.

(32)   Bosman, A. W.; Vestberg, R.; Heumann, A.; Frechet, J. M. F.; Hawker, C. J. *J. Am.Chem. Soc.,* **2003**, *125,* 715.

(33)   Binder, W. H.; Gloger, D.; Weinstabl, H.; Allmaier, G.; Pittenauer, E. *Macromolecules,* **2007**, *40*, 3097.

(34)   Rademacher, J. T.; Baum, M.; Pallack, M. E.; Brittain, W. J. *Macromolecules,* **2000**, *33,* 284.

(35)   Teodorescu, M.; Matyjaszewski, K. *Macromolecules,* **1999**, *32,* 4826.

(36)   Teodorescu, M.; Matyjaszewski, K. *Macromol. Rapid Commun.,* **2000**, *21,* 190.

(37)   Huang, X.; Wirth, M. J. *Macromolecules,* **1999**, *32,* 1694.

(38)   Neugebauer, D.; Matyjaszewski, K. *Macromolecules,* **2003**, *36,* 2598.

(39)   Senoo, M.; Kotani, Y.; Kamigaito, M.; Sawamoto, M. *Macromolecules,* **1999**, *32,* 8005.

(40)   Coskun, M.; Temuz, M. M. *Polym. Int.,* **2005**, *54,* 342.

(41)   Mehmet, M. T.; Mehmet, C. *J. Polym. Sci Part A: Polym. Chem.,* **2005**, *43,* 3771.

(42)   Konak, C.; Ganchev, B.; Teodorescu, M.; Matyjaszewski, K.; Kopeckova, P.; Kopecek, J. *Polymer,* **2002**, *43,* 3735.

(43)   Chiefari, J.; Chong, Y. K. B.; Ercole, F.; Krstina, J.; Jeffery, J.; Le, T. P. T.; Mayadunne, R. T. A.; Meijs, G. F.; Moad, C. L.; Moad, G.; Rizzardo, E.; Thang, S. H. *Macromolecules,* **1998**, *31,* 5559.

(44)   Moad, G.; Chiefari, J.; Chong, B. Y.; Krstina, J.; Mayadunne, R. T.; Postma, A.; Rizzardo, E.; Thang, S. H. *Polym. Int.,* **2000**, *49,* 993.

(45)   Sumerlin, B. S.; Donovan, m. S.; Mitsukami, Y.; Lowe, A. B.; McCormick, C. L. *Macromolecules,* **2001**, *34,* 6561.

(46)   Donovan, M. S.; Lowe, A. B.; Sumerlin, B. S.; McCormick, C. L. *Macromolecules,* **2002**, *35,* 4123.

(47)   Donovan, M. S.; Sanford, T. A.; Lowe, A. B.; Sumerlin, B. S.; Mitsukami, Y.; McCormick, C. L. *Macromolecules,* **2002**, *35,* 4570.

(48)   Baum, M.; Brittain, W. J. *Macromolecules,* **2001**, *35,* 610.

(49)   Donovan, M. S.; Sumerlin, B. S.; Lowe, A. B.; McCormick, C. L. *Macromolecules,* **2002**, *35,* 8663.

(50)   Perrier, S.; Davis, T. P.; Carmichael, A. J.; Haddleton, D. M. *Chem. Comm.,* **2002**, 2226.

(51)   Millard, P.-E.; Barner, L.; Stenzel, M. H.; Davis, T. P.; Barner-Kowollik, C.; Muller, A. H. E. *Macromol. Rapid Commun.,* **2006**, *27,* 821.

(52)   Relogio, P.; Charreyre, M.-T.; Farinha, J. P. S.; Martinho, J. M. G.; Pichot, C. *Polymer,* **2004**, *45,* 8639.

(53)   Le, T. P.; Moad, G.; Rizzardo, E.; Thang, S. H. PCT Int Appl WO 9801478A1, 1998; *Chem. Abstr.* **1998**, *128*, 115390.

(54)   Taton, D.; Wilczewska, A.; Destarac, M. *Macromol. Rapid Commun.,* **2001**, *22,* 1497.

(55)   Thomas, D. B.; Sumerlin, B. S.; Lowe, A. B.; McCormick, C. L. *Macromolecules,* **2003**, *36,* 1436.

(56)   Ganachaud, F.; Monteiro, M. J.; Gilbert, R. G.; Dourges, M.-A.; Thang, S. H.; Rizzardo, E. *Macromolecules,* **2000**, *33,* 6738.

(57)   Schilli, C.; Lanzendörfer, M. G.; Müller, A. H. E. *Macromolecules,* **2002**, *35,* 6819.

(58)   Arotcarena, M.; Heise, B.; Ishaya, S.; Laschewsky, A. *J. Am. Chem. Soc.,* **2002**, *124,* 3787.

(59)   Ray, B.; Isotobe, Y.; Morioka, K.; Habaue, S.; Oskamoto, Y.; Kamigaito, M.; Sawamoto, M. *Macromolecules,* **2003**, *36,* 543.

(60)   Donovan, M. S.; Lowe, A. B.; McCormick, C. L. *ACS Polym. Prep.,* **2000**, 281.

(61)   Sumerlin, B. S.; Lowe, A. B.; Thomas, D. B.; McCormick, C. L. *Macromolecules,* **2003**, *36,* 5982.

(62)   de Lambert, B.; Charreyre, M.-T.; Chaix, C.; Pichot, C. *Polymer,* **2005**, *46,* 623.

(63)   D'Agosto, F.; Charreyre, M.-T.; Veron, L.; Llauro, M.-F.; Pichot, C. *Macromol. Chem. Phys.,* **2001**, *202,* 1689.

(64)   Favier, A.; Charreyre, M.-T.; Chaumont, P.; Pichot, C. *Macromolecules,* **2002**, *35,* 8271.

(65)   Favier, A.; Charreyre, M.-T.; Pichot, C. *Polymer,* **2004**, *45,* 8661.

(66)   Favier, A.; Ladaviere, C.; Charreyre, M.-T.; Pichot, C. *Macromolecules,* **2004**, *37,* 2026.

(67)   D'Agosto, F.; Hughes, R. J.; Charreyre, M.-T.; Pichot, C.; Gilbert, R. G. *Macromolecules,* **2003**, *36,* 621.

(68)   Jo, Y. S.; van der Vlies, A. J.; Gantz, J.; Antonijevic, S.; Demurtas, D.; Velluto, D.; Hubbell, J. A. *Macromolecules,* **2008**, *41,* 1140.

(69)   Ferruti, P.; Bettelli, A.; Fere, A. *Polymer,* **1972**, *13,* 462.

(70)   Favier, A.; D'Agosto, F.; Charreyre, M.-T.; Pichot, C. *Polymer,* **2004**, *45,* 7821.

(71)   Eeckman, F.; Moes, A. J.; Amighi, K. *Eur. Polym. J.,* **2004**, *40,* 873.

(72)   Li, Y.; Akiba, I.; Harrisson, S.; Wooley, K. L. *Adv. Funct. Mat.,* **2008**, *18,* 551.

(73)   Wyatt, P. J. *Analytica Chimica Acta,* **1993**, *272,* 1.

(74)   Flodin, P., in *Dextran gels and their applications in gel filtration,* (Uppsala), **1962**.

(75)   Leamen, M. J.; McManus, N. T.; Penlidis, A. *J. Appl. Polym. Sci.,* **2004**, *94,* 2545.

(76)   Coto, B.; Escola, J. M.; Suarez, I.; Caballero, M. J. *Polymer Testing,* **2007**, *26,* 568.

(77)   Medrano, R.; Laguna, M. T.; Saiz, E.; Tarazona, M. P. *Phys. Chem. Chem. Phys.,* **2003**, *5,* 151.

(78)   Zimm, B. *J. Chem. Phys.,* **1948**, *16,* 1093.

(79)   Moad, G.; Rizzardo, E.; Thang, S. H. *Aust. J. Chem.,* **2005**, *58,* 379.

(80)   Cao, Y.; Zhu, X. X.; Luo, J.; Liu, H. *Macromolecules,* **2007**, *40,* 6481.

(81)   Convertine, A. J.; Lokitz, B. S.; Lowe, A. B.; Scales, C. W.; Myrick, L. J.; McCormick, C. L. *Macromol. Rapid Commun.,* **2005**, *26,* 791.

(82)   Schilli, C.; Zhang, M.; Rizzardo, E.; Thang, S. H.; Chong, Y. K. B.; Edwards, K.; Karlsson, G.; Muller, A. H. E. *Macromolecules,* **2004**, *37,* 7861.

(83)   Thomas, D. B.; Convertine, A. J.; Myrick, L. J.; Scales, C. W.; Smith, A. E.; Lowe, A. B.; Vasilieva, Y. A.; Ayres, N.; McCormick, C. L. *Macromolecules,* **2004**, *37,* 8941.

(84)   Barner-Kowollik, C.; Coote, M. L.; Davis, T. P.; Radom, L.; Vana, P. *J. Polym. Sci. Part A: Polym. Chem.,* **2003**, *41,* 2828.

(85)   Muller, A. H. E.; Zhuang, R.; Yan, D.; Litvenko, G. *Macromolecules,* **1995**, *28,* 4326.

(86)   Muller, A. H. E.; Litvenko, G. *Macromolecules,* **1997**, *30,* 1253.

(87)   Moad, G.; Moad, C. L.; Rizzardo, E.; Thang, S. H. *Macromolecules,* **1996**, *29,* 7717.

(88)   Goto, A.; Sato, K.; Fukuda, T.; Moad, G.; Rizzardo, E.; Thang, S. H. *Polym. Prepr.,* **1999**, *40,* 397.

(89)   Barner-Kowollik, C.; Quinn, J. F.; Nguyen, T. L. U.; Heuts, J. P. A.; Davis, T. P. *Macromolecules,* **2001**, *34,* 7849.

Chapter 6

Novel siloxane block copolymers

Abstract

RAFT appears to be a suitable technique for the synthesis of controlled block copolymers using PDMS as a macroCTA to copolymerize with NAM. To our knowledge these are the first examples of PDMS-*b*-poly(acryloylmorpholine) (PDMS-*b*-polyNAM) (25) block copolymers synthesized in solution by RAFT polymerization. These novel block copolymers with length-varying polyNAM block were synthesized with a very efficient control over $\bar{M}_n$, $\bar{M}_w$ as well as PDIs, as determined by MALS. High performance liquid chromatography (HPLC) results were performed on these novel materials. It was possible to separate PDMS-*b*-polyNAM from the starting materials (polyNAM and PDMS). The presence of polyNAM was negligible in all cases. Finally, TEM results confirmed the amphiphilic nature of these novel block copolymers.

6.1   Objectives

The objectives for this study include:

- confirmation by analytical characterization techniques that a block copolymer structure consisting of both PDMS and polyNAM has been synthesized.
- use of MALS and HPLC to determine molecular weights and estimate the degree to which the monomer was incorporated into the block copolymer, respectively.
- TEM images to confirm the self-assembly of these materials.

6.2   What is an amphiphilic block copolymer?

In summary, an amphiphilic block consists of hydrophilic and hydrophobic segments and is a self-assembling material which is capable of forming polymeric associates in aqueous solutions. Their application in biological fields is extensive.[1,2]

6.3   Can one obtain a (dn/dc) value of a copolymer?

The quick answer to this is yes, but it has to be used with caution.

The theory of light scattering was covered in Section 5.6.2. It was explained in that section that when analyzing polymers by means of LS it is necessary to determine the (*dn/dc*) of the polymer. For homogenous homopolymers and copolymers it is usually sufficient to determine a mean (*dn/dc*) value as this value remains essentially constant over a range of masses measured,[3] but if one is analyzing heterogeneous copolymers, the situation becomes a little bit more complicated. If the copolymer composition varies with molecular weight, a single (*dn/dc*) value cannot always be assumed[4] as the (*dn/dc*) will change over the whole sample, and this quantity must be measured at each elution slice since it may be a function of molecular weight.[3] However, if the composition is invariant with molecular weight, it may be sufficient to use a mean value for (*dn/dc*) for the sample determined by making an off-line measurement of (*dn/dc*) from the bulk.[3,5] When using average (*dn/dc*) values and the copolymer composition is not homogenous, uncertainties are introduced and apparent molecular weights can only be obtained.[6,7] Therefore, when using LS to analyze your polymers, and wanting to use a mean(*dn/dc*), it is important that they are monodisperse. From the results of the block copolymers synthesized in this chapter (results presented in Section 6.6), it can be seen that the MWD of the block copolymers is fairly narrow, therefore, it can be assumed that the criteria for allowing a mean (*dn/dc*) value for the block copolymers to be used (*i.e.* the block copolymers are monodisperse) is valid.

There are however some shortfalls when using LS techniques. Since the scattered light is proportional to the molecular weight (equation (5.8)), it is important that the concentration of your polymer is high enough for it to be detected by the LS detector. It is also possible that experimental error can occur during the measurement of the (*dn/dc*)*,* or, in the case of copolymers, that the polymer is polydisperse and can lead to an erroneous mean (*dn/dc*) value. The effects of temperature differentials between the off-line refractometer (used to determine (*dn/dc*)) and the LS detector can also lead to deviations of observed molecular weights from theoretical molecular weights.

It is possible to determine the (*dn/dc*) by measuring the DRI response,[8] in combination with the UV response,[4] however, these methods rely on an accurately calibrated DRI detector, as well as no absorption of the polymer on the SEC column. This method was not used for the purposes of this project as the software package could not allow determination of 100% polymer recovery. The (*dn/dc*) for the homopolymers and copolymers were determined using a refractometer. Since the author was strongly considering using this technique to confirm the (*dn/dc*) values obtained with the refractometer –but was prohibited from doing this due to the software limitations – it was

thought valuable information for the reader to include a summary of the theory behind these methods.

The (*dn/dc*) of a copolymer may be expressed as a function of the corresponding values for the homopolymers and the chemical composition following the expression[9]

$$\left(\frac{dn}{dc}\right) = \left(\frac{dn}{dc}\right)_1 w_1 + \left(\frac{dn}{dc}\right)_2 (1 - w_1)$$

(6.1)

where the subscripts 1 and 2 represent the two homopolymers, $(dn/dc)_1$ and $(dn/dc)_2$ are the refractive index increment for monomer 1 and 2 respectively, and w_1 is the weight fraction of monomer units of monomer 1. One does not know the weight fractions of each homopolymer, therefore, it is necessary to try and calculate w_1.

One method in which the w_1 can be calculated is by using a refractive index (RI) detector (mass sensitive) in combination with a UV detector (concentration sensitive) to determine molecular weights of polymers.[9] The RI signal is proportional to both the mass concentration of the solution and the refractive index increment (*dn/dc*), by

$$S^{RI} = k^{RI} c \left(\frac{dn}{dc}\right)$$

(6.2)

where k^{RI} is the absolute response factor of the detector that does not depend on the kind of polymer and can be assumed to be constant; c is the mass concentration and (*dn/dc*) is the mean refractive index increment. On the other hand, the UV signal is only proportional to the concentration as seen by

$$S^{UV} = k^{UV} c$$

(6.3)

where k^{UV} is the response factor of the instrument to the kind of sample detected. Since the response factor of the DRI detector is independent of chemical nature of the eluted sample, equation (6.2) may be applied to the *i*th slice of the chromatogram produced by the copolymer with the only modification of particularizing the mass concentration and refractive index increment to the values appropriate for that particular slice

$$S_i^{RI} = k^{RI} c_i \left(\frac{dn}{dc}\right)_i$$

(6.4)

If one knows the exact concentration of polymer in the sample, then one can determine the $(dn/dc)_i$ value for that slice. However, if the $(dn/dc)_i$ does not coincide with the known

concentration, one can obtain the apparent concentration c_i^{app} by a ratio of the $(dn/dc)_i$ for each slice versus the mean value (dn/dc) by equation (6.5)

$$c_i^{app} = c_i \frac{(dn/dc)_i}{(dn/dc)}$$

(6.5)

Through substituting c_i^{app} into the light scattering equation (5.10), using a mean value (dn/dc) and extrapolating to zero angle, the apparent molecular weight from the RI signal (M^{RI}) can be calculated by

$$M_i^{RI} = \frac{(\Delta R_\Theta)_i}{K'\left(\frac{dn}{dc}\right)c_i\left(\frac{dn}{dc}\right)_i}$$

(6.6)

where

$$K' = \frac{4\pi^2\eta^2}{\lambda_0^4 N_A}$$

(6.7)

On the same token, an apparent molecular weight from the UV signal (M^{UV}) can be calculated and the ratio of M^{RI}/ M^{UV} will allow one to determine w_1 which can be used in equation (6.1) to determine the refractive index of the copolymer. For more details on this method, the reader is referred to the specified reference.

6.4   Experimental

6.4.1   Materials

n-Acryloylmorpholine (NAM) (Aldrich, 97%, 1,000ppm monomethyl ether hydroquinone as inhibitor), 1,4-dioxane [123-91-1] (Merck, 99+%), cyclohexane [110-82-7] (Merck, ≥99%), diethyl ether [60-29-7] (Merck, 98%), acetonitrile [75-05-8] (Merck, ≥99%) and trioxane [110-88-3] (Riedel De Haen) were used as received. The PDMS macroCTA (11b) used in these block copolymerizations were synthesized and purified as described in Chapter 3. 2,2'-azobis(isobutyronitrile) [78-67-1] (AIBN) (Riedel De Haen) was purified by recrystallization from methanol.

6.4.2   Polymerization procedure

All solution experiments were performed in the same manner. A ratio of 1,4-dioxane and cyclohexane was used as solvent for all polymerizations that follow. Ratios were optimized to the point just before the solution (containing the PDMS macroCTA, AIBN and

trioxane) would become turbid (not clear). For the different chain lengths of the polyNAM blocks synthesized, it was found that a *different ratio* of these solvents were necessary. AIBN was used as initiator in all polymerizations. It was also realized that it was necessary to subject a solution containing solvent (1,4-dioxane and cyclohexane), PDMS macroCTA, trioxane and AIBN to freezing cycles *separate* from the monomer (which was also subjected to freezing cycles). If this was not performed, the monomer would permanently separate from the rest of the contents (*i.e.* form a separate layer). It was also found that the solvents in the flask containing the PDMS macroCTA had to be weighed in a *specific order* or there would be yet again a permanent turbid solution prior to freezing cycles. A typical experimental procedure is described. A solution of PDMS macroCTA, cyclohexane, 1,4-dioxane, AIBN and trioxane were introduced in a 250mL Schlenk tube equipped with a magnetic stirrer and degassed by freeze–evacuate–thaw cycles until no more oxygen was present. The monomer (NAM) was weighed in a separate Schlenk tube and degassed by freeze–evacuate–thaw cycles until no more oxygen was present. Prior to starting the polymerization the monomer was transferred to the rest of the contents by means of a degassed syringe and then heated in a thermostated oil bath at 80°C. It was opted that no samples were drawn during the polymerization in order to avoid the possible uptake of oxygen. The precipitation of the block copolymers were done in different solvents depending on the ratio of the second polyNAM block. The block copolymer synthesized in experiment 9 was precipitated in acetonitrile; whilst the block copolymers synthesized in experiments 10 and 11 were precipitated by first removing the solvent and then swelling the polymer in acetonitrile followed by diethyl ether. After polymer was recovered they were dried *in vacuo*. Trioxane (internal reference for ^{1}H-NMR determination of monomer consumption) was used in all reactions. The complete elimination of residual monomers was confirmed by ^{1}H-NMR spectroscopy.

6.4.3   Analyses and sample preparation

Conversion. As a result of the high boiling point of the monomer (257°C at 1atm (760mm)), conversion had to be determined by an analytical method. ^{1}H-NMR spectroscopy was used to monitor the conversion of NAM. ^{1}H-NMR spectra were recorded on a Varian VXR 300MHz spectrometer and were performed at room temperature using deuterated chloroform (CDCl$_3$) (99.8%) as the solvent. Trioxane (CDCl$_3$, 5.1ppm) was used in all reactions in order to monitor the conversion. Approximately 120mg of sample was transferred to an NMR tube and deuterated chloroform added. Since each sample analyzed was a separate reaction, a ^{1}H-NMR spectrum was recorded at the beginning of *each* experiment, and by comparing the ratio of the monomer peaks at the beginning of the experiment to those remaining at the

respective times, the conversion of polymer was determined by monitoring the depletion of the monomer peaks (5.68, 6.28 and 6.53ppm, ref. trioxane, 5.1ppm)) relative to a constant trioxane peak for each individual reaction.

Molecular Weight Analyses (Relative). Molecular weights were determined using SEC. Samples were prepared for SEC analysis by precipitating each solution aliquot, washing it several times, and then drying it to completion in a vacuum oven for 12 hours. The dried polymers were weighed off (~10mg), and dissolved in 3mL HPLC grade THF (containing 0.012% BHT), filtered through a 0.2μm filter and then submitted for SEC analysis. UV wavelengths used to analyze samples were 240nm and 320nm as the maximum absorption of polyNAM and the thiocarbonyl is at 240nm and 325nm respectively. The SEC instrument specifications can be seen in Chapter 3.

Molecular Weight Analyses (Absolute). The absolute molecular weights of the polymers were determined by MALS in THF containing 0.012% BHT at 30°C on a Dawn-F DSP instrument (Wyatt Technology; He-Ne laser operating at 632.8nm). The dried polymers were weighed off, dissolved in the solvent, filtered through a 0.2μm filter and then submitted for analysis. The column specifications and sample procedure were the same as that for determining molecular weights (relative) (as above). Data processing was performed using Astra (V4.73.04) software.

Measuring differential refractive increments (dn/dc). The (*dn/dc*) of PDMS-*b*-polyNAM was determined with the same eluent used in SEC and MALLS - namely THF (c<10.0mg/mL) - using a *Scan*Ref (NFT) differential refractometer equipped with a filtered light source at 632.8nm. Solutions were filtered through a 0.2μm filter. Data sampling and evaluation of the raw data were performed using Data Labview 4 Run-Time (National Instruments). No external thermostat was used.

Gradient elution chromatography (GEC). This technique is widely used in the separation of polymers according to chemical composition. One is able to separate block copolymers from any homopolymer or unreacted species by varying the mobile phase solvent composition. The HPLC instrument consisted of a Waters 2690 Separations module (Alliance), and Agilent 1100 series variable wavelength detector, a PL-ELS 1000 detector and data was recorded and processed using PSS WinGPC unity (Build 2019) software. The mobile phase was maintained at 1mL/min and the composition was varied as described in Section 6.4.2. A C18 column (Nucleosil C18 5μm, 250mm x 4.6mm) was used at 30°C. Samples were prepared in a solution of THF at a concentration of 5mg/mL after which they were filtered through a 0.2μm filter before analysis.

Morphology was determined using transmission electron microscopy (TEM). TEM was carried out at the University of Cape Town, Electron Microscope Unit A. The apparatus used was a Leo 912 TEM operating at 120kV attached to a digital camera. All the samples were analyzed on copper grids. The sample analyzed in water was stained with a 2% uranyl acetate solution before being mounted onto the copper grid. The other two samples analyzed were taken directly from the reaction mixture and further diluted with cyclohexane/1,4-dioxane. These samples were not stained.

6.5   Results and Discussion

After establishing appropriate conditions in the previous chapter for the homopolymerization of NAM in dioxane, slightly modified reaction conditions were used for the block copolymers of PDMS-*b*-polyNAM (25) prepared by RAFT polymerization using the macroCTA technique as shown in Scheme 6.1. The experimental conditions are summarized in Table 6.1.

 Three experiments were performed, each targeting a different molecular weight for the second block (B$_m$) consisting of polyNAM. Notation for each block copolymer is represented as A$_1$B$_m$ where A$_1$ is the PDMS block which has a constant molecular weight in all experiments 5000 (g/mol for purposes of calculations), and *m* represents the block length of the second polyNAM (in terms of $\overline{M}_{n\,Theor}$) block divided by the 5000. Refer to Table 6.1 for these chain lengths (*m* being 4.8, 3.2 or 2.1 times the length of block A$_1$ for experiments 9, 10 and 11 respectively). Scheme 6.1 is a simplification of the reaction performed to obtain the desired end product, a PDMS-*b*-polyNAM (25) copolymer.

Table 6.1   Experimental conditions for block copolymerizations of PDMS-*b*-PolyNAM (experiments 9–11).

| E	S	m	$\overline{M}_{n\,Theor}$ (g/mol)	[M]/ [CTA]	[CTA]/ [AIBN]	M [mol/L]	P	AIBN [mmol/L]	R	Solvent % *	PDMS %	NAM %
9	A$_1$B$_{4.8}$	24 000	28 900	170	16.7	1.28	7.5	0.45	57/43	80	3.9	16
10	A$_1$B$_{3.2}$	16 100	21 100	115	16.7	0.95	8.3	0.50	65/34	84	4.3	12
11	A$_1$B$_{2.1}$	10 400	15 300	74	16.7	0.79	10.7	0.68	74/26	85	5.5	10

E = experiment

S = sample

M = PolyNAM chain length (g/mol)

P = PDMS macroCTA [mmol/L]

R = CH/Dioxane solvent ratio

* total volume percentage of solvent in reaction
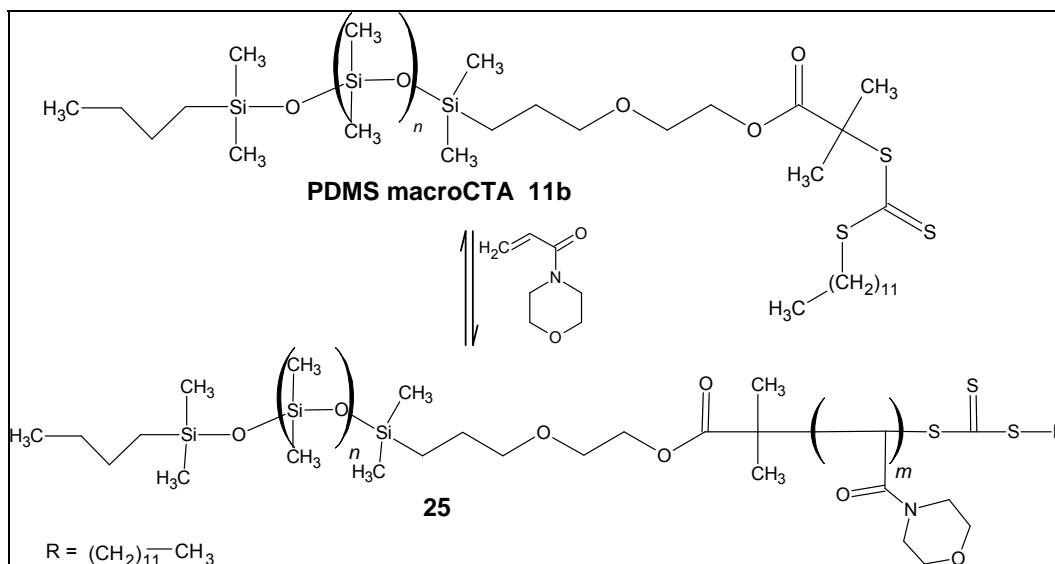
Scheme 6.1   Simplified reaction scheme for the synthesis of PDMS-*b*-polyNAM (25) block copolymers.

Figure 6.1 presents the SEC chromatograms for the final PDMS-*b*-polyNAM ((25) in Scheme 6.1) copolymers each with different target block lengths. In each chromatogram, the DRI signal of the initial PDMS macroCTA (11b) is included. In all experiments it can be seen that there is a clear shift in the unimodal copolymer peak from the peak of macroCTA which confirms the formation of a block copolymer. It does appear as though there is a slight tail on the low molecular weight side of the block copolymer peak which could be as a result of minor termination reactions occurring or some unreacted PDMS macroCTA. However, it would seem that an insignificant percentage of this took place. Ideally, higher targeted molecular weights would have confirmed whether unreacted PDMS is included in these tails, however these sorts of targets were not part of the scope of this project. In all three chromatograms there is a good overlay of the UV signals with the shifting block. Of particular importance is the UV 325nm signal which is solely due to the presence of the thiocarbonyl moiety, therefore, it is a given that this peak contains the PDMS macroCTA (11b) (block (A$_1$)).

An important consideration in RAFT polymerizations is the leaving ability of the R· group. The better the leaving group ability, the better the chances of radicals being preferentially formed upon fragmentation of CTA adduct radicals, thereby ensuring a narrower PDI.[10] Also, R· must be a good/fast re-initiator of monomer in order to avoid termination and/or transfer of the macroCTA and leading to a mixture of homopolymers/copolymers, or no polymerization at all.[10] Both these characteristics will influence the molecular weights and PDI of the block copolymers. From the results in Figures 6.1 and 6.2, it is reasonable to assume that the macroCTA used in these reactions has a good leaving group (a tertiary radical) relative to the incoming propagating poly(acryloylmorpholine) radical and is also

efficient at re-initiating NAM monomer. HPLC results (shown in Section 6.5.1.1) also confirm this assumption.
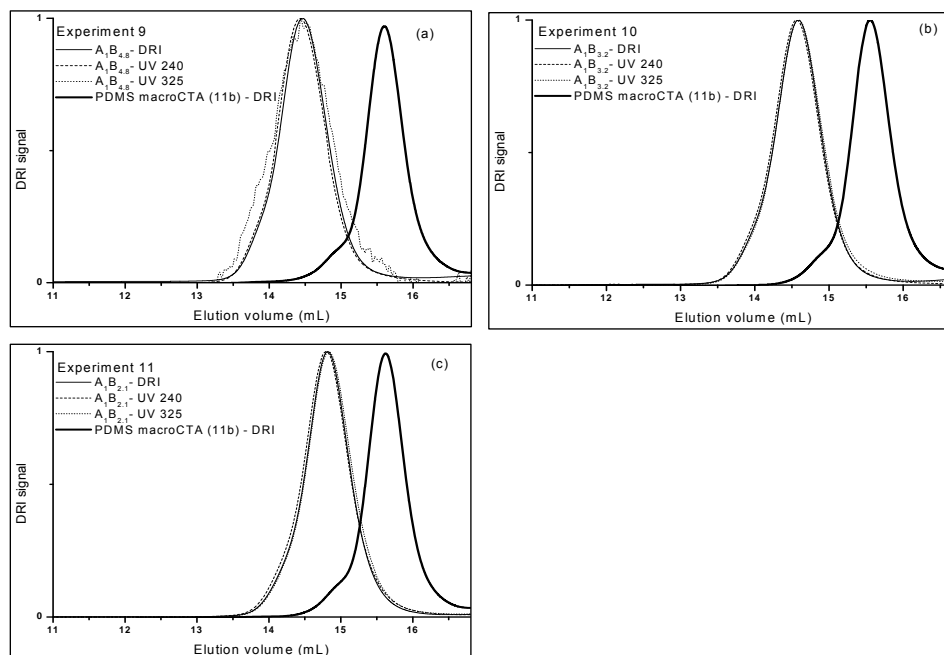
Figure 6.1 **SEC chromatograms of PDMS-*b*-polyNAM (25) (experiments 9–11) (a) DRI and UV data for A$_1$B$_{4.8}$ (b) DRI and UV data for A$_1$B$_{3.2}$ (c) DRI and UV data for A$_1$B$_{2.1}$. In all graphs, the DRI signal of the PDMS macroCTA (11b) is shown.**

However, the $\overline{M}_n$'s measured by SEC for the block copolymers were significantly lower than the theoretical $\overline{M}_n$ values (refer to Table 6.2). The reason for this difference can be ascribed to the hydrodynamic properties of the copolymer versus PSt standards used for calibration. Since the SEC separation mechanism is based on the effective hydrodynamic volume of macromolecules rather than on their molecular weight, application of this method to copolymer systems heterogeneous in composition and architecture is complicated because of an overlap of similar molecular sizes of various topology and composition. As noted in the previous chapter, when using SEC to determine the molecular weights of polyNAM, there were large deviations from the theoretical molecular weights. For this reason, it was thought necessary to use LS to determine molecular weights of these novel block copolymers.

Concerning light scattering analysis, we made the approximation that all copolymers have a corresponding (*dn/dc*) value equal to the one determined for $A_1B_{4.8}$, which is 0.099mL/g (in THF). Thus, the molecular weights must be considered with care. Nevertheless, there is good agreement between the theoretical and molecular weights obtained with MALS. In order to confirm the (*dn/dc*) value of block $A_1B_{4.8}$, a mixture of PSt ((*dn/dc*) value taken as 0.2mL/g) and block $A_1B_{4.8}$ were analyzed by SEC. Since the area under the peak is directly proportional to the mass × (*dn/dc*) (equation (6.8)), the (*dn/dc*) value could be determined by using equation (6.9). The calculated (*dn/dc*) was 0.097mL/g, which is within 2% error of the one determined from the external refractometer.

$$\frac{Area_1}{Area_2} = \frac{\left(\frac{dn}{dc}\right)_1}{\left(\frac{dn}{dc}\right)_2} \times \frac{mass_1}{mass_2} \qquad (6.8)$$

$$\left(\frac{dn}{dc}\right)_2 = \frac{\left(\frac{dn}{dc}\right)_1 \times mass_1 \times Area_2}{Area_1 \times mass_2} \qquad (6.9)$$

The three experiments (Table 6.2, experiments 9–11) all showed very high conversions (>99.0%) and have been isolated by precipitation and analyzed by SEC/LSD. The experimental $\bar{M}_n$ values obtained with conventional SEC as well as MALS are included for the purpose of identifying the need for a LS technique for molecular weight characterization. $\bar{M}_{w\,MALS}$ has also been included as it is sometimes believed that these numbers are more reliable than $\bar{M}_{n\,MALS}$. From the results, it can be seen that there is not a large discrepancy between these values as the samples are fairly monodisperse (narrow PDIs). There is very good agreement with the $\bar{M}_{n\,Theor}$ and the $\bar{M}_{n\,MALS}$. PDI values remain very low which indicate the control of the second block.

In order to monitor the conversion of the PDMS-*b*-polyNAM (25) copolymerization, a series of individually sealed reactions were weighed off and run until different percentages of conversion. Figure 6.2 shows the series of kinetic runs performed for determining conversion of PDMS-*b*-polyNAM (experiment 12 - same reaction conditions as experiment 10). As can be learned from this graph, within 90 minutes (1.5h) the reaction already reached 99% conversion.

Table 6.2 **Experimental results for block copolymerizations of PDMS-*b*-PolyNAM (experiments 9–11).**

| Sample	Time (h)	Conversion (%)	M_{nTheor} (g/mol)	M_{nSEC} (g/mol)	M_{nMALS} (g/mol)*	M_{wMALS} (g/mol)*	PDI_{SEC}	PDI_{MALS}*
$A_1B_{4.8}$	3	99.8	28 900	18 800	30 500	31 700	1.14	1.04
$A_1B_{3.2}$	3	> 99.8	21 100	15 400	23 900	24 800	1.14	1.04
$A_1B_{2.1}$	3	> 99.0	15 300	12 600	16 700	17 400	1.15	1.04
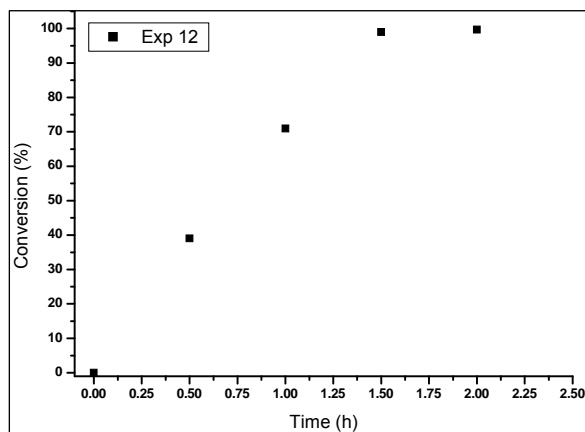
Figure 6.2 **Conversion versus time graph for a series PDMS-*b*-polyNAM (25) copolymer kinetic runs (experiment 12).**

Figure 6.3 is the ^{1}H-NMR spectrum of purified $A_1B_{4.8}$ identifying the presence of both polyNAM and PDMS peaks. Since the molecular weight of polyNAM is almost 5 times as long as PDMS, the peaks of the latter material are less pronounced.
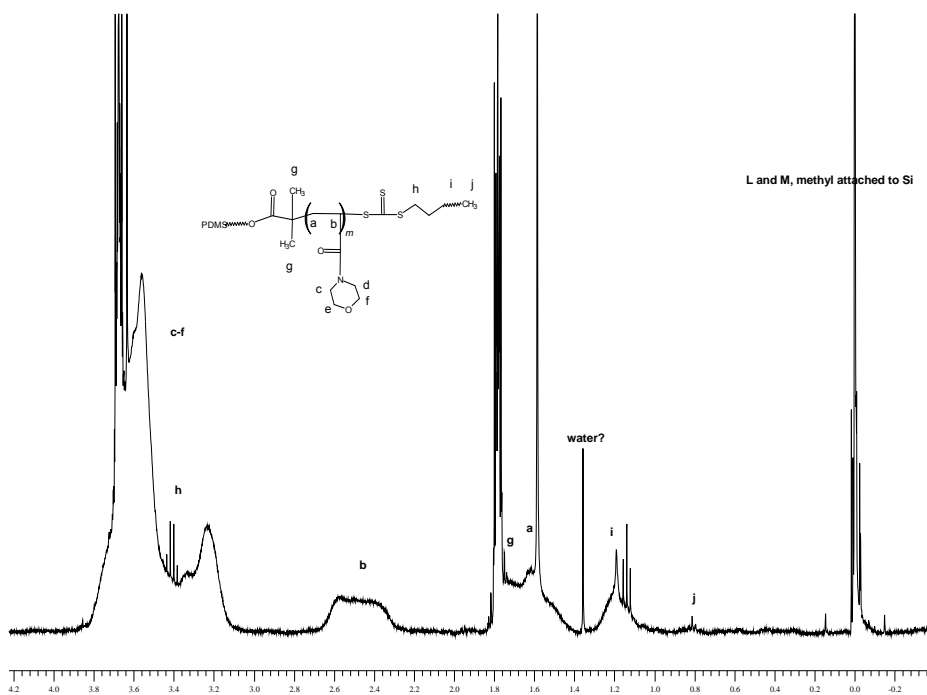

Figure 6.3 **^{1}H-NMR spectrum of PDMS-*b*-polyNAM (25) compound $A_1B_{4.8}$ (experiment 9).**

6.5.1 HPLC Analysis

6.5.1.1 Development of GEC system and characterization of siloxane block copolymers

This section discusses the development of a gradient elution LC technique suitable for the analysis of the block copolymers synthesized in this chapter. This principle of this technique is based on the separation of the polymer chains according to relative solubilities or polarities. After great difficulty in terms of separating the various polymeric species using a polar silica column, it was decided that a non-polar stationary phase C^{18} column would be suitable for separation as there was no signs of column interaction. The solvent combination used was THF and Hexane. The gradient profile is illustrated in Figure 6.4.
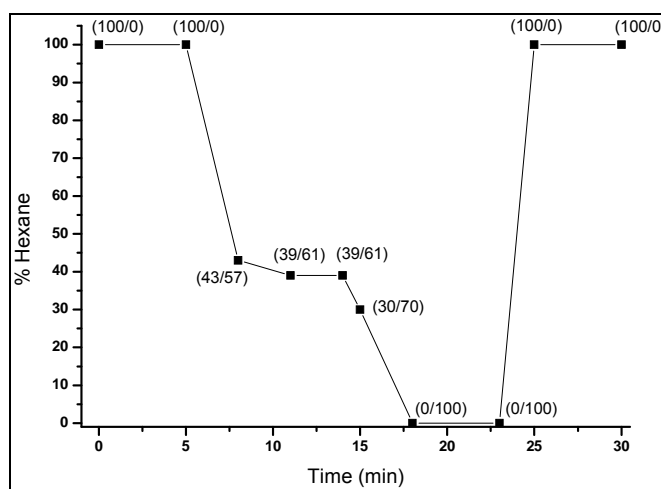

Figure 6.4 **Gradient profile of HPLC system with % hexane plotted against time.**

It was found during optimization of the gradient method that the PDMS macroCTA eluted very early on through the column when using either 100% hexane or 100% THF. Since the polyNAM-containing block copolymer and polyNAM are not soluble in hexane, it was considered optimal to separate the PDMS macroCTA from the rest of the polymeric species by using 100% hexane within the first 5 minutes in SEC mode. PDMS macroCTA and polyNAM samples were run using the optimized method in order to verify their respective retention times in the block copolymer sample runs in order to avoid the possibility of mistaken identity in these samples.

Figure 6.5 displays the overlay of the HPLC chromatograms obtained for each of the three PDMS-*b*-polyNAM samples that were synthesized, each differing in the target molecular weight. There seems to be good correspondence for the peak retention times of the block copolymer species (PDMS-*b*-polyNAM) ((25) in Scheme 6.1) for all three of the samples. It is important to note that the UV trace may not always be a perfect overlay which is due to the constant changing mobile phase composition along the gradient profile, although it

can clearly be seen where a strong UV signal is overlapping with an ELSD response. In all three samples analyzed, the peak maximum of the PDMS-*b*-polyNAM species occurs at 10.64 minutes. The $A_1B_{2.1}$ sample shows signs of a shoulder on the low molecular weight side. Since this sample was the lowest targeted molecular weight of the three samples analyzed, the reason for this low molecular weight shoulder could possibly be as a result of termination of intermediate radicals due to the fact that there are more thiocarbonylthio end-groups present per monomer molecule (a higher CTA concentration leads to a greater chance of cross-termination to occur). For all three samples, polyNAM eluted at approximately the same retention time (peak maximum varied between 18.6–18.88 minutes). It is postulated that these slight differences in retention times can be due to the different possible lengths of polyNAM formed during polymerization. The PDMS macroCTA species is a bit more complicated to interpret as there appear to be multiple peaks occurring in the 1.6–3.3 minute retention time region. Figure 6.5 includes an enlarged insert of this region. As can be seen in this insert, the peaks at 2.14 (no UV 254nm), 2.34 (shoulder with UV 254nm), 2.9 (UV 254nm) and 3.28 minutes (UV 254nm) appear to be present in all three samples analyzed. A peak at 1.7 minutes (no UV 254nm) appears to be present only in samples $A_1B_{4.8}$ and $A_1B_{2.1}$. The largest of these peaks is the peak at 2.14 minutes which contains no UV 254nm, therefore it cannot be a thiocarbonythio-terminated material. The peaks present that do not show any UV absorbance are assumed to be impurities present in the original PDMS-OH.
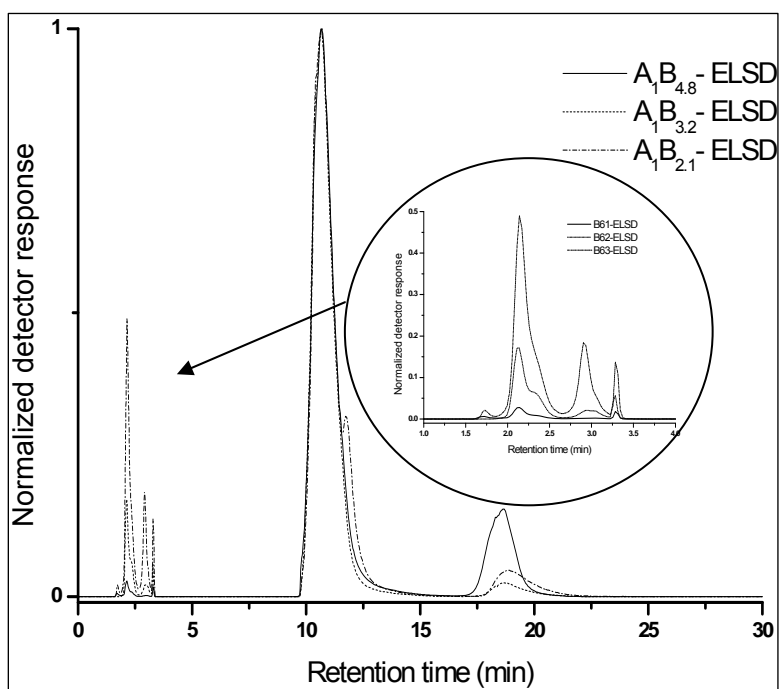

Figure 6.5   **Overlaid GEC chromatograms of PDMS-*b*-polyNAM (25) block copolymer samples (samples from experiment 9–11).**

To assist in the interpretation of these multiple peaks, Figure 6.6 is the GEC chromatogram of a PDMS macroCTA that was run with the optimized GEC method. It can be learned from this chromatogram that there are multiple species present (2.25, 2.87 and 3.19 minutes) containing UV 254nm in the starting macroCTA, presumably all containing PDMS. Although they are not occurring at the same retention times in the block copolymer samples that were analyzed, the author believes that with every batch of PDMS macroCTA that is synthesized, there is the possibility of minor impurities forming at some point along the synthetic process (from original PDMS-OH to esterification reactions to block copolymerizations). It is possible that these impurities may in turn react further during the block copolymerizations to account for the peaks seen in the enlarged insert of Figure 6.6. Alternatively, the author believes that, due to the presence of some peaks in the aforementioned region containing no UV 254nm signal that they may occur during the block copolymerization.
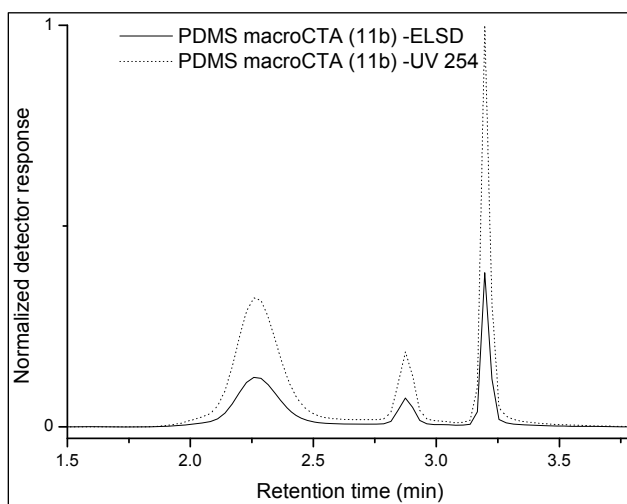

Figure 6.6   **GEC chromatogram of a PDMS macroCTA.**

As seen in Figures 6.7 (a–c), the areas of these PDMS-containing species are however relatively small in comparison to the areas of the respective block copolymer species. The sample (Figure 6.7 (a)) with the highest targeted molecular weight appears to have the least unreacted PDMS/PDMS containing species present, whilst the sample with the lowest targeted molecular weight (Figure 6.7 (c)) appears to have the most unreacted PDMS/PDMS containing species present. The reasons for this are not clear at this point.
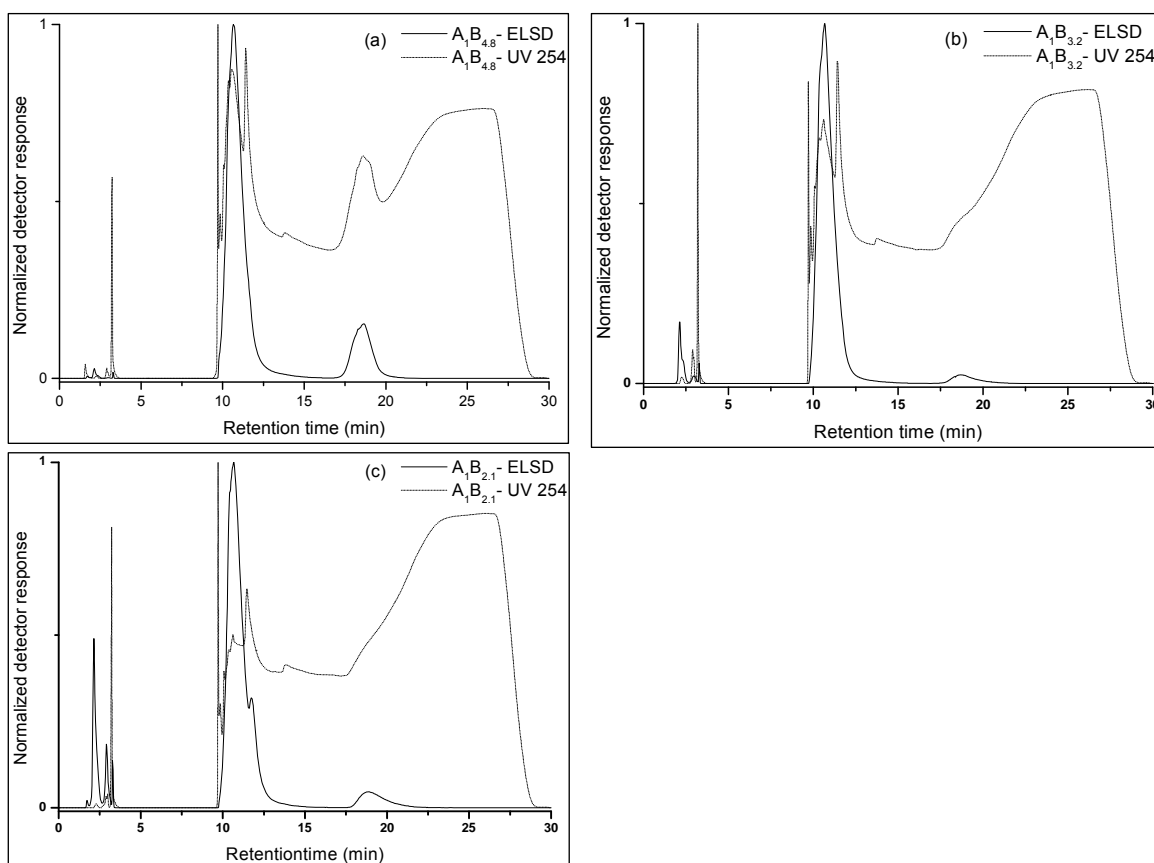
Figure 6.7 **GEC chromatograms for PDMS-*b*-polyNAM (25) block copolymers with ELSD and UV 254nm overlays: (a) $A_1B_{4.8}$ ($\overline{}$, $M_{n\text{Theor}}$ = 28 900g/mol); (b) $A_1B_{3.2}$ ($\overline{}$, $M_{n\text{Theor}}$ = 21 100g/mol); (c) $A_1B2.1$ ($\overline{}$, $M_{n\text{Theor}}$ = 15 300g/mol).**

6.5.2   Solubility studies

Solubility studies of PDMS-*b*-polyNAM were performed at room temperature, and it was found that, unlike PDMS, the block copolymer is soluble in water. In addition to water, it is also soluble in a relatively broad range of organic solvents, including dioxane, THF and chloroform. Therefore, it can be seen that the incorporation of polyNAM with PDMS results in the block being soluble in aqueous environments. It is envisaged that this property would be useful for cosmetic applications in which a water soluble polymer is desired, yet the soft, silky benefits of PDMS can be retained.

Table 6.3   **List of solvents tested for solubility of PDMS-*b*-polyNAM (25) block copolymers.**

Solvent	Sample			
	Exp 9	**Exp 10**	**Exp 11**	**polyNAM**
Hexane	-	-	-	-
Acetonitrile	s	s	s	+
DMF	+	+	+	+
Chloroform	+	+	+	+
THF	+	+	+	+
Dioxane	+	+	+	+
Water	+	+	-	+
Diethyl ether	-	-	-	-
Cyclohexane	-	-	-	

s = swells; (-) = not soluble; (+) = soluble

6.5.3 TEM analysis

Figures 6.8 (a–c) show the TEM images obtained of the three PDMS-*b*-polyNAM (25) block copolymers synthesized in this chapter. In all three cases it is evident that these materials have the ability to self-assemble. They assemble into spherical core-shell materials with varying particle sizes. Material $A_1B_{4.8}$ (Figure 6.8 (a)) was pre-dissolved in water and stained before analysis, whilst materials $A_1B_{3.2}$ and $A_1B_{2.1}$ (Figures 6.8 (b) and (c)) were pre-dissolved in the original reaction mixture, cyclohexane/1,4-dioxane, and not stained before analysis. The latter materials were prepared differently to the former as hazy-like TEM images were consistently observed for all samples pre-dissolved in water. It has been reported that the direct dissolution of amphiphilic block copolymers in water can often be problematic.[11] In all three examples, however, more evident in the last two ((b) and (c)), there is clear evidence of a dark-outer layer on each particle. Since no stain was used in the last two images, this dark layer (presumably the high density PDMS) can allow one to assume that this layer is a true observation of the material.

a)   **b)**
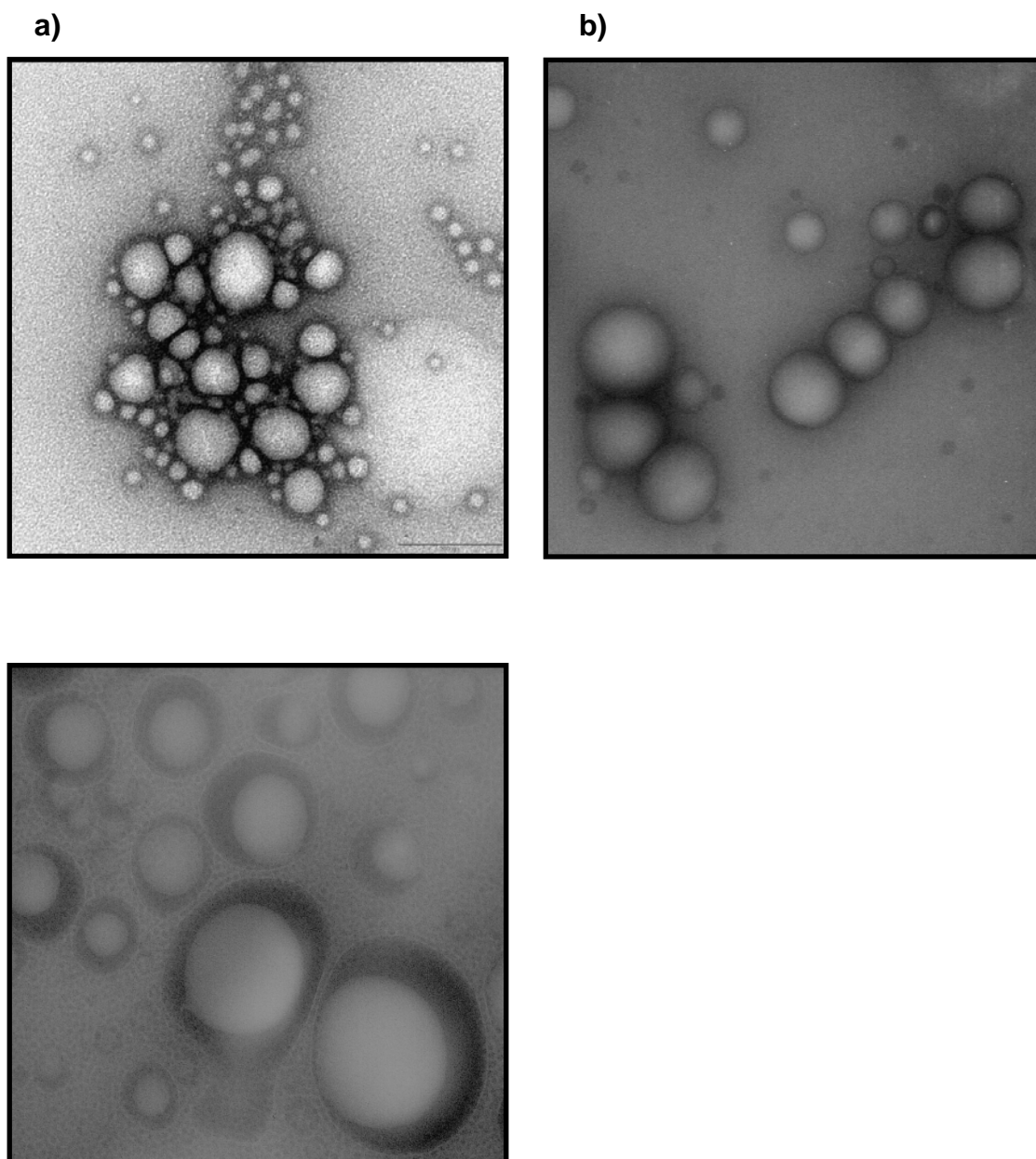
Figure 6.9   TEM images of PDMS-b-polyNAM (25) block copolymers.

6.6   Conclusion

The work presented in this chapter shows that living/controlled radical polymerization, namely RAFT, can be used for the synthesis of a novel PDMS-*b*-polyNAM (25) block copolymer. A PDMS-containing thiocarbonylthio macroCTA is used to react with polyNAM, hereby producing a novel material with both aqueous and organic solubility. Characterization of these novel materials was obtained by SEC/MALS in order to determine molecular weights and PDIs; ^{1}H-NMR in order to identify the presence of both PDMS and polyNAM peaks in the material; and HPLC in order to guage the effectiveness of these block copolymerizations. Finally, TEM images were obtained which gave evidence of the block copolymer reassembling into spherical core-shell particles.

Since the thiocarbonylthio moiety is retained on this block copolymer, it is envisaged by the author that this polymer can be modified to produce a material with applications in the fields of cosmetic science as well as biomedical research.

References

(1)   Chaibundit, C.; Ricardo, N. M. P. S.; Crothers, M.; Booth, C. *Langmuir,* **2002**, *18,* 4277.

(2)   Moffitt, M.; Eisenberg, A. *Macromolecules,* **1997**, *30,* 4363.

(3)   Wyatt, P. J. *Analytica Chimica Acta,* **1993**, *272,* 1.

(4)   Coto, B.; Escola, J. M.; Suarez, I.; Caballero, M. J. *Polymer Testing,* **2007**, *26,* 568.

(5)   Grinshpun, W.; Rudin, A. *J. Appl. Polym. Sci.,* **1986**, *32,* 4303.

(6)   Radke, W.; Simon, P. F. W.; Mueller, A. H. E. *Macromolecules,* **1996**, *29,* 4926.

(7)   Netopilik, M.; Bohdanecky, M.; Kratochvil, P. *Macromolecules,* **1996**, *29,* 6023.

(8)   Leamen, M. J.; McManus, N. T.; Penlidis, A. *J. Appl. Polym. Sci.,* **2004**, *94,* 2545.

(9)   Medrano, R.; Laguna, M. T.; Saiz, E.; Tarazona, M. P. *Phys. Chem. Chem. Phys.,* **2003**, *5,* 151.

(10)   Pound, G.; Aguesse, F.; McLeary, J. B.; Lange, R. F. M.; Klumperman, B. *Macromolecules,* **2007**, *40,* 8861.

(11)   Willet, N.; Gohy, J.-F.; Auvray, L.; Varshney, S.; Jerome, R.; Leyh, B. *Langmuir,* **2008**, *24,* 3009.

Chapter 7

Conclusions and recommendations

7.1 Conclusions

The primary objective of this research is the synthesis of a novel block copolymer containing PDMS and polyNAM using RAFT polymerization. This dissertation has been the first report on the successful synthesis hereof using a LRP technique such as RAFT polymerization.

The first step towards the synthesis of the block copolymers was the esterification of a monohydroxy-terminated PDMS material. This was achieved by using an excess of CTA/DCC as well as catalytic amounts of DMAP at room temperature over a period of 10 hours. Prior to column chromatography, there were no signs of unreacted PDMS in the ^{13}C-NMR and ^{1}H-NMR spectra of the esterified products (PDMS macroCTAs) using the optimized reaction conditions. However, there were numerous unidentified peaks in the NMR spectra, presumably due to side products. These reaction conditions were a significant improvement over that reported in the literature.[1] In addition to obtaining improved reaction conditions, another important objective was to obtain as pure as possible a material as impurities could potentially lead to undesirable side reactions in further polymerizations. By column chromatography, the unidentified peaks in the NMR spectra were removed and a purity of ~99.9% was obtained for the PDMS macroCTA (11b). This compound was used in further block polymerizations with styrene and NAM.

As a model reaction, the above synthesized PDMA macroCTA was used in the block copolymerization with styrene using RAFT polymerization in both solution and emulsion media (specifically miniemulsion). It could be concluded through SEC and TEM results from these experiments that there was indeed formation of a block copolymer and that these materials underwent self-assembly, however conversion rates were very low for the reactions performed in solution. This is expected and an improvement in kinetics should be observed when performing the reactions using miniemulsion techniques. Significantly enhanced kinetics resulted when synthesizing the blocks using RAFT in miniemulsion polymerization, however, samples were not able to be filtered and run through the SEC for molecular weight and PDI analysis. Interesting phase behaviour was observed for the PDMS-*b*-PSt copolymers synthesized in both solution and emulsion media (acorn-like and onion-like structures).

Since it could be identified in the PDMS/PSt system that this technology was working, the next step was to identify suitable reaction conditions for the PDMS/polyNAM system. The first point of concern was the type of CTA to be used. Since it is of great value that the CTA used fragments in such a way that upon addition of a polymeric radical species, the thiocarbonyl moiety is placed at the terminal end of the block copolymer, it was opted to use the trithiocarbonate CTA (10b) as the leaving group in the block copolymerization reactions. The advantage of this is that if one needs to remove the thiocarbonylthio moiety with regard to the desired application, the removal hereof is easily performed without having to cleave the second block of the copolymer. Therefore, the PDMS macroCTA (11b) (functionalized with the trithiocarbonate CTA (10b)) was chosen as the most suitable CTA to use in the block copolymerizations with NAM. However, before the block copolymerizations were attempted, homopolymerizations with NAM and CTA (10b) were performed and the optimized results (*i.e.* temperature, solvent choice) reinforced the initial reasons for choosing this CTA (*i.e.* conversion and molecular weight/PDI results were satisfactory). Also, through performing homopolymerizations with NAM, the author was able to better understand and anticipate which reaction conditions would be suitable for the block copolymerizations of PDMS and polyNAM.

Well-controlled PDMS-*b*-poly(NAM) chains were obtained in a range from 16 000 to 30 000g/mol (as determined by MALS) with narrow PDIs and high monomer conversions (>99.0%). There was good agreement between the $\bar{M}_{n\,Theor}$ and $\bar{M}_{n\,MALS}$ results, however, large discrepancies existed between the molecular weights obtained with conventional SEC. This confirmed the importance of not using PSt standards to measure molecular weights for polyNAM when wanting to obtain reliable results. In order to analyze the block copolymers using HPLC, a gradient elution liquid chromatography technique had to firstly be developed. It was possible to separate PDMS-*b*-polyNAM from the starting materials (polyNAM and PDMS). The presence of polyNAM was negligible in all cases. TEM analysis was performed on these materials in the anticipation of finding evidence of self-assembly. The results indicated that these materials self-assembled into spherical core-shell materials with varying particle sizes.

Solubility studies on these novel siloxane block copolymers indicated that they are soluble both in organic solvent (chloroform, dioxane, THF, DMF) and in aqueous media, contrary to PDMS which is not soluble in water. Therefore, these novel siloxane block copolymers may be used in applications requiring water solubility whilst providing some of the physical and chemical benefits possessed by the superhydrophobic PDMS.

7.2   Recommendations

Both PDMS and polyNAM are widely used in personal care and cosmetic formulations, as well as medicinal and biological field, and are non-toxic and biocompatible to the human body. It is anticipated that this novel material would find application in the personal care and cosmetic field, or even the medicinal field, as it is amphiphilic in nature which is a very useful property in the abovementioned areas.

Since the thiocarbonylthio moiety is retained on this block copolymer, it is envisaged by the author that this polymer can be modified through removal of this moiety to produce a material with applications in the fields of cosmetic science as well as biomedical research.

References

(1)   Pai, T. S. C.; Barner-Kowollik, C.; Davis, T. P.; Stenzel, M. H. *Polymer,* **2004**, *45,* 4383.

Appendix 1

PDMS chemical shift values

PDMS	A	B	C	Impurities		
^{1}H	3.72	3.52	3.43	6.1	3.8	3.48
^{13}C	61.9	71.7	74.07			

Thin-layer chromatography plates for purification of PDMS macroCTA

Pre-extraction

1:1 Hexane/Ethyl acetate or
1:1 Hexane/Diethyl ether

Post extraction

1:1 Hexane/Ethyl acetate or
1:1 Hexane/Diethyl ether

Post column

1:1 Hexane/Ethyl acetate or
1:1 Hexane/Diethyl ether
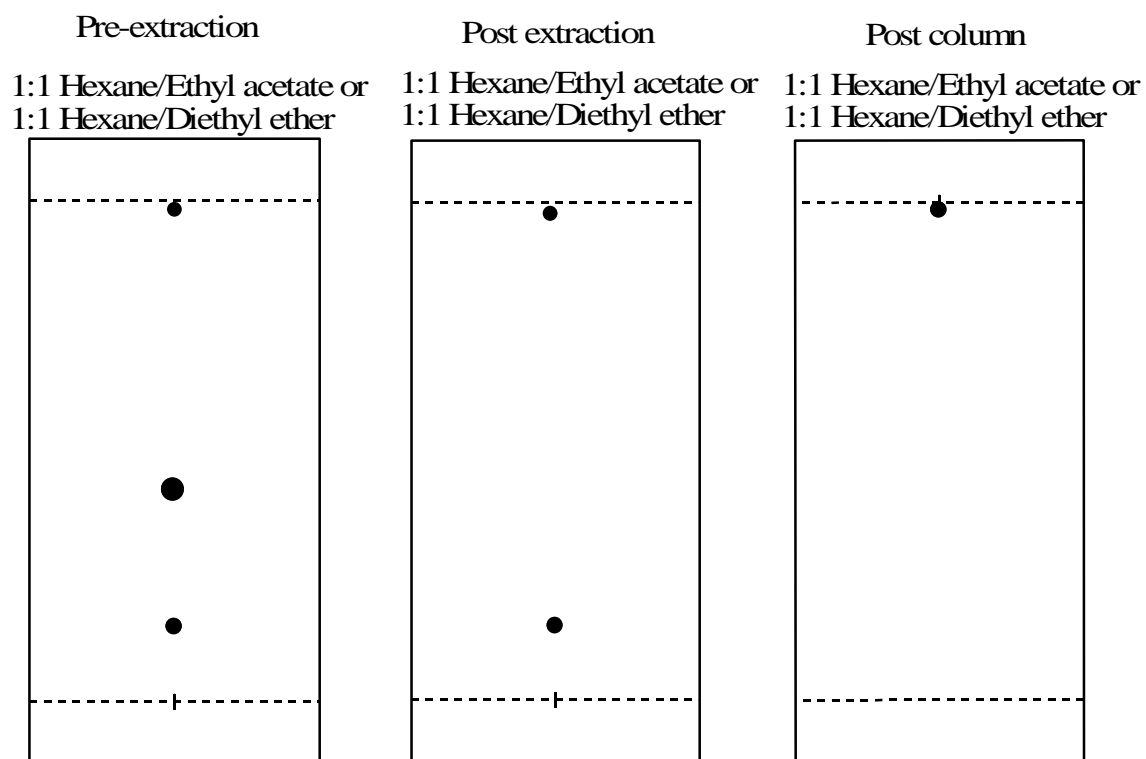
Appendix 2

TEM images as observed for the synthesis of PDMS-*b*-PSt block copolymers using RAFT in miniemulsion.

(a)
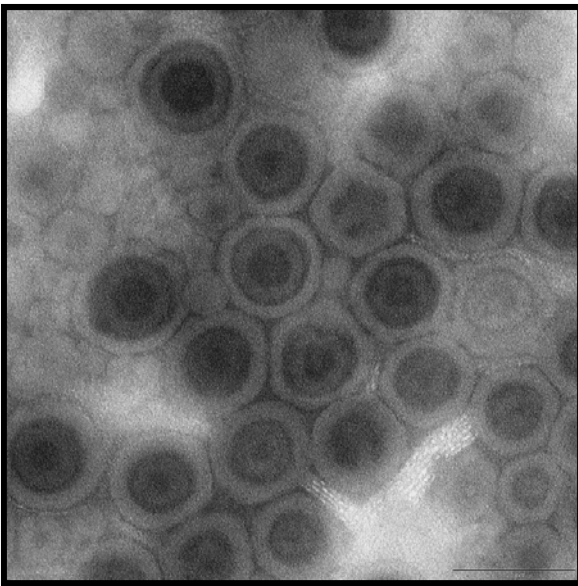
(b)
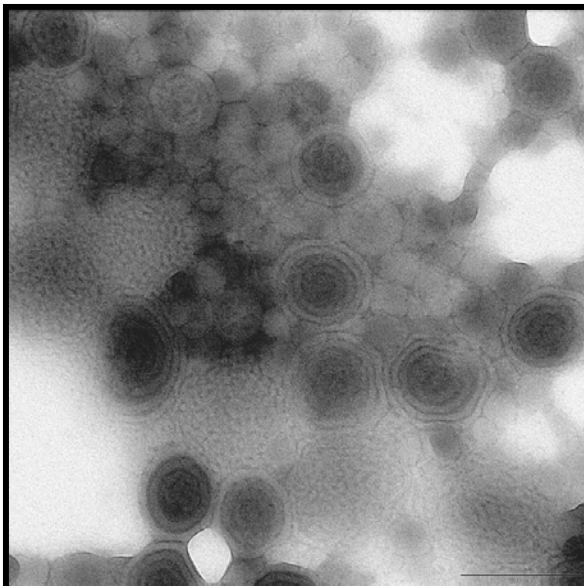
(a) experiment performed using 3% sodium dodecyl sulphate (SDS) and hexadecane (HD) with respect to styrene; [PDMS macroCTA]:[AIBN] = [10:1], sonication time 45 minutes and temperature = 75°C.

(b) experiment performed using 3% Brij 98 and hexadecane (HD) with respect to styrene; [PDMS macroCTA]:[AIBN] = [10:1], sonication time 30 minutes and temperature = 75°C.